

Physical and Molecular Processes Controlling the Formation, Structure and Breakdown of the Salivary Pellicle

Anthony Ash

A thesis submitted for the degree of Doctor of Philosophy to the
University of East Anglia, for research conducted at the Institute of Food
Research

March 2014

© This copy of the thesis has been supplied on condition that anyone who consults it is understood to recognise that its copyright rests with the author and that use of any information derived there from must in accordance with current UK Copyright Law. In addition, any quotation or extract must include full attribution.

English Abstract

Objectives:

Despite the importance of the pellicle in oral physiological and pathological processes, an understanding of the fundamental physical and molecular mechanisms underlying the structural formation and breakdown of this protein film remains unresolved. Therefore the work carried out herein attempts to elucidate the structural changes that the pellicle undergoes upon exposure to intrinsic and extrinsic factors. Such as; the role that mucins play in pellicle formation, the effect of a changing acidic environment or the structural changes that occur upon contact with dentifrice components.

Methods:

in vitro adsorbed pellicles were formed from the saliva (stimulated parotid saliva and stimulated whole mouth saliva) of 14 healthy volunteers, and studied using techniques including a quartz crystal microbalance with dissipation monitoring and a dual polarisation interferometer. The pellicles were then exposed to certain food and oral hygiene ingredients to observe the physical (e.g. surface mass, density, thickness and viscoelasticity) and chemical (e.g. protein composition) modifications that the pellicle undergoes when challenged in this way.

Results:

Mucins present in whole mouth saliva were shown to help form a more viscous pellicle compared to a pellicle formed from mucin free saliva (parotid saliva). Whereas, the pellicle formed from saliva containing 10 mM CaCl₂ was more diffuse and less stable compared to pellicles formed from saliva containing 1mM CaCl₂. Structural changes in the pellicle also took place upon exposure to pH4 and pH3

citrate buffers, changes that may be related to the isoelectric points of the proteins present in the pellicle. Finally, the polyanionic STP molecule was shown to be more effective than SDS at displacing pellicle from hydroxyapatite.

Conclusion:

This research demonstrated that the composition of saliva has an important effect on the physical properties of the adsorbed pellicle; and lays the foundations as to how regulating the calcium concentration of saliva provides a mechanism that can control the physical properties of the in-vitro formed pellicle. In addition, the structural changes that the pellicle undergoes under differing acidic environments, and upon exposure to components of oral hygiene products, were observed to help understand the mechanisms underlying the formation and breakdown of the salivary pellicle.

Riassunto Italiano

Obiettivi:

Nonostante l'importanza della pellicola nei processi orali fisiologici e patologici, la comprensione dei meccanismi fisici e molecolari fondamentali alla base della formazione strutturale e la ripartizione di questo film proteina rimane irrisolta. Pertanto il lavoro svolto qui cerca di illustrare i cambiamenti strutturali che la pellicola subisce in seguito all'esposizione a fattori intrinseci ed estrinseci. Ad esempio, il ruolo che svolgono le mucine nella formazione della pellicola, l'effetto di un ambiente acido o i cambiamenti strutturali che si verificano al contatto con componenti di dentifricio.

Metodi:

Per comprendere ulteriormente tali caratteristiche fisiche, furono formate pellicole in vitro estratte da saliva di quattordici volontari sani (saliva stimolata intera e saliva stimolata dalla ghiandola parotide) utilizzando un microbilancia cristallo di quarzo con dissipazione, e un interferometro a doppia polarizzazione. Le pellicole furono poi esposte a determinati alimenti e determinati ingredienti di igiene orale per poter notare quali modificazioni avessero subito. Modificazioni fisiche tali superficie di massa, densità, spessore e viscosità; e modificazioni chimiche tali identificazione delle proteine.

Risultati:

Si è dimostrato che le mucine presenti nella saliva, aiutano a formare una pellicola più viscosa rispetto ad una pellicola formata da saliva senza mucine (saliva parotide). In più, la pellicola formata da saliva che conteneva 10 mM CaCl_2 era più diffusa e meno stabile rispetto ad una pellicole formata da saliva che conteneva 1 mM CaCl_2 . I cambiamenti strutturali della pellicola hanno avuto luogo anche in seguito

all'esposizione pH4 e pH3 buffer citrate. Queste modifiche possono essere correlate ai punti isoelettrici delle proteine presenti nella pellicola. Infine, il polyanionic molecola STP ha dimostrato di essere più efficace dello SDS a spostare la pellicola dall'idrossiapatite.

Conclusione:

Questa ricerca ha dimostrato non solo che la composizione della saliva ha un effetto importante sulle proprietà fisiche della pellicola, ma anche che cambiando la concentrazione di calcio della saliva, si può creare un meccanismo in grado di controllare le proprietà fisiche della pellicola in vitro. Inoltre, i cambiamenti strutturali che la pellicola subisce quando sotto le diverse condizioni acide e quando esposta agli elementi dei prodotti di igiene orale, aiutano a capire i meccanismi alla base della formazione e della ripartizione della pellicola salivare.

Acknowledgements

I would like to express my profound gratitude to Prof. Peter Wilde and Dr. Gary Burnett for giving me the opportunity to carry out this research and supporting me throughout the progression of this PhD. In four years of study I have never been denied a single opportunity to publish my research or present my work at international conferences in the USA, Brazil or to attend training schools in Switzerland, Germany and Holland. I can't imagine having better supervisors for my PhD, Thank you very much.

I am also very grateful to Mike Ridout, Dr. Roger Parker, Dr. Rob Penfold, Dr. Patrick Gunning and Andrew 'make it so' Kirby for their scientific expertise and insightful suggestions. The amount of time that you gave up to explain techniques or difficult concepts to me was remarkable. All I can say is that I have been very lucky to have had the chance to work alongside you all, and I am very grateful for the guidance and supervision that you gave me. Thank you.

Finally, I would like to thank everyone at the Institute of Food Research, past and present, for making my time here so productive; not only from a work perspective but a social one too. Our many visits to the Fat Cat certainly helped oil the progression of this PhD, and I always felt that the group meetings held there were the most productive. Although it is not possible to mention every single person who has influenced my time here, I would like to thank all the amazing people I have met over the past 4 years. Thank you for being a part of this amazing and fulfilling journey. I have had the time of my life!

Dedicated to my Mother; '*Gabriella Anna Paronuzzi Ash*' and Father; '*Julian Horace Ash*'. You have given me the happiest life a son could ask for,

Thank you.

“You don’t miss the water until the well runs dry”

Publications

1. A. Ash, G.R. Burnett, R. Parker, M.J. Ridout, N.M. Rigby and P.J. Wilde, Structural characterisation of parotid and whole mouth salivary pellicles adsorbed onto DPI and QCMD hydroxyapatite sensors, *Colloids Surf B Biointerfaces*, (2013). In Press doi: 10.1016/j.colsurfb.2013.10.024. Based on chapter 4

2. A. Ash, M.J. Ridout, R. Parker, A.R. Mackie, G.R. Burnett and P.J. Wilde, Effect of calcium ions on in vitro pellicle formation from parotid and whole saliva, *Colloids and Surfaces B: Biointerfaces*, 102 (2013) 546-553. Based on chapter 5

Table of Contents

Thesis Title.....	1
English Abstract.....	2-3
Italian Abstract.....	4-5
Acknowledgments.....	6
Publications.....	8
List of Figures	18-25
List of Tables.....	26
Chapters 1– 8.....	27–223
References.....	224

Chapter 1 The Salivary Pellicle.....	27
Introduction.....	28
History of pellicle exploration.....	31
Function of the acquired enamel pellicle (AEP).....	33
Lubrication of tooth surfaces.....	33
Semi permeable membrane & mineral homeostasis.....	35
Bacterial adherence.....	37
Formation of the AEP.....	38
Composition of the AEP.....	44
Protein composition of AEP.....	46
Lipid composition of AEP.....	47
Carbohydrate composition of AEP.....	48
Structure of the AEP.....	49
Food components that influence the AEP.....	53
pH changes.....	53
Calcium changes.....	54
Components of oral hygiene products that influence the AEP.....	56
Research Aims.....	59

Chapter 2 Techniques used to Investigate the Formation, Structure and	
Composition of the Salivary Pellicle.....	61
Introduction.....	62
Quartz Crystal Microbalance with Dissipation monitoring (QCMD).....	63
Change in the frequency of the oscillating sensor to calculate mass.....	64
Measuring change in dissipation to determine viscoelasticity.....	65
Voigt model for viscoelasticity.....	67
Dual Polarisation Interferometer (DPI).....	69
Atomic Force Microscopy (AFM).....	75
Protein Analysis.....	79
Fast protein liquid chromatography.....	80
Hydroxyapatite packed column.....	81
1-dimension Sodium dodecyl sulfate polyacrylamide gel electrophoresis.....	83
2-dimensional polyacrylamide gel electrophoresis (2D-PAGE).....	85
First dimension separation (isoelectric focussing).....	85
Second dimension separation (SDS-PAGE).....	85
Liquid chromatography tandem mass spectrometry (LC-MS/MS).....	87
Saliva.....	90
Saliva collection.....	90
Saliva protein concentration.....	93

Chapter 3 Salivary Pellicle Adsorption and Characterisation Relative to Hydrophobic, Silica and Hydroxyapatite surfaces.....	95
Introduction.....	96
Materials and Methods.....	99
Sensor cleaning.....	100
Contact angles.....	100
Surface roughness.....	101
2-D gel electrophoresis and mass spectrometry.....	101
In situ trypsin hydrolysis of protein bands.....	101
Statistics.....	102
Results.....	103
Surface roughness.....	103
Contact angle.....	103
Surface charge.....	106
QCMD.....	107
DPI.....	110
Identification of <i>in vitro</i> hydroxyapatite bound pellicle proteins.....	113
Discussion.....	118

Chapter 4 Structural Characterisation of Parotid and Whole Mouth Salivary

Pellicles Adsorbed onto DPI and QCMD Hydroxyapatite Sensors.....125

Introduction.....	126
Materials and methods.....	128
Saliva collection.....	128
Saliva adsorption protocol.....	128
Simulated salivary buffer.....	129
Sensor properties.....	129
Sensor cleaning.....	130
Mucin immuno-blotting.....	130
Statistics.....	131
Results.....	132
Mucin composition.....	132
QCM-D pellicle adsorption.....	133
Protein concentration.....	135
Viscoelastic properties.....	137
DPI Pellicle adsorption.....	138
Pellicle density.....	141
Discussion.....	142

Chapter 5 Effect of Calcium Ions on <i>in vitro</i> Pellicle Formation from Parotid and Whole Mouth Saliva.....	149
Introduction.....	150
Materials and methods.....	152
Saliva collection.....	152
Saliva adsorption.....	152
Sensor properties.....	154
DPI sensor cleaning.....	154
QCMD sensor cleaning.....	155
Statistics.....	155
Results.....	156
DPI.....	156
Pellicle ‘polymer’ mass.....	156
Pellicle Thickness.....	156
Pellicle Density.....	157
QCMD.....	160
Pellicle hydrated mass & thickness.....	160
Pellicle viscoelasticity.....	163
Discussion.....	166

Chapter 6 Structural Changes of the Salivary Pellicle Under Acidic

Conditions.....	172
Introduction.....	173
Materials & Methods.....	176
Solutions.....	176
Sensor properties.....	176
Quartz crystal microbalance with dissipation monitoring (QCMD).....	177
Dual polarisation interferometer (DPI).....	178
Statistics.....	179
Results.....	180
QCMD.....	180
DPI.....	182
Discussion.....	185

Chapter 7 Structural and Compositional Changes in the Salivary Pellicle

Induced Upon Exposure to SDS and STP.....190

Introduction.....	191
Materials & Methods.....	193
Saliva collection.....	193
Solutions.....	193
Quartz crystal microbalance with dissipation monitoring (QCMD).....	193
Dual polarisation interferometer (DPI)	194
Sensor properties.....	195
Fast protein liquid chromatography (FPLC).....	196
SDS-PAGE.....	195
AFM.....	197
Results.....	198
QCMD.....	198
DPI.....	200
FPLC Protein identification.....	203
LC-MS/MS.....	205
Discussion.....	210

Chapter 8 Conclusion.....218

List of Figures

Figure 1.0. Release of ordered water molecules drives the formation of protein adsorption to enamel. In **(a)**, a salivary protein and an enamel surface are shown surrounded by ordered water molecules, which represent a low entropy system. **(b)** then shows how adsorption of the salivary protein to the tooth enamel surface releases some of the ordered water molecules surrounding them. This increase in entropy provides the thermodynamic push toward protein adsorption and consequently formation of the AEP.....**40**

Figure 1.1. Current proposed outline of pellicle formation: **(a)** initial salivary protein adsorption occurs rapidly, followed by; **(b)** the formation of a dense basal layer. Subsequently, **(c)** protein aggregates and mucins adsorb to form a more globular outer layer, when finally **(d)** bacteria adsorb and colonise the outer pellicle. Initially the pellicle provides a protective barrier for teeth, preventing enamel abrasion and demineralisation. However, over time the pellicle becomes the primary site for the attachment of acid producing bacteria.....**50**

Figure 2.0.1. (a) Photograph of the QCMD fitted with a QAFC 302 axial flow measurement chamber. (b) Inner chamber of the QCMD where the sensor is placed on top of the green o-ring. (c) Photograph of gold coated QCMD sensors that sandwich the quartz crystal disc. The front of the sensor is where the proteins adsorb; and the gold electrode on the back of the sensors is where the electrical voltage is applied.....**63**

Figure 2.0.2. Thickness shear mode oscillation of the QCMD sensor. Due to the piezoelectric properties of quartz, it is possible to excite the crystal to oscillate by applying an alternating flow of electricity across its electrodes at a frequency to which the crystal resonates (i.e 5MHz). When applying a direct current (DC) to the sensor it shifts the sensor in one direction **(a)**. When the current is switched off the sensor returns to its original position **(b)**. By reversing the flow of electricity the sensor will move in the opposite direction **(c)**. Thus by applying an alternating current (AC) to the sensor (where the flow of electric charge periodically reverses direction) will result in the sensor oscillating left and right in what is known as the thickness shear mode **(d)**.....**64**

Figure 2.0.3 An example of dissipation differences between (a) an elastic film and (b) a more viscous film.....**66**

Figure 2.0.4. **(a)** The QCMD sensor oscillates at different frequencies (or overtones). This results in a decrease in the detection or penetration depth of the film at increasing overtones of the oscillating sensor.....**67**

Figure 2.0.5. Photos: (a) PC, pump and DPI unit (b) Temperature control unit where sensor is clamped (c) sensor holding unit.....**69**

Figure 2.0.6. (a) Plan view of the DPI silicon oxynitride sensor: arrows 1 and 3 indicate the position of the measuring channels of the sensor; and arrow 2 indicates the reference channel where no contact with the sample was made. (b) Side view, schematic representation of the sensor, showing the dual slab waveguides, and the passage of polarised light through the sensing and reference waveguides.....70

Figure 2.0.7. The electric field profile of light in a waveguide of the DPI sensor. The evanescent field extends only a few hundred nanometers from the waveguide surface, an area known as the near field. Any changes in the refractive index in this nearfield region will influence the speed at which light passes down the waveguide. The higher the refractive index of an adsorbed material, the greater the slowing effect on light passing through the sensor.....70

Figure 2.0.8. Output from both waveguides combine to generate interference patterns. Changes in these patterns are directly related to both the refractive index and the thickness of the molecular layer. (a) Principle of interferometry; when light waves interact. (b) Screen image of a fringe pattern as light passes through a sensor. 1 and 3 represent the fringe pattern from measuring channels 1 and 3 of the sensor; whereas 2 represents the fringe pattern of the reference channel of the sensor where no contact with the sample was made.....71

Figure 2.0.9. TE and TM evanescent fields passing through a DPI sensor with an adsorbed monolayer of proteins. The TE mode evanescent field is more closely confined to the surface of the waveguide than the TM mode evanescent field; and is therefore more sensitive to adsorbed material close to the surface than the TM mode. This difference is exploited to obtain information about the structure of the layer on the waveguide surface.....72

Figure 2.1.0. (a) Graph displaying the phase change of an adsorbing film over time. (b) The converted phase data from time point t to generate a range of thickness and RI values that satisfy the observed phase change observed in TM and TE mode. The point of intersection corresponds to the layer condition on the waveguide surface at time t73

Figure 2.1.1. (a) Photo of the MFP-3D-BIO AFM sat on a vibration isolation platform (right side) with controller unit and PC (left side). Padded room reduces environmental vibrations which can impact image quality. (b) (i) MFP-3D head where cantilever tip is held and moves the tip in the vertical z direction. (ii) Stage or MFP-3D XY scanner that moves the sample in the horizontal x and y direction. (c) Scanning electron micrograph of the AFM tip and cantilever used to ‘feel’ the surface of a sample.....76

Figure 2.1.2. Schematic overview of the AFM that illustrates the main features.....77

Figure 2.1.3. The apparatus (i) consists of a Biocad Sprint liquid chromatography equipped with an internal PC running Windows 95 and used for controlling the system and storing and processing data. (ii) schematic overview of the system.....81

Figure 2.1.4. schematic representation of the binding mechanisms of salivary proteins to the hydroxyapatite.....82

Figure 2.1.5. schematic representation of peptides separated by mass in a polyacrylamide gel.....84

Figure 2.1.6. (a) schematic of isoelectric focusing: a mixture of salivary proteins were resolved on a pH3-10 Immobilized pH gradient strip according to each proteins isoelectric point, independent of the protein size. **(b)** Schematic diagram showing the second dimension separation of proteins by SDS-PAGE after separation by IEF.....86

Figure 2.1.7. A typical experimental workflow for salivary protein identification and characterisation using LC-MS/MS data; and a schematic outline of the LTQ-Orbitrap.....89

Figure 2.1.8. Image of a Lashley cup and the collection of parotid saliva (a) placement of the Lashely cup in preparation for the collection of parotid saliva; (b) Parotid duct (also known as Stensen’s duct) located in the upper cheek next to the maxillary second molar; (c) Inner structure of the Lashley cgup showing ;(i) the vacuum chamber that allows the attachment of the device to the surrounding buccal surface; and (ii) Parotid saliva collection chamber where the parotid saliva flows.....92

Figure 2.1.9. Bacterial growth derived from PS and WMS. PS and WMS was swabbed onto 3 different media: **(a)** M17 medium supplemented with either glucose only; **(b)** de Man, Rogosa and Sharpe and **(c)** Blood Agar Base 1% Yeast Extract 5%Horse Blood. Plates were then incubated for 24 hours at 37°C.....93

Figure 3.0.1. AFM imaging and contact angle photo of: (a) DPI hydroxyapatite coated sensor; (b) a QCMD hydroxyapatite coated sensor; (c) DPI silica sensor; (d) QCMD silica sensor; (e) DPI C18 functionalised sensor; (f) QCMD polystyrene functionalised sensor. Differences between either surface roughness or wettability can clearly be observed in all sensors, apart from (b) and (d)104

Figure 3.0.2. Bar chart displaying the different contact angles of all the DPI and QCMD sensors used. No significant difference between DPI and QCMD hydroxyapatite sensors. The hydrophobic DPI C18 and QCMD polystyrene sensors display the highest contact angle of all the sensors. But surprisingly DPI and QCMD silica sensors display significantly different contact angles.....105

Figure 3.0.3. (a) Graph showing the change in frequency of the sensor (\approx pellicle hydrated mass) over time. (b) Bar chart showing the adsorbed pellicle hydrated mass after rinsing with buffer.....107

Figure 3.0.4. (a) Graph showing the change in dissipation of the sensor (\approx pellicle softness) over time. (b) Bar chart showing the dissipation value of the sensor, and thus, adsorbed pellicle softness after rinsing with buffer.....108

Figure 3.0.5. Bar chart displaying ΔD (dissipation) as a function of Δf (frequency) measured for the 3rd overtone reflecting qualitative viscoelastic properties of the pellicle (less negative = more elastic) on three different surfaces. Pellicle adsorbed to the hydroxyapatite sensor was shown to be more rigid than pellicle adsorbed to silica and polystyrene.....109

Figure 3.0.6. (a) Adsorption profile of salivary pellicle ‘dry’ mass onto three DPI sensors (Silica, C-18 and hydroxyapatite). (b) Bar chart showing the ‘dry’ mass of the adsorbed pellicle after rinsing with buffer.....110

Figure 3.0.7. (a) Adsorption profile of salivary pellicle thickness on three DPI sensors (Silica, C-18 and hydroxyapatite). (b) Bar chart showing the thickness of the adsorbed pellicle after rinsing with buffer.....111

Figure 3.0.8. (a) Adsorption profile of salivary pellicle density on three DPI sensors (Silica, C-18 and hydroxyapatite). (b) Bar chart showing the density of the adsorbed pellicle after rinsing with buffer.....112

Figure 3.0.9. Two-dimensional gels obtained in pH range between 3 and 10 and 12.5% of SDS–PAGE stained with colloidal Coomassie blue of: (a) original WMS sample and (b) a hydroxyapatite incubated WMS sample (identifying non-adsorbed proteins) and (c) gels a and b overlaid to reveal salivary proteins that do adsorb (orange) and those that do not (Black/blue).....114

Figure 3.1.0. A section of 2D gel displaying the selective adsorption of spot B8 (Calgranulin – A) to hydroxyapatite from 3 different volunteers (a), (b) and (c); and the limited adsorption of spots B7 (Cystatin-SN); B12 (Cystatin-SN); and D3 (Cystatin-B).....116

Figure 4.1. Immunoblot displaying the presence of mucins (MUC 1, 2, 5AC, 5B, 6 and 7) in WMS and their general absence from PS in 4 of the 14 volunteers’ saliva used in this study. MUC 7 and MUC 5B being the primary mucins present in saliva; with traces of epithelial derived mucins (MUC 1 and MUC 2); and very faint blots of pulmonary (MUC 5AC) and human gastric (MUC6) mucins.....132

Figure 4.2. The adsorption profile of an example (a) WMS and (b) PS sample; with raw data and fitted Voigt modelled data (WMS $\chi^2 = 9.3 \times 10^5$; PS $\chi^2 = 13.5 \times 10^5$). Adsorption profile of (c) mean frequency and (d) mean dissipation changes versus time; measured for the 3rd overtone by QCM-D for the adsorption of WMS (n=10) and PS (n=10) pellicle on hydroxyapatite coated sensors. Frequency decreases instantly, with a concomitant rapid increase in dissipation, as the saliva rapidly adsorbs to the sensor surface. Following 120 minutes adsorption a simulated salivary buffer was used to remove loosely adsorbed material from the pellicle.....133

Figure 4.3. Box plot displaying the variation in the protein concentration of PS (n = 33) and WMS (n = 42).....136

Figure 4.4. linear regression analysis of Sauerbrey mass as a function of the protein concentration for (b) PS (n=10) and (c) WMS (n=10) derived pellicles. This suggests that the PS protein concentration had a positive association to the adsorbed Sauerbrey mass of the adsorbed salivary pellicle.....136

Figure 4.5. Bar chart displaying the ratio of $\Delta f/\Delta D$ for WMS and PS derived pellicles at three different stages of pellicle formation. Throughout the experiment the PS formed a pellicle that had a lower $\Delta f/\Delta D$ ratio than WMS derived pellicle. This suggests that the PS derived pellicle was more elastic relative to WMS derived pellicle.....138

Figure 4.6. Adsorption profile of (a) WMS (n=10) and (b) PS (n=10) forming a pellicle over time on a DPI hydroxyapatite coated sensor. Thickness, mass and density of the pellicle increase rapidly as the saliva rapidly adsorbs to the sensor surface. Following 120 minutes adsorption a simulated salivary buffer was used to remove loosely adsorbed material from the pellicle.....139

Figure 4.7. Box plot displaying the rate of pellicle formation derived from PS and WMS after 2 hours adsorption. The PS continually adsorbs to the surface of both QCMD and DPI sensors for the duration of the experiment. Whereas WMS formed pellicle stopped adsorbing and actual desorption of pellicle mass was observed.....140

Figure 4.8. Density difference between PS and WMS pellicle at different stages of formation. Throughout the experiment the density of the PS derived pellicle was higher than that of the WMS derived pellicle. This suggest that the WMS derived pellicle is more diffuse relative to the PS derived pellicle.....141

Figure 4.9 Proposed model of pellicle formation: (a) The mucins contain a number of sites that can potentially promote adsorption to a surface. These include hydrogen bonding and hydrophobic interactions (via the carbonyl groups and methyl groups) and electrostatic interactions (via sialic acid residues). (b) The smaller MW surface active proteins (i.e statherin, histatins) that are entrapped in the mucin network begin to diffuse through the network adsorbing onto the enamel surface. (c) These low MW proteins crosslink to form a dense basal layer. (d) Mucins and protein aggregates then arrange themselves in a way that results in a small amount of syneresis to take place.....147

Figure 5.1. Adsorption profile of WMS forming a pellicle over time on a DPI sensor. (a) Real time TM and TE phase changes that show: **I** the baseline recorded in deionised water, **II** the peak value of the adsorbed pellicle, **III** the phase shift post calcium rinse. **IV** & **V** the phase shifts post water rinse. (a) The derived thickness, polymer mass and density changes derived from TE and TM phase changes using Maxwell's equations. (b) Thickness, mass and density of the pellicle increase rapidly as the saliva rapidly adsorbs to the sensor surface. Following 20 minutes adsorption a calcium rinse removed loosely adsorbed material from the pellicle. Upon rinsing the pellicle with water, the thickness and mass was reduced with a concomitant increase in pellicle density.....154

Figure 5.2. (a) Box plot of DPI measured polymer mass, thickness and density changes formed from WMS containing 0 mM Calcium (2 mM EDTA) (n=10); the natural concentration of WMS + 1 mM CaCl₂ (n=10); and natural concentration of WMS +10 mM CaCl₂ (n=10). **(b)** PS containing 0 mM Calcium (2 mM EDTA) (n=12); the natural concentration of PS + 1 mM CaCl₂ (n=12); and natural concentration of PS +10 mM CaCl₂ (n=12). Values reported are peak, post calcium rinse and post water rinse values (* = Significant difference (p ≤ 0.01)).....158

Figure 5.3. (a) Frequency and **(b)** dissipation changes versus time measured for the 3rd overtone (15 MHz) by QCMD for the adsorption of WMS at different calcium concentrations of saliva. **I** baseline recorded in deionised water. **II** Peak value. **III** post calcium rinse. **IV & V** water rinse. Increasing concentrations of calcium in saliva display lower frequency oscillations with respective higher dissipation values.....160

Figure 5.4. Comparison of frequency changes to pellicle formed from **(a)** WMS and **(b)** PS containing 0 mM Calcium (+2mM EDTA) (n=12), natural concentration of WMS + 1mM CaCl₂ (n=12), and natural concentration of PS + 10 mM CaCl₂ (n=12). (* = Significant difference (p ≤ 0.05)).....163

Figure 5.5. Comparison of dissipation changes to pellicle formed from **(a)** WMS and **(b)** PS containing 0 mM Calcium (+2mM EDTA) (n=12), natural concentration of WMS + 1mM CaCl₂ (n=12), and natural concentration of PS + 10 mM CaCl₂ (n=12). (* = Significant difference (p ≤ 0.05)).....164

Figure 5.6. ΔD as a function of Δf measured at the 3rd overtone by QCM-D for the adsorption of **(a)** WMS pellicle and **(b)** PS pellicle containing: 0 mM Calcium (+2mM EDTA); + 1mM CaCl₂, and +10 mM CaCl₂.....165

Figure 5.7. Proposed model for the changes in the structure of the pellicle derived from saliva containing different concentrations of calcium: **(a)** Pellicle formed from saliva containing 0mM CaCl₂ or 1mM CaCl₂. **(b)** Pellicle formed from saliva containing 10mM CaCl₂. Proteins in saliva aggregate at 10mM CaCl₂, prior to pellicle adsorption. The aggregates subsequently deposit onto the sensor surface forming thicker more diffuse films.....170

Figure 6.1. Salivary pellicle adsorption profile on a QCMD silica sensor after **(a)** 2 hour adsorption of the salivary pellicle and then subsequent rinsing of the adsorbed pellicle with citrate buffer at: **(b)** pH7 **(c)** pH6 **(d)** pH5 **(e)** pH4 **(f)** pH3 and **(g)** pH7.....178

Figure 6.2. Salivary pellicle adsorption profile on a DPI silica sensor after **(a)** 2 hour adsorption of the salivary pellicle and then subsequent rinsing of the adsorbed pellicle with citrate buffer at: **(b)** pH7 **(c)** pH6 **(d)** pH5 **(e)** pH4 **(f)** pH3 and **(g)** pH7.....179

Figure 6.3. Bar charts representing the mean (n=5) **(a)** Dissipation, **(b)** Sauerbrey mass, thickness and **(c)** ratio of $\Delta f/\Delta D$ for salivary pellicles under different pH conditions (i.e. pH 3- pH7). The pellicle undergoes predominant structural changes at pH 4 and pH 3.....181

Figure 6.4. Bar charts representing the mean (n=5) (a) Thickness, (b) Mass and (c) Density changes of the salivary pellicle under different pH conditions (i.e. pH 3- pH7). Significant changes in Mass and density but not thickness were observed.....183

Figure 6.5. (a) salivary pellicle showing glycosylated mucins over a layer of low-molecular weight proteins bathed in pH7 citrate buffer solution, representing a densely packed rigid film relative to (b) where a more diffuse and viscous salivary pellicle was observed when bathed in a more acidic (i.e. pH3 and pH4) citrate buffer solution.....186

Figure 7.1. QCMD Experimental procedure: Salivary pellicle adsorption profile for a parotid saliva sample on a QCMD hydroxyapatite sensor. (i) Addition of saliva (ii) phosphate buffer rinse (iii) 10 mM STP or SDS rinse (iv) phosphate buffer rinse.....194

Figure 7.2. DPI Experimental procedure: Salivary pellicle adsorption profile for parotid saliva sample on a DPI hydroxyapatite sensor. (i) Addition of saliva (ii) phosphate buffer rinse (iii) 10 mM STP or SDS rinse (iv) phosphate buffer rinse.....195

Figure 7.3. Box plot displaying the Sauerbrey mass (primary axis) and thickness (secondary axis) of the combined WMS and PS salivary pellicles on hydroxyapatite and silica sensors before and after rinsing with 10mM STP and 10mM SDS; and the statistical differences between them.....199

Figure 7.4. $\Delta f / \Delta D$ plot displaying the different elastic properties of the combined WMS and PS salivary pellicles before and after rinsing with SDS and STP on both hydroxyapatite and silica surfaces. (A test for outliers was performed using the “outlier test” function in the R statistical package and removed from the plots.....200

Figure 7.5. Box plot displaying the changes in thickness, mass and density of combined WMS and PS salivary pellicles adsorbed to a DPI hydroxyapatite and silica sensor before and after rinsing with 10mM STP and 10mM SDS.....202

Figure 7.6. (a) Chromatogram showing the displacement of saliva proteins from hydroxyapatite by 10mM STP (three repeats) and the fractions collected (labelled 1-4); and the accompanying typical electrophoretic profile observed of those fractions separated by SDS-PAGE (lanes 1-4). (b) Chromatogram showing the displacement of saliva proteins from hydroxyapatite by 10mM SDS (three repeats) and the fractions collected (labelled i - iv); and the accompanying typical electrophoretic profile observed of those fractions separated by SDS-PAGE (labelled i - iv).....204

Figure 7.7. Qualitative classification of the in vitro pellicle proteins displaced by 10mM STP and 10 mM SDS according to (a) molecular weight and (b) isoelectric point. **N.B** STP displaced significantly more proteins than SDS. The following pie charts only show relative contributions of proteins displaced out of 100% and do not represent the total amount of protein displaced.....209

Figure 7.8. AFM image of a (a) 2 hour adsorbed salivary pellicle. (b) The same pellicle after exposure to 10mM STP. The holes in the pellicle represent areas where the pellicle network has been displaced by STP entering defects within the pellicle.....**212**

List of Tables

Table 3.1. Surface properties of the DPI and QCMD sensors.....	106
Table 3.2. List of proteins identified from gel in Figure 3.0.9. (c). Several spots were assigned as the same protein, due to possible post-translational modifications, protein isoforms and peptides.....	137
Table 4.1. QCM-D values of the adsorbed Sauerbrey and Voigt mass, thickness and rate of formation for WMS (n=10) and PS (n=10) determined on hydroxyapatite surfaces after 1 minute and 2 hour saliva adsorption; and after rinsing with simulated salivary buffer.....	135
Table 4.2. DPI values of the adsorbed polymer mass, density and thickness for WMS (n=10) and PS (n=10) determined on hydroxyapatite surfaces after 1 minute and 2 hour saliva adsorption; and after rinsing with simulated salivary buffer.....	140
Table 5.1. Effect of the calcium concentration of WMS and PS on Sauerbrey and Voigt modelled thickness and hydrated mass changes to pellicle formed from (a) WMS containing 0 mM Calcium (2 mM EDTA) (n=10); natural concentration of WMS + 1 mM CaCl ₂ (n=10); and natural concentration of WMS +10 mM CaCl ₂ (n=10). And pellicle formed from (b) PS containing 0 mM Calcium (2mM EDTA) (n=12), natural concentration of PS + 1mM CaCl ₂ (n=12), and natural concentration of PS + 10 mM CaCl ₂ (n=12).....	162
Table 6.1. QCMD data of the salivary pellicle under neutral and acidic conditions (pH7 – pH3).....	182
Table 6.2. DPI data of the salivary pellicle under neutral and acidic conditions (pH7 – pH3).....	184
Table 7.1. (a) Identified proteins displaced from hydroxyapatite using 10mM STP.....	206
Table 7.1. (b). Identified proteins displaced from hydroxyapatite using 10mM SDS.....	208

Chapter 1

The Salivary Pellicle

Introduction

The formation of the acquired enamel pellicle (AEP) at the tooth/saliva interface is a result of the selective adsorption of proteins, including enzymes and glyco-proteins that are present in saliva [1]. The saliva is a fluid that is secreted via three pairs of major salivary glands (parotid, sublingual and submandibular) and by hundreds of minor salivary glands located throughout the mouth [2]. The glands differ in the type of secretion they produce, which is subject to the ratio of mucous to serous glandular cells within the respective glands. Serous cells are found in parotid, submandibular, palatal and lingual glands that secrete a watery fluid, essentially devoid of mucins. Mucous cells, present in submandibular, sublingual, labial, palatal and lingual glands, produce mucin rich saliva, which generates a more viscoelastic fluid [3]. Parotid saliva therefore generates a serous secretion devoid of mucins, whereas whole saliva generates a secretion formed from a mixture of all the salivary glands within the mouth, alongside oral tissue fragments and bacterial components found within the oral cavity. The amount and composition of saliva however, depends on factors, such as: the flow rate [4], circadian rhythm [5], drugs [6], age [7], gender [8] and physiological status [9]. Although the average secretion of saliva ranges from 0.3 to 7.0 ml/min[10], with about 0.5 – 1.5 l of saliva produced per day [11].

Whole mouth saliva is mainly composed of water (99.5%), proteins (0.3%) and inorganic trace substances (0.2%) [11, 12]. Saliva's relatively low protein and ion concentration change a fluid that is predominantly water into a solution with physical characteristics very unlike that of water. These characteristics allow saliva to perform its multifunctional roles in speech, lubrication, digestion of food and importantly the formation of the salivary pellicle which helps to maintain oral health [13]. As the

salivary pellicle constitutes an interface between teeth and the oral environment, it is universally accepted to be of prime importance for several protective functions within the oral cavity. For example, the AEP aids the lubrication of teeth, protecting dentition against abrasion and erosion [14]; and behaves as a perm-selective membrane promoting tooth re-mineralisation, whilst protecting against the de-mineralization of teeth caused by acids [15-17]. However, the beneficial effect of the AEP is ambivalent, as it not only protects the enamel but also provides the primary site for bacterial attachment and the build-up of plaque, which can increase the risk of caries [18]. This is important, as the Adult Dental Health Survey carried out in the UK in 1998 showed that nearly 72% of dentate adults presented visible plaque on their teeth [19]. Despite the importance of the AEP in oral physiological and pathological processes, an understanding of the fundamental physico-chemical mechanisms underlying the structural formation of this protein film has been difficult to achieve. This has been because only minuscule amounts of *in vivo* formed pellicle can be collected from tooth surfaces [20]. Despite this hurdle, several authors [20-27] have studied the composition of the AEP using a number of methods which has allowed identification of mucins, amylase, albumin, IgA, S-IgA, proline-rich proteins (PRPs), cystatins, lysozyme, carbonic anhydrase, lactoferrin, statherin and histatins as key pellicle components. However, more recently, greater attention has been given to the structural appearance of the adsorbed pellicle layer using a number of techniques, such as: scanning electron microscopy (SEM), transmission electron microscopy (TEM) confocal laser scanning microscopy (CLSM), Quartz Crystal Microbalance (QCMD), Dual polarisation interferometry (DPI) and atomic force microscopy (AFM) which has resulted in a greater understanding of AEP [28-34]. Current thinking suggests that the formation of the AEP takes place in two stages.

The initial pellicle forms almost instantaneously via non-covalent interactions; whereby proteins with a high affinity to hydroxyapatite, the primary mineral of enamel, are the first proteins to adsorb to the tooth surface [35]. This then permits a slower secondary phase of continuous adsorption of biomolecules present in saliva. These two phases of protein adsorption can be viewed as two distinct zones under electron microscopes: one as a primary electron dense basal layer, and the second, an outer globular layer, porous in nature [32, 36]. It is believed that the dense basal layer consists extensively of proline rich proteins (PRPs), whereas the outer globular, porous structure contains a combination of mucins and protein aggregates. However, other components foreign to saliva also influence pellicle formation and structure. For example, it is thought that the effects of eating certain foods and/or the use of certain oral hygiene products may alter the structure of the pellicle. Some components of toothpaste (e.g. sodium tripolyphosphate (STP) and Sodium lauryl sulphate (SLS)) are known to remove some of the proteins from the AEP [37]. In addition, certain components of foods, such as calcium found in dairy products or the low pH of soft drinks, may change the structure of the AEP [33, 38, 39]. Unfortunately, the effects that these extrinsic factors have on the AEP remain to a large extent unknown. This review therefore sets out to help illuminate the significance of the pellicle by covering a brief history of the AEP; followed by its function: in terms of enamel protection; its formation: in terms of the thermodynamic aspects of protein bio-adhesion; Its composition: in terms of the proteins, carbohydrates and lipids that have been hitherto identified; and finally, its structure: in terms of thickness, mass and morphology.

History of pellicle exploration

Alexander Nasmyth is credited as being the first person to become aware that the surfaces of teeth were encapsulated with an organic pellicle. In the 1830's he observed that "...*detached portions of membrane floating on the surface of the solution in which human teeth had been submitted to the action of acid*", and described this membrane as "*the persistent dental capsule*" [40]. Later, this capsule was referred to as "Nasmyth's membrane" and was commonly believed to be of embryological origin. However, this was soon proved not to be the case, as in 1926, Chase [41] was able to show that organic films were present not only on enamel surfaces but also on surfaces of amalgam fillings and dentures. These findings indicated that Nasmyth's membrane could not be of embryologic origin and that the membrane on the enamel surface had to be accrued by other means. Sometime later in 1949, Frank [cited in, 42] described two types of enamel membranes. One was a prematurely formed membrane, which developed prior to tooth eruption, and was found to be rich in ameloblastic cellular remnants; whilst the other membrane coating only appeared after exposure of the tooth to the oral environment. These findings explain to a certain extent why some early authors [43, 44] exploring the enamel pellicle had been convinced by its embryological origins. Subsequently, it became accepted that embryologic integuments are lost after eruption of the teeth, and that these are replaced by an acellular, bacteria-free, protein rich membrane termed the "acquired enamel pellicle" an expression introduced by Dawes *et al.* in [45]. Subsequently, Hay [46], studied the adsorption of whole saliva to various forms of hydroxyapatite, including ground enamel. He found that the proteins removed from the surface of freshly extracted teeth had the same electrophoretic mobility as

saliva proteins adsorbed by the hydroxyapatite and enamel powder *in vitro*. This was significant; as it was now possible to hypothesize that the AEP that forms on tooth surfaces originates from precursors present in saliva. Over the years similar techniques were used to examine deposits on enamel via a variety of electrophoretic techniques [47, 48]. Observations from these studies permitted the identification of individual members of different salivary protein families and demonstrated the selective nature of salivary protein adsorption to the enamel surface; as only certain members of salivary protein families seemed to be involved in AEP formation. Today a number of *in vivo* [49, 50], *in situ* [51, 52] and *in vitro* [53, 54] experiments have been performed in order to tease out additional information about the nature of the AEP. Collectively, these studies have furthered knowledge about the structure, formation, composition and function of the AEP. However, they have also raised many more questions that still remain to be addressed. It is perhaps for this reason that the AEP is still an area of science that continues to stimulate a great deal of interest, one hundred and seventy four years after Nasmyth's first discovery.

Function of the acquired enamel pellicle (AEP)

The AEP appears to have a number of functions that primarily involve protecting the enamel surfaces of teeth. For example the AEP protects teeth from abrasive forces by means of lubrication; it is able to regulate demineralisation/remineralisation of calcium phosphate ions present in the enamel and helps neutralize acid produced by oral bacteria [12]. However, the function of the pellicle in protecting tooth enamel is somewhat ambivalent; this is because AEP also provides sites for the initial attachment of bacteria to the tooth surface, which is the first step in plaque formation. Therefore, AEP plays a major role in the interactions that take place at the tooth/saliva interface which are important both physiologically and pathologically [55].

Lubrication of tooth surfaces

Lubrication can be defined as an attribute of a substance that reduces friction between two moving surfaces; in this case, oral surfaces. The AEP provides lubrication for teeth that facilitates speech, mastication and plays a key role in the sensory perception of food and food components [56]. Without suitable lubrication, damage to teeth and epithelial surfaces in the mouth occur, as a result of excessive wear between surfaces (i.e. tooth/tooth or tooth/mucosae abrasion). Evidence of the importance that lubrication plays can be seen in individuals who suffer from Xerostomia (i.e. hyposalivation)[57]. Without adequate saliva in the mouth, functions such as speech, mastication and swallowing become difficult to perform and if left untreated over time impairment of oral health is likely to occur. For

example, onset of dental caries, mucous membrane damage or dental wear are all conditions that are more likely to occur in individuals who hyposalivate [58]

The lubricative properties of the AEP have been attributed to several salivary proteins, including mucins, statherin, amylase, proline-rich glycoproteins and acidic proline-rich proteins [39, 59, 60]. Early studies found that MUC5B was a better lubricant than MUC7[61]. However, proteins do not always behave the same *in vitro* as they would *in vivo* and so the lubricating properties of salivary proteins are heavily dependent on the method and model surfaces used [62]. Consequently no straightforward correlations have yet been made between viscosity, protein adsorption and lubrication [56]. For example, early studies suggested that lubrication depended upon viscosity of saliva as well as the physical properties of the adsorbed surface [63, 64]. However, experiments by Aguirre *et al.* [61] observed that while the viscosity of Submandibular/sublingual saliva was almost double that of PS, there was little difference in lubrication between the two, which suggests that lubrication and viscosity at the tooth surface are independent of each other. Later, Douglas *et al.* [65] showed that statherin functions as an important boundary lubricant in the pellicle perhaps as a consequence of its amphipathic nature. Evidence for the importance of the amphipathic nature of molecules for lubrication was also shown by Reeh *et al.* [66]; whereby friction between opposing tooth surfaces was reduced by amphipathic molecules. These studies suggest that perhaps the configuration of proteins maybe the key characteristic for the lubricant properties of AEP.

The mechanisms of salivary lubrication have been quantitatively measured by means of a reduction in the coefficient of friction [see 66 for more details]. Using this

method Berg *et al.* [59, 67] monitored the lubrication effect of salivary proteins between silica surfaces, using AFM. They found that the presence of adsorbed salivary pellicles between hard surfaces reduced the friction coefficient by a factor of 20 when compared to a NaCl solution. It appears that the salivary proteins which adsorb onto enamel permit surfaces to slide over each other with a reduced friction as a result of repulsive van der Waal forces between opposing salivary films. All of these studies briefly touched upon suggest that the pellicle layer rather than the bulk salivary fluid is of more importance to lubrication than previously thought [68].

Semi permeable membrane & mineral homeostasis

The pellicle acts as a semi permeable barrier, which helps maintain the structure of the enamel surface by preventing demineralisation and/or facilitating enamel remineralisation. At neutral pH (7.0) saliva is supersaturated with respect to calcium and phosphate ions[69]. If the pH of saliva surrounding the tooth is lowered (increasing H^+ ions) it ceases to be supersaturated as the H^+ ions react with (PO_4^{3-}) or (OH) ions in the saliva reducing their concentration. This is important because the demineralisation of hydroxyapatite in the enamel is governed by the law of mass action, so that the loss of calcium and phosphate ions present in saliva is directly related to the loss of calcium and phosphate ions in teeth. In other words, as the saliva becomes less saturated with calcium phosphate, as a consequence of low pH, the hydroxyapatite in enamel disassociates to counteract the change. Thus, hydroxyapatite is not attacked directly by H^+ ions but simply responds to a shift in ion concentrations in the saliva; so as long as the tooth surface is in an acidic environment that is undersaturated with respect to calcium and phosphate, the tooth will dissolve. Interestingly it is actually water that is responsible for disrupting the

crystal lattice bonds of hydroxyapatite by reducing the attractive forces between calcium and phosphate ions [see 70 for more details].

Mostly small chain acids (*e.g.* formic, lactic, acetic, and propionic acids) produced by bacteria when exposed to fermentable carbohydrates are responsible for demineralising the enamel [71]. However, AEP is able to behave as a semi permeable membrane which permits it to manage acid diffusion and transport of calcium and phosphate ions into and out of the enamel surface slowing down the demineralisation of enamel in acidic environments and promoting remineralisation in basic/neutral environments [72, 73]. Further evidence supporting the role of AEP as a protective film against acid erosion has come from a number studies. For example, an electron microscopic study demonstrated that the presence of a salivary pellicle drastically reduced erosion of enamel by an acidic cola drink [74]. Amaechi *et al.* [75] also found that a 60-min *in situ* formed pellicle layer gave some protection to the enamel surface against the erosive challenge of orange juice, and Hannig *et al.* [14] found that even a 3-min *in situ* formed pellicle layer provides some protective effect on the enamel surface against citric acid attack. More recently Hannig *et al.* [38], showed that during consumption of acidic beverages *in situ*, the erosive effects on pellicle coated bovine enamel were modest and that orange juice seemed to be less damaging when compared to low pH cola beverages. However, it is not only the semi permeable structure that is responsible for the protective nature of the pellicle but specific components of the pellicle also contribute to the shielding of the enamel surface from a hostile environment.

Bacterial adherence

As briefly mentioned the nature of AEP is not solely protective in its nature and is in fact somewhat ambivalent in its defence of tooth enamel. For example, several pellicle components such as, proline-rich proteins, mucin MG 2 and fibrinogen serve as specific receptor sites for bacterial adherence [68, 76]. These salivary proteins present epitopes or peptide sequences on their surface that are recognized by a variety of antennae systems on the bacterial cells (i.e. pili, fibrils and fimbriae). *Streptococcus soralis*, *S. sanguis* and *S. mitis* account for 80% of primary colonizers [77]. This Initial bacterial adhesion passes through a phase of weak and reversible binding before an irreversible attachment is established [78]. Over time this initial layer is subsequently displaced by anaerobic bacteria such as, *S. mutans*, *S. sobrinus*, and *Lactobacilli* [79]. These bacteria are responsible for the fermentation of carbohydrates in food and subsequent production of organic acids in the oral environment; this can result in a decrease in pH and potentially promotes tooth demineralisation. Conversely, certain bacteria in dental biofilms may lessen the effects of acid-producing bacteria. For example, *Veillonella* metabolises lactic acid produced by some bacteria; and *S. salivarius* contain urease that produces ammonia compounds, which can raise the pH of the saliva, thus delaying tooth demineralisation [71]. Interestingly, Comelli *et al.* [80] found that bacterial strains used in the dairy industry such as *S. thermophilus* and *Lactobacillus lactis* ssp. *lactis* were able to integrate into a biofilm present on a hydroxyapatite surface and to interfere with development of the cariogenic species *S. sobrinus*. This is important, as it shows that the AEP may not only be manipulated by components native to the oral cavity but can also be affected by factors of non salivary origin, such as the ingredients found in food.

Formation of the AEP

The AEP is an organic pellicle on the tooth surface formed by selective adsorption of mostly salivary proteins derived from the continuous exposure of enamel to whole saliva [81]. The formation of this pellicle is considered to be a selective process, as only a limited number of the proteins that have been detected in whole saliva are found to reside in the AEP [22]. Currently, phosphor-proteins such as, acidic proline rich proteins (aPRPs), histatin and statherin are the main salivary proteins thought to play an important role as pellicle precursor proteins (PPPs). As such, these proteins have been widely studied with respect to their ability to adsorb onto enamel surfaces and thus influence early pellicle formation [1, 82].

The adsorption of proteins required for pellicle formation is influenced by a number of variables inherent to the individual, making it difficult to elucidate the respective roles that pellicle proteins play in AEP formation. For example, protein adsorption will be affected by factors such as an individual's circadian cycle, the location of teeth in the mouth and the tooth's physical (e.g. surface roughness) and chemical (e.g. hydrophobicity of enamel) properties [35, 83-85]. Therefore numerous methodical approaches have been designed to explore AEP formation. For example, *in vivo* studies have been used where the pellicle is scraped off of the tooth surface [86]; *in situ* studies, where enamel, often bovine, is exposed in the oral cavity [72]; or *in vitro* studies, where different dental components are exposed to collected saliva extra-orally [87]. Although data from these studies are not always comparable, as a consequence of diverse methodologies, it is generally accepted that the basic rate determining steps of AEP formation comprise the following steps:

1. Diffusion of salivary proteins towards the enamel surface,
2. Attachment of proteins to the enamel surface,
3. Potential conformational changes and cross-linking of proteins
4. Potential detachment from the enamel surface and transport away from the tooth

In explaining these rate determining steps, researchers have emphasized the nonspecific physicochemical mechanisms of adhesion [88]. This involves either a thermodynamic model (see Figure 1.0.) or mathematical models such as the Derjaguin, Landau, Verwey, Overbeek (DLVO) principle, in which protein adhesion is regarded as the total sum of Van der Waals, acid–base, and electrostatic interactions[See 89 for more details]. Although these electrostatic interactions are imperative in the binding of proteins to solid surfaces, protein adsorption is driven by an increase in entropy [90]. In other words, the formation of the AEP can be directly related to the second law of thermodynamics. This states that the tendency in nature is toward ever-greater disorder in the universe, a law that initially appears to be somewhat unrelated to describe AEP formation. However, by referring to Gibbs's law of free energy (equation 1) it is possible to see how the second law of thermodynamics directly affects protein adsorption at the tooth– saliva interface.

Protein adsorption, and thus AEP formation, will occur spontaneously if more energy is released in a system than gained, either by a gain in entropy (disorder) or a decrease in enthalpy (heat), respectively [91]. For the formation of AEP, an increase in entropy is central as the changes in enthalpy at high coverage of tooth surface are

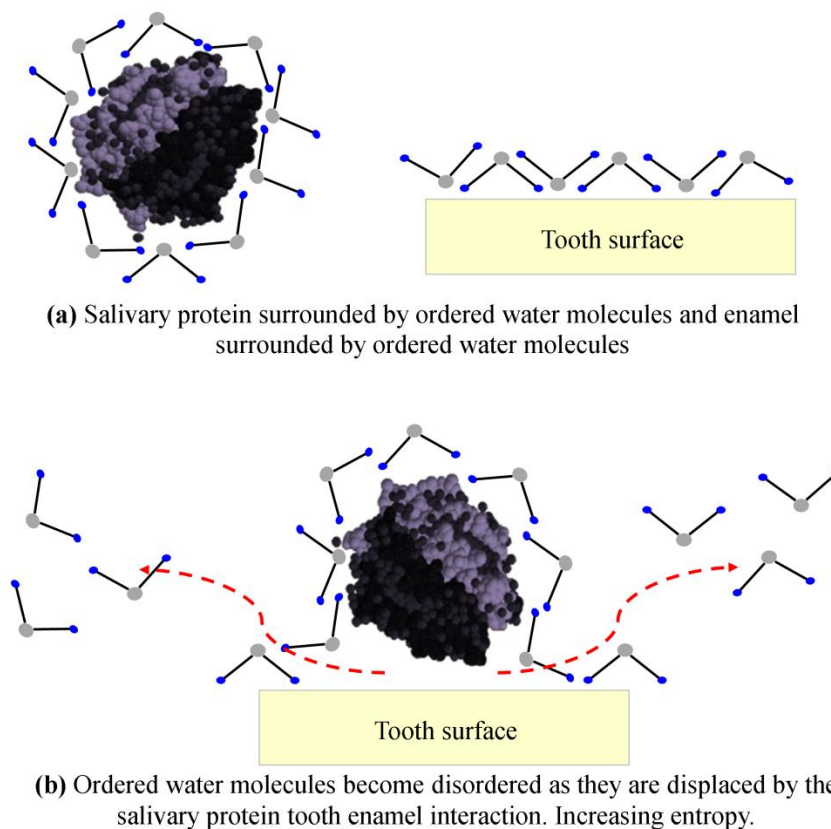
negligible [92] . Where, G = Gibbs free energy, H = enthalpy, T = absolute temperature, S = entropy and Δ_{ads} = net change of the thermodynamical parameters.

Equation 1. Gibbs's law of free energy

$$\Delta_{\text{ads}}G = \Delta_{\text{ads}}H - T \Delta_{\text{ads}}S < 0$$

The increase in entropy, and thus the driving force of protein adsorption in the above equation, is displayed graphically in Figure 1.0.

Figure 1.0. Release of ordered water molecules drives the formation of protein adsorption to enamel. In (a), a salivary protein and an enamel surface are shown surrounded by ordered water molecules, which represent a low entropy system. (b) then shows how adsorption of the salivary protein to the tooth enamel surface releases some of the ordered water molecules surrounding them. This increase in entropy provides the thermodynamic push toward protein adsorption and consequently formation of the AEP.



Studies have shown that there are a small group of salivary proteins that show an increased selective adsorption to enamel over other proteins found in saliva. These include acidic PRPs, statherin and histatins, also known as pellicle precursor proteins (PPPs) [26, 93]. When PPPs adsorb to the surface of teeth, they appear to undergo a conformational change, whereby they increase their cross-sectional area and provide a fast coverage of the tooth surface [94]. This occurs because there is a driving force for the reduction of excess surface energy on the tooth surface; somewhat analogous to when a liquid forms a spherical drop to reduce excess energy by reducing its total interfacial area [95]. Obviously the tooth is unable to adopt a spherical shape as it is a solid; however, the driving force (i.e. reduction of surface energy) is the same, and thus the solid tooth overcomes its high surface energy via the adsorption of proteins, rather than the energetically favourable shape change seen in liquids. Despite these somewhat abstract theories (Gibbs free energy/surface energy) used to describe protein adsorption to tooth enamel, formation of the AEP can be thought of more tangibly as taking place in two stages. The first stage being characterised by a rapid adsorption of proteins to the enamel surface (proteins with a high diffusion coefficient and high affinity for hydroxyapatite), followed by a second, slower phase, due to larger components, such as larger proteins and aggregates with a lower affinity for hydroxyapatite.

The initial stage of pellicle formation can be visualised as an electron dense basal layer observed via transmission electron microscopy micrographs Hannig [35]. They showed that the dense basal layer of the AEP starts to form within seconds taking between 2 - 3 minutes to complete, reaching an estimated thickness of 10 - 20 nm, where it remains for about 30 minutes. The rapid first stage of AEP formation is

followed by a slower second phase, whereby pellicle thickness is increased by continuous adsorption of biopolymers from saliva. However, rather than a continued adsorption of single PPPs, studies have now shown that micelle like globules and heterotypic complexes, together known as supramolecular pellicle precursors (SPPs), maybe responsible for the second stage increase in pellicle thickness. This is because SPPs are structurally much larger than individual PPPs and are therefore more likely to be responsible for the increase in thickness of the AEP. Evidence to support this comes from the similarities that are shown to exist between the amino acid profiles of SPPs and the amino acid profiles of 2 hour *in vivo* AEP [96]. This has also been confirmed by electron microscopic investigations of *in situ* pellicles, showing globular structures of 80–120 nm in diameter [97].

Under *in vivo* conditions the AEP is continually exposed to proteolytic activity of enzymes (of bacterial origin) which could potentially be important for the development of the pellicle structure over time [21]. In addition, other enzymes such as amylase, glucosyltransferases and lysozyme are a few of the active enzymes that have been detected in the pellicle that may affect the AEP [98]. Furthermore, in a recent study by Hannig [27], amino transferase and alanine amino transferase were also found in active conformations after only 3 minutes of pellicle formation. These enzymes are important as they may influence AEP formation by complexing adsorbed molecules [99] and/or by influencing enzymatic cross-linking of pellicle proteins [100]. Although a full comprehension of the role that active enzymes play in AEP is yet to be fully understood, they do give an appreciation of how AEP can behave as a dynamic film due to the continuous remodelling of adsorbed pellicle

proteins via these enzymes. However, the dynamic nature of the AEP also makes it difficult to characterize the *in vivo* formation of AEP.

Composition of the AEP

Elucidation of the composition of AEP remains relatively obscure as a consequence of the minute quantities of pellicle that can be collected from the tooth surface. These amounts have been estimated at approximately 1.0 μg per labial tooth surface, a quantity that makes it difficult to analyse under standard chromatographic techniques [20]. In addition, it can also be difficult to selectively remove pellicle material from tooth surfaces without contaminating it with salivary secretions and bacteria, which can result in erroneous analysis of pellicle composition. As a result, a number of studies have been performed through the incubation of saliva with hydroxyapatite powder [87, 101] or hydroxyapatite plaques [28, 82] under *in vitro* conditions in order to imitate the formation of AEP *in vivo*. These *in vitro* studies have provided valuable information on the way certain salivary proteins can display different affinities for hydroxyapatite surfaces and thus give clues as to which proteins are likely to adhere to tooth surfaces. However, these methods are not completely reliable as a number of studies comparing *in vivo* enamel pellicles with *in vitro* hydroxyapatite pellicles found that the electrophoretic characteristics and amino acid profile differed significantly between the two surfaces [20, 86]. Yao *et al.* [20] also found that the pellicle appeared to undergo extensive enzymatic changes *in vivo*, as a greater number of intact proteins had been found in *in vitro* pellicles when compared to *in vivo* pellicles. This highlights how AEP, under *in vivo* conditions, is not a static structure but is in a state of dynamic equilibrium with the surrounding saliva. The AEP should therefore be viewed as an ever-changing, dynamic film that shows continual adsorption and desorption of bio-molecules and is very sensitive to changes in its environment [102]. For example, Rykke and Sonju [103] found that pellicles

formed for 24 hrs when food and beverage intake was avoided were similar; whilst pellicles formed for 24 hrs when subjects consumed a normal diet, exhibited significant differences. This suggests that even the components of food can modify *in vivo* pellicle composition. Furthermore, the proteolytic activity of enzymes present in saliva also contribute to changes in pellicle composition via their inherent enzymatic functions and by providing sites for bacterial adherence [104]. In fact, the effect of enzymes on pellicle composition is multifactorial, as they also have relevance as structural pellicle constituents [99]. For example, the enzymes alpha-amylase and lysozyme have been shown to be integral parts of salivary micelle like globules that are believed to contribute to pellicle formation [97, 105]. This has been supported by electron microscopic investigations of *in situ* pellicles, showing globular structures of 80–120 nm in diameter [28]. In addition, pellicle composition may differ from where it is collected in the mouth. For example, Vacca Smith & Bowen [82] showed that the overall protein composition of *in vivo* formed pellicles displayed characteristics typical of the saliva prevailing in the area of the mouth where the pellicles were formed. Transmission electron microscopic and confocal laser-scanning microscopic studies of *in situ* pellicles have shown that pellicles formed on buccal sites are thicker than those formed on palatal sites and are therefore more likely to differ in composition [35, 75]. In addition to the enzymes within secretions of different salivary glands, Kajisa *et al.* [106] and Boackle *et al.* [107] both suggest that gingival crevicular fluid, serum, bacteria, mucosal tissues, epithelial cells and fluids from the respiratory tract should also be regarded as possible sources for pellicle-immobilized enzymes. Therefore, the maturation of AEP and subsequent exposure to enzymes and components within saliva over time is likely to lead to modifications of adsorbed molecules within the AEP, resulting in compositional changes of AEP over time.

Furthermore, Zimmerman *et al.* [108] also showed that there can be differences in the proteome of deciduous teeth compared to permanent enamel; again, highlighting the difficulties surrounding the identification of AEP proteins. None the less Mass Spectrometry (MS) techniques and database search algorithms are constantly improving [109]; and if used correctly [110], are powerful methods in the identification of pellicle proteins.

Protein composition of AEP

Early compositional analysis of AEP using histo-chemical staining techniques suggested that it was mainly proteinaceous in nature. Such results were confirmed by the observation of Dobbs [111] and later Meckel [112] who found that pellicle was lost upon incubation of teeth with proteolytic enzymes. A number of other different techniques have since been used to expose the composition of AEP, via chromatographic, electrophoretic and immunological techniques. Most of these studies showed that the most abundant components of the pellicle are proteins, glycoproteins, enzymes, and mucins [36]. For example, several authors have identified the presence of mucins MG1 and MG2, amylase, albumin, IgA, S-IgA, proline-rich proteins (PRPs), cystatins, lysozyme, carbonic anhydrase, lactoferrin and histatins as major pellicle components [23, 87, 113].

Improvements in methods of mechanical and chemical removal of pellicle have also made it possible to selectively harvest AEP from the tooth surfaces *in vivo*. The tooth surface is either swabbed with a polyvinylidene fluoride membrane filter soaked in 0.5M sodium bicarbonate [114] or rubbed with a foam sponge soaked with 2% sodium dodecyl sulphate [115]. Using these methods Yao [22] identified components

in pellicle included histatins, lysozyme, statherin, cytokeratins, and calgranulin; whilst Carlen [116] was able to reveal that proteins in plasma, such as fibrinogen, albumin and IgG were also incorporated in experimentally formed pellicles.

Other developments have seen improvements in mass spectrometric techniques which have allowed characterisation of peptides to femtomole levels. For example, Siqueria [50] used - Liquid chromatography electrospray ionisation tandem MS - to identify 130 pellicle proteins, of which 89 were found in three of the five experiments, suggesting a degree of uniformity between different pellicles. Vittorino *et al.* [26] used- Matrix assisted laser desorption ionisation time of flight MS- to identify more than 90 peptides/proteins in AEP. The majority of the identifications corresponded to peptide/protein fragments belonging aPRPs, basic PRPs, statherin, cystatins and histatins. Further progress in the elucidation of the composition of *in vivo* pellicle has been achieved by using indirect detection methods, such as the use of immunological assays to identify AEP components [22]. These techniques have also provided evidence for the presence of alpha-amylase, lysozyme and statherin as components of the acquired salivary pellicle [60, 117]

Lipid composition of AEP

Information pertaining to lipid composition of the AEP is very limited even though Slomiany *et al.* [118] reported that lipids account for 22-23% of the dry weight of pellicle. They found glycolipids and neutral lipids and phospholipids. However, only the presence of phosphatidylcholine has been confirmed by other researchers Kautsky & Featherstone [119]. Despite the scarcity of data surrounding the lipid composition of AEP, it is potentially an area of interest to oral hygiene. This is

because in 1990, Slomiany *et al.* [120] found that the interaction of salivary phospholipids with enamel may influence the susceptibility of the tooth surface to demineralization by acids produced by plaque. Although only limited information is available about the nature of lipids in the pellicle, current work carried out in 2012 by Reich *et al.* [121] suggests a new technique for the determination of the fatty acid profile of the pellicle, which has the potential to shed new light on the lipid profile of the pellicle.

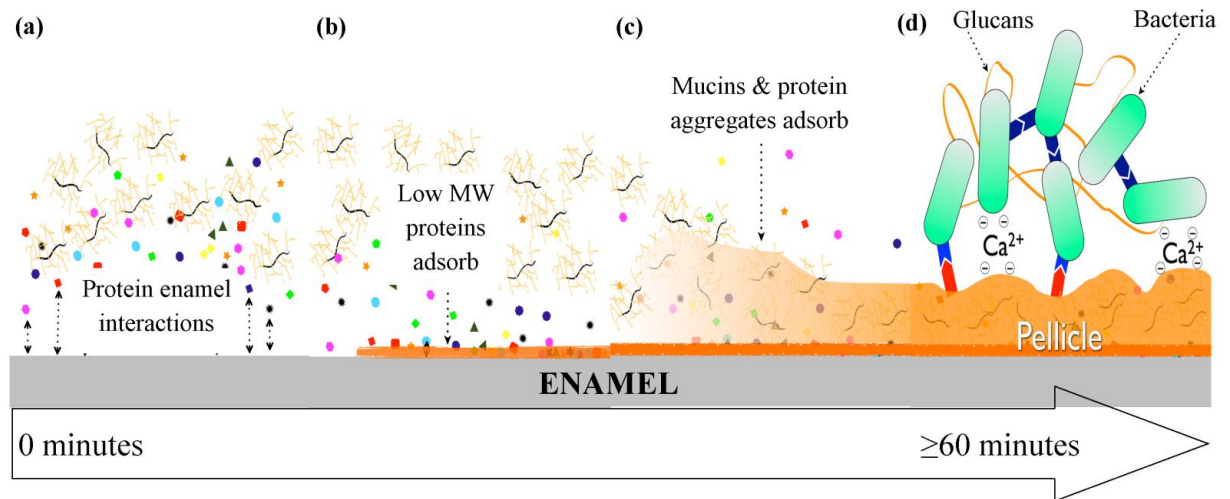
Carbohydrate composition of AEP

As with lipids, studies relating to the carbohydrate composition of pellicle are scarce and rather dated. In 1975, Sonju [122] reported that the pellicle contains several sugars of which glucose dominates (67%) with traces of glucosamine (18%); galactose (9%) and mannose (6%) also present. Mayhall & Butler [123] suggested that the glucose sugar was likely to originate from glycoproteins, whilst Slomiany *et al.* [118] believed that glycol-lipids may be partly responsible for the high proportion of the glucose monosaccharide found in the pellicle. However, Hannig & Joiner [68] proposed more recently that the origin of glucose is much more likely to be as a consequence of adsorption of glucans, bacterial in origin. Unfortunately, the inter-relationships between all these components (e.g. proteins, peptides, lipids and carbohydrates) and how they are structurally organised on the tooth surface has yet to be clarified.

Structure of the AEP

Hitherto a complete understanding of the three dimensional structure of *in situ* formed AEP has not yet been fully characterised; even though significant inroads are being made. Current knowledge of the surface structure of AEP has been founded upon microscopic investigations such as SEM, TEM and AFM [28-30, 113]; whereas the structural physical properties (i.e. mass, thickness and density) of the AEP have been investigated using QCMD, DPI and ellipsometry [33, 34, 124]. These investigations generally reveal a pellicle that is composed of a tightly adsorbed electron dense basal layer and a loosely arranged outer globular layer. Rupp *et al.* [125] observed a two-step adsorption process that may indicate the structural heterogeneity of the salivary pellicle between a dense basal layer and a more hydrated outer layer. It was suggested by Skjorland *et al.* [126] that these dense and hydrated layers were due to compositional differences between the two stages of pellicle formation (see Figure 1.1.).

Figure 1.1. Current proposed outline of pellicle formation: (a) initial salivary protein adsorption occurs rapidly, followed by; (b) the formation of a dense basal layer. Subsequently, (c) protein aggregates and mucins adsorb to form a more globular outer layer, when finally (d) bacteria adsorb and colonise the outer pellicle. Initially the pellicle provides a protective barrier for teeth, preventing enamel abrasion and demineralisation. However, over time the pellicle becomes the primary site for the attachment of acid producing bacteria.



Early electron microscopy analyses of pellicle displayed an irregular and rutted morphological pattern on the pellicle's surface [127, 128]. This was also seen on more recently performed SEM and AFM studies which showed that the surface of the *in vivo* formed pellicle has a structure similar to a sponge like matrix, made up of a network of spherical like particles [28, 29]. The diameters of these particles was shown to be between 10nm and 20nm after a few minutes of pellicle formation, whereas after 2 hours of pellicle formation diameters of adsorbed proteins were shown to be between 20nm and 60nm [28]. These studies also showed that palatal formed pellicle displays an uneven surface characterized by an intricate network of 20nm to 40nm wide tentacle like structures that interconnect larger globules between 60nm and 150 nm in diameter. The reason for these differences in pellicle thickness remains uncertain, however, it has been suggested that factors acting locally in the mouth, such as shearing forces of the tongue and differing supply of salivary components at different locations of the mouth may be responsible for the assorted

pellicle thicknesses seen on tooth surfaces. However, Sonju Clasen [129] provided evidence that the action of the tongue does not influence pellicle thickness or its structural appearance; and therefore, differences in pellicle thickness are more likely to be related to the varying supply of salivary components in different regions of the oral cavity. This is because salivary glands produce secretions that are made up of many different types of proteins with varying molecular weights at different concentrations that can vary significantly between glands [130]. For example, the parotid gland produces watery, serous saliva essentially devoid of mucins, whilst submandibular and sublingual glands produce viscous saliva that is rich in mucins. Consequently, certain salivary glands have the potential to bathe teeth with distinctly different secretions depending on the location of teeth in the mouth. For example, upper posterior buccal molars are likely to receive a continuous flow of components from parotid saliva, whilst lower anterior lingual incisors are likely to receive a continuous flow of components from submandibular and sublingual glands. How these differences affect pellicle thickness however is still uncertain. As apart from differences between secretions of certain salivary glands, it is known that the composition of saliva also depends on circadian cycle, sex, age, diet and general health of an individual, all of which is also likely to affect the structural differences seen in pellicle samples [131].

In 2009, Hannig *et al.* [38] studied the pellicle structure *in situ* using bovine enamel slabs fixed onto a tooth surface and found that the electron dense layer had a thickness of $\approx 5\text{nm} - 30\text{ nm}$. This layer was then covered by a less dense globular structure of variable thickness. For example, the thickness of globular structures on the 1st molar ranged between 100 nm and 500 nm on the buccal surface; and 20nm –

40 nm on the palatal surface. They also estimated that the thickness of the globular structures on incisors was 100nm on the labial surface and 20nm – 40 nm on the palatal surface. Furthermore, in the mandible pre-molars the buccal pellicles were 300 nm in thickness, whilst the lingual pellicles were between 20– 40 nm. As with previous studies they also concluded that the structure of pellicle is indeed dependent on the site of formation. This is important because variations in pellicle thickness and composition may influence early bacterial attachment and subsequent tooth-related diseases in various parts of the mouth [132]. For example, it is possible that a thick, continuous pellicle has the potential to play a significant role in protecting underlying enamel acting as a diffusion barrier inhibiting the demineralization of enamel [75]. Furthermore, the pellicle thickness and structure may be important for the lubrication of tooth surfaces [133] and may also alter its function as a semi-permeable membrane to ionic conductivity, which is important for remineralisation of enamel surfaces [134].

Food components that influence the AEP

The adsorption of salivary components on tooth surfaces during pellicle formation has been shown to be influenced by a number of dietary components [82, 135, 136]. For example, Vacca Smith & Bowen [82, 136] showed that rinsing hydroxyapatite discs with milk as well as rinsing with sucrose, sorbitol or xylitol caused changes in the composition and formation of the salivary pellicle. Early *in vitro* studies also showed that certain casein derivatives of milk can adsorb onto the tooth surface and integrate into the salivary pellicle in exchange for albumin [137]. Thus, certain dietary components may well be considered integral components of the pellicle. This is important because the pellicle provides binding receptors for a number of bacteria. Therefore, any modifications in the composition of the pellicle induced by dietary components are likely to alter its microbial binding preferences.

pH changes

The consumption of acidic beverages such as fruit juices and sports drinks are increasing in the western diet. This may be a problem, as consumption of these drinks has been linked with dental erosion. For example, *in vitro* and *in situ* studies have clearly demonstrated the erosive properties of soft drinks on tooth enamel [138, 139]. Although it is important to measure enamel loss in relation to consumption of acidic beverages, it is perhaps more important to assess the effect that acidic challenges have on the morphology and thickness of the pellicle layer itself; as it is the pellicle that has first contact with any acidic challenges. In an *in situ* study, Hannig *et al.* [38] showed that the consumption of erosive beverages removed

considerable amounts of the outer layer of the pellicle; but the basal layer remained unaffected (Cardenas *et al.* [140] showed that Mucin MUC5B may be responsible for the tenacity of the basal layer). This was considered important as protection against tooth erosion has been related to the thickness of the pellicle layer. For example, Amaechi *et al.* [75] showed an inverse relationship between the degree of enamel dissolution and the thickness of the AEP. However more recently it was shown that even a 3 minute *in situ* formed pellicle layer provides protection against citric acid attack that does not differ significantly from the protective effect of a 2 hour *in situ* formed pellicle [14]. Therefore pellicle thickness may not be as important in protecting tooth surfaces against acids as previously thought. Furthermore, the pH of a beverage is likely to be more relevant to the extent of erosive demineralisation of teeth *in vitro* than pellicle thickness [141]. Hannig [38] found that pellicle limits diffusion of acids to the tooth surface in a pH-dependent manner. For example, they found that orange juice (pH 3.8) had no effect on micro-hardness of pellicle coated enamel, whereas Coke Light ® (pH 2.85) did manage to cause a decrease in the micro-hardness of pellicle coated enamel; however, the calcium in the orange juice may have had a modulating effect on the erosive process [138]. This is an interesting point, as calcium may also alter the structure of the AEP.

Calcium changes

Phosphoproteins such as, acidic proline rich proteins (aPRPs), histatin and statherin found in saliva are thought to play an important role as pellicle precursor proteins. [1, 25, 36, 68, 82]. These proteins contain calcium binding domains that may serve to provide a region of high calcium concentration close to the tooth surface, thus facilitating the mineralisation of teeth. A number of studies have looked at the

interplay between the structure of the pellicle and the ionic composition of the saliva [142-146]. However, it is of particular interest to understand the role calcium ions play on pellicle structure, as calcium ions are thought to have a bearing on the attraction between pellicle proteins and the surface to which pellicle proteins adsorb [18, 144]. For example, Tanizawa *et al.* [143] showed that calcium ions were able to enhance pellicle formation onto hydroxyapatite surfaces via calcium bridging of proteins. Whilst Proctor *et al.* [39] showed that chelation of calcium from saliva caused a dramatic decrease in the mechanical properties of an adsorbed salivary film, consistent with the breakdown of pellicle structure. Ash *et al.* [33] also observed changes in the hydrated mass, polymer mass, thickness and polymer concentration of the pellicle for both WMS and PS formed pellicles when the natural calcium concentration of the respective salivas was increased from 0 mM to 10 mM. These studies provide information that help elucidate the mechanisms behind pellicle formation and structure.

Components of oral hygiene products that influence the AEP

It is well known that dentifrices used in conjunction with tooth brushing act to remove stains and discolorations as well as to reduce plaque and calculus deposits on teeth [147]. Certain basic ingredients such as, detergents (e.g. sodium dodecyl sulphate), abrasives (e.g. sodium carbonate), and fluoride are common to most dentifrices. These ingredients are added to dentifrices in order to remove stained pellicle from dentition and loosen deposits on tooth surfaces that may become cariogenic. Ideally, dentifrices should effectively remove stains and cariogenic bacteria from the tooth surface without excessive removal of the protective pellicle. *in vitro* and *in vivo* studies have shown that brushing with certain dentifrices significantly reduces the pellicle film thickness [148, 149]. Joiner *et al.* [150] showed that the thickness of a six hour *in situ* formed pellicle, followed by ten seconds of *ex vivo* tooth brushing with a toothpaste slurry, reduced the pellicle to a 1–30 nm basal layer. Confirming previous findings indicating that the basal pellicle layer has a higher resistance against abrasion compared to the outer globular layer [151].

The incomplete removal of the basal layer of the pellicle from the tooth surface is important, as this would suggest that it can continue to impart protection to enamel even after short tooth brushing cycles. Furthermore, Hannig *et al.* [14] found that even a 3-min *in situ* formed pellicle layer provides some protective effect on the enamel surface against acid attack; suggesting that even if the pellicle was completely removed by brushing teeth with a dentifrice, the rapid accumulation of pellicle on the tooth surface is likely to prevent any excessive damage occurring.

Other components of dentifrices that have been found to influence the formation of pellicle are chelants known as, condensed phosphates, that display strong reactivity to enamel surfaces, producing significant anti-stain and anti-calculus effects [152, 153].

The anionic condensed phosphates used in dentifrices have been shown to remove pellicle proteins that have become stained and can prevent the development of calculus [37]. Pyrophosphate was one of the first condensed phosphates used in dentifrices, demonstrating clinical efficacy in the prevention of dental calculus [154] and chlorhexidine promoted dental stains [155]. However, the efficacy of pyrophosphate is reduced over time, either by hydrolytic breakdown of its intermolecular bonds, or because it becomes displaced by re-adsorbing salivary proteins in the pellicle [156]. Consequently, longer chain variants of pyrophosphate (e.g. sodium hexametaphosphates, sodium tripolyphosphates or “polypyrophosphates”) have been developed in order to overcome the limitations of pyrophosphate as an intraoral cleaner [152]. This is mainly because condensed phosphates have more anionic phosphate bonds and more binding sites than pyrophosphate. Consequently condensed phosphates have a greater surface affinity for tooth enamel because they present more binding sites to the tooth surface. Subsequently they also display an increased retention and activity on the tooth surface as they can withstand hydrolytic challenge from pellicle enzymes for longer and thus continue inhibiting calculus formation or stain development for longer than the smaller chain pyrophosphates [157].

The safety of pyrophosphate salts in dentifrices are well established now [145] and today condensed phosphates are found in most dentifrices worldwide [158]. For example, Sodium tripolyphosphate, a linear condensed phosphate is used in many teeth whitening products which have been shown to be effective in removing stain *in vitro* [159]. Of particular interest is that the pre-treatment of teeth with STP has been shown to reduce the adsorption of both protein and stain by more than 50% [37]. This suggests that STP can modify the pellicle in such a way as to prevent certain proteins or chromogens from adsorbing. Baig *et al.* [160] suggested that the condensed phosphates do this by blocking sites on the enamel surface that have an affinity for certain chromogens; and that the condensed phosphates also have a higher affinity for enamel which may be responsible for the competitive desorption of chromogens. Therefore, unlike abrasives that physically remove pellicle proteins, condensed phosphates have the additional benefit of being able to alter the adsorption and desorption of pellicle proteins over time by altering the pellicle's physicochemical composition. This is important as cleaning teeth with dentifrices that contain condensed phosphates may prevent the adsorption of cariogenic bacteria and chromogens for longer than the smaller chain length pyrophosphates. Whilst SDS is known to remove pellicle proteins[30], and STP has been shown to be effective in the *in vitro* removal of stain [161]; the impact of SDS and STP on salivary pellicle structure has not been investigated or characterised in great detail.

Research Aims

As the pellicle is the primary interface between the oral environment and the hard and soft tissue of the mouth it plays an important role in oral physiological and pathological processes. For example, the pellicle serves as a protective barrier against acids that can damage teeth but also lubricates tissues in the mouth which helps to make the consumption and processing of food easier and tastier. Consequently, a deeper understanding of the structural changes that take place when the pellicle is exposed to different environments will help our understanding of the structural adaptation that the pellicle undergoes upon exposure to everyday food and oral hygiene products. This research sets out to determine the underlying mechanisms responsible for the formation and breakdown of the pellicle on hard tissue substrates; information that has implications for the development of more effective oral hygiene products and the potential generation of simulated salivas.

Experiments were designed to:

- Determine the role of mucins on the formation of the pellicle by comparing how whole mouth saliva and mucin free parotid saliva, form their respective pellicles.
- Determine the physical structure of the pellicle under varying calcium concentrations to establish the role calcium plays in pellicle formation.
- Determine the changes that the pellicle undergoes in the presence of an increasing acidic environment at pH concentrations commonly consumed in human diets.

- Determine the mechanisms by which detergents (i.e. SDS) and preservatives (i.e. STP) from dental hygiene products control the breakdown of the salivary pellicle
- Identify proteins that are present in the pellicle and identify proteins that are removed via SDS or STP

Chapter 2

Techniques used to Investigate the Formation, Structure and Composition of the Salivary Pellicle

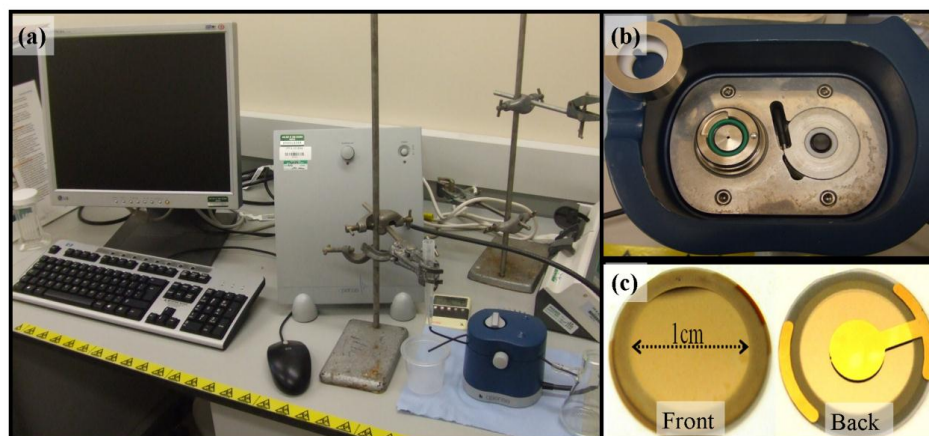
Introduction

The following description of the techniques used in this investigation of the salivary pellicle provides a concise coverage of the fundamental principles that lay behind each instrument operated during the course of this research. However, the exact details of most experimental procedures are to be found in the results chapters. The explanation of the techniques used will be described from the perspective of a non-physicist. Thus, equations, formulas and physical phenomenon that the instruments exploit to measure salivary pellicle structure and composition, will be explained in a way that makes the understanding of the instrumentation simple and accessible to undergraduate, post-graduate and post-doctoral researchers. The intention therefore, is to remove the mystery that lies behind these methods in order to give researchers who are interested in exploiting these techniques a running start with their research. In so doing this also demonstrates that the techniques carried out in this thesis have been understood and applied correctly.

Quartz Crystal Microbalance with Dissipation monitoring (QCMD)

The QCMD (see Figure 2.0.1.) is a technique that can be used to determine the mass and viscoelastic properties of adsorbed films [162]. The technique is based on changes in the frequency of an oscillating quartz crystal sensor when mass is adsorbed onto its surface. The oscillation of a quartz crystal is brought about by what is known as the piezoelectric effect [163]. A piezoelectric material is one that produces an electrical charge when a mechanical stress is applied (the material is squeezed or stretched); or conversely, a mechanical deformation is produced when an electric field is applied.

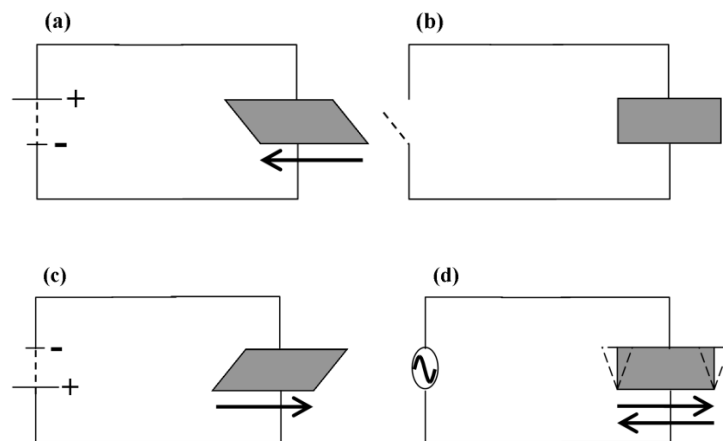
Figure 2.0.1. (a) Photograph of the QCMD fitted with a QAFC 302 axial flow measurement chamber. (b) Inner chamber of the QCMD where the sensor is placed on top of the green o-ring. (c) Photograph of gold coated QCMD sensors that sandwich the quartz crystal disc. The front of the sensor is where the proteins adsorb; and the gold electrode on the back of the sensors is where the electrical voltage is applied.



Quartz (which is a single-crystal form of SiO_2) is piezoelectric. However, because quartz crystals are also highly anisotropic (i.e. the mechanical deformation varies

greatly with crystallographic direction) it is important that the crystals are cut at a specific angle to the crystal planes. An AT-cut quartz crystal was used as the sensor, because at this cut the sensor oscillates in the thickness shear mode, the mode most sensitive to the addition or removal of mass (see Figure 2.0.2.).

Figure 2.0.2. Thickness shear mode oscillation of the QCMD sensor. Due to the piezoelectric properties of quartz, it is possible to excite the crystal to oscillate by applying an alternating flow of electricity across its electrodes at a frequency to which the crystal resonates (i.e 5MHz). When applying a direct current (DC) to the sensor it shifts the sensor in one direction (a). When the current is switched off the sensor returns to its original position (b). By reversing the flow of electricity the sensor will move in the opposite direction (c). Thus by applying an alternating current (AC) to the sensor (where the flow of electric charge periodically reverses direction) will result in the sensor oscillating left and right in what is known as the thickness shear mode (d).



Change in the frequency of the oscillating sensor to calculate mass

Changing the mass of the sensor (by adsorbing material to it) will change its resonant frequency. Changes in the resonant frequency of the oscillating sensor can then be related to changes in mass adsorbing on to the quartz surface through the Sauerbrey relationship [164].

Equation 2.1. The Sauerbrey relationship

$$\Delta m = -\frac{\rho_0 v_0}{2 f_n^2} \Delta f$$

Where Δm is change in adsorbed mass (ng cm^{-2}), ρ_0 is the density of the quartz crystal (2650 kg m^{-3}), v_0 is the shear velocity in quartz (3340 m s^{-1}), f_n is the resonant frequency (5.0 MHz), and Δf is the actual change in frequency recorded by the instrument. The Sauerbrey relation is valid for rigid, evenly distributed, and thinly adsorbed layers. However, for viscoelastic films, the Sauerbrey relationship underestimates the hydrated mass and thus another method of analysis is needed to fully characterise such a film. Therefore, in addition to recording frequency changes, the QCM-D measures a second parameter known as Dissipation (D).

Measuring change in dissipation to determine viscoelasticity

Dissipation (D) is inversely proportional to the decay time (τ) and resonant frequency (f) of the oscillating sensor as follows:

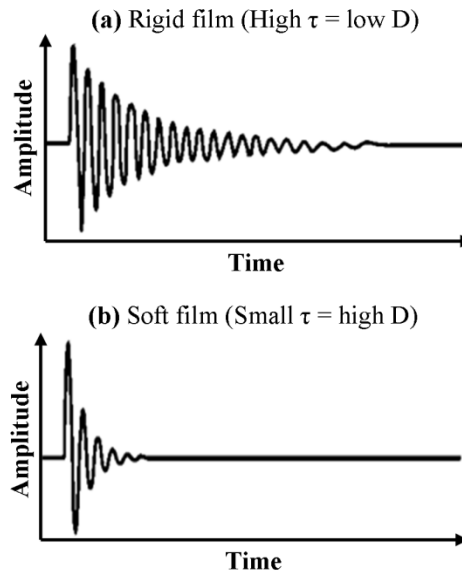
Equation 2.2. Dissipation relationship to Frequency

$$D = \frac{1}{\pi f \tau}$$

The instrument measures the decay time (τ) by stopping the current to the crystal sensor and allowing the crystal to freely oscillate to a standstill. The decrease in the amplitude of the oscillation with time is dependent on the viscoelasticity of the adsorbed layer. This is because the more elastic and rigid the adsorbed layer on the sensor surface is, the longer it takes for the sensor to stop oscillating. Conversely, the more viscous the adsorbed layer on the sensor surface is, the less time it takes for the

sensor to stop oscillating (see Figure 2.0.3.).

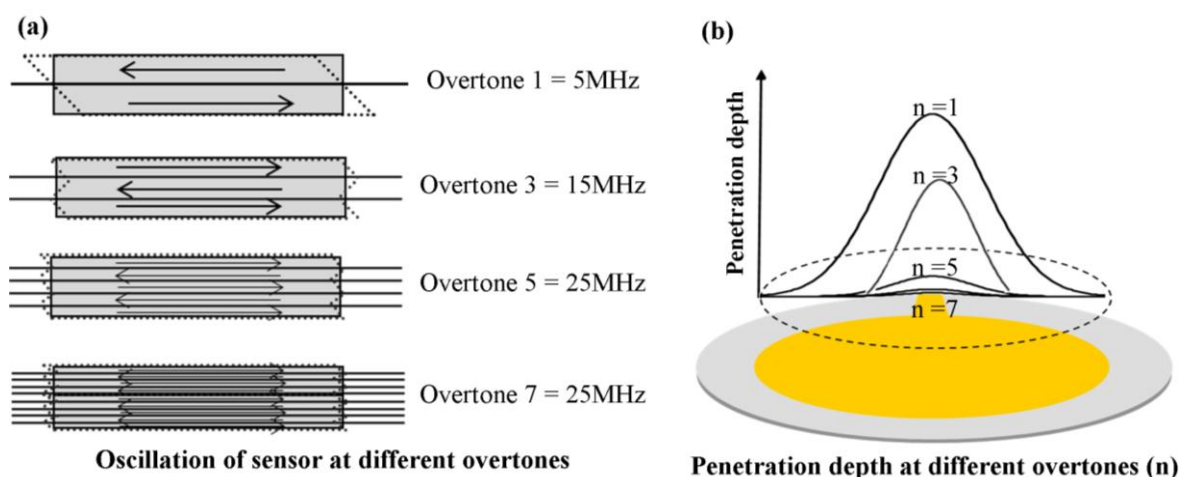
Figure 2.0.3 An example of dissipation differences between (a) an elastic film and (b) a more viscous film



So far it has been observed that Δf and ΔD can be used to measure adsorbed mass and viscoelasticity respectively. However, at the fundamental frequency (i.e. the lowest frequency at which the crystal sensor resonates/vibrates (5MHz) only the top layer of the adsorbed layer is disturbed. Consequently measuring the Δf and ΔD at this frequency alone, only gives a sense of the physical properties of the upper, outer layer of the film. This is because the detection range away from the sensor surface decreases with increasing overtone number. In other words, low frequencies of oscillation monitor the events at the top of the film furthest from the sensor surface, whilst higher frequencies of oscillation monitor the events closer to the bottom of the film nearest to the sensor surface (see Figure 2.0.4.). This is important because different overtones are measuring different parts of the layer and can therefore give information about the homogeneity of the adsorbed layer. Therefore, assuming that the adsorbed film has a uniform thickness and density the instrument combines frequency (f) and dissipation (D) measurements from multiple harmonics

(overtones), which can be used to extract unknown parameters (i.e. thickness, hydrated mass and viscoelasticity) of the adsorbed film when applied to the Voigt model for viscoelasticity[165].

Figure 2.0.4. (a) The QCMD sensor oscillates at different frequencies (or overtones). This results in a decrease in the detection or penetration depth of the film at increasing overtones of the oscillating sensor. (b) Plan view of the sensor and penetration depth at different overtones.



Voigt model for viscoelasticity

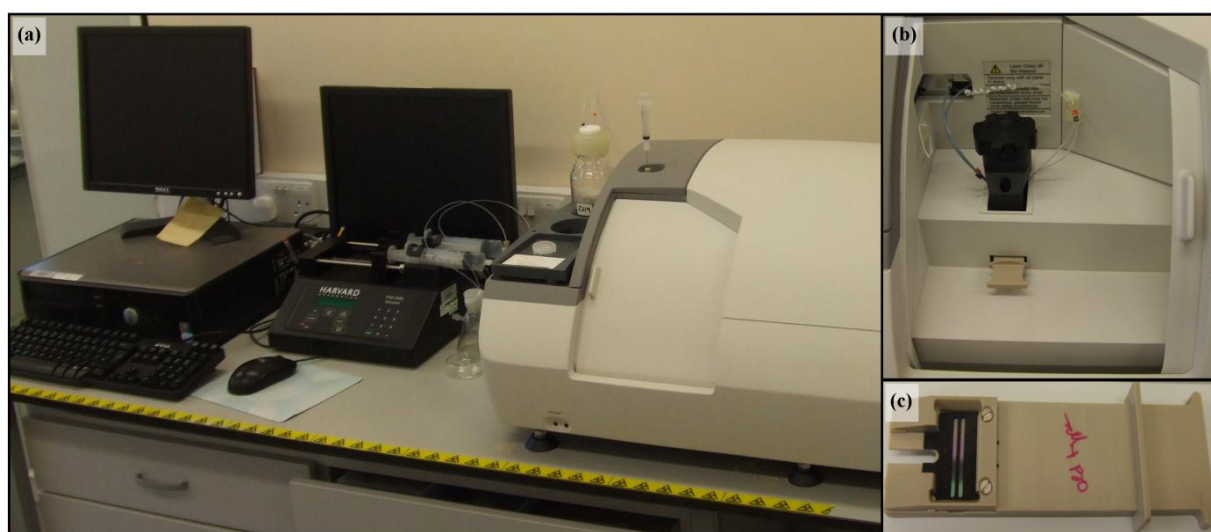
The QCMD instrument comes equipped with a software package to model the thickness and viscoelastic properties of the adsorbed layers. The QTools package is based on either the Maxwell or Voigt model for viscoelasticity. It is the latter of these models that is most commonly employed for modelling viscoelastic layers as it is applied for polymers that conserve their shape and do not flow. The work by Voinova *et al.* [165] used this model to derive a general solution of a wave equation to describe the dynamics of viscoelastic polymer materials adsorbed on a quartz crystal chip. The QTools package incorporates the solutions from this work that describes the changes in frequency and dissipation when a single viscoelastic layer is adsorbed from a Newtonian liquid. In short, the Voigt model tries to account for the

viscoelastic behaviour of an adsorbed film, and thus more accurately estimates the adsorbed hydrated mass for this type of film compared to the assumption of a purely elastic film by the Sauerbrey model.

Dual Polarisation Interferometer (DPI)

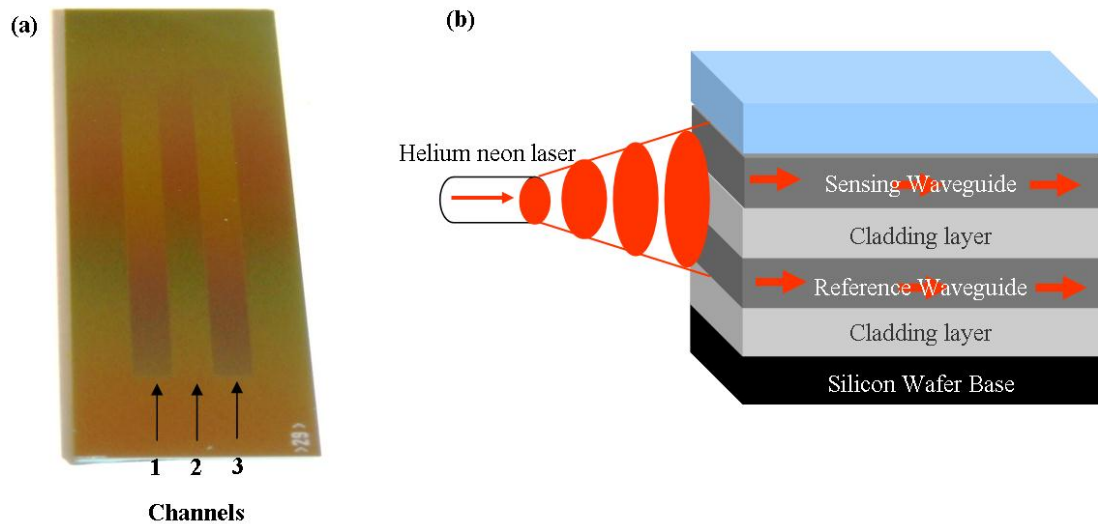
In contrast to the QCMD, which measures the hydrated mass of an adsorbed film; the DPI measures the dry mass of a film. The measurements of mass, thickness and density were performed in real time using an AnaLight Bio200 dual polarization interferometer (Farfield Sensors Ltd., Manchester, UK) [166]. The device uses a silicon oxynitride sensor chip that was clamped in a temperature-controlled enclosure that allowed the temperature to be maintained constant for all experiments. A gasket on top of the sensor forms two measurement chambers, each 1 mm wide, 17 mm long and 1 mm deep (see Figure 2.0.5.).

Figure 2.0.5. Photos: (a) PC, pump and DPI unit (b) Temperature control unit where the sensor is clamped (c) sensor holding unit.



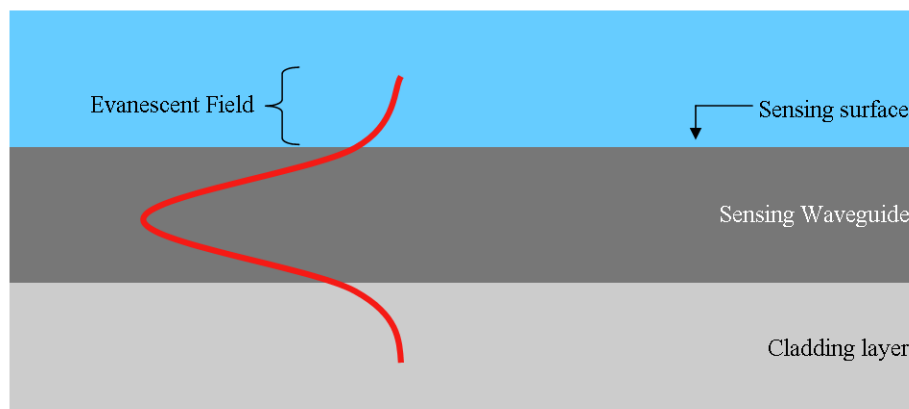
The sensor chip itself has a five layer structure consisting of two horizontally stacked waveguides, a sensing waveguide on top of a reference waveguide which is then separated by an opaque cladding material. The two optical paths (waveguides) present within the sensor allows polarised light from a helium neon laser (wavelength, 632.8 nm) to pass through the sensor (see Figure 2.0.6.).

Figure 2.0.6. (a) Plan view of the DPI silicon oxynitride sensor: arrows 1 and 3 indicate the position of the measuring channels of the sensor; and arrow 2 indicates the reference channel where no contact with the sample was made. (b) Side view, schematic representation of the sensor, showing the dual slab waveguides, and the passage of polarised light through the sensing and reference waveguides.



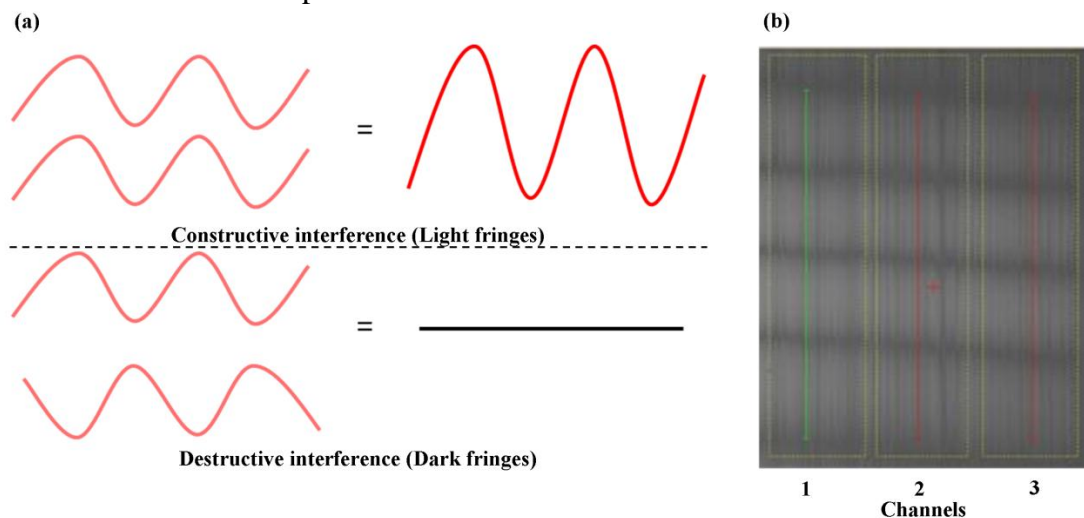
However, the polarised light is not completely confined within the waveguide structures. The light decays exponentially away from the borders of the waveguide; this part of the light wave is known as the evanescent (vanishing) field (see Figure 2.0.7).

Figure 2.0.7. The electric field profile of light in a waveguide of the DPI sensor. The evanescent field extends only a few hundred nanometers from the waveguide surface, an area known as the near field. Any changes in the refractive index in this nearfield region will influence the speed at which light passes down the waveguide. The higher the refractive index of an adsorbed material, the greater the slowing effect on light passing through the sensor.



Molecules at the surface of the sensing (upper) waveguide will interact with the evanescent field and the speed at which the light passes through the waveguide will be altered according to the refractive index (RI) of the adsorbing material. In contrast, the light in the reference (lower) waveguide is covered by cladding and is therefore not exposed to any RI changes and thus progresses at a constant velocity through the waveguide. This provides an optical reference for when the two beams of light diverge from the ends of the upper and lower waveguides combining to form dark and light interference fringes (See Figure 2.0.8.).

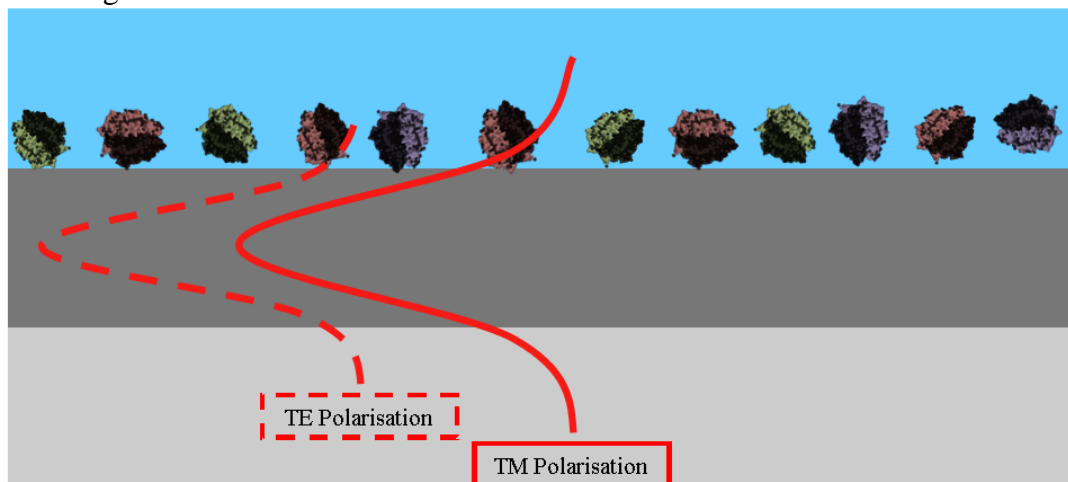
Figure 2.0.8. Output from both waveguides combine to generate interference patterns. Changes in these patterns are directly related to both the refractive index and the thickness of the molecular layer. **(a)** Principle of interferometry; when light waves interact. **(b)** Screen image of a fringe pattern as light passes through a sensor. 1 and 3 represent the fringe pattern from measuring channels 1 and 3 of the sensor; whereas 2 represents the fringe pattern of the reference channel of the sensor where no contact with the sample was made.



As further protein are added or removed from the sensor surface the speed that light travels through the upper waveguide is changed and thus the position of the interference fringes also moves in response. Furthermore, the polarisation of light that passes through the waveguide is alternately switched between two polarisations: transverse magnetic (TM) and transverse electric (TE) by a ferroelectric liquid

crystal half-wave plate (or polariser switch) that oscillated at 50 Hz (See Figure 2.0.9.). After traversing the chip length the emergent light forms an interference fringe pattern that was detected by a 1024x1024 camera, located at the far field (6 mm from the output face of the chip) and passes the output to a digital signal processor that is linked to the polariser switch where the type of polarised light is linked to the fringe pattern being produced. TE and TM respond differently to protein adsorption/displacement and therefore provide independent measurements of the adsorbed material, enabling two optical phase change measurements to be made.

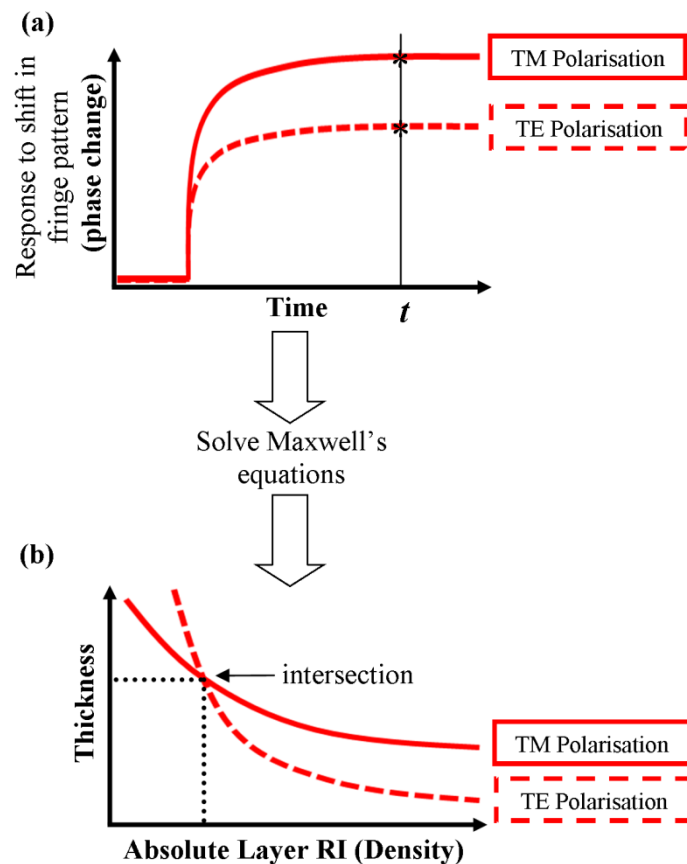
Figure 2.0.9. TE and TM evanescent fields passing through a DPI sensor with an adsorbed monolayer of proteins. The TE mode evanescent field is more closely confined to the surface of the waveguide than the TM mode evanescent field; and is therefore more sensitive to adsorbed material close to the surface than the TM mode. This difference is exploited to obtain information about the structure of the layer on the waveguide surface.



By assuming that the adsorbed film behaved as a single homogeneous layer (e.g. uniform composition & density along the chip length) and was isotropic (e.g. RI of TM = RI of TE); a range of thickness and RI values that satisfy the observed interference fringe movement are obtained. By solving Maxwell's equations simultaneously for the phase change of the TE and TM the mean refractive index and

thickness of the adsorbed film was obtained (See Figure 2.1.0.). As would be expected the thickness and RI values obtained in TM polarisation mode and TE polarisation mode are not identical, a direct consequence of their different evanescent fields. However, when the two series of computed layer thickness and refractive index values obtained for the two polarisation modes are overlaid there is a single point where TE and TM meet, which corresponds to the layer condition on the waveguide surface at time t . By carrying out this calculation at all time points of the experiment; layer thickness and refractive index measurements for the entire time course of the experiment can be acquired.

Figure 2.1.0. (a) Graph displaying the phase change of an adsorbing film over time. (b) The converted phase data from time point t to generate a range of thickness and RI values that satisfy the observed phase change observed in TM and TE mode. The point of intersection corresponds to the layer condition on the waveguide surface at time t .



Because RI is a linear function of protein concentration over a wide range of protein concentrations [167], the absolute amount of the adsorbed molecules, Γ (referred to as 'polymer' mass) can be obtained via the de Feijter formula [168].

Equation 2.3. The Feijter equation to calculate adsorbed mass of a film

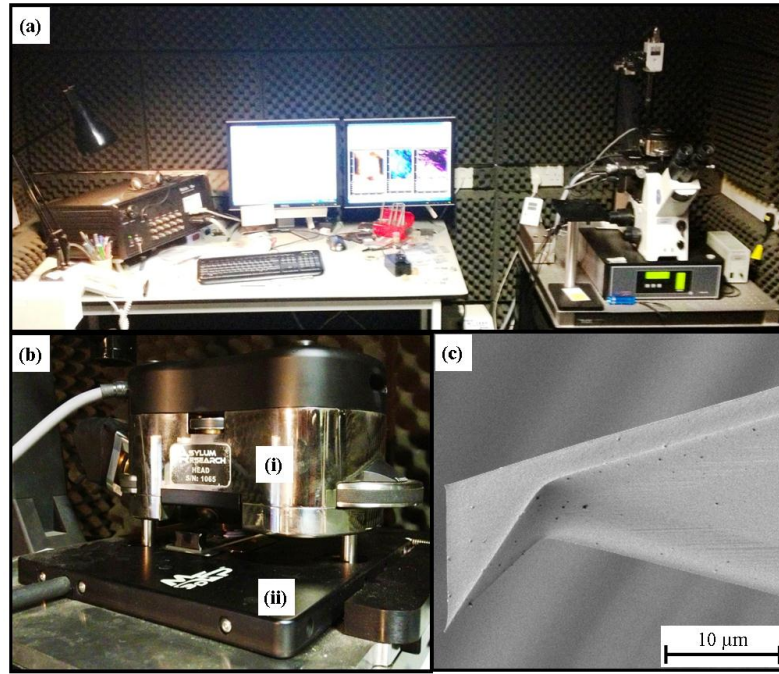
$$\Gamma = d_f \frac{n_f - n_{buffer}}{dn/dc}$$

Where n_f and d_f represent the RI and thickness of the adsorbed film, n_{buffer} the RI of the buffer used in the experiment and dn/dc the RI increment of the adsorbing proteins. The surface adsorbed mass densities determined from this formula depend only on the difference in the refractive index of the adsorbed film (n_f) and the RI of the buffer (n_{buffer}) therefore the coupled solvent molecules of the film do not contribute to the mass as they do for the QCMD technique. These calculations were carried out using the Analight Explorer software (version 1.5.4.18811, Farfield Scientific, Manchester, UK). The assumed refractive index increment dn/dc was 0.15, a value typical for protein films [169].

Atomic Force Microscopy (AFM)

AFM is a technique that images the 3 dimensional topography of a surface and is a method that does not require any chemical treatment of a sample that would potentially alter the structure of the sample under examination. Furthermore, AFM can carry out measurements in both air and liquid so that the *in vivo* conditions of the pellicle can be more closely matched. The primary purpose of the Asylum Research MFP-3D AFM (see Figure 2.1.1.) in this research was to quantitatively measure surface roughness of substrates that were used to measure the adsorption of the salivary pellicle and the surface roughness of the salivary pellicle itself. The following details how topographical images of the pellicle and sensor surfaces reproduced in this thesis were constructed by plotting the sample height of a surface against the AFM probe tip position.

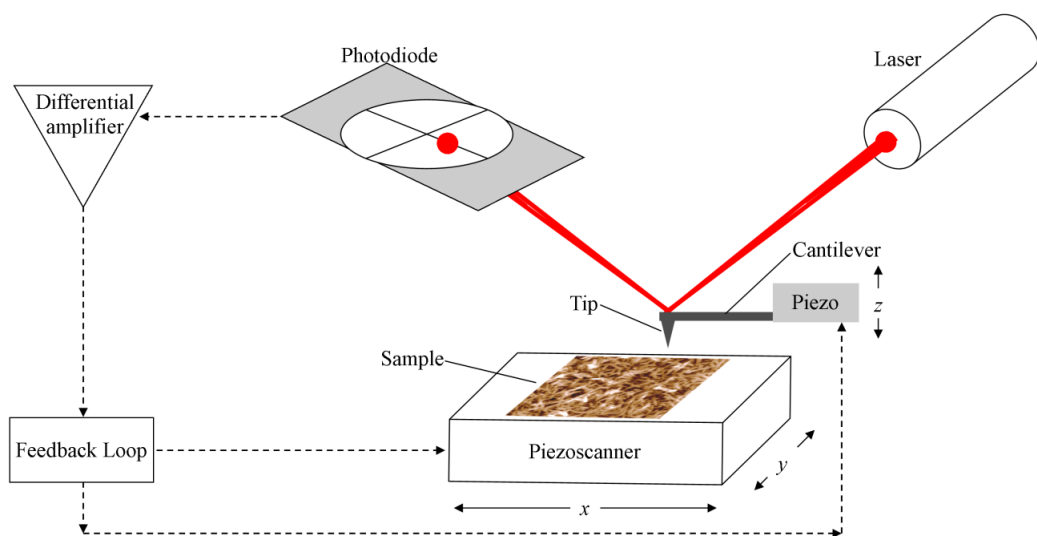
Figure 2.1.1. (a) Photo of the MFP-3D-BIO AFM sat on a vibration isolation platform (right side) with controller unit and PC (left side). Padded room reduces environmental vibrations which can impact image quality. (b) (i) MFP-3D head where cantilever tip is held and moves the tip in the vertical z direction. (ii) Stage or MFP-3D XY scanner that moves the sample in the horizontal x and y direction. (c) Scanning electron micrograph of the AFM tip and cantilever used to ‘feel’ the surface of a sample.



The AFM is a probe microscope that ‘feels’ the surface of a sample, somewhat analogous to how a blind person uses their fingertips to probe Braille. Unlike human fingers however, the probes that were used in the AFM are in the order of nanometres in size, which permits nanometre (10^{-9} m) scale resolution of an untreated sample. The pointed tip, or probe, that touches the sample surface extends down from the end of the cantilever. When the tip was scanned over a surface, forces between the tip and the sample lead to a deflection of the cantilever. The deflection was measured by the reflection of a laser that was focused on the back of the cantilever (See Figure 2.1.2.). As the tip scans (scan rate 2 Hz) the surface of a sample, the cantilever moves up and down relative to the contours of the surface which deflects the laser beam into a photodiode. The photodiode is split into four

sections and measures the difference in light intensities from where the reflected laser beam lands; so that lateral motions of the tip can be calculated. Feedback from this photodiode enables the piezoelectric scanners to maintain the tip at a constant force above the sample to obtain the correct height information of the surface. This feedback mechanism is important to inform the instrument to adjust the tip-to-sample distance to prevent damaging the sample.

Figure 2.1.2. Schematic overview of the AFM that illustrates the main features.



For this whole process to work accurately it was important to ensure that any deflection observed in the cantilever was a consequence of the surface roughness of the sample. To do this the stiffness of the cantilever must be accounted for; where the application of force and the deflection of the cantilever is expressed via Hooke's law:

$$F = -ks,$$

F = force

k = spring constant (stiffness of the cantilever)

s = distance the cantilever is bent.

In this thesis Olympus AC 160 cantilevers with a spring constant quoted at 42 N m⁻¹ were used. In order to prevent the tip from scraping and damaging the sample, an

AFM technique known as tapping mode was employed. In tapping mode, the cantilever was driven to oscillate, in an up down motion near its resonance frequency by a small piezoelectric element mounted in the AFM tip holder. This resulted in the cantilever oscillating at about 300 kHz at an amplitude of a few nanometres. The oscillating tip was then moved toward the surface until it began to lightly touch, or tap the surface. Whenever the tip passed over a peak in the surface of the sample, the oscillation of the cantilever becomes restricted and consequently the amplitude of oscillation decreases. Conversely, when the tip passed over a fissure in the sample surface, the oscillation of the cantilever was less restricted and the amplitude increases. These changes in amplitude are measured by the photodiode and passed onto a computer which generates the AFM image in three dimensions; the horizontal x and y plane, and the vertical z dimension [170]. Software analysis then permits root mean square surface roughness to be calculated; an important factor when discussing protein adsorption kinetics.

Protein Analysis

The following methods describe the techniques used to identify pellicle protein composition and protein concentration in this study. The order in which each technique is described follows the chain of techniques that lead to the identification of pellicle proteins in this research.

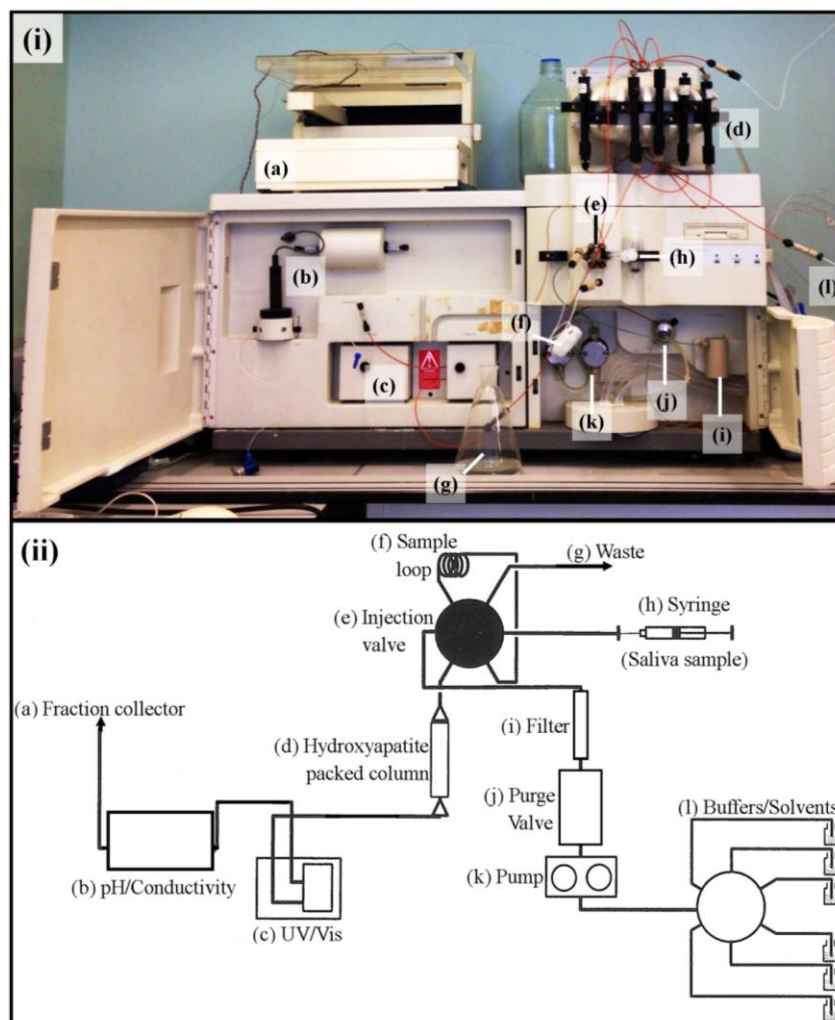
Basic chromatography principles

Column chromatography is a technique that separates proteins into different fractions by taking advantage of differences in protein charge, size and binding affinities. The technique used has a stationary phase (hydroxyapatite) that was held in a column; and a mobile phase (saliva and subsequently buffer) that permeates through the stationary phase. Individual proteins migrate through the column at different rates, depending on the properties of the proteins and their affinity for stationary phase, in this case hydroxyapatite. The stationary phase contains chemical groups that only specific salivary proteins bind to. The passage of these proteins through the column was delayed and their emergence from the column was detected by measuring the absorbance at 280nm and 220nm recorded via UV/Vis detectors.

Fast protein liquid chromatography

For the separation of salivary proteins a technique called Fast protein liquid chromatography was used. This is an improvement on traditional column chromatography techniques because instead of the mobile phase (saliva) being allowed to drip through a column under gravity, it is forced through under pressure ($\leq 3,000$ psi & flow rate range between 0.2 to 100.0 ml/min) via a peristaltic pump. In addition, small hydroxyapatite particle sizes (≤ 40 nm) were used for the column packing material which gave a larger surface area for interactions with the saliva. This reduced the diffusion of the sample throughout the column, and improved the ability to distinguish between the separation of proteins measured by the UV/Vis detector. Salivary protein fractionation was performed via a BioCAD SPRINT Perfusion Chromatography workstation (PerSeptive Biosystems, Massachusetts, USA) (see Figure 2.1.3.) ; using ceramic hydroxyapatite particles (Bio-Rad Laboratories, Hertfordshire, UK) as the column packing media. Detection of proteins was performed at 280nm and 220nm and effluent was collected using an Advantec SF-2120 super fraction collector (California, USA). Subsequent 2 ml fractions were then dehydrated in a Speed-vac SPD131DDA (Thermo Scientific, Hampshire, UK) and frozen for later protein analysis (e.g. SDS-PAGE).

Figure 2.1.3. The apparatus (i) consists of a Biocad Sprint liquid chromatography equipped with an internal PC running Windows 95 and used for controlling the system and storing and processing data. (ii) schematic overview of the system.

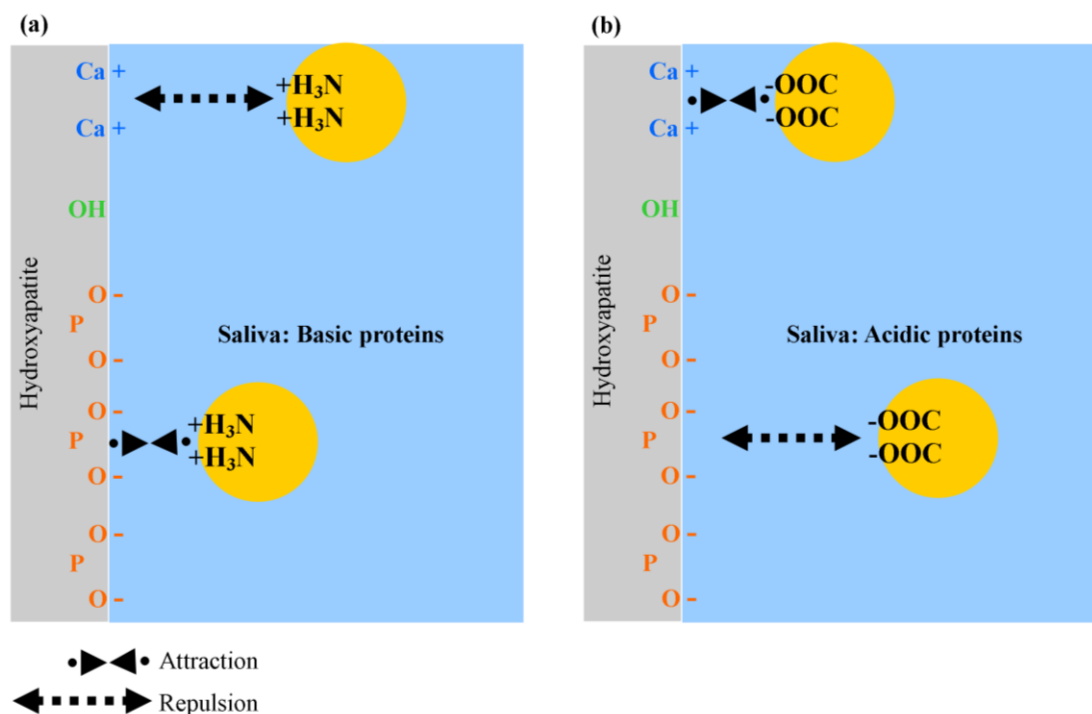


Hydroxyapatite packed column

Hydroxyapatite ($\text{Ca}_{10}(\text{PO}_4)_6\text{OH}_2$) is the main component of tooth enamel (~ 98%). Thus it was deemed appropriate to pack the column and separate salivary proteins relative to their affinity to hydroxyapatite particles. Although the protein interactions with hydroxyapatite are complex (see [171] for a detailed review), the following description attempts to elucidate the most significant features of the hydroxyapatite

protein interaction. Hydroxyapatite contains two types of binding sites, positively charged calcium and negatively charged phosphates. As a result, predominantly basic proteins from saliva will bind via cation exchange interactions with the negatively charged phosphate ions of hydroxyapatite. However, the positive amino groups on these proteins will also be repelled by the calcium sites on the hydroxyapatite packing; consequently, overall binding will depend upon the combined effects of these repulsion/attraction interactions. On the contrary, acidic proteins from saliva adsorb with the positively charged calcium ions of hydroxyapatite and are repelled by the negatively charged phosphate sites (see Figure 2.1.4.). These interactions were disrupted using components found in dentifrice products and fractions collected (See chapter 7) and separated using 1D SDS-PAGE.

Figure 2.1.4. schematic representation of the binding mechanisms of salivary proteins to the hydroxyapatite.



1-dimensional Sodium dodecyl sulphate polyacrylamide gel electrophoresis (1D SDS-PAGE)

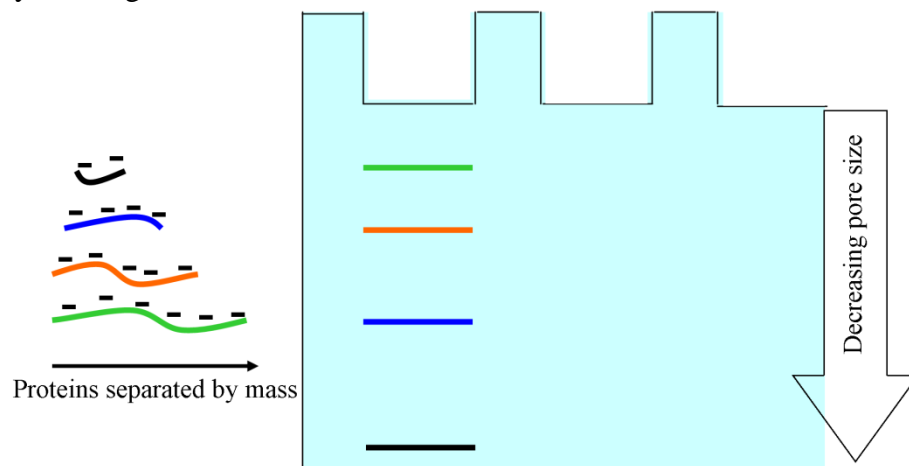
Sodium dodecyl sulphate (SDS) is an anionic (negatively charged) detergent that denatures proteins down to their primary structure (addition of dithiothreitol breaks the disulfide bonds that SDS cannot). Furthermore, SDS applies a negative charge to each protein in proportion to the mass of the protein, so that one molecule of SDS binds to every two amino acid residues of a protein. This treatment has two functions:

- (1) In an electric field all polypeptides are driven toward the anode (+ve charge).
- (2) Proteins are denatured so that only protein mass will influence migration rates.

Therefore, depending on the molecular mass of each peptide, the peptide will move differently through a polyacrylamide gel; depending on the pore size of the gel being used. The pore size of a gel can be varied by changing the total percentage of acrylamide present in the gel. Gels with a gradient of 4% acrylamide at the top of the gel, increasing to 12% acrylamide at the bottom of the gel were used.

This gradient generated a sieving effect that separated proteins according to their size. Therefore, as each protein moves through the gel, the pore sizes become progressively smaller. The combination of gel pore size and protein charge, size, and shape determines the migration rate of the protein (see Figure 2.1.5).

Figure 2.1.5. schematic representation of peptides separated by mass in a polyacrylamide gel



2-dimensional polyacrylamide gel electrophoresis (2D-PAGE)

A widely used approach is two-dimensional gel electrophoresis (2-DE). Introduced in the seventies [172]. The purpose of this method was to separate salivary proteins by two dimensions; firstly by isoelectric point (pI) using isoelectric focussing (IEF), then by size using SDS PAGE to obtain individual proteins which are observed as individual spots on a stained gel. Spots of interest can be excised from the gel and subjected to in-gel tryptic digestion to allow identifications via MS/MS analysis.

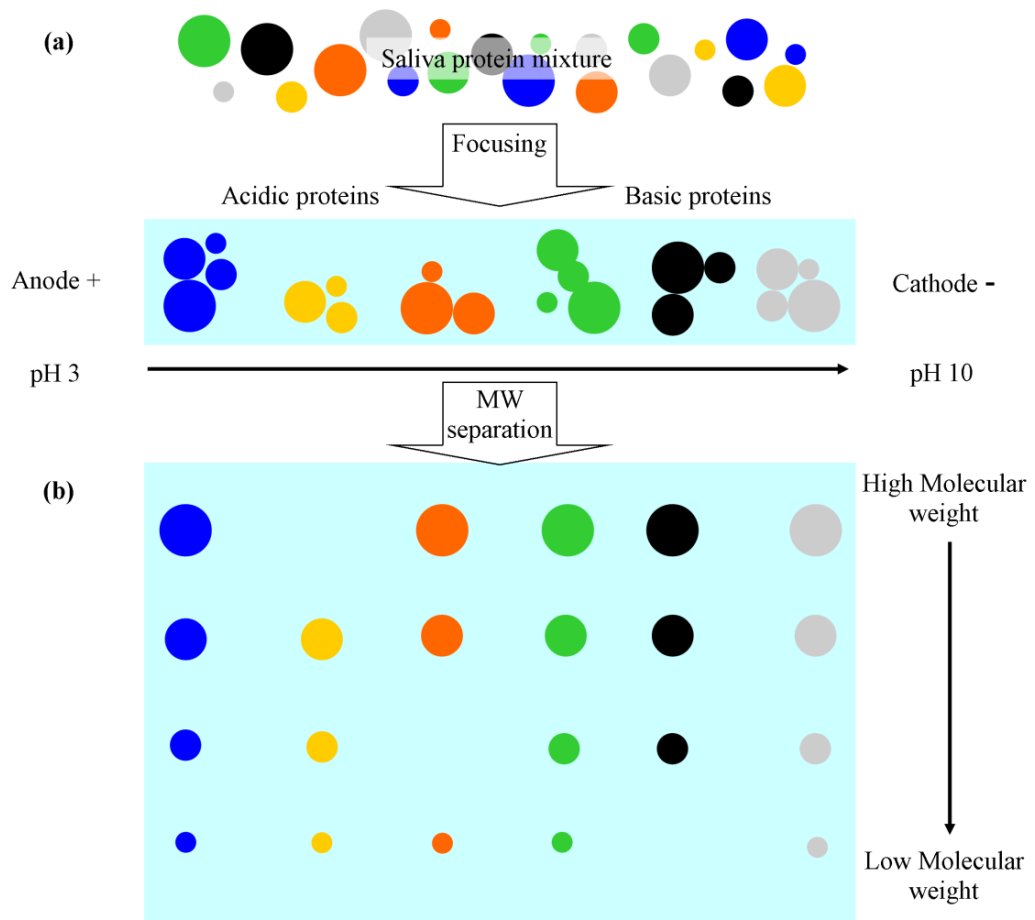
First dimension separation (isoelectric focussing)

The experiment involves the separation of proteins according to their isoelectric point (pI) by isoelectric focusing (IEF). IEF works by applying an electric field to proteins within a pH gradient. The proteins separate as they migrate through the pH gradient in response to the applied voltage. When a protein reaches a pH value that matches its pI, its net electrical charge becomes neutral, and stops migrating. In this way, each protein in a sample becomes "focused" according to its pI. Immobilized pH gradient (IPG) with ampholytes covalently bound to a gel are used to (See Figure 2.1.6. (a))

Second dimension separation (SDS-PAGE)

The proteins resolved by IEF are then applied to SDS-PAGE and separated by molecular weight (as previously described) in a direction perpendicular to the first dimension (see Figure 2.1.6. (b)). Separated proteins can then be excised from the gels and identified using mass spectrometry

Figure 2.1.6. (a) schematic of isoelectric focusing: a mixture of salivary proteins were resolved on a pH3-10 Immobilized pH gradient strip according to each proteins isoelectric point, independent of the protein size. **(b)** Schematic diagram showing the second dimension separation of proteins by SDS-PAGE after separation by IEF.

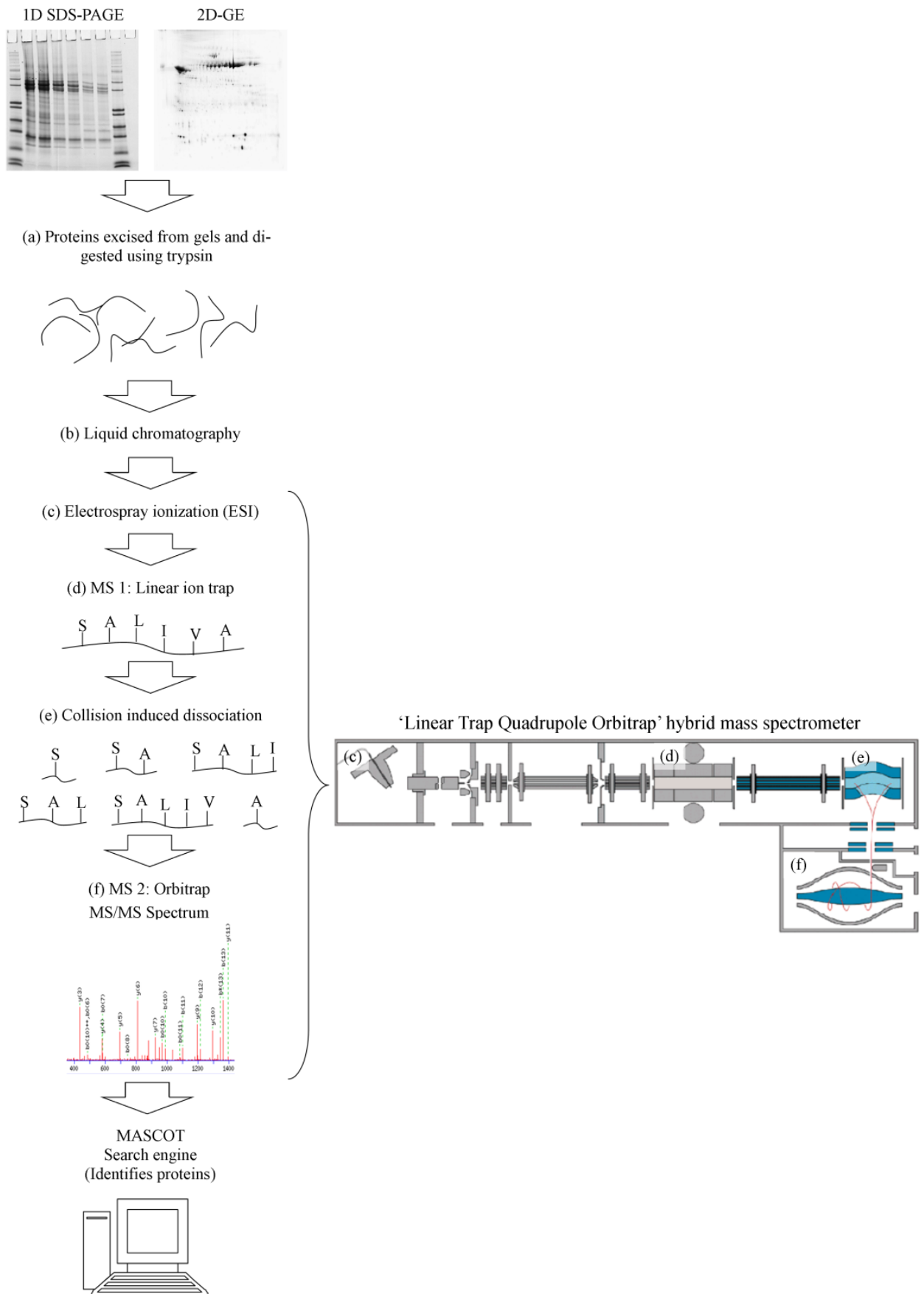


Liquid chromatography tandem mass spectrometry (LC-MS/MS)

Figure 2.1.7. illustrates the typical experimental workflow for protein identification using liquid chromatography (LC) and electrospray ionization tandem mass spectrometry (MS/MS) in this research. This technique was performed using a 'linear trap quadrupole' (LTQ)-Orbitrap mass spectrometer (Thermo) and a nanoflow-HPLC system (nanoACQUITY: Waters) [173]. Prior to LC-MS/MS analysis however, 1D-PAGE and 2D-PAGE separation was performed so as to reduce the complexity of the saliva/pellicle samples. Proteins of interest were then excised from the gels and the enzyme trypsin, which selectively cleaves peptides at the C-terminal side of arginine and lysine, was used to digest the proteins into peptides. These peptides were then introduced into the nanoflow-HPLC system which regulates the flow of peptides into the mass spectrometer. Upon exiting the HPLC system, the peptides were sprayed under high-voltage via the electrospray ionization (ESI) source, where small droplets of the peptides were formed and vaporised giving rise to ionised peptides. The first stage of mass analysis (MS1) takes place in the linear ion trap which separated the ionised peptides with respect to their mass-to-charge ratios (m/z). Each isolated ionised peptide was then induced to fragment by collision induced dissociation (CID); and the fragmented peptides were then passed into the Orbitrap for the second stage of mass analysis (MS2). Here, fragmented ionized peptides revolve about the central electrode and oscillate harmonically along the orbitrap's axis (the z-direction) with a frequency characteristic of the peptides m/z values. This permits the generation of an MS/MS spectrum that identifies the sequence of the peptide. This sequence is then correlated with theoretical sequences

generated *in silico* using database search algorithms. Proteins in this research were identified using the MASCOT v2.2.06 search engine [174]; where the degree of matching between each experimental and theoretical mass spectrum was assigned a score and the peptide sequence in the database with the most significant score was assumed to be correct. Analysis was performed using a LTQ-Orbitrap mass spectrometer (Thermo) and a nanoflow-HPLC system (nanoACQUITY: Waters). Peptides were trapped on line to a Symmetry C18 Trap (5 μm , 180 μm x 20 mm) which was then switched in-line to a UPLC BEH C18 Column, (1.7 μm , 75 μm x 250 mm) held at 45°C. Peptides were eluted by a gradient of 0–80% acetonitrile in 0.1% formic acid over 50 min at a flow rate of 250 nl min^{-1} . The mass spectrometer was operated in positive ion mode with a nano-spray source at a capillary temperature of 200°C. The Orbitrap was run with a resolution of 60,000 over the mass range m/z 300–2,000 and an MS target of 106 and 1 sec maximum scan time. The MS/MS was triggered by a minimal signal of 2000 with an Automatic Gain Control target of 30,000 ions and maximum scan time of 150 ms. For MS/MS events selection of 2+ and 3+ charge states selection were used. Dynamic exclusion was set to 1 count and 30 sec exclusion time with an exclusion mass window of ± 20 ppm. Proteins were identified by searching the Thermo RAW files converted to Mascot generic format by Proteome Discover 1.1 (Thermo) and proteins were identified by interrogating the Sprot_trembl20121031 proteome database (taxonomy Homo Sapiens) using the MASCOT v2.4.1 search engine [174].

Figure 2.1.7. A typical experimental workflow for salivary protein identification and characterisation using LC-MS/MS data; and a schematic outline of the LTQ-Orbitrap.



Saliva

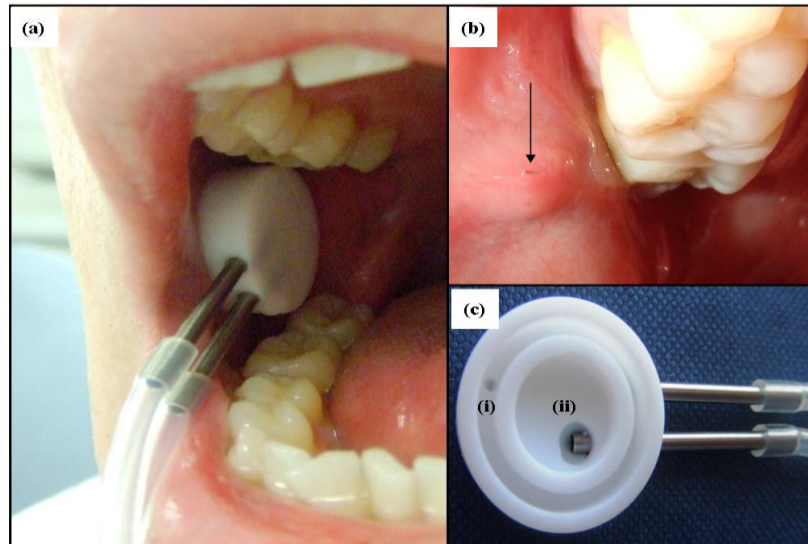
The composition of stimulated and unstimulated differs significantly. About 70 % of the unstimulated whole saliva is derived from the submandibular/sublingual glands; about 15-20 % from the parotid and 5-8 % from the minor salivary glands. When saliva is stimulated, the parotid saliva contributes up to 50% of the total WMS [4]. However, the proteins of WMS are susceptible to hydrolysis by proteolytic enzymes,[175]. Consequently, when no pre-treatment of saliva is implemented (e.g. protease inhibition, centrifugation and temperature control) rapid changes in the nature and composition of the saliva takes place [176]. Due to the rapid degradation, low secretion rate, coupled with the relatively large volumes of saliva required for analysis (≥ 10 ml for WMS and ≥ 30 ml for PS samples), unstimulated saliva was not used in this study. Furthermore, the rapid secretion of stimulated saliva minimised the time between collection and measurement, thus eliminating the need for protease inhibitors and centrifugation of the saliva. The consequence of which were saliva samples that were more representative of the saliva produced *in vivo*.

Saliva collection

Saliva collection of stimulated Whole Mouth Saliva (WMS) and stimulated Parotid Saliva (PS) was undertaken according to a protocol approved by the National Research Ethics Service, by the Hertfordshire Research Ethics Committee. Study reference number: 10/H0311/15 registered online at ClinicalTrials.gov ID: NCT01167504; Protocol ID: IFR03-2010. The saliva was obtained from 14 apparently healthy nonsmoking male and female volunteers, ranging in age from 20 to 50 years. The subjects had no history or current signs of oral conditions that could

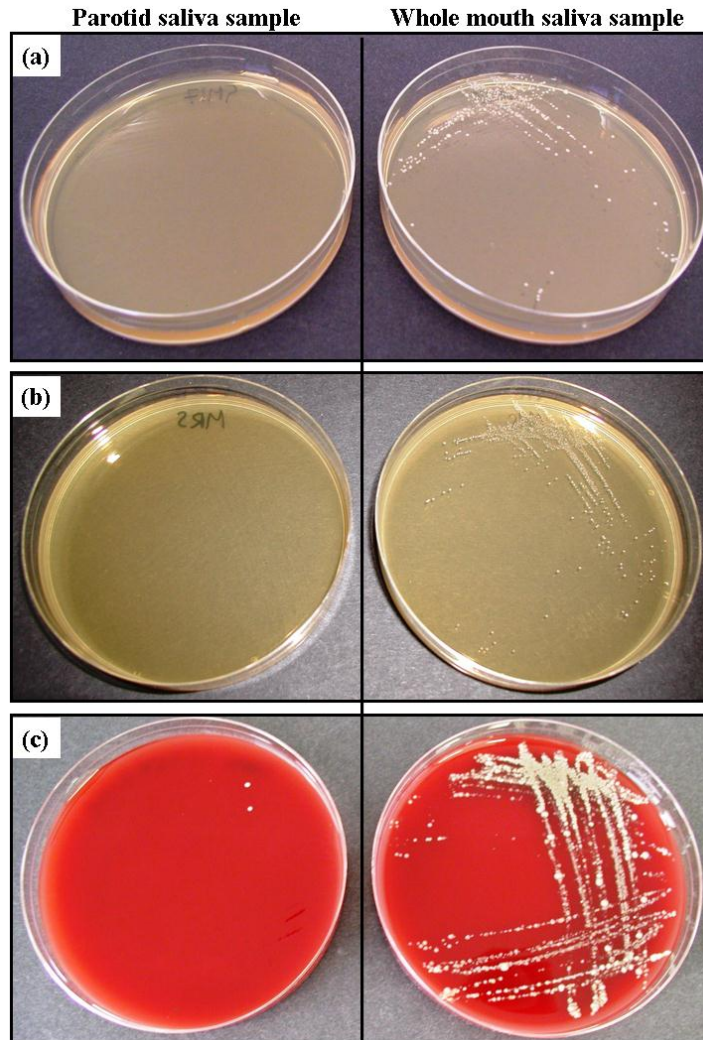
affect oral fluid composition. In order to collect WMS, volunteers rinsed their mouth with 10ml of bottled still water (Waitrose, Norwich, UK) twice. Volunteers then chewed on flavour-free gum (Gumlink, Dandyvej, Denmark) and expectorated the saliva into a small sterile collection bottle for up to 15 min, or until they had produced 10 mL of saliva. The PS was collected using a sterilised Lashley suction cup which was placed over the parotid duct (see Figure 2.1.8) after the nurse cleaned the inside of the cheek around the parotid duct area with sterile gauze [177]. Once the cup was in position the volunteer was asked to gently draw back the plunger of the syringe attached to the tubing on the cup to create mild suction in the outer, suction chamber of the cup until the cup is held securely but comfortably in place. The salivary secretion was stimulated by sucking 'Rosey Apples' boiled sweets (Asda, Norwich, UK). This continued for up to 45 minutes, or until 20-30 mls of saliva had been produced. Salivas were kept in ice upon expectoration, and were used immediately for study; and therefore it was deemed that no protease inhibitors were required. Moreover, this would mimic the behaviour of the *in vivo* pellicle as closely as possible, including potential proteolysis of the pellicle and pre-cursor proteins.

Figure 2.1.8. Image of a Lashley cup and the collection of parotid saliva (a) placement of the Lashley cup in preparation for the collection of parotid saliva; (b) Parotid duct (also known as Stensen's duct) located in the upper cheek next to the maxillary second molar; (c) Inner structure of the Lashley cup showing (i) the vacuum chamber that allows the attachment of the device to the surrounding buccal surface; and (ii) Parotid saliva collection chamber where the parotid saliva flows.



In order to ensure that the collection procedure was being carried out correctly; and to validate that no mixing of PS was taking place during the collection of volunteers PS, three different media were used to observe bacterial growth within WMS and PS samples. Because PS is ductal saliva, and is therefore essentially bacteria free, no/limited bacterial growth was observed. Conversely, plates that contained WMS did, as expected, show bacterial growth and thus confirmed that the protocol was effective at separating the two types of saliva (See Figure 2.1.9).

Figure 2.1.9. Bacterial growth derived from PS and WMS. PS and WMS was swabbed onto 3 different media: (a) M17 medium supplemented with either glucose only; (b) de Man, Rogosa and Sharpe and (c) Blood Agar Base 1% Yeast Extract 5% Horse Blood. Plates were then incubated for 24 hours at 37°C.



Saliva protein concentration

Total protein concentration of whole mouth saliva and parotid saliva of the volunteers' saliva samples was carried out via BCA (bicinchoninic acid) assay kits from Pierce Biotechnology Inc., (Rockford, IL, USA). This assay is based on two chemical reactions; the first is the Biuret reaction, where cupric ions (Cu^{2+}) are reduced (i.e. gain electrons) to cuprous ions (Cu^{+}) by the peptide bonds of proteins in an alkaline environment. The amount of Cu^{2+} reduced is proportional to the amount

of protein present in the solution within concentrations of 20 – 2,000 µg/ml [178].

The second step involves the chelating of one Cu^{1+} with two BCA molecules forming a purple coloured solution, which absorbs light at a wavelength of 562nm. This was measured with a 'Benchmark Plus Microplate Spectrophotometer (Bio-Rad Laboratories Ltd., Hertfordshire, UK). The protein concentration of saliva samples were then determined by comparing there absorbance values with a standard curve of absorbances from nine concentrations (0 ug/ml to 2,000 ug/ml) of bovine serum albumin (BSA) provided with the kit.

Chapter 3

Salivary Pellicle Adsorption and Characterisation Relative to Hydrophobic, Silica and Hydroxyapatite Surfaces

Introduction

In 2001 Nakanishi described the event of proteins adsorbing to a solid interface as: “a common but very complicated phenomenon” [179]. Common, because proteins are amphipathic molecules which renders them intrinsically surface-active molecules; and complicated because protein adsorption is confounded by numerous variables that render a simple description of the subject area very difficult. This is because protein adsorption is influenced by many factors (e.g. properties of the protein; properties of the surface, temperature, pH and ion concentration).

Consequently, even though significant progress in certain areas of protein adsorption has been achieved (see Vroman effect [180]) differing opinions on how to explain protein adsorption continue (see Daly *et al.* [181] Vs. Wertz [182] *et al.*) to this day.

Added to this complexity is that saliva is a heterogeneous and variable fluid that contains hundreds of proteins that vary in concentration and depend on many factors such as; saliva flow rate, circadian rhythm[183]; type and size of the salivary gland [184]; and physiological status of the subject [56]. Therefore, developing a model that predicts the adsorption behavior of saliva to a surface, with the currently available methods, is very challenging. In addition, the dynamic nature of enamel pellicle once adsorbed to a surface results in a film that is constantly evolving with its oral environment, making it difficult to be certain of an exact structure. In order to circumvent these issues a number of studies have identified proteins within the pellicle, which have then been isolated to observe their individual adsorption behaviors. For example, proline-rich proteins [62], statherin [51], mucin [185], serum albumin [115] and lysozyme [186] have all been studied to help understand in greater detail the adsorption phenomenon of the pellicle that occurs in the mouth. However,

once isolated the adsorption characteristic of an isolated protein is no longer representative of how it behaves in a mixture of solutes such as that found in the mouth. Therefore another way pellicle adsorption can be observed is by using several whole mouth saliva samples from numerous volunteers, and then following pellicle adsorption onto surfaces that are representative of surfaces in the mouth.

Consequently, the formation of salivary pellicles derived from stimulated whole mouth saliva samples on 6 different surfaces (3 DPI sensors: Silica; hydroxyapatite; C18 and 3 QCMD sensors: Silica; hydroxyapatite; polystyrene) that vary in charge and hydrophobicity was observed. Observing the adsorption of the WMS on each of these surfaces helps to envisage the formation of the salivary pellicle as it may take place in the oral cavity, as it too consists of physically diverse surfaces (i.e. hard enamel and soft mucosa) that impact the adsorption behaviour of salivary proteins and gives an indication as to how different surface properties (i.e hydrophobicity, roughness) can affect salivary protein adsorption. Furthermore, in order to push our understanding of salivary pellicle formation on the tooth surface a little further it was decided that distinguishing which of the salivary proteins were involved in pellicle forming process should be identified. This was because the formation of the enamel pellicle is the result of selective adsorption of salivary components to the tooth surface; thus, not all proteins in saliva are involved in the pellicle forming process. As the dental enamel is primarily made of hydroxyapatite this was used as a model for the tooth surface. Subsequently the types of proteins that bind to hydroxyapatite were exposed via a combination of 2D-gel and mass spectrometry. This was also considered a useful step in explaining the adsorption isotherms of the hydroxyapatite sensors observed in this chapter and subsequent chapters where hydroxyapatite was used. The aim of this chapter therefore is three fold. Firstly, to observe the

adsorption profiles of stimulated WMS on hydrophilic hydrophobic and hydroxyapatite coated sensors. Secondly to introduce the reader to some of the complexities of protein adsorption; and thirdly, to identify the selective proteins from saliva that are adsorbing to hydroxyapatite, which are potentially the same proteins adsorbing to enamel in the mouth.

Materials and Methods

Hydroxyapatite, hydrophilic and hydrophobic sensors were used to observe the pellicle forming properties and physical structure of WMS derived pellicle. Two instruments (QCMD and DPI) were used to investigate the adsorption profiles of the following 3 different surfaces:

For the DPI experiments the following sensors were used:

- Hydroxyapatite coated
- C18 functionalised (Hydrophobic)
- Silicon oxynitride (Hydrophilic)

and for the QCMD experiments the following sensors were used:

- Hydroxyapatite coated
- Amorphous Fluoropolymer 1600/Teflon-like (Hydrophobic)
- Silicon dioxide (Hydrophilic)

Two surface properties of these sensors (roughness and wettability) were investigated via AFM and contact angle measurements (See Figure 3.0.1.) in order to highlight potential surface effects on subsequent pellicle formation and structure data produced from the DPI and QCMD.

Stimulated whole mouth saliva was collected as previously mentioned in Chapter 2.

Once the sample had been expectorated, 2 ml of the saliva was used for QCMD analysis and 2 ml of the same saliva sample was used for DPI analysis. The saliva

was allowed 2 hours to adsorb and was then rinsed with a 10mM pH 7 phosphate buffer in order to remove any loosely adsorbed material. These experiments were repeated five times per sensor, using a different saliva sample per experiment. No sensor was used more than three times.

Sensor cleaning

After the completion of the experiment, QCMD and DPI surfaces were cleaned with 2% w/v SDS (Sigma-Aldrich, UK), followed by 2% w/v Hellmenax then copiously rinsed with buffer followed by MiliQ water. QCMD sensors were further dried with oxygen free nitrogen gas and exposed to UV-ozone (Bio-Force Nanosciences Inc., Iowa, USA) for 20 min. Whereas the DPI sensors were not removed from the instrument, but had 20% isopropanol flowing over the sensor at 20 $\mu\text{l}/\text{min}$ until the next experiment.

Contact angles

The contact angle is a quantitative measure of the wetting of the solid by the liquid. This wettability of the sensors was measured by Attension Theta optical tensiometer (Biolin Scientific) in order to predict the hydrophobic nature of the sensors surfaces. Contact angles were measured with Mili-Q water (drop size $\approx 15\mu\text{l}$) as static contact angles using the sessile drop technique with an Attension Theta optical tensiometer (Biolin Scientific). The computer captures an image of the drop which is analyzed with a drop profile fitting method in order to determine contact angle. When attracted by the solid, the liquid forms a drop with low contact angles ($\theta < 90^\circ$). If repelled, the contact angles are high ($\theta > 90^\circ$).

Surface roughness

An MFP-3D atomic force microscope (Asylum Research, CA, USA) was used to measure the root mean square surface roughness (RMS) of the sensors. See chapter 2 for methods.

2-D gel electrophoresis and mass spectrometry

These techniques were used to identify which salivary proteins were selectively binding to hydroxyapatite. WMS was collected from 3 volunteers as described in chapter 2. Each sample was analyzed via 2D gel electrophoresis (See chapter 2) to identify salivary proteins present in WMS. However, 0.1ml of each of the volunteer's WMS sample was also added to 0.01mg of HA powder. The WMS/hydroxyapatite mixture was incubated for 2 h at 37 °C under continuous mixing. After 2 hours, the resulting suspensions were centrifuged at 10000 rpm for 10 min at 4 °C and the supernatants were then analyzed via 2D electrophoresis to identify salivary proteins that had not adsorbed to hydroxyapatite. By comparing the gels from the saliva samples that had or hadn't been exposed to hydroxyapatite, it was possible to observe which proteins had been selectively adsorbed to the hydroxyapatite.

In situ trypsin hydrolysis of protein bands

Gel pieces of interest were excised using a 5ml Diamond pipette tip (Gilson) and then washed with two 15 min incubations in 200mM ammonium bicarbonate (ABC) in 50% (v/v) acetonitrile (500µl) to equilibrate the gel to pH 8 and remove the stain, followed by 10 min incubations with acetonitrile (Fisher) (500µl). Any cysteine thiol side chains were then reduced by incubation with 10mM dithiothreitol in 50mM ABC (500µl) for 30 min at 60°C before being alkylated with 100mM iodoacetamide

in 50mM ABC (500µl) for 30 min in the dark at room temperature. The gel pieces were then washed with two 15 min incubations in 200mM ammonium bicarbonate (ABC) in 50% (v/v) acetonitrile (500µl) followed by 10 min in acetonitrile (500µl) to dehydrate and shrink the gel pieces before air drying. The protein was digested by the addition of 100ng Trypsin in 10µl of 10mM ABC (modified porcine trypsin; Promega), or a mixture of 100ng Trypsin and 100ng Endoproteinase GluC (Roche) in 10µl of 10mM ABC before incubated overnight at 37°C. Following digest the samples were acidified by incubating with 10µl of 1% (v/v) formic acid for 10 min. The digest solution removed from tube into an Eppendorf tube and the gel pieces were then washed with 50% Acetonitrile (20µl) for 10mins to recover more digest peptides from the gel. The combined extracted digest samples were then dried down at the Low Drying setting (some heat) on a Speed Vac SC110 (Savant) fitted with a Refrigerated Condensation Trap and a Vac V-500 (Buchi). The samples were then frozen at -80°C until ready for Orbitrap analysis.

Statistics

Significant differences in pellicle mass, thickness and density of WMS derived pellicle between sensors was determined by two sample t tests after the post buffer rinse of the pellicle. This was carried out using GenStat (14th Edition, VSN International Ltd, Hemel Hempstead, UK). Two sample t tests were also used to determine significant differences between the measured contact angles of the sensors. A p value < 0.05 was considered significant in all statistical analysis.

Results

Surface roughness of the hydroxyapatite coated DPI sensor (RMS = 18.7nm) was higher compared to the silica oxynitride (RMS = 4.7 nm) and the C18 (RMS = 8.9nm) sensors. The surface roughness of the QCMD sensors was much more uniform; Hydroxyapatite (RMS = 1.4nm) silicon dioxide (RMS = 1.2nm) and polystyrene (RMS = 1.6nm) (See Figure 3.0.1. and Table 3.1.).

Contact angles (three repeats on each DPI and QCMD sensor) did not differ significantly between the DPI ($42 \pm 13^\circ$) and the QCMD ($43 \pm 4^\circ$) hydroxyapatite sensors. Whilst unsurprisingly, the C18 and polystyrene functionalised sensors were shown to be the most hydrophobic of the sensors, with contact angles of $99 \pm 1^\circ$ and $80 \pm 3^\circ$ respectively, what was surprising was the large difference in contact angles between the DPI ($68 \pm 1^\circ$) and QCMD ($32 \pm 1^\circ$) silica sensors; a difference of $\sim 36^\circ$ (See Figure 3.0.2.).

Figure 3.0.1. AFM imaging and contact angle photo of: **(a)** DPI hydroxyapatite coated sensor; **(b)** a QCMD hydroxyapatite coated sensor; **(c)** DPI silica sensor; **(d)** QCMD silica sensor; **(e)** DPI C18 functionalised sensor; **(f)** QCMD polystyrene functionalised sensor. Differences between either surface roughness or wettability can clearly be observed in all sensors, apart from **(b)** and **(d)**.

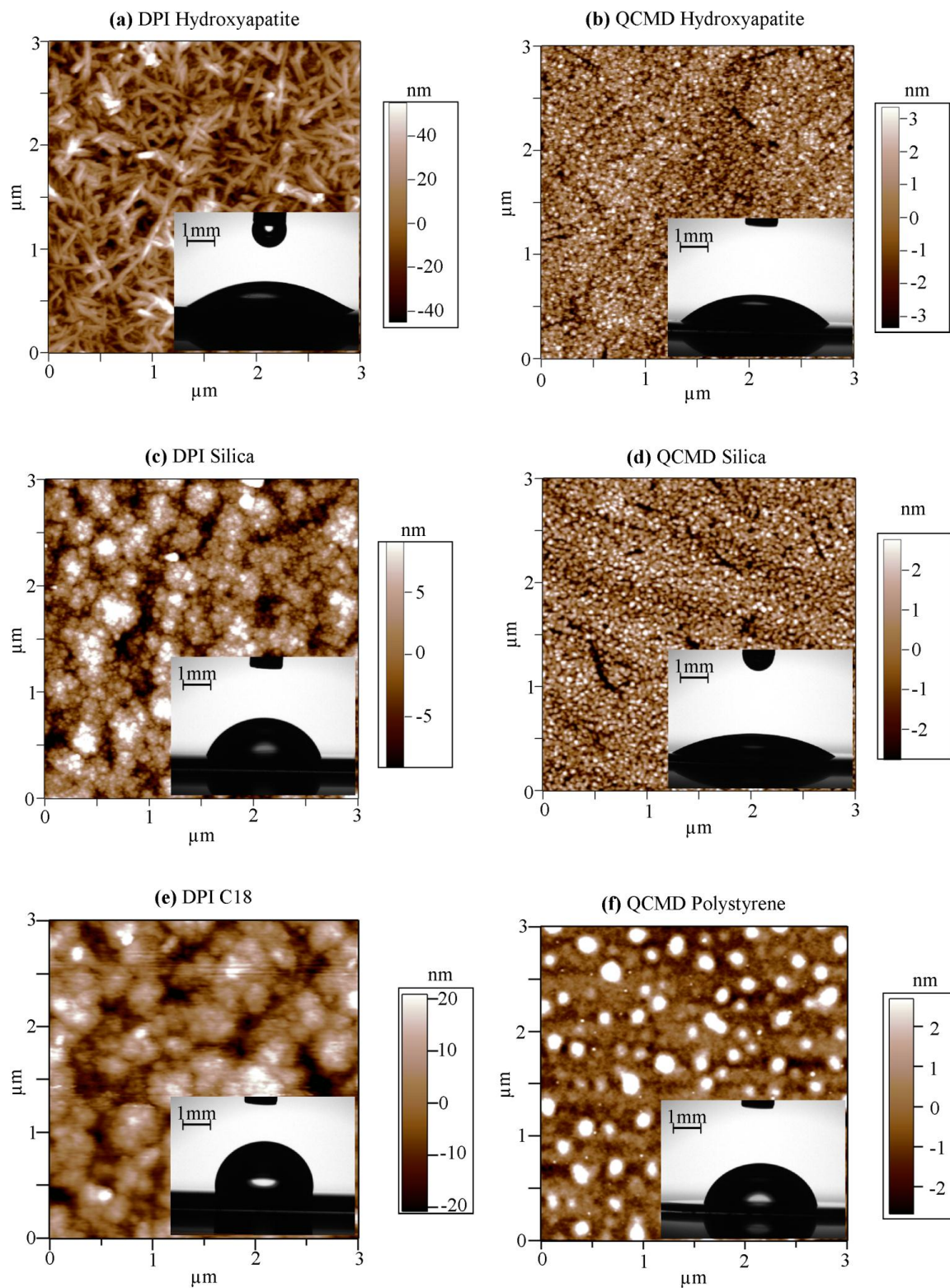
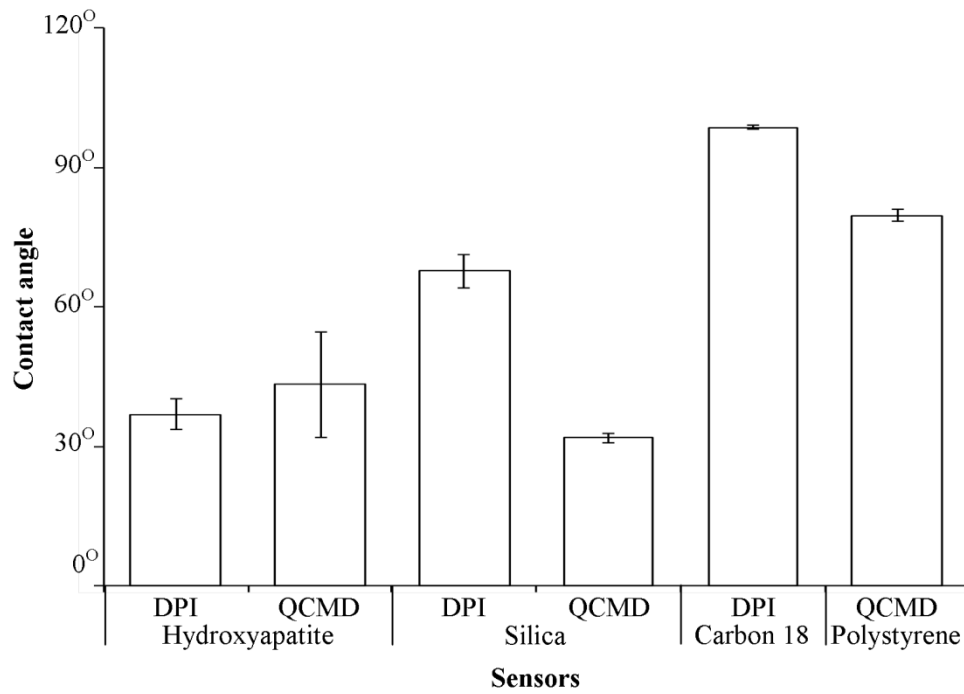


Figure 3.0.2. Bar chart displaying the different contact angles of all the DPI and QCMD sensors used. No significant difference between DPI and QCMD hydroxyapatite sensors. The hydrophobic DPI C18 and QCMD polystyrene sensors display the highest contact angle of all the sensors. But surprisingly DPI and QCMD silica sensors display significantly different contact angles.



Surface charge

The isoelectric point of hydroxyapatite is estimated at \approx pH 8 [187]; and under the neutral (pH7) conditions used for the adsorption of saliva in this study the hydroxyapatite surface would have carried a slight positive charge. The isoelectric point of silica is \approx pH 2 [188] so under the conditions used in this study, the silica would have carried a negative charge. Finally the C18 and polystyrene sensors were assumed to be uncharged, even though some residual charge of the underlying silica may have some influence on adsorption this was not verified (See Table 3.1.).

Table 3.1. Surface properties of the DPI and QCMD sensors

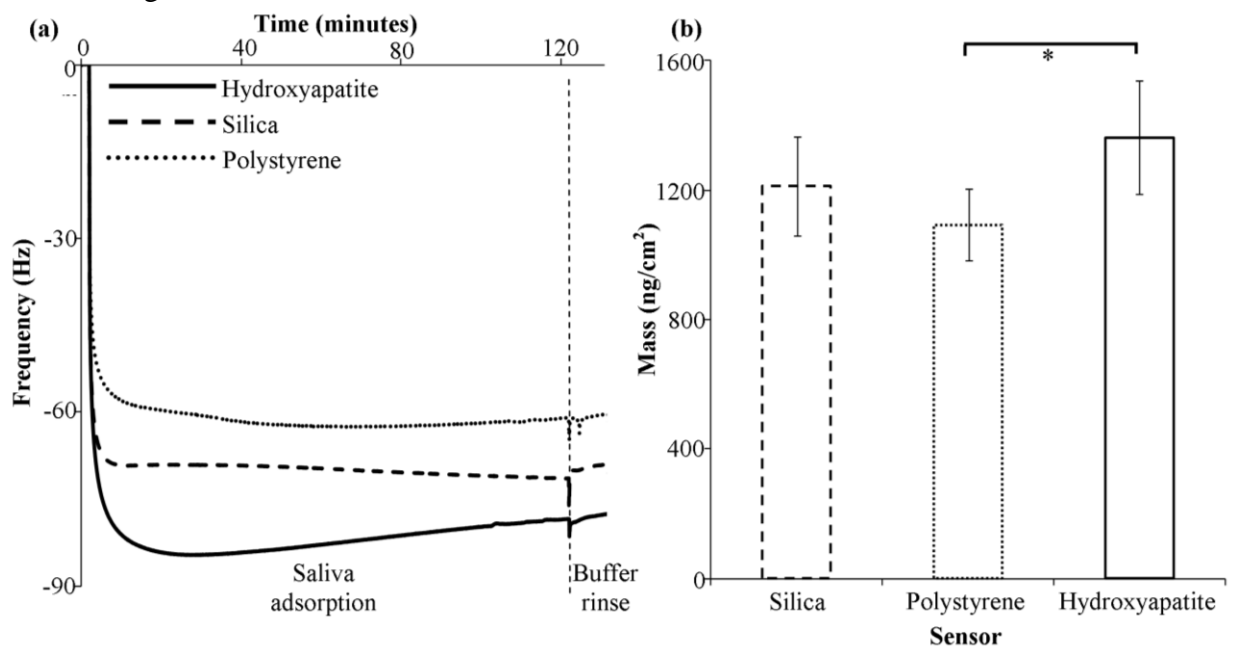
Surface Properties of Sensors	Sensor Type					
	DPI			QCMD		
	Hydroxyapatite	Silica Oxynitride	C-18	Hydroxyapatite	Silicon Dioxide	Polystyrene
Contact angle	42 \pm 13 °	68 \pm 1 °	99 \pm 1 °	43 \pm 4 °	32 \pm 1 °	80 \pm 3 °
Roughness (RMS)	18.7 nm	4.7 nm	8.9	1.4 nm	1.2 nm	1.6
Chemical Composition	Ca ₁₀ (PO ₄) ₆ (OH) ₂	(SiON) _n	C ₁₈ H ₃₇	Ca ₁₀ (PO ₄) ₆ (OH) ₂	(SiO ₂) _n	(C ₈ H ₈) _n
Surface Charge at pH 7	Positive	Negative	Uncharged*	Positive	Negative	Uncharged*

*- C18 and polystyrene sensors were assumed to be uncharged. Any residual charge would be that of the underlying silica

QCMD

The adsorption of the salivary pellicle was very rapid for all three surfaces (See Figure 3.0.3. (a)). The hydrated mass of the pellicle after rinsing away any loosely adsorbed material with phosphate buffer was: 1212 ± 154 ng/cm² on the silica surface; 1094 ± 111 ng/cm² on the polystyrene surface; and 1363 ± 176 ng/cm² on the hydroxyapatite. The pellicle adsorbed to the hydroxyapatite sensor measured the highest hydrated mass compared to the other two sensors, but this difference was only statistically significant when compared against the polystyrene sensor (See Figure 3.0.3. (b)).

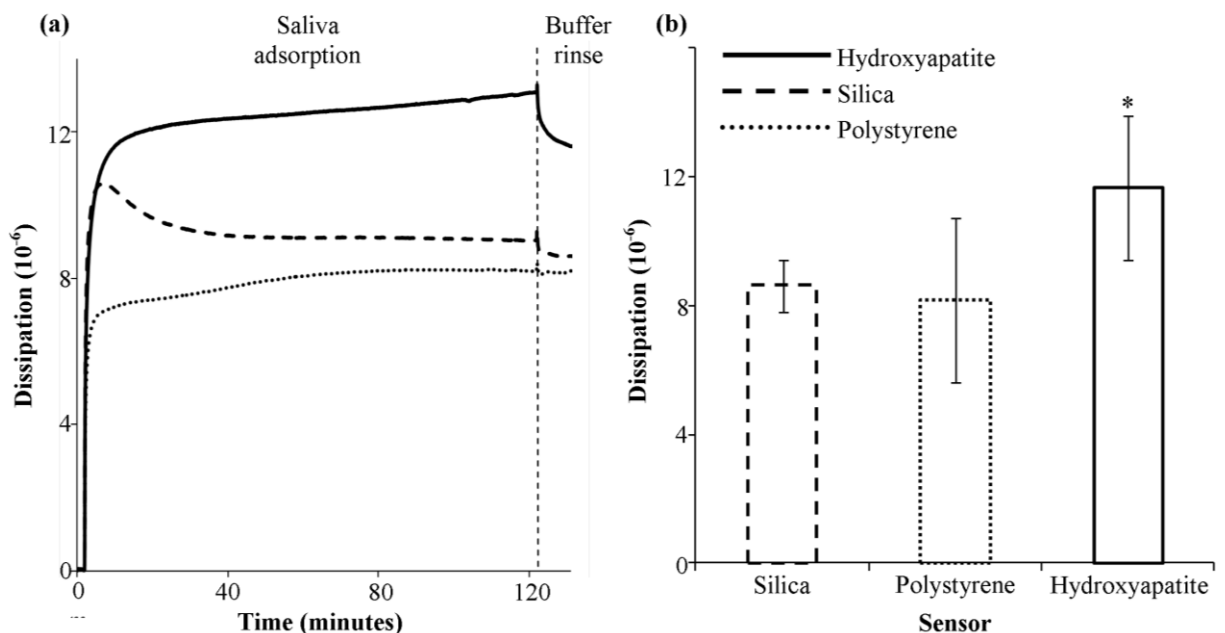
Figure 3.0.3. (a) Graph showing the change in frequency of the sensor (\approx pellicle hydrated mass) over time. (b) Bar chart showing the adsorbed pellicle hydrated mass after rinsing with buffer.



As the pellicle adsorbed to the sensor surface an increase in dissipation (measured at the 3rd overtone) was observed. This dissipation increase gives an independent qualitative insight into the viscoelasticity of the pellicle, corresponding to an decrease in rigidity or elasticity of the film. For the hydroxyapatite and polystyrene sensors the increase in dissipation was proportional to the increase in pellicle mass

(See Figure 3.0.4. (a)). However, for the pellicle adsorbed to the silica sensor a slightly different phenomenon was observed. Initially an increase in dissipation of the sensor as the proteins adsorb to the surface occurred (as was observed with the polystyrene and hydroxyapatite sensors); but then a rapid drop in the dissipation of the sensor occurs after 2 minutes adsorption. This suggests some viscoelastic changes taking place in the early stages of pellicle formation on the silica sensor that was not observed on the other sensors. The dissipation of the pellicle after rinsing away any loosely adsorbed material with phosphate buffer was: $9 \pm 1 \times 10^{-6}$ on the silica surface; $8 \pm 3 \times 10^{-6}$ on the polystyrene surface; and $12 \pm 2 \times 10^{-6}$ on the hydroxyapatite. The pellicle adsorbed to the hydroxyapatite sensor measured the highest dissipation and was significantly different statistically when compared to the other two sensors (See Figure 3.0.4. (b)).

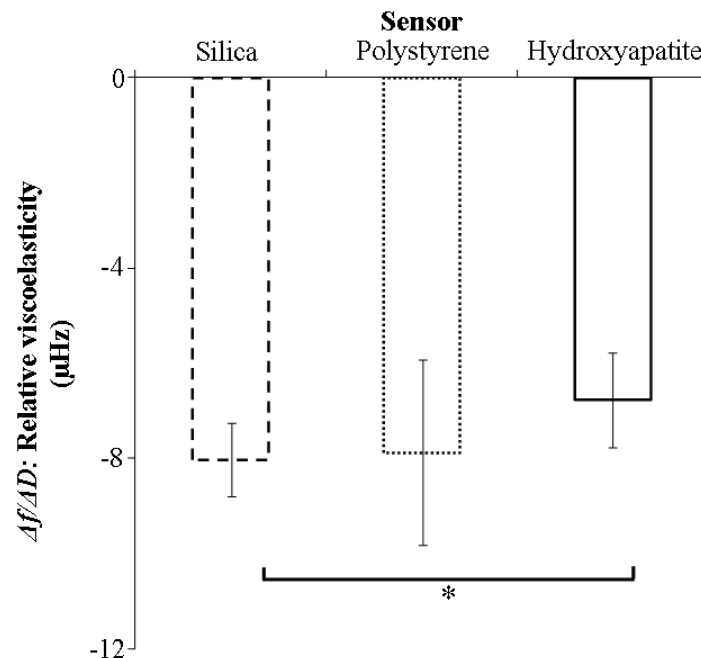
Figure 3.0.4. (a) Graph showing the change in dissipation of the sensor (\approx pellicle softness) over time. **(b)** Bar chart showing the dissipation value of the sensor, and thus, adsorbed pellicle softness after rinsing with buffer.



This data showed that the decrease in frequency (i.e. increase in hydrated mass) was highly associated to an increase in dissipation for WMS derived pellicle on all three

surfaces. By comparing the ratio between Δf (Hz) and ΔD (unitless) (see Figure 3.0.5) after rinsing with buffer, the viscoelastic properties of the adsorbing pellicle, with respect to the induced energy dissipation of the sensor per coupled unit mass, can be observed. Such that a more negative $\Delta f/\Delta D$ value indicates the addition of mass without eliciting a significant dissipation increase, which is characteristic of a more rigid salivary pellicle. Conversely a less negative $\Delta f/\Delta D$ value indicates a more viscoelastic, dissipative, salivary pellicle. This data shows that the pellicle adsorbed to the hydroxyapatite sensors contained a significantly greater viscous component ($-6 \pm 1 \Delta f/\Delta D$) within its structure than the pellicle adsorbed to the silica ($-7 \pm 1 \Delta f/\Delta D$) and polystyrene ($-8 \pm 2 \Delta f/\Delta D$) sensors.

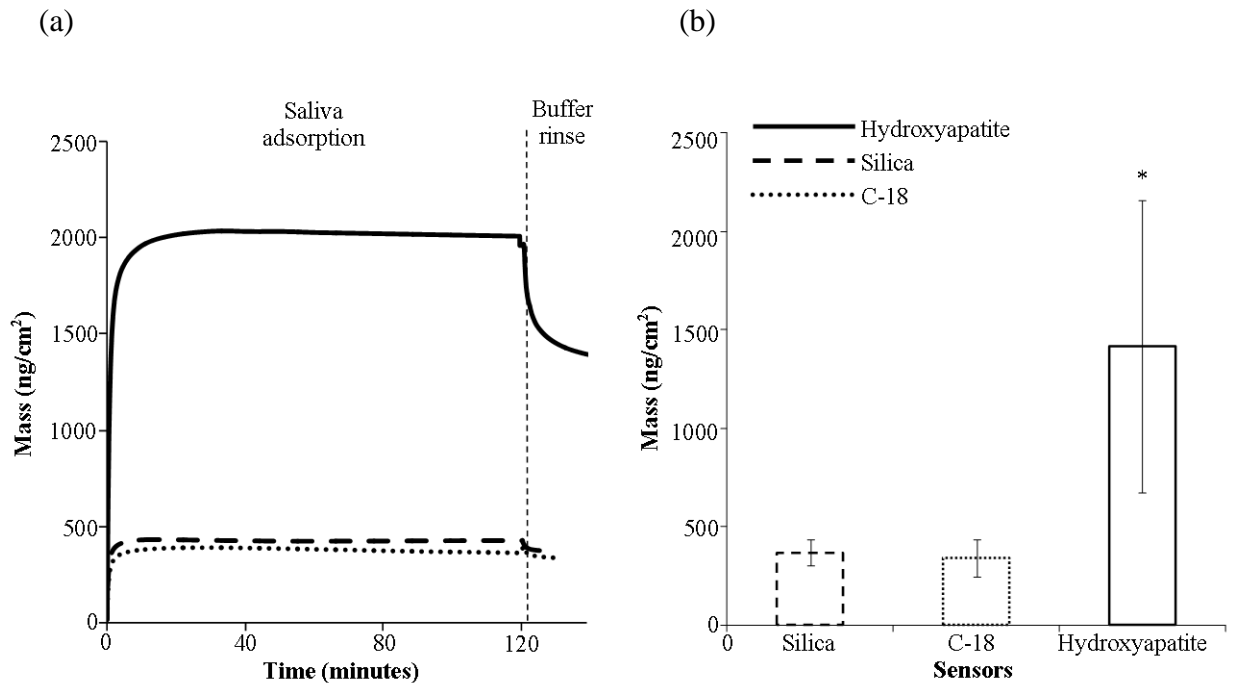
Figure 3.0.5. Bar chart displaying ΔD (dissipation) as a function of Δf (frequency) measured for the 3rd overtone reflecting qualitative viscoelastic properties of the pellicle (less negative = more elastic) on three different surfaces. Pellicle adsorbed to the hydroxyapatite sensor was shown to be more rigid than pellicle adsorbed to silica and polystyrene.



DPI

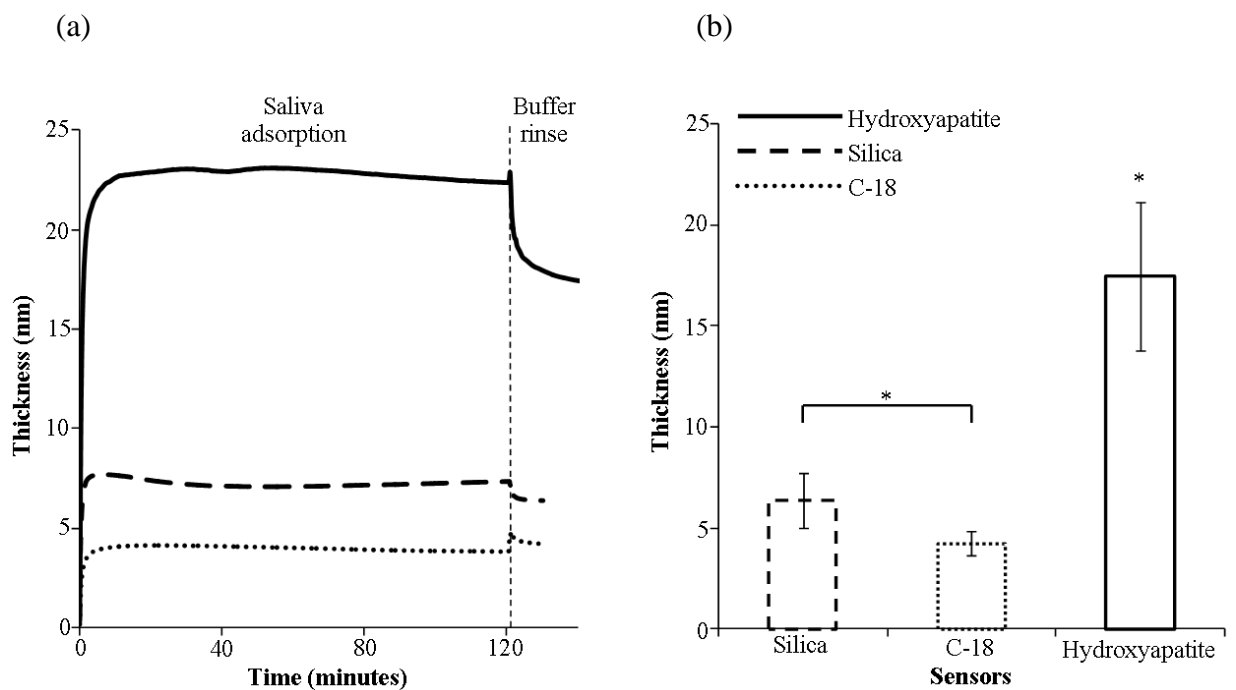
Pellicle ‘dry’ mass The formation of the salivary pellicle onto all three DPI sensors occurs very rapidly. The peak ‘dry’ mass was reached after circa 20 minutes adsorption time. Subsequently no further adsorption, or desorption, was observed (See Figure 3.0.6. (a)). After rinsing loosely adsorbed material from the sensor with phosphate buffer, a larger decrease in mass was observed from the hydroxyapatite coated sensor, relative to the silica and C-18 sensors. Post buffer rinse the silica and C-18 sensors showed similar quantities of adsorbed mass (369 ± 68 ng/cm² and 339 ± 94 ng/cm² respectively). Whereas the pellicle formed onto the hydroxyapatite formed a pellicle of significantly higher mass (1416 ± 742 ng/cm²) relative to the other two sensors (See Figure 3.0.6. (b)).

Figure 3.0.6. (a) Adsorption profile of salivary pellicle ‘dry’ mass onto three DPI sensors (Silica, C-18 and hydroxyapatite). **(b)** Bar chart showing the ‘dry’ mass of the adsorbed pellicle after rinsing with buffer.



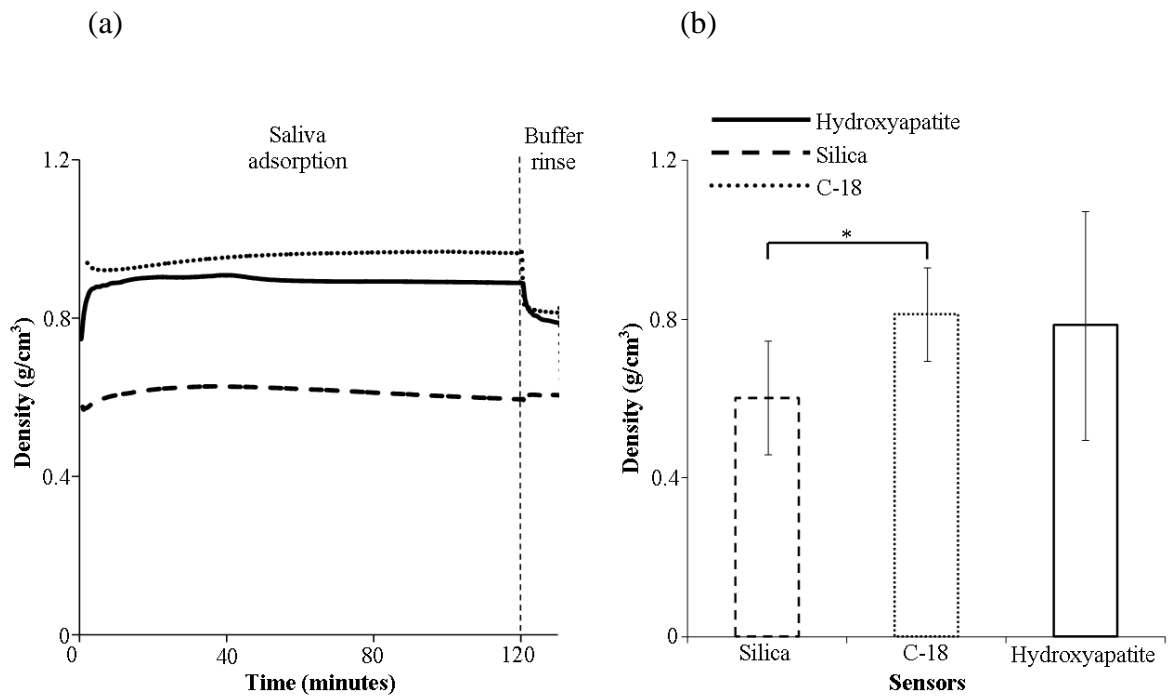
Pellicle Thickness Although peak pellicle thickness was reached under ~20 minutes adsorption time for all three sensors, the thickness of the pellicle differed significantly for all three sensors (See Figure 3.0.7. (a)). After the buffer rinse, the pellicle adsorbed to the C-18 sensor was the thinnest (4 ± 1 nm). Pellicle formed onto the silica sensor was slightly thicker (6 ± 1 nm) but the pellicle with the largest thickness was that formed on the hydroxyapatite-coated sensor (17 ± 3 nm) (See Figure 3.0.7 (b)).

Figure 3.0.7. (a) Adsorption profile of salivary pellicle thickness on three DPI sensors (Silica, C-18 and hydroxyapatite). **(b)** Bar chart showing the thickness of the adsorbed pellicle after rinsing with buffer.



Pellicle Density The peak density of the pellicle is reached very quickly for all three sensors observed. However, the pellicle adsorbed onto the silica sensor had a much lower density when compared to the density of the pellicles adsorbed onto the C-18 and hydroxyapatite sensors (See Figure 3.0.8. (a)). After rinsing with buffer the density of the pellicle on silica was measured at $0.6 \pm 0.1 \text{ g/cm}^3$; whilst on the C-18 and hydroxyapatite sensors the density of the pellicle was measured at $0.8 \pm 0.1 \text{ g/cm}^3$, $0.8 \pm 0.3 \text{ g/cm}^3$ respectively (See Figure 3.0.8 (b)).

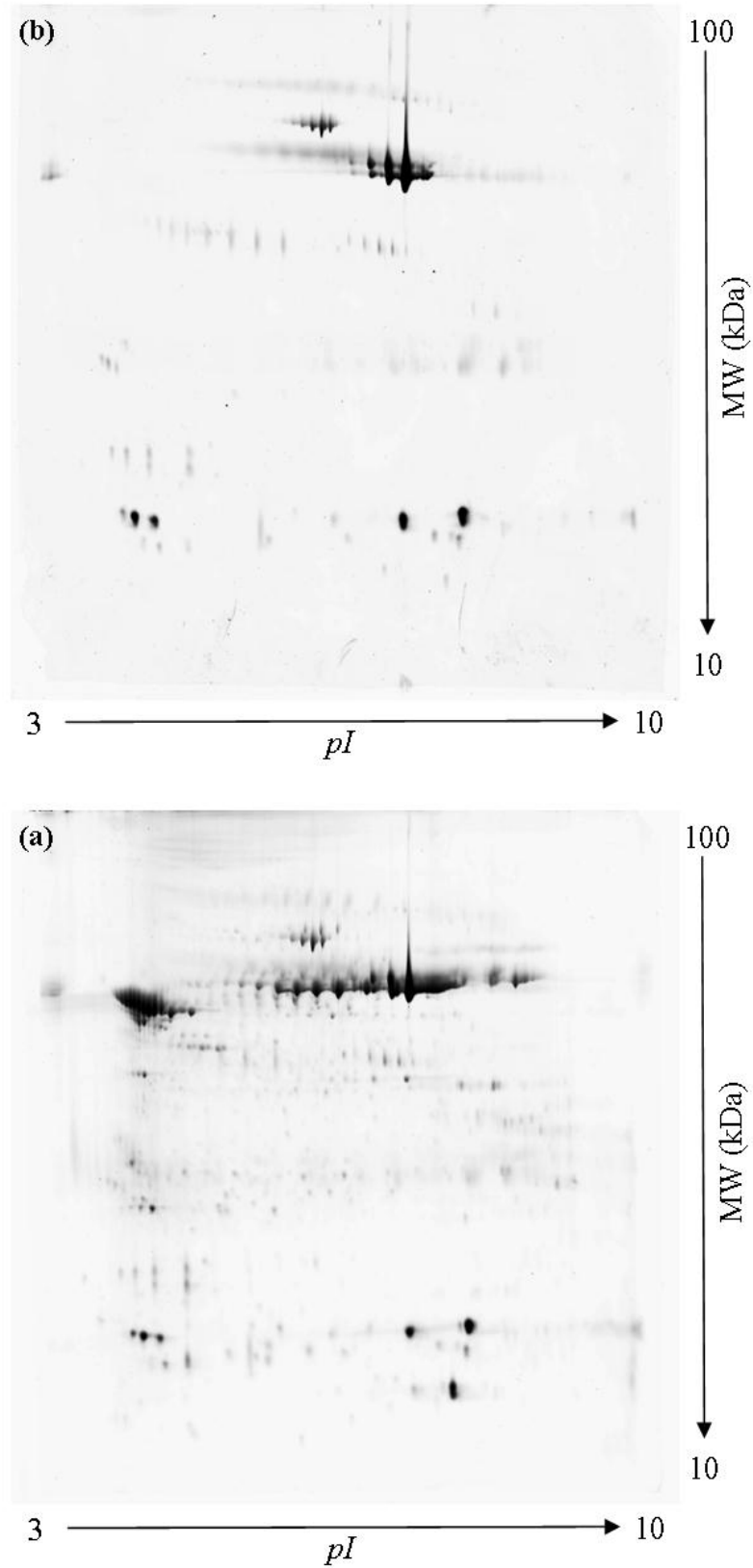
Figure 3.0.8. (a) Adsorption profile of salivary pellicle density on three DPI sensors (Silica, C-18 and hydroxyapatite). **(b)** Bar chart showing the density of the adsorbed pellicle after rinsing with buffer.

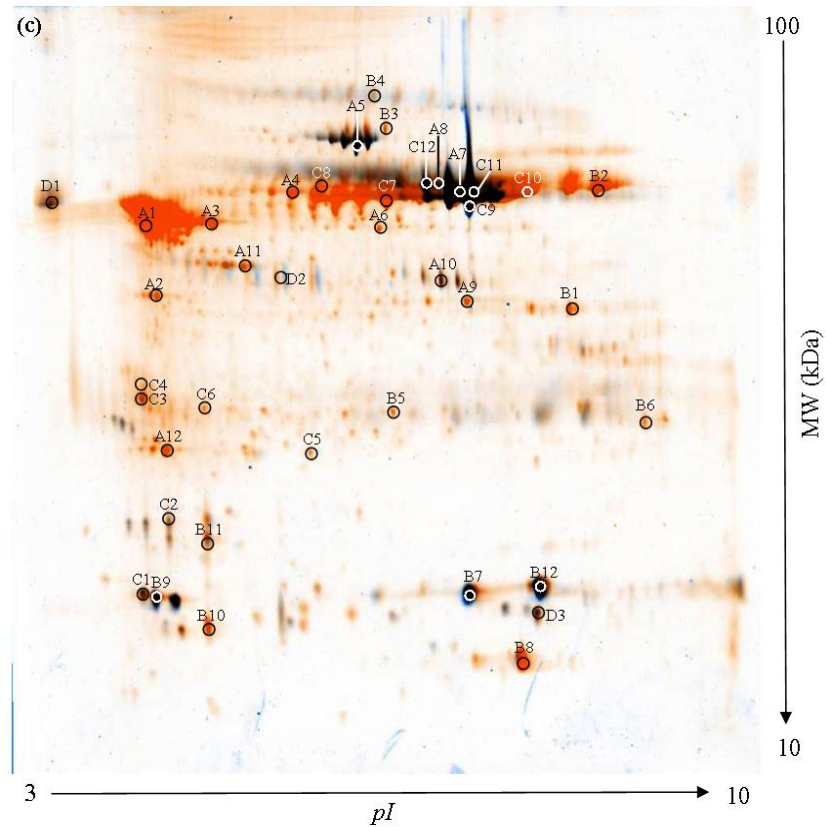


Identification of in vitro hydroxyapatite bound pellicle proteins

Comparison of the 2D gel electrophoresis patterns obtained from WMS samples (Figure 3.0.9(a)) with those obtained after incubation of WMS with HA (Figure 3.0.9 (b)) showed a similar pattern of protein distribution for all samples, from all three subjects (See Figure 3.1.0.). The number of spots observed on the 2D gel of saliva exposed to hydroxyapatite was much smaller than that observed on the 2-D gels of the saliva that was not exposed to hydroxyapatite. These missing proteins were assumed to be proteins adsorbing to hydroxyapatite, which can be considered to be good candidates for actual *in vivo* pellicle proteins.

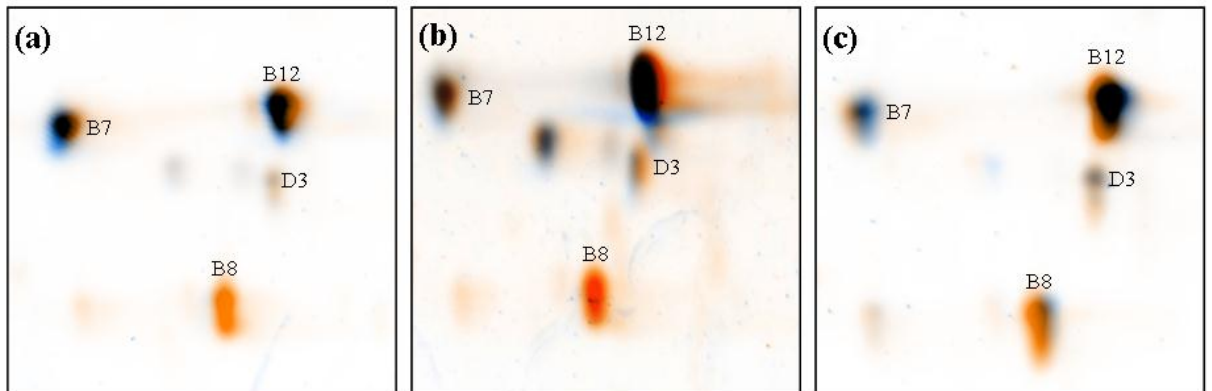
Figure 3.0.9. Two-dimensional gels obtained in pH range between 3 and 10 and 12.5% of SDS-PAGE stained with colloidal Coomassie blue of: (a) original WMS sample and (b) a hydroxyapatite incubated WMS sample (identifying non-adsorbed proteins) and (c) gels a and b overlaid to reveal salivary proteins that do adsorb (orange) and those that do not (Black/blue).





The specific adsorption of salivary proteins to hydroxyapatite was highlighted in Figure 3.1.0. Here it was observed that calgranulin-A (Spot B8) was present in all three volunteers saliva and selectively adsorbed to hydroxyapatite in all experiments. Whilst proteins Cystatin-SN and Cystatin-B were also present in all three volunteers saliva the adsorption of these proteins to hydroxyapatite was limited; highlighting the specific adsorption taking place between salivary proteins and hydroxyapatite.

Figure 3.1.0. A section of 2D gel displaying the selective adsorption of spot B8 (Calgranulin – A) to hydroxyapatite from 3 different volunteers (a), (b) and (c); and the limited adsorption of spots B7 (Cystatin-SN); B12 (Cystatin-SN); and D3 (Cystatin-B).



A total of 39 spots (highest scoring proteins) were identified from the 2D gels (See Table 3.2.). Many of the identified proteins were shown to be present in more than one form (Figure 3.1.0. and Table 3.2.). This could be due to fragmentation caused by bacterial degradation or by, phosphorylation, or glycosylation. For example, major proteins identified in different forms were salivary α -amylase, cheek mucosal cytokeratins, and the cystatins. The cystatins were identified in a number of isoforms (cystatin S, cystatin SN and cystatin B) that may differ with respect to phosphorylation and/or glycosylation [189]. In addition, a number of cytokeratins from oral epithelia were also present, such as, cytokeratin -4, -5, -13 and -16 which have all been shown to be present in the mouth [190].

Table 3.2. List of proteins identified from gel in Figure 3.0.9. (c). Several spots were assigned as the same protein, due to possible post-translational modifications, protein isoforms and peptides.

Spot	Accession number	protein name	Score	Mass (Da)	Significant (<0.05) sequences	PI
A1	P02533	Cytokeratin-14	900	51872	8	5.09
A2	P13646	Cytokeratin-13	1783	49900	23	4.91
A3	P08779	Cytokeratin-16	1201	51578	17	4.99
A4	P12035	Cytokeratin-3	448	64549	7	6.12
A5	P02768	Serum albumin	890	71317	28	5.92
A6	P19013	Cytokeratin-4	1737	57649	35	6.25
A7	P04745	Alpha-amylase 1	752	58415	18	6.47
A8	P04083	Annexin A1	217	38918	12	6.57
A9	P04083	Annexin A1	847	38918	15	6.57
A10	P23280	Carbonic anhydrase 6	185	35459	6	6.51
A11	P60709	Beta-actin	426	42052	12	5.29
A12	P31947	Stratifin	101	27871	3	4.68
B1	P07355	Annexin-2	700	38808	23	7.57
B2	P04259	Cytokeratin-6B	2020	60315	44	8.09
B3	Q08188	Transglutaminase E	811	76926	24	5.62
B4	P01833	Poly-Ig receptor	418	84429	11	5.58
B5	P04792	Heat shock protein β -1	327	22826	11	5.98
B6	P04083	Annexin A1	450	38918	15	6.57
B7	P01037	Cystatin-SN	317	16605	6	6.73
B8	P05109	Calgranulin-A	590	10885	12	6.51
B9	P01036	Cystatin-S	283	16489	5	4.95
B10	P06702	Calgranulin-B	66	13291	1	5.71
B11	P31025	Lipocalin-1	72	19409	2	5.39
B12	P01037	Cystatin-SN	952	16605	7	6.73
C1	P01036	Cystatin-S	127	16489	4	4.95
C2	P01036	Cystatin-S	290	16489	6	4.95
C3	P08779	Cytokeratin-16	108	51578	4	4.99
C4	P08780	Cytokeratin-16	221	51578	8	4.99
C5	P02533	Cytokeratin-14	658	51872	6	5.09
C6	P19013	Cytokeratin-4	884	57649	14	6.25
C7	P04745	Alpha-amylase 1	179	58415	8	6.47
C8	P13647	Cytokeratin-5	1207	62568	37	7.59
C9	P04745	Alpha-amylase 1	3810	58415	27	6.47
C10	P02538	Cytokeratin-6A	933	60293	29	8.09
C11	P04745	Alpha-amylase 1	2838	58415	31	6.47
C12	P04745	Alpha-amylase 1	828	58415	16	6.47
D1	P04745	Alpha-amylase 1	264	58415	12	6.47
D2	P25311	Zinc- α -2-glycoprotein	662	34465	19	5.71
D3	P04080	Cystatin-B	321	11190	6	6.96

Discussion

This chapter attempts to attain a general insight into the adsorption of saliva and focus on the way the salivary pellicle forms onto hydrophobic, silica and hydroxyapatite coated surfaces. Despite the different surfaces used, the amphipathic nature of proteins allowed a salivary pellicle to form instantaneously on to all of the surfaces. This is not to say that the surface had no effect on the pellicle structure. On the contrary, differences in pellicle structure were observed in many cases and these differences are likely to depend on the type of surface the saliva was adsorbing too, as all other conditions such as buffer concentration, temperature, adsorption time and rinsing steps were kept the same for all experiments.

QCMD: The salivary pellicle with the highest hydrated mass was observed on the QCMD hydroxyapatite coated sensor. This may suggest that a higher number of the proteins in saliva have a higher affinity to hydroxyapatite than polystyrene or silica, and subsequently more proteins adsorb to the hydroxyapatite sensor than the polystyrene or silica sensors. Santos *et al.* [124] also observed higher adsorbed amounts on hydroxyapatite compared to silica sensors via QCMD and ellipsometry. However, it may also be the case that it is in fact the type of proteins adsorbing to the hydroxyapatite sensor, rather than the quantity of proteins. This was because the QCMD measured all the adsorbed material on the sensor, including the water content of the pellicle. Consequently, the proteins that adsorb to hydroxyapatite may produce a pellicle that is capable of absorbing more water into its structure than the types of proteins adsorbing onto the polystyrene and silica sensors. This would help explain the higher hydrated mass observed, and it may not therefore simply be a matter of increased protein adsorption. Supporting this description of increased pellicle

hydration on the hydroxyapatite sensor was the dissipation data. This showed that the pellicle adsorbed to hydroxyapatite formed a softer, less rigid film compared to the pellicles adsorbed to silica and polystyrene; a less elastic pellicle would be suggestive of a more hydrated film. This would also compliment work by Veeregowda *et al.* [34] where the hydration of the pellicle is described to play an important role in the lubricating processes of the mouth. However, despite the evidence produced by the QCMD it was not possible to be explicit as to the precise mechanisms that resulted in a pellicle with a higher hydrated mass when salivary proteins adsorb to hydroxyapatite (increased protein adsorption vs. increased pellicle hydration). Consequently, pellicle formation was also observed via the DPI to measure the dry mass of the pellicle (i.e. pellicle layer without water content) using hydroxyapatite, silica and C-18 sensors; in order to mirror as closely as possible the sensors used for the QCMD.

DPI: The pellicle adsorbed to the hydroxyapatite sensor was much thicker and had a significantly higher mass than the silica and C-18 sensors. However, this difference was likely due to the difference in the surface roughness of the DPI hydroxyapatite sensor relative to the C-18 and silica sensors. The RMS surface roughness of the hydroxyapatite sensor was 4 times greater than the silica sensor and 2 times higher than the C-18 sensor. Rechendorff *et al.* [191] showed that the adsorption of fibrinogen increased with increasing RMS roughness, and that this increase in adsorption was beyond the accompanying increase in surface area. Subsequently, it was no surprise that the hydroxyapatite sensor adsorbed a pellicle that was thicker and was of a higher mass when compared to the smoother silica and C-18 surfaces. However, because the effective RI of the waveguide (i.e. DPI hydroxyapatite sensor)

changes in proportion to the amount of added material, the change in mass observed was still a valid measurement of the amount of added protein to the hydroxyapatite surface; only, the hydroxyapatite surface is microcrystalline and has a much larger surface area. As a result, this difference in surface area made it difficult to compare saliva adsorption and pellicle formation on hydroxyapatite sensors relative to the other smoother DPI sensors. Subsequently, the principle mechanism behind the observed increased mass on the hydroxyapatite sensors remains unresolved. Nevertheless, because hydroxyapatite is the main component of dental enamel the use of a DPI hydroxyapatite sensor is desirable when looking at pellicle formation. This is because hydroxyapatite is considered a good model for the chemical properties of the tooth surface [192]. As a result, the DPI hydroxyapatite sensor was a surface that could still be used to observe how pellicle structure changes depending on the type of saliva used (Chapter 4) and how the pellicle was affected by surfactants (see Chapter 7) when used as an independent measurement. Even though there isn't a comparable positively charged surface, to compare with the hydroxyapatite, it only has a small positive charge, yet has a very large adsorption of proteins, some of which are neutral and basic. Thus it would suggest that there is a more specific interaction with the substrate, especially as some of the identified proteins are known to bind calcium or have discrete negatively charged regions in their structure [193] and thus may well bind strongly to hydroxyapatite.

2D-gel & LC-MS/MS: The identification of proteins adsorbing to hydroxyapatite was also analysed via 2-dimensional SDS-PAGE of in vitro (hydroxyapatite) formed pellicle, and subsequent mass spectrometry of excised gels. Due to the miniscule quantities of protein that can be extracted from the DPI and QCMD sensors and from

the *in vivo* formed pellicle, experiments were performed *in vitro*. In this way the identification of the salivary proteins adsorbing to hydroxyapatite powder may help identify the proteins adsorbing to the QCMD and DPI hydroxyapatite sensors. Identification of these proteins may also provide supporting evidence to the structural observations made from the QCMD and DPI hydroxyapatite sensors. For example, there is clear evidence that enzymes perform a structural role in the pellicle [24]. This evidence was supported by the identification of proteins adsorbed to hydroxyapatite herein; where enzymes such as amylase, transglutaminase and carbonic anhydrase were identified. It has been suggested that protein aggregates that form in the mouth play a significant role in the formation of the pellicle [97]. The amino acid composition of these micelles is similar to that of a 2-hour *in vivo* pellicle layer [96]. Furthermore, electron microscope studies have also identified globular structures on *in situ* formed pellicles [35]. Consequently the rapid increase in pellicle mass and thickness observed from QCMD and DPI data maybe a result of protein aggregates adsorbing to the surface, rather than the adsorption of individual proteins. Although a full explanation behind the complexities of salivary protein adsorption to a surface is beyond the scope of this work (see reviews [194, 195] for more detail) it is understood that the adsorption of proteins from saliva onto the hydroxyapatite solid surface is the result of a number of non covalent interactions that simultaneously occur between components of saliva and hydroxyapatite.

At the surface of hydroxyapatite, calcium ions have a stronger tendency than the phosphate ions to dissolve, resulting in an overall negative charge at the surface [62]. This surface is subsequently coated with cationic calcium counter ions, resulting in an ionic double layer [68]. Consequently, although a number of forces dictate the

adsorption of proteins to a surface, basic proteins are more likely to be bound by ionic interactions via their positively charged amino groups with the negatively charged phosphate ions of hydroxyapatite. Whilst acidic proteins will bind via their negatively charged carboxyl groups with the positively charged calcium ions of hydroxyapatite [25]. In addition to these short range (< 5nm) ionic interactions, Van der Waals forces and hydrophobic interactions also contribute to the formation of AEP as these have a longer range of attraction (50 – 100nm and 10-50nm respectively) and therefore may help overcome potential repulsive forces between prospective pellicle components of the same charge [196]. These interactions result in the selective adsorption of only a certain number of proteins found in saliva (see Figure 3.1.0.); a phenomenon that has also been observed for salivary enzymes, where only a fraction of enzymes present in oral fluids have been detected in the pellicle [24].

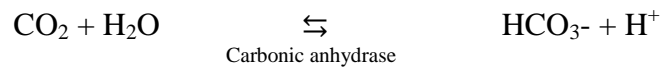
In addition to the evidence that enzymes are structural elements of the pellicle [105] it has been shown that amylase, lysozyme, carbonic anhydrases, glucosyltransferases and fructosyltransferase are immobilized in an active conformation in the pellicle layer where they exhibit buffering properties and antibacterial effects in addition to their influence on the structural modification of AEP [24]. Two of these salivary enzymes (amylase & carbonic anhydrase) were also identified herein and are worthy of particular focus. The reader is also referred to references [24, 27, 60] for more detailed discussion on other enzymatic properties of the pellicle.

Amylase: Using various techniques, amylase has been shown to be one of the major components of AEP. It has been detected in both experimental pellicles and *in situ*

formed pellicles [60] and is known to be the most abundant enzyme in human saliva [197]. The enzymatic role of amylase is to catalyse the breakdown of dietary starch to glucose and maltose saccharides, to facilitate absorption into the body [77]. However, glucose and maltose can be further metabolized by cariogenic bacteria to organic acids, which can lead to tooth demineralisation [102]. So why does the pellicle contain an enzyme that appears to promote cariogenic bacteria so close to the tooth surface? Firstly, amylase is an important structural component of AEP as it forms heterotypic complexes with Mucin Glycoprotein 1, which is the most abundant mucin detected in the pellicle. Consequently, amylase is considered to be an important precursor protein in the initial formation of the pellicle [105]. Secondly, the amylase adsorbed into the AEP undergoes conformational changes, so that pellicle-bound amylase has a lower affinity to starch than the amylase found free in saliva [198]. In other words, pellicle bound amylase does not produce as much fermentable carbohydrates for bacteria as unbound amylase, free in saliva. Subsequently, amylase adsorbed onto AEP provides protection for tooth enamel via its structural role in pellicle formation, whilst its capacity to produce fermentable carbohydrates for cariogenic bacteria is negligible.

Carbonic anhydrase (CA): CA exists as a number of isoenzymes, though CA II and CA VI are the two that are dominant in AEP. CA II and VI has been shown to be present *in situ* formed pellicles [23]; and van der Mei [135] showed that the immobilized enzyme retains its biological activity *in vivo*. The CAs catalyse the reversible reaction seen in equation below. This has an important protective function for teeth, as CA accelerates acid removal in the local environment of the tooth surface, thus preventing carie formation.

Equation 1. Carbonic anhydrase drives the reaction converting carbonic acid to carbon dioxide and water (see below), which effectively takes up accessible hydrogen ions.



Salivary flow ensures that there is enough bicarbonate [HCO₃⁻] present to take up excess [H⁺] so that when acid is produced within the mouth the increase in [H⁺] will move the position of equilibrium to the left, producing more carbon dioxide and water. Now, although carbon dioxide is also an acid, in an open system such as the mouth, carbon dioxide is converted from a dissolved state into a volatile gas where it is lost to the atmosphere. Thus the acidic environment has been neutralised and demineralisation of teeth prevented. From the above discussion, enzymes not only play a role in pellicle structure, but are also involved in pellicle function.

In conclusion, this chapter has summarised the physical properties of the pellicle and how these properties can be influenced by the surface to which the pellicle adsorbs. Furthermore, identification of the proteins that adsorb to hydroxyapatite help explain the structural formation of the pellicle that adsorbs to the hydroxyapatite coated DPI/QCMD sensors and how some of these proteins maintain some activity.

Although this work raises some interesting points regarding pellicle structure and pellicle composition the reader should be made aware that the systems used in this work do not reflect the dynamic conditions of the mouth, such as, the continual flow and clearance of saliva. As a result, several differences have been found between pellicles formed *in vitro* and those *in vivo* [35, 117]. Furthermore, enzymes from bacterial cells, mucosal tissues and from consumed foods can also integrate into the pellicle *in vivo* and may too influence pellicle structure [for more details see 36, 106]; factors that could not be simulated in this work.

Chapter 4

Structural Characterisation of Parotid and Whole Mouth Salivary Pellicles Adsorbed onto DPI and QCMD Hydroxyapatite Sensors

Introduction

In the previous chapter the selective adsorption of salivary proteins, including enzymes and glyco-proteins at the tooth/saliva interface resulting in the formation of a salivary pellicle was observed [1]. As this pellicle constitutes an interface between teeth and the oral environment, it is universally accepted to be of prime importance for several protective functions within the oral cavity [14, 15, 34]. Despite the importance of the pellicle in oral physiological and pathological processes, an understanding of the fundamental physical and molecular mechanisms underlying the structural formation of this protein film remains unresolved. This is because the adsorption of salivary proteins required for pellicle formation is influenced by a number of variables inherent to the individual, making it difficult to elucidate the respective roles that salivary proteins play in pellicle formation. For example, protein adsorption may be affected by the location of teeth in the mouth and the tooth's physical (e.g. surface roughness) and chemical (e.g. hydrophobicity of enamel) properties [35, 83-85]; a phenomenon that was also observed in the previous chapter. Other factors such as the dynamic protein composition of individual's saliva and the effect that exogenous proteins (food- or bacterially-derived) may have on the pellicle can complicate the interpretation of results. Therefore numerous methodical approaches have been designed to explore pellicle formation. For example, *in vivo* studies have been used where the pellicle is scrapped from the tooth surface [50, 86]; or *in situ* studies, where enamel, often bovine, is exposed in the oral cavity [72]; or *in vitro* studies where different substrates are exposed to collected saliva extra-orally [87, 192, 199]. In this study the differences in the properties of pellicles formed from stimulated parotid saliva (PS), which contains little or no mucin; and stimulated

whole mouth saliva (WMS), which contains mainly two types of mucin: MUC5B and MUC7[200] was investigated. By combining the data from quartz -crystal microbalance with dissipation monitoring (QCM-D) and a dual polarisation interferometer (DPI) the formation and structure of the salivary pellicle by contacting WMS and PS with hydroxyapatite (the main component of enamel[201]) coated sensors was observed. Combining these techniques not only allowed us to measure the hydrated mass, dry mass, thickness and viscoelastic properties of the pellicle; but also to record the density of the PS and WMS formed pellicles. The pellicle density was a physical parameter of pellicle structure that had hitherto been assumed and not directly measured. Therefore, this study takes our understanding of the formation and structure of this salivary film a step further; as one can now comment on the packing of the pellicle proteins (i.e. low density \equiv diffuse pellicle or high density \equiv compact pellicle). With this added information the kinetic adsorption processes involved in the formation of PS and WMS salivary pellicles were observed. Subsequently, the role that different salivary components (e.g. mucins) have on the formation and structure of the salivary pellicle as it takes place on the tooth surface was hypothesized.

Materials and methods

Saliva collection

10 WMS and 10 PS samples were obtained from 14 apparently healthy, non-smoking, male and female volunteers, ranging in age from 20 to 50 years. Volunteers refrained from eating 1 hour prior to donation, and rinsed their mouths twice with 10 mL of bottled still water (Waitrose, UK). To collect WMS, volunteers then chewed on flavour-free gum (Gumlink, Denmark) and expectorated the saliva into a small sterile collection until they had produced 10 mL of saliva. The stimulated PS was collected using a sterilised Lashley suction cup [177]. The salivary secretion was stimulated by sucking citric acid containing boiled sweets ('Rosey-Apples', ASDA, UK). This continued until 20-30 mL of saliva had been produced. Samples were kept on ice upon expectoration, and were used as soon as possible upon collection. The protein content of each collection was measured via the bicinchoninic acid (BCA) assay (Pierce Chemical Co., Illinois, USA) using bovine serum albumin as a protein standard[178].

Saliva adsorption protocol

All substrates used were coated in hydroxyapatite (HA). QCM-D measurements were performed using a D300 QCMD (Q-Sense AB, Vastra Frolunda, Sweden) with a QAFC 302 axial flow measurement chamber maintained at 36.8°C. HA coated AT-cut piezoelectric quartz crystals sandwiched between gold electrodes (QSX-303, Q-Sense AB, Vastra Frolunda, Sweden) were used as the substrate. Measurements of pellicle thickness and refractive indices (RI) were performed using an AnaLight Bio200 DPI (Farfield Sensors Ltd., Manchester, UK). The device used a silicon-nitride sensor that was coated with HA. The sensor was clamped in a

temperature-controlled enclosure and maintained at 36.8°C for all experiments. A 0.5 ml sample of saliva (PS or WMS depending on the experiment) was injected into the QCMD and DPI instruments at the same time (both used static adsorption systems i.e. not a flow-cell). Pellicle formation was monitored for 120 minutes before rinsing with a 0.5ml simulated salivary buffer solution (see below). Three data points were collected during the time course of the experiment: at 1 minute adsorption, 120 minutes adsorption and at 130minutes (i.e. post buffer rinse).

Simulated salivary buffer

A simulated salivary buffer of similar ionic strength to saliva was used (100 mM NaCl, 1 mM CaCl₂, 3 mM Na₃PO₄ and HEPES, pH 7.5). Solutions were prepared in deionised and filtered ultra-pure water (Nanopure Diamond, Barnstead Int., USA).

Sensor properties

The substrates used for the adsorption of saliva were ten QCMD hydroxyapatite (Q-Sense AB, Vastra Frolunda, Sweden) and ten DPI hydroxyapatite coated sensors (Farfield Scientific, Manchester, UK); each one used a maximum of three times. The HA sensors were calibrated to take into account the R.I. (1.52) and thickness (940nm) of this hydroxyapatite layer when measuring the thickness, mass and density of the salivary pellicle. This was done by stripping the hydroxyapatite from one of the sensors (using phosphoric acid at pH1.7) and measuring the subsequent phase change of TE and TM upon removal of hydroxyapatite. The R.I. and thickness values of the hydroxyapatite sensors could then be calculated and entered manually into the software for subsequent salivary film analysis; assuming that all of the DPI hydroxyapatite sensors were coated with similar quantities of hydroxyapatite.

Sensor cleaning

After the completion of the experiment, QCMD and DPI surfaces were cleaned with 2% w/v SDS (Sigma-Aldrich, UK), followed by 2% w/v HX then copiously rinsed with simulated salivary buffer followed by MiliQ water rinsing and dried with oxygen free nitrogen gas. Finally, QCMD sensors were exposed to UV-ozone (Bio-Force Nanosciences Inc., Iowa, USA) for 20 min.

Mucin immuno-blotting

Immuno-blotting a 1 µl sample from each of the whole mouth and parotid saliva dilutions (dilution factor: 5, 10, 15) were transferred onto an Immuno-Blot PVDF membrane (0.2 µm pore, Bio-Rad) and were left to dry for 2 h. Unoccupied protein-binding sites of the membrane were then blocked by incubation (2 h, 25°C) with 5% Bovine Serum Albumin (Sigma) in phosphate buffered saline and Tween 20 (PBST) solution (137 mM NaCl, 10 mM Na phosphate, 2.7 mM KCl, 0.1% v/v Tween 20, pH 7.5) followed by washing in PBST (3 x 5 min, 50 mL). The membranes were then incubated separately in a 1:250 dilution of MUC 1, MUC 2, MUC5AC, MUC5B and MUC7 rabbit polyclonal antibody and MUC6 goat polyclonal antibody respectively (Santa Cruz Biotechnology, inc. Dallas, USA); and placed on a shaker in fridge at 4°C for 10 h. The membranes were then washed in PBST (3 x 5 min, 50 mL) and then incubated in a 1:1000 dilution of goat anti-rabbit alkaline phosphatase conjugate and rabbit anti-goat for MUC6 (Santa Cruz Biotechnology, inc. Dallas, USA) for 3 h at 25°C and then washed in PBST (as above). Bound antibody was located by briefly washing the membrane in water (1 x 30 s, 100 mL) and then staining using 10 mL of a SIGMA FAST™ BCIP/ NBT substrate tablet solution (1

tablet in 10 mL of water). The washing step was sufficient to remove any inhibitory effect of phosphate on the alkaline phosphatase.

Statistics

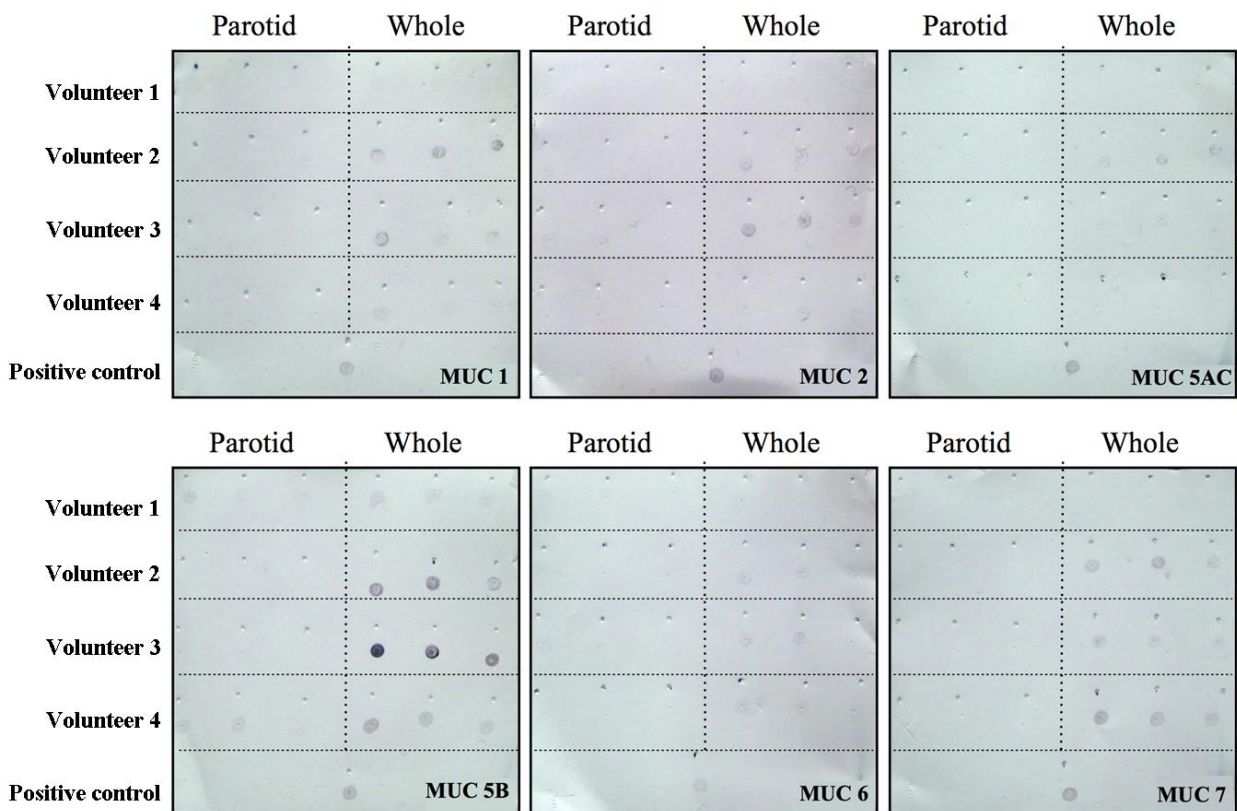
Significant differences in pellicle mass, thickness and density in relation to WMS and PS formed pellicles was determined by two sample t tests at three points of the experiment (i.e. pellicle formed after 1 minute; pellicle formed after 2 hrs and pellicle post buffer rinse) using GenStat (14th Edition, VSN International Ltd, Hemel Hempstead, UK). In addition, simple linear regression analysis of pellicle mass as a function of the protein concentration of saliva was carried out; also using GenStat. A p value < 0.05 was considered significant in all statistical analysis.

Results

Mucin composition

An immunoblot test was performed using rabbit and goat polyclonal antibodies against MUC 1, 2, 5AC, 5B, 6 and 7. A number of mucins were present in the WMS of all volunteers tested (See Figure 4.1.) were observed. Conversely all these mucins were absent from PS with only traces of MUC 5B being detected in the PS of volunteer 1 and 4, possibly due to the presence of minor salivary glands close to the parotid gland duct on PS collection. Despite this, the immunoblot used confirmed the scarcity of all 5 types of mucins from PS, but their presence in WMS.

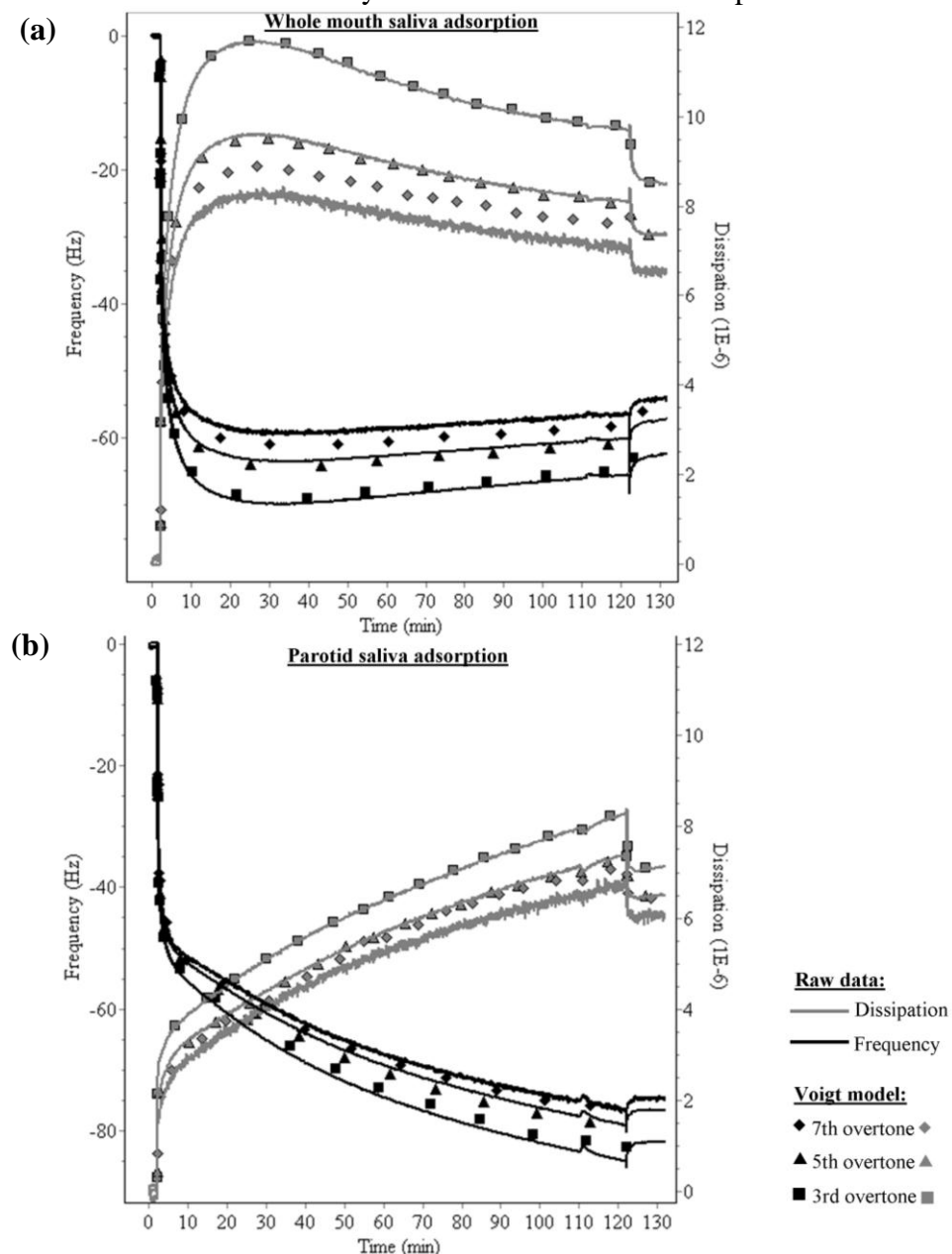
Figure 4.1. Immunoblot displaying the presence of mucins (MUC 1, 2, 5AC, 5B, 6 and 7) in WMS and their general absence from PS in 4 of the 14 volunteers' saliva used in this study. MUC 7 and MUC 5B being the primary mucins present in saliva; with traces of epithelial derived mucins (MUC 1 and MUC 2); and very faint blots of pulmonary (MUC 5AC) and human gastric (MUC6) mucins.

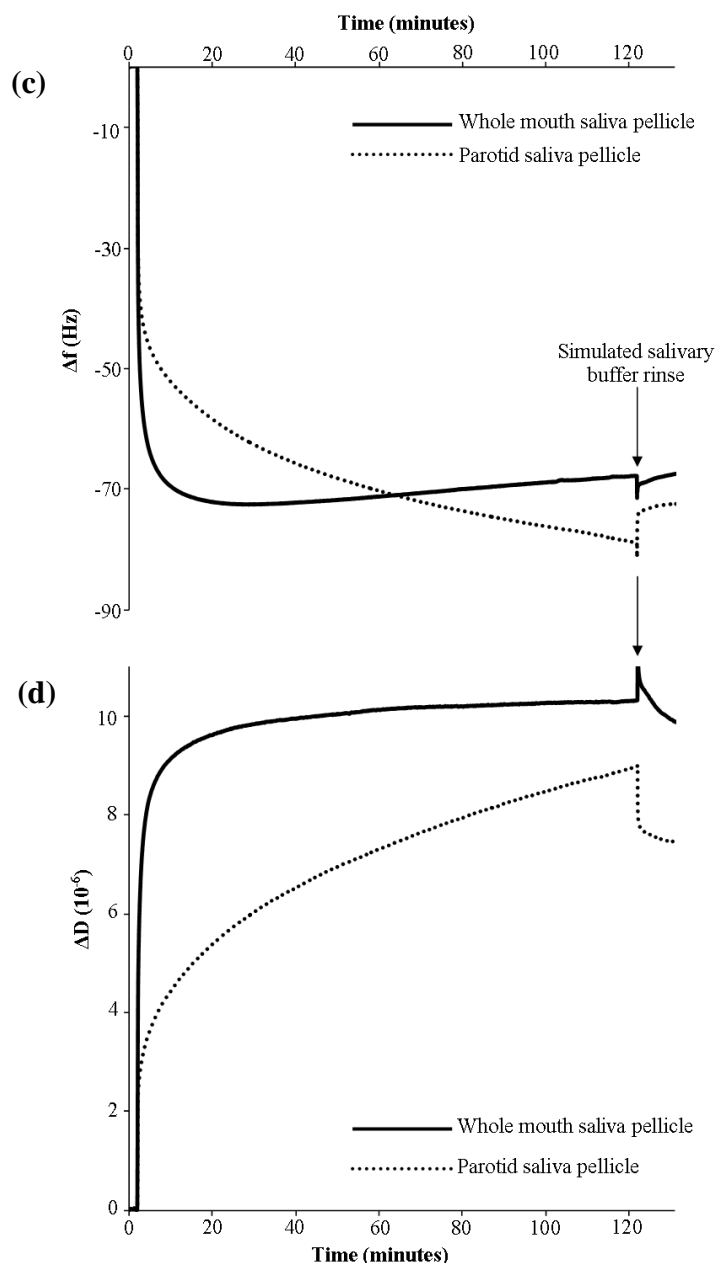


QCM-D pellicle adsorption

Figure 4.2. shows the frequency and dissipation profile for WMS and PS adsorption onto hydroxyapatite surfaces measured at the 3rd overtone. Upon addition of WMS and PS a rapid decrease in frequency, due to an increase in adsorbed hydrated mass, was observed. While the WMS pellicle reached a plateau after 20 min adsorption, the proteins from PS continually adsorb to the surface even after 120 minutes.

Figure 4.2. The adsorption profile of an example (a) WMS and (b) PS sample; with raw data and fitted Voigt modelled data (WMS $\chi^2 = 9.3 \times 10^5$; PS $\chi^2 = 13.5 \times 10^5$). Adsorption profile of (c) mean frequency and (d) mean dissipation changes versus time; measured for the 3rd overtone by QCM-D for the adsorption of WMS (n=10) and PS (n=10) pellicle on hydroxyapatite coated sensors. Frequency decreases instantly, with a concomitant rapid increase in dissipation, as the saliva rapidly adsorbs to the sensor surface. Following 120 minutes adsorption a simulated salivary buffer was used to remove loosely adsorbed material from the pellicle.





When Δf and ΔD were used in Voigt model analysis the initial rate of adsorption for WMS and PS was recorded at 868 ± 475 ng/cm²/min and 520 ± 240 ng/cm²/min respectively (see Table 4.1.). This reduced to -1 ± 3 ng/cm²/min for WMS and 7 ± 2 ng/cm²/min for PS in the last hour of pellicle adsorption. The mass uptake was also accompanied by a rapid increase in energy dissipation. The PS pellicle had a slower increase in dissipation in the early stages of pellicle formation, compared to WMS, which inferred that the PS pellicle was more rigid with respect to the WMS pellicle.

In fact, the dissipation value for WMS pellicle reached a plateau almost instantly, as opposed to the dissipation value for PS pellicle, which increased incrementally over time.

Table 4.1. QCM-D values of the adsorbed Sauerbrey and Voigt mass, thickness and rate of formation for WMS (n=10) and PS (n=10) determined on hydroxyapatite surfaces after 1 minute and 2 hour saliva adsorption; and after rinsing with simulated salivary buffer.

Saliva	<i>Raw data</i>		<i>Sauerbrey Model</i>			<i>Voigt Model</i>		
	ΔF_3 (Hz)	ΔD_3 (10^{-6})	Thickness (nm)	Mass (ng/cm ²)	Rate of formation (ng/cm ² /min)	Thickness (nm)	Mass (ng/cm ²)	Rate of formation (ng/cm ² /min)
1 minute adsorption								
Whole	-55 (± 14)	7 (± 3)	10 (± 2)	963 (± 246)	305 (± 126)	25 (± 13)	2450 (± 1280)	868 (± 475)
Parotid	-40 (± 9)*	3 (± 2)*	7 (± 2)*	712 (± 155)*	167 (± 41)*	15 (± 6)*	1462 (± 645)*	520 (± 240) ^a
2 hour adsorption								
Whole	-70 (± 16)	10 (± 4)	12 (± 3)	1220 (± 281)	-1.1 (± 1)	27 (± 8)	2683 (± 820)	-1 (± 3)
Parotid	-78 (± 11)	9 (± 3)	14 (± 2)	1362 (± 192)	5.38 (± 3)*	27 (± 9)	2689 (± 868)	7 (± 2)*
post buffer rinse								
Whole	-69 (± 15)	9 (± 4)	12 (± 3)	1203 (± 207)	-3 (± 2)	27 (± 9)	2681 (± 902)	-14 (± 32)
Parotid	-72 (± 12)	8 (± 2)	13 (± 2)	1254 (± 208)	-2 (± 4)	24 (± 10)	2424 (± 1028)	-4 (± 7)

* = $p < 0.05$; a = 0.054

N.B. modelled mass differs from the modelled thickness due to the assumed density of the adsorbed pellicle and therefore the two parameters are statistically identical.

Protein concentration

The mean protein concentration of WMS was 1.6 ± 0.6 mg/ml and PS 0.9 ± 0.3 mg/ml, samples collected were shown to be significantly different ($p < 0.05$) (see Figure 4.3.). Although few studies, if any, have directly compared the protein concentration of WMS with PS from the same group of volunteers, the results are similar to individual studies of PS [202] and WMS [203] protein concentration. PS protein concentration was shown to have a significant ($p < 0.05$) positive association to the adsorbed hydrated Sauerbrey mass of the adsorbed salivary pellicle (Figure 4.4. (a)). Thus, with increasing protein concentration of PS, an increase in the hydrated Sauerbrey mass of the pellicle was observed. Conversely, the WMS protein

concentration was shown to have no significant ($p=0.3$) association to the adsorbed hydrated Sauerbrey mass of the pellicle; and therefore, was independent of protein concentration (Figure 4.4. (b)).

Figure 4.3. Box plot displaying the variation in the protein concentration of PS ($n = 33$) and WMS ($n = 42$).

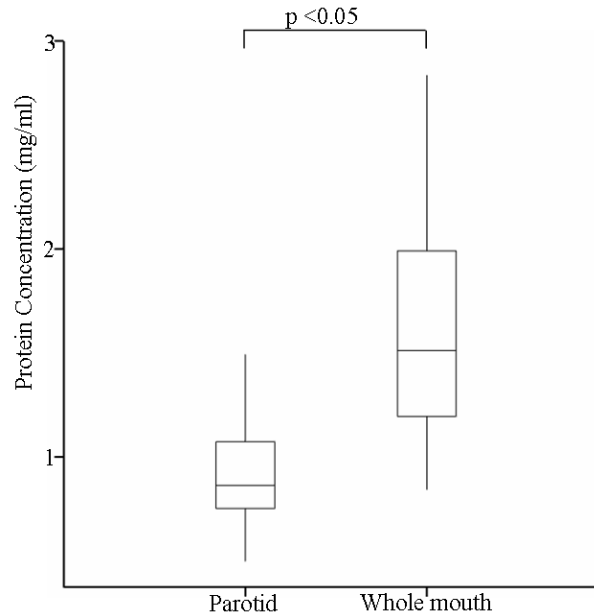
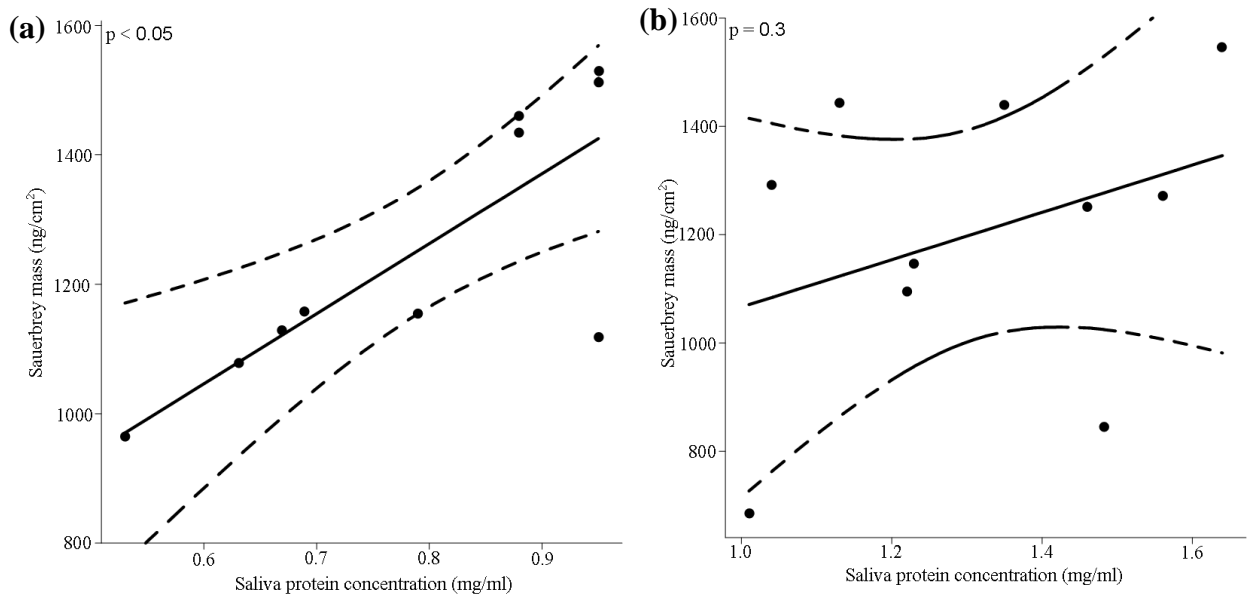


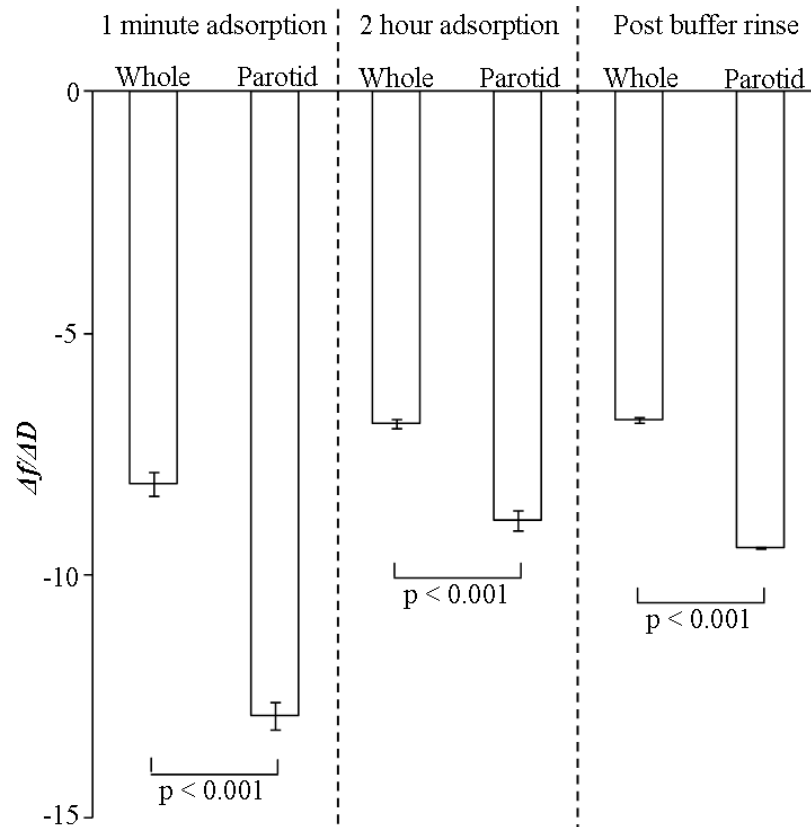
Figure 4.4. linear regression analysis of Sauerbrey mass as a function of the protein concentration for (a) PS ($n=10$) and (b) WMS ($n=10$) derived pellicles. This suggests that the PS protein concentration had a positive association to the adsorbed Sauerbrey mass of the adsorbed salivary pellicle.



Viscoelastic properties

By comparing the ratio between Δf (Hz) and ΔD (unitless) (see Fig. 4.5.) one can observe the viscoelastic properties of the adsorbing pellicle with respect to the induced energy dissipation of the sensor per coupled unit mass. Such that a more negative $\Delta f / \Delta D$ value indicates the addition of mass without eliciting a significant dissipation increase, which is characteristic of a rigid, elastic salivary pellicle. Conversely a less negative $\Delta f / \Delta D$ value indicates a viscoelastic, more dissipative, salivary pellicle. PS formed pellicle was predominantly more elastic after 1 min adsorption ($-12.8 \Delta f / \Delta D$), 2 h adsorption ($-8.8 \Delta f / \Delta D$) and after rinsing with buffer ($-9.4 \Delta f / \Delta D$) with respect to the WMS pellicle where the $\Delta f / \Delta D$ ratio at the same time points was -8.1 , -6.8 and -6.8 , respectively.

Figure 4.5. Bar chart displaying the ratio of $\Delta f/\Delta D$ for WMS and PS derived pellicles at three different stages of pellicle formation. Throughout the experiment the PS formed a pellicle that had a lower $\Delta f/\Delta D$ ratio than WMS derived pellicle. This suggests that the PS derived pellicle was more elastic relative to WMS derived pellicle.



DPI Pellicle adsorption

On the introduction of WMS and PS to the DPI hydroxyapatite sensor, a rapid increase in the polymer mass, thickness and density of the pellicle was observed (see Figure 4.5. (a) and (b)). PS and WMS formed a salivary pellicle at a mean rate of $1576 \pm 392 \text{ ng/cm}^2/\text{min}$ and $954 \pm 493 \text{ ng/cm}^2/\text{min}$ in the 1st minute of pellicle adsorption respectively (see Table 4.2.). Consequently, the PS formed pellicle deposited more mass ($1576 \pm 392 \text{ ng/cm}^2$) compared to the WMS formed pellicle ($954 \pm 493 \text{ ng/cm}^2$) after 1 minute of adsorption. However, over time (>1hour) no statistical difference between WMS and PS pellicle mass and thickness was

observed; and the rate of formation for WMS effectively stops at $-0.2 \pm 1 \text{ ng/cm}^2/\text{min}$; whilst for PS it slows considerably to $1 \pm 2 \text{ ng/cm}^2/\text{min}$ (see Figure 4.6.). The pellicle thickness of both PS and WMS formed pellicles ranged from 12 – 24 nm at different stages of pellicle formation (similar to the Voigt modelled pellicle thickness measured via QCM-D) and at no point of the experiment was a statistical difference observed. Nevertheless, a consistent difference in pellicle density between PS and WMS formed pellicles was consistently observed.

Figure 4.6. Adsorption profile of (a) WMS (n=10) and (b) PS (n=10) forming a pellicle over time on a DPI hydroxyapatite coated sensor. Thickness, mass and density of the pellicle increase rapidly as the saliva rapidly adsorbs to the sensor surface. Following 120 minutes adsorption a simulated salivary buffer was used to remove loosely adsorbed material from the pellicle.

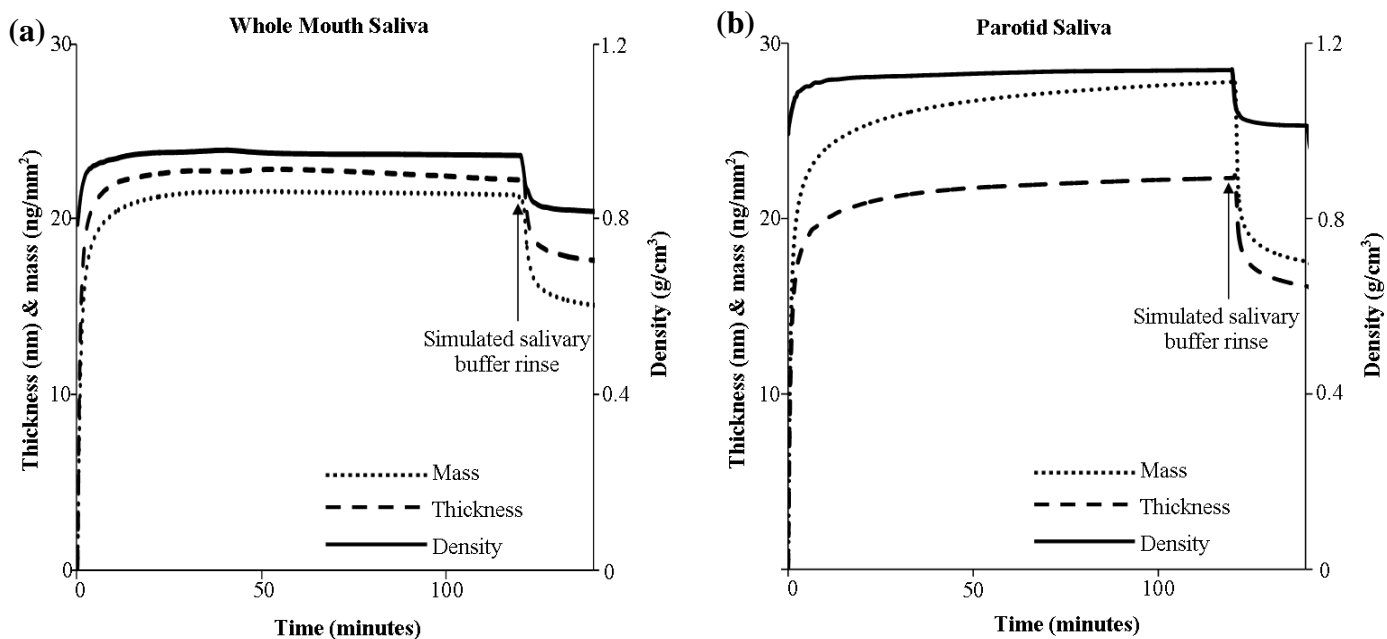


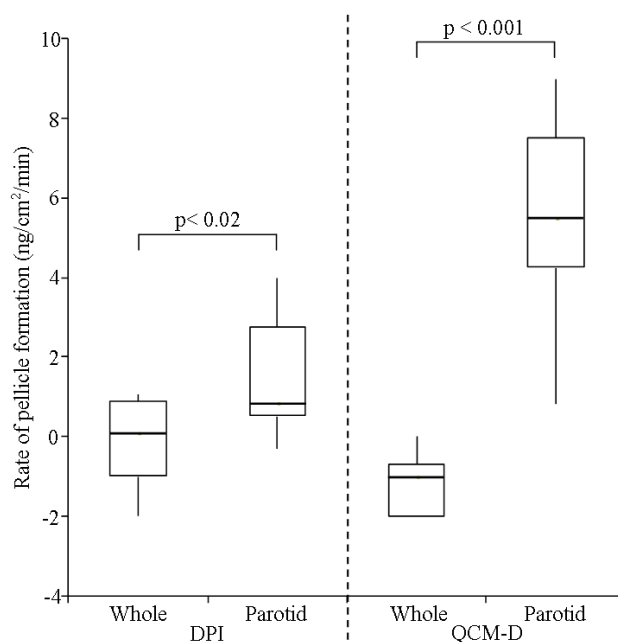
Table 4.2. DPI values of the adsorbed polymer mass, density and thickness for WMS (n=10) and PS (n=10) determined on hydroxyapatite surfaces after 1 minute and 2 hour saliva adsorption; and after rinsing with simulated salivary buffer.

Saliva	Mass (ng/cm ²)	Density (g/cm ³)	Thickness (nm)
1 minute adsorption			
Whole	954(±493)	0.8(±0.2)	12(±6)
Parotid	1576(±392)*	1.0(±0.1)*	15(±5)
2 hour adsorption			
Whole	2195(±1160)	0.9(±0.2)	22(±8)
Parotid	2781(±797)	1.1(±0.1)*	24(±8)
Post buffer rinse			
Whole	1442(±744)	0.8(±0.3)	17(±5)
Parotid	1758(±705)	1.0(±0.2) ^a	17(±6)

*= p < 0.05;

^a = 0.058

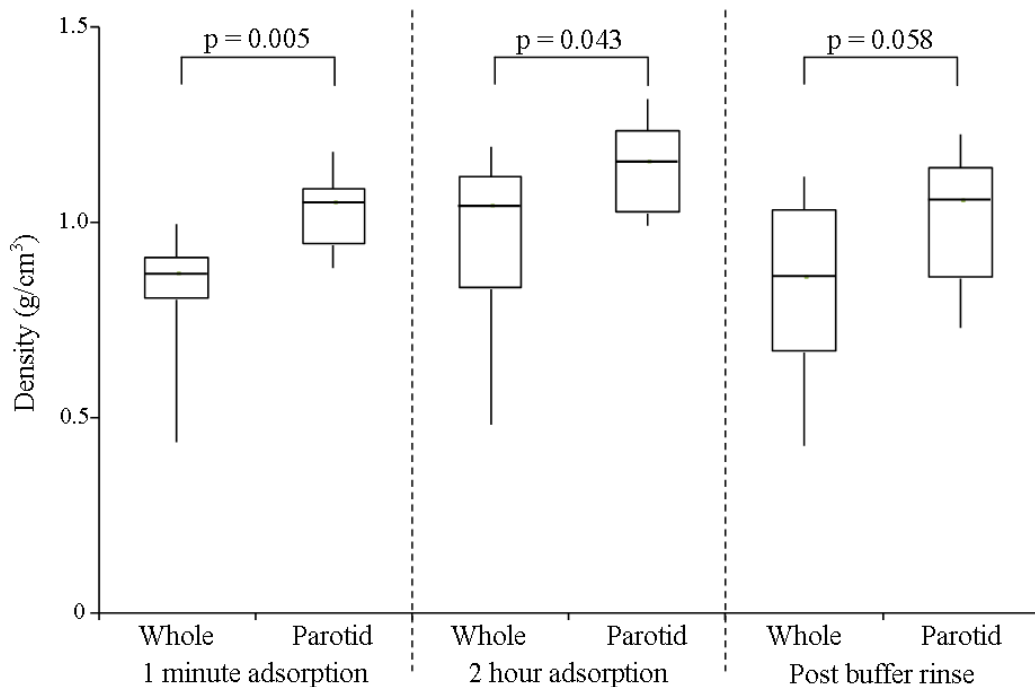
Figure 4.7. Box plot displaying the rate of pellicle formation derived from PS and WMS after 2 hours adsorption. The PS continually adsorbs to the surface of both QCMD and DPI sensors for the duration of the experiment. Whereas WMS formed pellicle stopped adsorbing and actual desorption of pellicle mass was observed.



Pellicle density

In the 1st minute of adsorption the densities of the PS ($1.0\pm 0.1\text{g/cm}^3$) and WMS ($0.8\pm 0.2\text{g/cm}^3$) formed pellicles differed significantly ($p < 0.05$). In fact, the difference in pellicle density for WMS and PS derived pellicle was consistently observed throughout the experiment (see Figure 4.8.). The maximum mean pellicle density ($1.1\pm 0.1\text{g/cm}^3$) occurred after 2 hours PS pellicle adsorption and the lowest pellicle density ($0.8\pm 0.3\text{g/cm}^3$) occurred after rinsing the WMS pellicle after 120 minutes of adsorption. This suggests that the pellicle formed from PS was more compact on the sensor surface; as opposed to the WMS pellicle, which produced a pellicle with a lower density, suggesting a more diffuse pellicle.

Figure 4.8. Density difference between PS and WMS pellicle at different stages of formation. Throughout the experiment the density of the PS derived pellicle was higher than that of the WMS derived pellicle. This suggest that the WMS derived pellicle is more diffuse relative to the PS derived pellicle.



Discussion

The focus of this study was to compare the differences in the pellicle structure formed from stimulated PS and stimulated WMS using optical (DPI) and acoustic (QCM-D) methods in order to explain how observed structural differences between PS and WMS pellicle came about. Furthermore, by comparing the pellicle forming properties of WMS with that of PS an indication of the role that salivary mucins play in pellicle formation and structure was provided; as the latter contains little or no mucins. The primary mucins detected in WMS i.e. MUC 5B (MG1) and MUC 7 (MG2), were to be expected, however it was also observed that traces of epithelial derived mucins (MUC 1 and MUC 2) were present. Faint blots of pulmonary (MUC 5AC) and human gastric (MUC6) mucins were observed; although, these signals were very weak and could easily be caused by some cross reactivity with mucins or aspecific binding to other compounds. Despite this, the literature often only cites the presence of MG1 and MG2 in saliva, which this study has shown not to be the case. Nevertheless, with respect to understanding the physical properties of the pellicle it is MG1 that generates most interest as it is not only the most concentrated mucin in saliva[200]; but also because it has a higher affinity for the tooth mineral (hydroxyapatite) than the other main salivary mucin, MG2 [204].

The mucins contain a number of sites that can potentially promote adsorption to a surface. These include hydrogen bonding and hydrophobic interactions via the carbonyl groups and methyl groups found in N-acetyl residues (i.e. N-acetyl glucoasamine, N-acetyl galactosamine) and electrostatic interactions via sialic acid residues [205].

In Table 4.2. and Figure 4.6. the polymer mass, thickness, density differences between WMS and PS pellicles using the DPI is presented. This shows that WMS and PS pellicles reach a thickness of ~20nm after 2 hours of adsorption. This compares well with our own QCMD data and that found in other studies [140, 144, 206]; where observed pellicle thicknesses ranged between ~20 and ~40nm. Considering that globular proteins of mass of 50kDa will have a diameter of approx 5nm [207] it is clear that the pellicles investigated here are likely be composed of multilayers, as seen in work by Baek *et al.* in 2009[32].

Considering that all salivary proteins are amphiphilic, regardless of their glandular origin, some relationship between salivary protein concentration and pellicle mass may be expected. However, it was observed that only the PS protein concentration was correlated with pellicle mass (Figure 4.4. (a)), and that increasing concentrations of salivary proteins contained within WMS did not necessarily result in a higher surface mass concentration of adsorbed pellicle (Figure 4.4. (b)). Whilst it was shown previously that low molecular proteins present in parotid saliva, primarily statherin, form a primary adsorbed layer [39, 51], which will typically follow monolayer adsorption behaviour, and adsorption will be self-limiting when the surface is saturated [195]; to suggest a typical adsorption profile for WMS is a difficult task considering the complex mixture of proteins present in WMS [208]. Hannig & Hannig [18] describe how adsorption of salivary proteins to form the pellicle will be driven by electrostatic and hydrophobic interactions. The smaller MW, surface active proteins that are rich in phosphor-serines (i.e. histatins and statherin) will have a higher diffusion coefficient, and a strong affinity for the hydroxyapatite surface, allowing them to adsorb more quickly and form the primary

layers in both PS and WMS. Subsequent adsorption will depend on the attractive interactions between the proteins present, perhaps enhanced by specific calcium mediated interactions [33].

For PS, the absence of the large mucins allows the smaller proteins to continually form a dense pellicle. The speed and hence extent of the pellicle formation with PS will therefore be influenced by the protein concentration. In contrast, the presence of the much larger MW mucin proteins in WMS will reduce the packing density and lead to a less dense pellicle, as observed in Figure 4.8. Therefore, the formation of the pellicle from WMS becomes complex, due to the presence of mucins. At low mucin concentrations, protein adsorption is rapid, forming a dense pellicle. At high mucin concentrations, higher viscosity will slow protein diffusion to the surface, particularly the large MW proteins, and the presence of mucins will reduce pellicle density. However, as the proportion of parotid saliva in WMS is not known in these samples, and may vary between individuals, no clear relationship between protein content and pellicle formation could be derived. Nevertheless, the PS pellicle was shown to be much denser than WMS pellicle which would suggest that the proteins present in PS are able to form a more compact pellicle when compared to WMS pellicle, as was suggested from the DPI analysis. This would infer that proteins from PS may be important for the formation of the dense basal layer of the enamel pellicle.

From the QCMD data it was observed that unlike PS pellicle formation, where adsorption of proteins never reached equilibrium, WMS pellicle reached a plateau, and began to lose mass, suggesting that components present in WMS are preventing

further pellicle growth after a certain point (see Figure 4.2. (c)). It is possible that mucins may be arranging themselves in a way that halts the continual adsorption of salivary proteins once the pellicle has formed. Santos *et al.* [124] also observed conformational changes in the pellicle after initial protein adsorption had taken place. However, it may be that under the current experimental procedure salivary proteins required for further pellicle growth become exhausted; whereas in the mouth, saliva, and thus pellicle proteins, are constantly being replenished. In Table 4.1. Here two estimates of the hydrated mass, thickness and rate of pellicle formation based upon a rigid elastic film (Sauerbrey model) and a softer more viscoelastic film (Voigt model) have been presented. It can be observed that the main differences between the way WMS and PS pellicles form occurs in the first minute of adsorption. Here, the WMS pellicle develops faster than the PS pellicle forming a pellicle that is thicker and higher in hydrated mass. Although after 60 min adsorption the mass of PS and WMS films is the same, which suggests that the proteins present in PS are able to continually adsorb to the surface forming multilayers of low molecular weight proteins; and although the mass may be similar, the density, thickness and rate of formation are different. So although there may be similarities during the primary formation due to the role of the parotid proteins in both samples, as the pellicle develops, differences in formation behaviour begin to emerge. It appears then that a combination of low MW proteins found in PS alongside the presence of proteins found in WMS appears to optimize the formation of the pellicle.

In this study it was also observed the structure of the pellicle formed from WMS and PS by comparing $\Delta f / \Delta D$ ratio (see Figure 4.5.) of the adsorbing pellicle with respect to the induced energy dissipation of the sensor per coupled unit mass. A lower $\Delta f / \Delta D$ ratio indicated the addition of pellicle mass without eliciting a significant dissipation

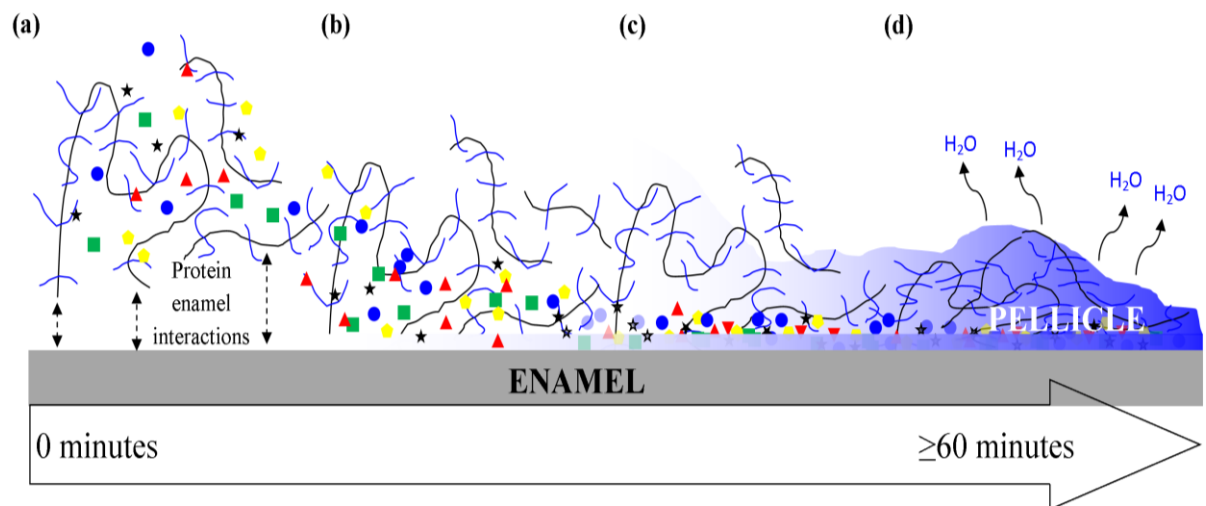
increase, which was characteristic of a rigid or elastic salivary pellicle. In the early stages of pellicle formation (< 1minute) PS pellicle was found to be more elastic ($-13 \Delta f/\Delta D$) than the WMS formed pellicle ($-8 \Delta f/\Delta D$). As the pellicle adsorption progressed, the PS formed pellicle was consistently more elastic relative to the WMS saliva formed pellicle. This phenomenon was also recently observed by Veeregowda *et al.* [34] where WMS (as well as submandibular saliva) produced 'softer' adsorbed films compared to the PS. This further suggests a more diffuse WMS pellicle, with weaker interactions between the components, which would be expected as more mucins adsorb into the film.

It appears then, that components of saliva absent in PS but present in WMS adsorb and interact with the hydroxyapatite surfaces that permit the WMS to form a more viscous and diffuse pellicle, compared to the more elastic and compact PS formed pellicles. Rupp *et al.* [125] also observed a similar structural heterogeneity of the salivary pellicle between a dense basal layer and a more hydrated outer layer. It was suggested by Skjorland *et al.* [126] that these dense and hydrated layers were due to compositional differences between the two stages of pellicle formation.

One can therefore propose that the presence of high MW mucins in WMS enhances the adsorption of low MW proteins to promote the formation of the dense basal layer. Possibly due to the water binding and network forming properties of the large MW mucins, which hinders the diffusion of the large proteins, but allows diffusion of the smaller proteins through the mucin network [209, 210]. This could ensure that low MW proteins are able to diffuse to the surface more rapidly, allowing a consistent order in the structure of the salivary pellicle. So that a dense basal layer (containing low MW proteins) can form first, followed by a more diffuse globular layer

(containing high molecular protein aggregates) arriving to the tooth surface afterwards (See Figure 4.9.). This is in agreement with *in situ* TEM studies of pellicle morphology where two distinct zones were found [30, 35].

Figure 4.9 Proposed model of pellicle formation: **(a)** The mucins contain a number of sites that can potentially promote adsorption to a surface. These include hydrogen bonding and hydrophobic interactions (via the carbonyl groups and methyl groups) and electrostatic interactions (via sialic acid residues). **(b)** The smaller MW surface active proteins (i.e statherin, histatins) that are entrapped in the mucin network begin to diffuse through the network adsorbing onto the enamel surface. **(c)** These low MW proteins crosslink to form a dense basal layer. **(d)** Mucins and protein aggregates then arrange themselves in a way that results in a small amount of syneresis to take place.



However, it is also important to recognise that protein adsorption to a solid/liquid interface is driven by many factors that should also be considered[195]. For example, protein adsorption to the enamel surface will be affected by the location of teeth in the mouth, and the tooth's physical (e.g. surface roughness) and chemical properties (e.g. hydrophobicity of enamel). Furthermore, the protein composition of an individual's saliva is highly variable [211]; which will also have an impact on the adsorption of the pellicle proteins to the enamel surface [85, 108]. Another consideration is that this study has focused on the absence of mucins from parotid saliva as a means to compare pellicle formation of saliva with and without mucins; it

should be noted that PS is a ductal fluid, and as such, bacteria free, as opposed to WMS, which contains copious amounts of micro-organisms[212]. Components that are released from bacterial and host cells are known to be incorporated into the pellicle. Therefore some of the differences in the way the pellicles form may also be due to the presence of bacteria in WMS and the absence of bacteria from PS. These effects however, were minimised by the salivary collection methods used and by utilising the saliva immediately after collection.

In conclusion, the data presented help to further define the mechanisms leading to the multi-layered structure of the salivary pellicle and demonstrate that salivary composition has an important effect on the properties of the adsorbed pellicle. In particular, this study has suggested that the mucins within saliva may play two key roles during pellicle formation; firstly they may promote the diffusion of low MW proteins to the enamel surface, and thereby promote a consistent order to the pellicle structure; and secondly the mucins also play an important role within the pellicle itself, by forming a less elastic, outer layer, which almost certainly possesses lubricating properties more suited to protecting the tooth surface from abrasive stresses. This knowledge augments our current understanding of the salivary pellicle, which is important for the development of more realistic salivary mimetics; something that has been hitherto untenable, due to difficulties in mimicking the complex interfacial properties of saliva. Furthermore, following the formation of the pellicle may help elucidate the mechanisms in which it is able to impede enamel demineralisation and subsequent dental carie formation.

Chapter 5

Effect of Calcium Ions on *in vitro* Pellicle Formation from Parotid and Whole Mouth Saliva

Introduction

Currently, phosphoproteins such as, acidic proline rich proteins (aPRPs), histatins and statherin are the main salivary proteins thought to play an important role as pellicle precursor proteins. As such, these proteins have been widely studied with respect to their ability to adsorb onto oral surfaces and thus influence early pellicle formation [1, 25, 36, 68, 82]. These proteins contain calcium-binding domains that may serve to provide a region of high calcium concentration close to the tooth surface, thus facilitating the mineralisation of teeth. The importance that the pellicle plays in preserving oral health becomes apparent in individuals who suffer from Xerostomia (i.e. dry mouth syndrome) [57, 58, 213]. Without adequate saliva in the mouth to produce an effective salivary pellicle, these individuals can suffer from increased dental caries and mucous membrane damage. Although artificial salivas are currently available as a treatment [214, 215], they only provide limited relief to the discomfort that Xerostomia inflicts, principally because current artificial salivas do not adequately mimic the complex interfacial film forming properties (i.e. thickness and viscoelasticity) of human saliva [216], which plays a key role in oral lubrication[39]. A number of studies have looked at the interplay between the structure of the pellicle and the ionic composition of the saliva [142-146]. Of particular interest has been to understand the role calcium ions play on pellicle structure, as calcium ions are thought to have a bearing on the attraction between pellicle proteins and the surface to which pellicle proteins adsorb [18, 144]. For example, Tanizawa *et al.* [143] showed that calcium ions were able to enhance pellicle formation onto hydroxyapatite surfaces via calcium bridging of proteins. Whilst Proctor *et al.* [39] showed that chelation of calcium from saliva caused a

dramatic decrease in the mechanical properties of an adsorbed salivary film, consistent with the breakdown of pellicle structure. Thus, information regarding the physical structure of the pellicle under varying calcium conditions should help elucidate the mechanisms behind pellicle formation. Therefore, in this study the *in vitro* formation of the salivary pellicle at different concentrations of calcium, from stimulated parotid saliva (PS) and stimulated whole mouth saliva (WMS) onto silicon oxide surfaces, using a quartz crystal microbalance with dissipation monitoring (QCMD) and a dual polarisation interferometer (DPI) was examined. Together these techniques yield information on changes in the pellicle structure in terms of adsorbed mass, thickness, polymer concentration, and density of the WMS and PS pellicles. Although there have been studies of the salivary pellicle formation using QCMD [124, 206, 217], It is possible that this is the first time that both DPI and QCMD have been used in combination to observe the real-time adsorption of the salivary pellicle in this way. It is hoped that this approach will also help us to understand the mechanisms underlying the formation and breakdown of the salivary pellicle. This new knowledge not only augments our current understanding of the salivary pellicle, which is important for the development of more realistic salivary mimetics, but also demonstrates how different interfacial techniques can be used to complement ones findings.

Materials and methods

Saliva collection

Saliva collection was undertaken according to a protocol previously assessed by an independent ethics panel. The saliva was obtained from 14 apparently healthy non-smoking male and female volunteers, ranging in age from 20 to 50 years.

Saliva adsorption

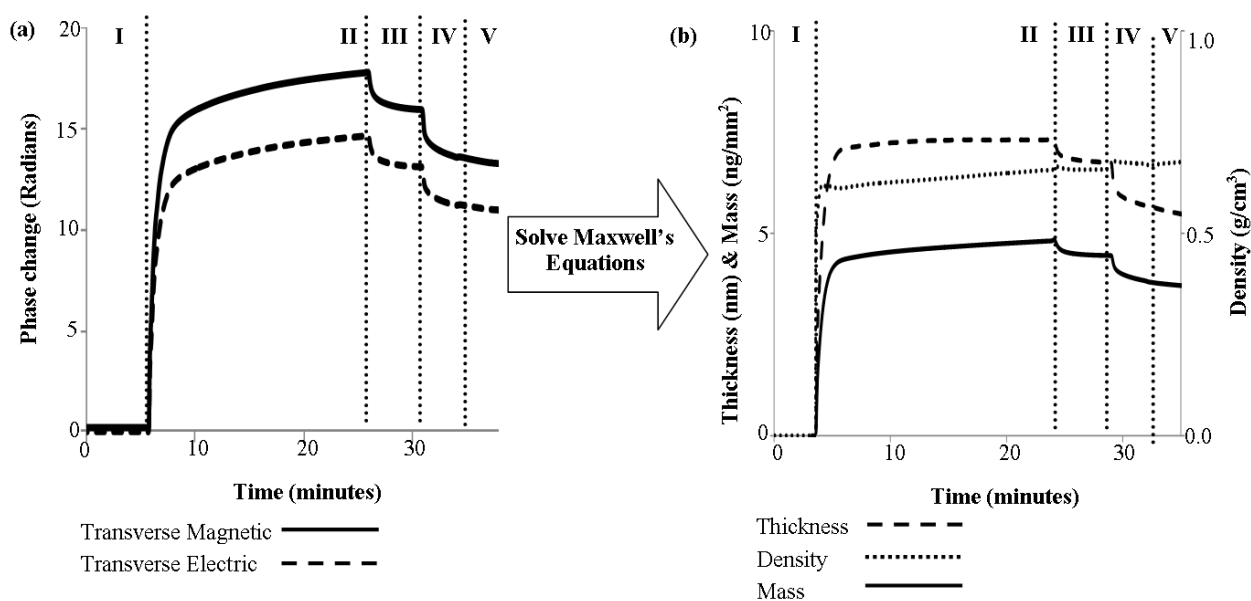
In addition to the calcium already present in saliva, the calcium concentration of both WMS and PS were increased by 1 mM Calcium chloride (CaCl_2 (Sigma-Aldrich, UK)) and 10mM CaCl_2 respectively. Furthermore, to test the adsorption of the salivary pellicle in the absence of free calcium, a 2 mM EDTA solution (VWR International Ltd., UK) was used to sequester all calcium-ions from WMS and PS (CaCl_2 and NaEDTA solutions were prepared in deionised and filtered ultra-pure water Nanopure Diamond, Barnstead Int., USA). Sewon *et al.* [218] showed that the average total calcium concentration of stimulated WMS was 1.3 ± 0.4 mM. Therefore 2 mM EDTA was used to sequester calcium from both parotid and whole mouth salivas. This was performed so that the salivas could be reduced to a known calcium concentration starting point. Thus the salivas containing EDTA were used as the control saliva sample.

The WMS and PS samples collected from each volunteer were divided into three aliquots respectively:

- (i) 0 mM CaCl₂
(1ml saliva + 1.5ml 4mM EDTA + 0.5 ml H₂O)
- (ii) 1 mM CaCl₂
(1ml saliva + 1.5ml 2mM CaCl₂ + 0.5 ml H₂O)
- (iii) 10 mM CaCl₂
(1ml saliva + 1.5ml 20mM CaCl₂ + 0.5 ml H₂O)

Each respective saliva sample was then measured concomitantly on the QCMD and DPI (both static adsorption systems i.e. not flow-cell). Upon injection of 0.5 ml of saliva, pellicle formation was monitored for 20 minutes, when pellicle formation plateaus (See Figure 5.1.). Subsequently the pellicle was rinsed with a 0.5ml calcium solution, which had a concentration equal to the calcium concentration of the saliva being used (i.e 0 mM, 1 mM or 10 mM CaCl₂). At this point the data was recorded as the post calcium rinse value. Finally the pellicle was rinsed twice with deionised water, and upon the second rinsing, the data was recorded as the post water rinse value.

Figure 5.1. Adsorption profile of WMS forming a pellicle over time on a DPI sensor. (a) Real time TM and TE phase changes that show: **I** the baseline recorded in deionised water, **II** the peak value of the adsorbed pellicle, **III** the phase shift post calcium rinse. **IV** & **V** the phase shifts post water rinse. (a) The derived thickness, polymer mass and density changes derived from TE and TM phase changes using Maxwell's equations. (b) Thickness, mass and density of the pellicle increase rapidly as the saliva rapidly adsorbs to the sensor surface. Following 20 minutes adsorption a calcium rinse removed loosely adsorbed material from the pellicle. Upon rinsing the pellicle with water, the thickness and mass was reduced with a concomitant increase in pellicle density.



Sensor properties

The substrates used for the adsorption of saliva were; silicon dioxide QCM-D sensors (Part No. QSX 303, Q-Sense AB, Vastra Frolunda, Sweden.) and silicon oxynitride DPI sensors (Part No. 2007-110c, Farfield Scientific, Manchester, UK.). See Chapter 3 for more details.

DPI sensor cleaning

After the completion of the experiment, surfaces were rinsed with 2% v/v Hellmanex (Müllheim, Germany), for 5 minutes, rinsed with ultra-pure water, followed by 2% w/v SDS (Sigma-Aldrich, UK), then rinsed with 50% v/v IPA (Sigma-Aldrich, UK).

QCMD sensor cleaning

After the completion of the experiment, surfaces were cleaned with 2% v/v Hellmanex rinsed with water, followed by 2% w/v SDS then rinsed with water and dried with nitrogen. Finally sensors were exposed to UV-ozone (Bio-Force Nanosciences Inc., Iowa, USA) for 30 minutes.

Statistics

Significant differences in pellicle mass, thickness and density in relation to calcium concentration of WMS and PS was determined by one-way ANOVA and Tukey post hoc analysis at three points of the experiment (i.e. peak, post calcium rinse and post water rinse values) using GenStat (14th Edition, VSN International Ltd, Hemel Hempstead, UK). Level of significance was set at $p < 0.05$. Linear regression functions were fitted and R^2 values calculated using Microsoft Office Excel 2007 (Microsoft Corporation, Redmond, WA, USA).

Results

DPI

Pellicle ‘polymer’ mass

The mean pellicle polymer mass for both WMS and PS did not change significantly with the addition of 1mM CaCl₂ or with the removal of calcium (using 2 mM EDTA) from saliva. However, the mass for WMS increased significantly when 10 mM CaCl₂ was added to WMS (See Figure 5.2. (a)) and PS (See Figure 5.2. (b)) respectively.

Upon rinsing each pellicle with a CaCl₂ solution (at a concentration equal to the CaCl₂ concentration present in the saliva) the pellicle formed maintained its additional mass. However, upon rinsing pellicles with de-ionised water any increase in mass that occurred in both WMS and PS was completely removed.

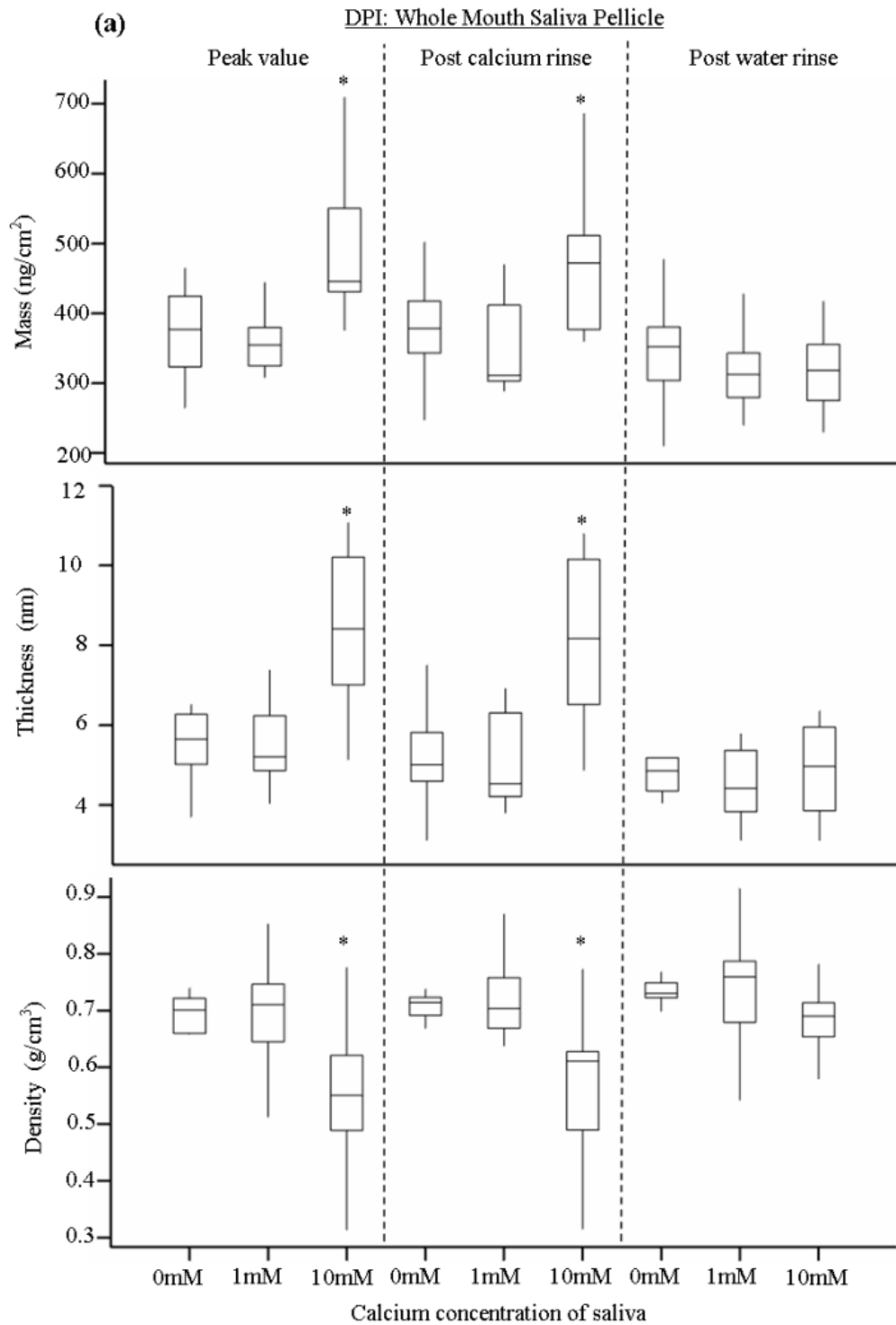
Pellicle Thickness

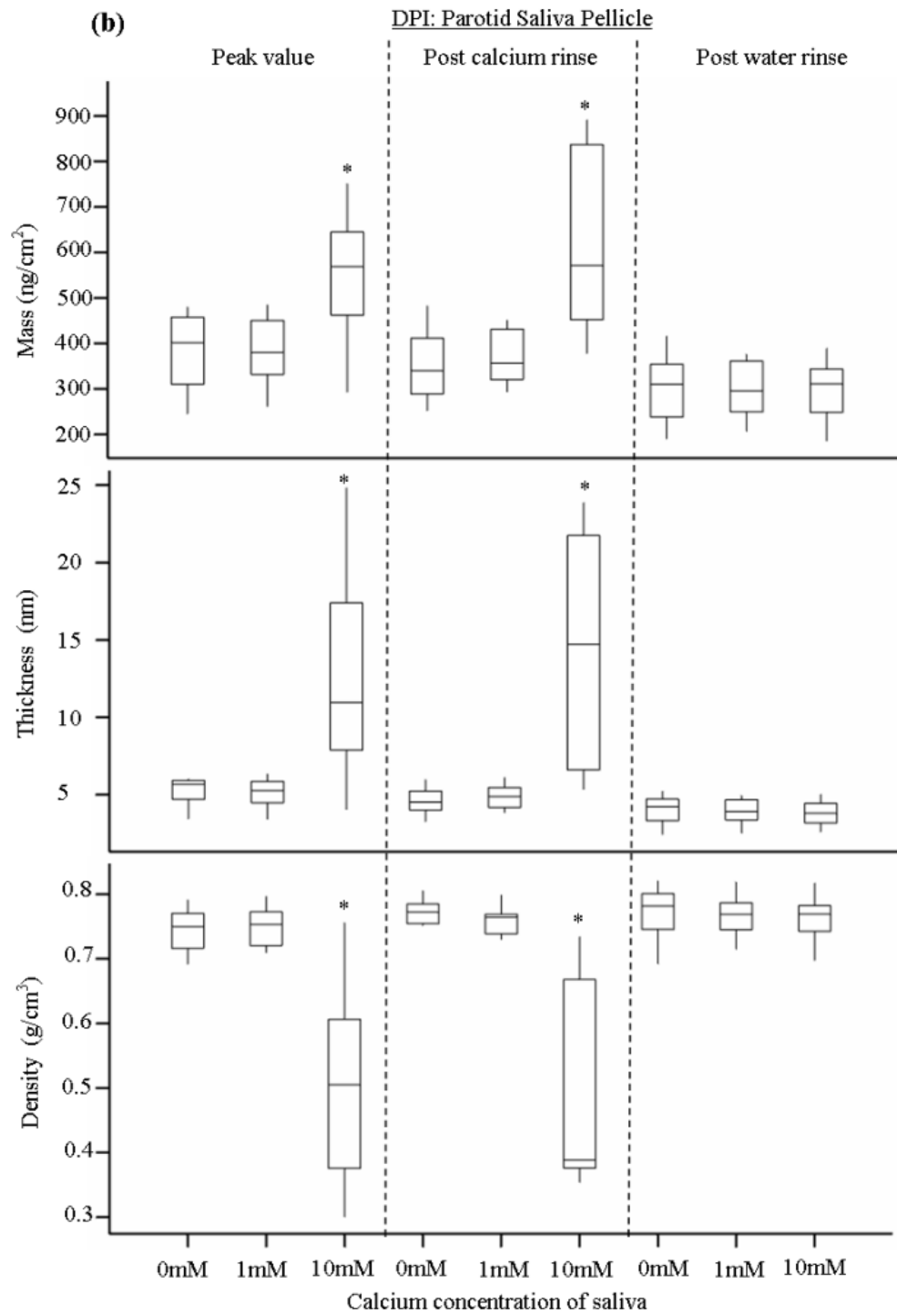
Increasing the natural concentration of calcium in WMS and PS by an additional 1 mM CaCl₂ had no effect on the thickness of the pellicle. However, increasing the natural calcium concentration of saliva by 10 mM resulted in a significant increase in the thickness of the resultant pellicle. Upon rinsing the pellicle with a calcium solution (at a concentration equal to the CaCl₂ concentration present in the saliva) the mean pellicle thickness for all three salivas (i.e. 0 mM CaCl₂ (natural saliva +2 mM EDTA), natural saliva + 1 mM CaCl₂ and natural saliva + 10 mM CaCl₂) remained similar. Upon rinsing with de-ionised water, a dramatic loss in pellicle thickness was again observed. In particular, WMS (See Figure 5.2. (a)) and PS (See Figure 5.2. (b)) containing an extra 10 mM CaCl₂ showed large losses in pellicle thickness when rinsed with de-ionised water.

Pellicle Density

The addition of 1 mM CaCl₂ or the removal of calcium from saliva had no significant effect on the density of PS or WMS pellicles. However, a large drop in the density of the pellicles formed from both WMS (See Figure 5.2. (a)) and PS (See Figure 5.2.(b)) occurred when the natural calcium concentration of saliva was increased by 10 mM CaCl₂. Subsequent rinsing of the pellicles with de-ionised water returned the density of all salivary pellicles to statistically similar values.

Figure 5.2. (a) Box plot of DPI measured polymer mass, thickness and density changes formed from WMS containing 0 mM Calcium (2 mM EDTA) (n=10); the natural concentration of WMS + 1 mM CaCl₂ (n=10); and natural concentration of WMS +10 mM CaCl₂ (n=10). **(b)** PS containing 0 mM Calcium (2 mM EDTA) (n=12); the natural concentration of PS + 1 mM CaCl₂ (n=12); and natural concentration of PS +10 mM CaCl₂ (n=12). Values reported are peak, post calcium rinse and post water rinse values (* = Significant difference ($p \leq 0.01$)).



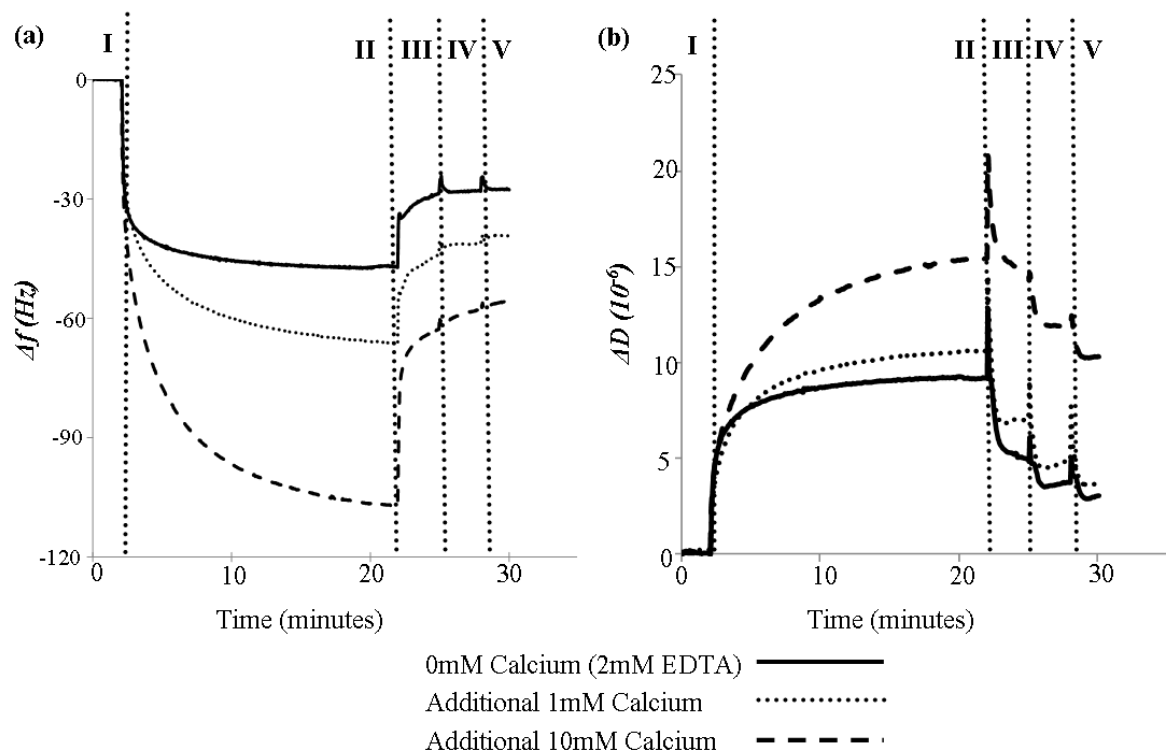


QCMD

Pellicle hydrated mass & thickness

Hydrated mass measured via QCMD takes into consideration the hydration, or water, contained within salivary pellicle. The viscous properties of softer films dampen the sensor's frequency of oscillation, and in such cases the Sauerbrey model underestimates the mass, whereupon another method of analysis is needed to fully characterise the film. Therefore, in addition to recording frequency changes, the QCMD measures a second parameter known as dissipation (D) (See Figure 5.3.).

Figure 5.3. (a) Frequency and (b) dissipation changes versus time measured for the 3rd overtone (15 MHz) by QCMD for the adsorption of WMS at different calcium concentrations of saliva. **I** baseline recorded in deionised water. **II** Peak value. **III** post calcium rinse. **IV** & **V** water rinse. Increasing concentrations of calcium in saliva display lower frequency oscillations with respective higher dissipation values.



The addition of 1 mM CaCl_2 to natural saliva or the removal of calcium (using 2 mM EDTA) from saliva had no significant effect on the hydrated mass of PS or WMS

pellicles. However, a notable increase in the hydrated mass for pellicles formed from both WMS and PS occurred when the natural calcium concentration of these salivas was increased by 10 mM CaCl₂ (see Table 5.1.). When the dissipation of the oscillations was also considered alongside the frequency of oscillation changes, the significant difference between pellicle thickness and mass was also observed with the addition of 1 mM CaCl₂ to saliva. This was reflected in an increase in peak values for Voigt fitted thickness and mass respectively (see Table 5.1.).

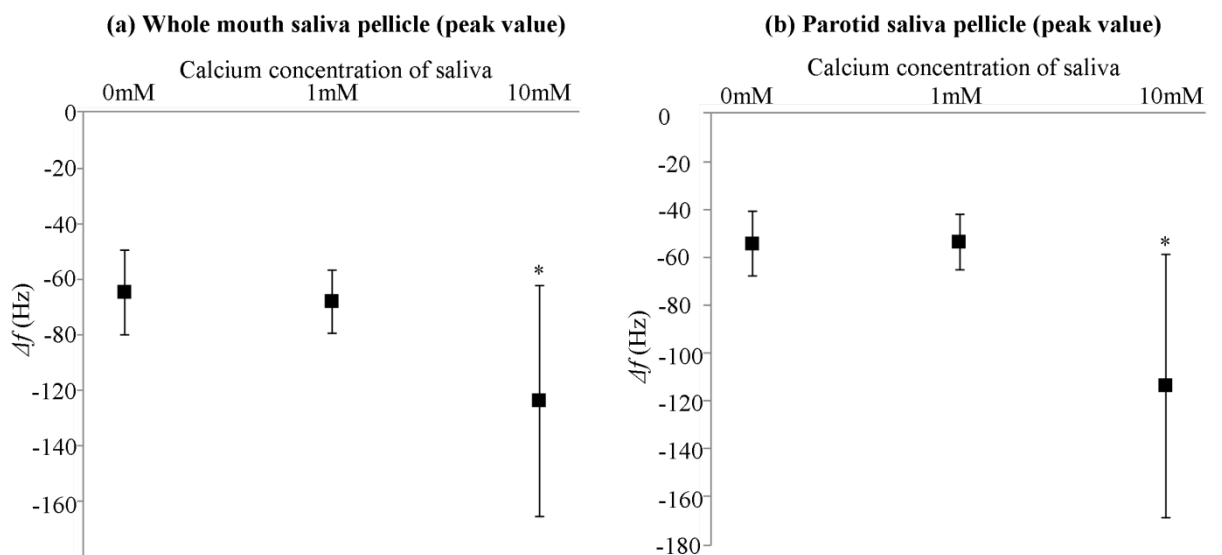
Table 5.1. Effect of the calcium concentration of WMS and PS on Sauerbrey and Voigt modelled thickness and hydrated mass changes to pellicle formed from (a) WMS containing 0 mM Calcium (2 mM EDTA) (n=10); natural concentration of WMS + 1 mM CaCl₂ (n=10); and natural concentration of WMS +10 mM CaCl₂ (n=10). And pellicle formed from (b) PS containing 0 mM Calcium (2mM EDTA) (n=12), natural concentration of PS + 1mM CaCl₂ (n=12), and natural concentration of PS + 10 mM CaCl₂ (n=12).

Calcium concentration (mM)	<i>Sauerbrey model</i>		<i>Voigt model</i>	
	Thickness (nm)	Mass (ng/cm ²)	Thickness (nm)	Mass (ng/cm ²)
Whole mouth saliva pellicle				
Peak values				
0	11.3(±2.7) ^a	1132(±266) ^a	25.7(8.9) ^a	2568(891) ^a
1	11.9(±2.0) ^a	1190(±196) ^a	37.2(10.6) ^b	3718(1063) ^b
10	18.2(±7.3) ^b	1815(±729) ^b	37.4(10.4) ^b	3742(1040) ^b
post calcium rinse values				
0	11.9(±2.1)	1186(±205) ^a	24.3(5.9) ^a	2428(588) ^a
1	11.8(±2.2)	1175(±221) ^a	32.2(5.3) ^{ab}	3217(533) ^{ab}
10	17.2(±8.2)	1718(±815) ^a	37.2(10.5) ^b	3724(1047) ^b
post water rinse values				
0	9.2(±2.7)	923(±271)	17.1(5.6)	1705(560)
1	9.3(±2.0)	929(±199)	25.0(11.2)	2500(1117)
10	9.5(±1.5)	955(±151)	26.3(11.0)	2630(1097)
Parotid saliva pellicle				
Peak values				
0	8.683(2.0) ^a	868(203) ^a	18.8(4.0) ^a	1882(398) ^a
1	8.6(1.7) ^a	864(169) ^a	15.3(6.5) ^a	1526(648) ^a
10	22.4(10.2) ^b	2239(1021) ^b	36.2(11.4) ^b	3617(1139) ^b
post calcium rinse values				
0	8.0(1.0) ^a	807 (95) ^a	16.3(5.1) ^a	1631(508) ^a
1	7.5(1.3) ^a	747 (131) ^a	12.4(6.6) ^a	1244(655) ^a
10	18.1(8.7) ^b	1807 (867) ^b	31.0(8.4) ^b	3101(836) ^b
post water rinse values				
0	6.2(1.5)	624.2(151)	14.6(4.4)	1464(443)
1	6.3(1.3)	633.2(134)	11.2(6.2)	1119(617)
10	5.1(1.6)	514.4(158)	12.8(6.5)	1280(647)

^a and ^b represent significant differences ($p \leq 0.05$) between respective means. ^{ab} is not significantly different between either ^a or ^b. **N.B.** Modelled mass differs from the modelled thickness due to the assumed density of the adsorbed pellicle and therefore the two parameters are statistically identical.

For example, the frequency change observed at the 3rd overtone, which by applying the Sauerbrey equation, is inversely proportional to the hydrated mass of the WMS pellicle, showed a decrease in frequency from -65 ± 15 Hz at 0 mM CaCl₂ down to -104 ± 42 Hz when the natural calcium concentration of WMS was increased by 10mM CaCl₂. A decrease in frequency from -55 ± 13 Hz at 0 mM CaCl₂ down to -113 ± 55 Hz when the natural calcium concentration of PS was increased by 10mM CaCl₂ was also observed (See Figure 5.4. (a) and (b)).

Figure 5.4. Comparison of frequency changes to pellicle formed from (a) WMS and (b) PS containing 0 mM Calcium (+2mM EDTA) (n=12), natural concentration of WMS + 1mM CaCl₂ (n=12), and natural concentration of PS + 10 mM CaCl₂ (n=12). (* = Significant difference ($p \leq 0.05$)).



Pellicle viscoelasticity

The dissipation value observed at the 3rd overtone also gave an independent qualitative insight into the viscoelasticity of the pellicle (i.e. the higher the dissipation value, the less elastic the film). WMS pellicle, showed an increase in dissipation from 8 ± 3 at 0 mM CaCl₂ up to 13 ± 6 when the natural calcium concentration of WMS was increased by 10mM CaCl₂. An increase in dissipation from -5 ± 2 Hz at 0 mM

CaCl₂ up to 10 ± 5 when the natural calcium concentration of PS was increased by 10mM CaCl₂ was also observed (See Figure 5.5. (a) and (b)). Dissipation values in this study were also used to improve modelling of hydrated mass and thickness from Sauerbrey model to the Voigt model. Overall the mean thicknesses and hydrated masses calculated using the Voigt model are a factor of 1.6 – 3.1 higher than the Sauerbrey values (see table 1).

Figure 5.5. Comparison of dissipation changes to pellicle formed from (a) WMS and (b) PS containing 0 mM Calcium (+2mM EDTA) (n=12), natural concentration of WMS + 1mM CaCl₂ (n=12), and natural concentration of PS + 10 mM CaCl₂ (n=12). (* = Significant difference (p ≤ 0.05)).

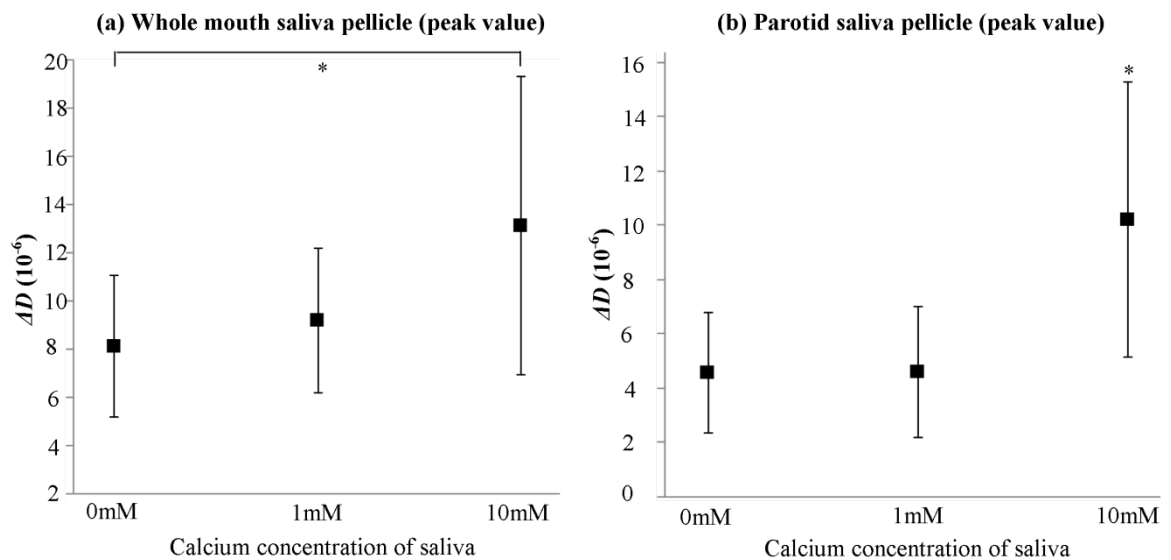
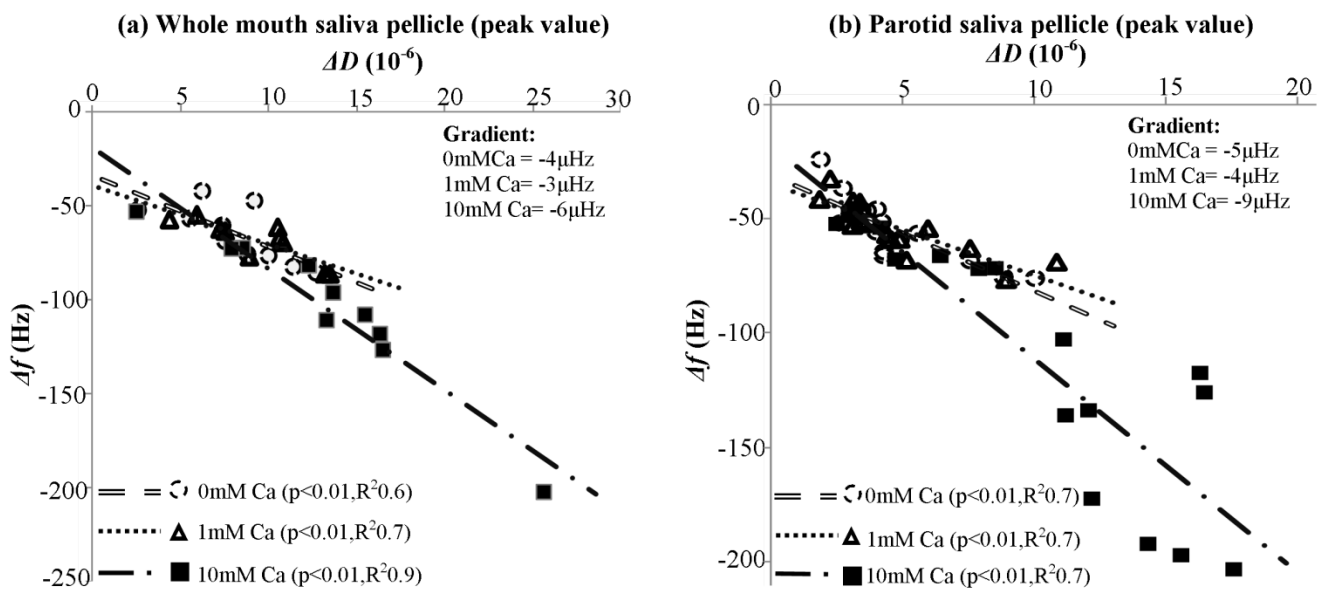


Figure 5.6. (a) and (b) show that the decrease in frequency is highly associated (p < 0.02) to an increase in dissipation for both PS and WMS at all three concentrations of calcium in saliva. This correlation is predicted by the Voigt model as both negative frequency shift and dissipation are proportional to the thickness for thin films [165]. However, the slope of the correlation indicates differences in the viscoelasticity of the films. This phenomenon was more pronounced in the saliva that had 0 and 1 mM CaCl₂ added to it. For example, the gradient of the curve for PS and WMS pellicle dissipation, as a function of frequency, was twice as high in WMS and PS that

contained an extra 10 mM CaCl₂ as opposed to saliva containing 0 mM CaCl₂, or an added 1 mM CaCl₂. For a given value of Δf the 0 mM and 1 mM CaCl₂ films have higher dissipations (ΔD) indicating they are relatively more viscous whereas the 10 mM CaCl₂ films are relatively elastic.

Figure 5.6. ΔD as a function of Δf measured at the 3rd overtone by QCM-D for the adsorption of (a) WMS pellicle and (b) PS pellicle containing: 0 mM Calcium (+2mM EDTA); + 1mM CaCl₂, and +10 mM CaCl₂.



Discussion

The formation of the salivary pellicle is a dynamic process that begins almost instantly (see Figure 5.1. and 5.3.) with the adsorption of low molecular weight proteins, followed by the adsorption of larger salivary proteins and protein aggregates with time [68]. Some evidence suggests that there is potential for Vroman-like [180] effects to take place, for example; between mucin MUC 5B with statherin and PRP1 [193]. However, Svendsen *et al.*[93] found that this exchange may be quite limited during the first hour of pellicle formation. Therefore under the experimental conditions used in this study the Vroman effect is unlikely to apply to the same extent in salivary proteins as is exhibited by blood serum proteins. Nevertheless, pellicles formed in this study showed striking similarities with work carried out by Hannig *et al.* [35]. They showed that after 1 minute the salivary adsorption process was able to form an electron dense pellicle layer, 10–20 nm thick, on an enamel surface; a thickness that was not dissimilar from our own results, despite the differences in the substrates being used. This not only augments confidence in the other physical parameters (i.e. mass and density) reported in this study, but also demonstrates that proteins in saliva are flexible with regard to the surfaces they adsorb to; thus permitting a salivary pellicle to form on diverse surfaces such as foods and dental implants [18].

The physical structure of the salivary pellicle has been thought to be influenced by calcium ions in saliva, as these divalent cations can permit the cross-linking of proteins [219]. Cross-linking of proteins has been shown to be important in maintaining micelle-like protein aggregates present in saliva, which may play an important role in the formation of the salivary pellicle [97, 220]. However, in this

study the DPI data showed little difference in the polymer mass, thickness and density of salivary pellicles formed from WMS and PS when calcium was sequestered using EDTA (i.e. 0 mM calcium) or when saliva was supplemented with 1 mM CaCl₂. Not until the natural calcium concentration of WMS and PS was increased by 10 mM CaCl₂ that a significant effect on the pellicle polymer mass, thickness and density was observed. The addition of 10 mM CaCl₂ to saliva resulted in a pellicle that was thicker, with a higher surface polymer mass; but more diffuse than pellicles formed from saliva containing no calcium or saliva with 1mM CaCl₂ added. This would suggest that the pellicle formed in the presence of an extra 10 mM CaCl₂ is much more nebulous than when a natural calcium concentration was used. This phenomenon was also more pronounced in pellicles formed from PS, where the increase in pellicle thickness and mass, and the concomitant decrease in density was higher than WMS pellicles. This was likely a consequence of the higher proportion of proteins in PS that contain calcium binding domains (i.e. statherin, histatins) [221], and therefore PS was more sensitive to the presence of calcium ions [222].

Further differences between PS and WMS adsorption also impact the physical nature of the respective salivas. For example, PS is a serous fluid that contains a number of low molecular weight proteins (≤ 15 kDa), such as cystatins, and acidic proline-rich proteins that have properties which make them suitable for forming the primary layer of the pellicle [223, 224]. These properties include being able to diffuse rapidly to the solid/liquid interface, re-arrange at the surface, and interact with neighbouring molecules [51]. In contrast, WMS contains high molecular weight proteins (≥ 180 kDa) such as mucins, which do not diffuse rapidly to the surface because of their size and highly glycosylated side chains. Moreover, mucins increase the viscosity of saliva

and thus concomitantly slow down the diffusion of other proteins present in saliva. These physical differences between PS and WMS also influence the conversion of raw data (i.e. Δf and ΔD) to modelled data (i.e. Sauerbrey and Voigt) when analysing QCMD data[225]. Consequently the qualitative changes in Δf and ΔD of the respective salivas, when observing differences in pellicle structure at different concentrations of calcium, were highlighted in this study.

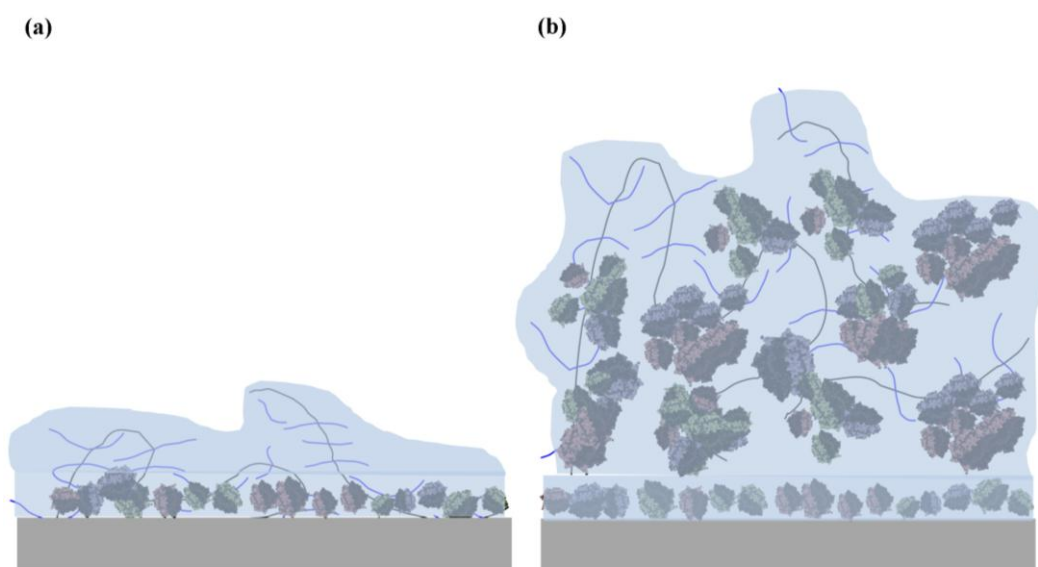
The QCMD data showed that by increasing the natural calcium concentration of WMS and PS by 10 mM CaCl_2 one could generate a statistically significant ($p < 0.05$) increase in hydrated mass of the pellicle. This, however, was reciprocated by an increase in pellicle elasticity, which was observed by a slower increase in dissipation with increasing negative frequency change (see Figure 5.4. and Figure 5.5.). All salivary pellicles, regardless of calcium concentration had a high association between the dissipation of the pellicle as a function of frequency. This correlates well with the work carried out by Voinova *et al.* [165], who show that dissipation increases with film thickness; so that as the salivary pellicle gets thicker, both the negative change in frequency, and the positive change in dissipation increase. This phenomenon was amplified by the addition of 10mM CaCl_2 to both PS and WMS, manifesting itself as the change in the gradient of the slope observed in Figure 5.6.. At 10 mM calcium the dissipation was increasing less with variation of frequency. This means that the salivary pellicles were becoming less dissipative and more elastic (closer to Sauerbrey behaviour) when 10 mM CaCl_2 was added to the saliva.

It was observed that little difference in the hydrated mass and thickness of salivary pellicles formed from WMS and PS when calcium was sequestered using EDTA (i.e.

0 mM calcium) or when 1 mM CaCl₂ was added to the calcium already present in the saliva. This raised an interesting question: why did adding 1 mM CaCl₂ to the natural calcium concentration of saliva show no response in terms of pellicle structure; but increasing the natural calcium concentration of saliva by an extra 10 mM CaCl₂ triggered a significant increase in mass, thickness and concomitant decrease in density and pellicle viscoelasticity. It appears that at low concentrations of calcium in saliva (i.e. 0 mM CaCl₂ and natural calcium concentration of saliva + 1 mM CaCl₂) there was no impact on the mass, thickness density and viscoelasticity of the pellicle, and that the salivary pellicle could readily form in the absence of calcium. This correlates well with the observations found by Proctor *et al.* [39] where they demonstrate that the surface tension of saliva at the air-water interface was unaffected by removal of calcium from saliva using 2 mM EDTA; thus also concluding that the passage of proteins to a surface is unaffected by the absence of calcium from saliva. They also showed that the elastic modulus of the adsorbed salivary film was significantly reduced upon removal of CaCl₂ by EDTA. However, this was measured at very low frequencies (0.2 Hz), which would detect changes in intermolecular interactions, whereas the high frequencies used by QCMD (>5MHz) were not as sensitive to these changes. This suggests that the change in viscoelasticity observed by Proctor *et al.* [39] was not due to a total breakdown of the adsorbed pellicle in the absence of CaCl₂ but more likely connected to the overall elasticity of the protein film through calcium mediated intermolecular interactions. It is possible that increasing the natural calcium concentration of saliva by 10 mM CaCl₂ increases the aggregation of proteins in saliva. Consequently, rather than small individual proteins packing to the surface forming densely packed salivary films, they form large protein aggregates in the saliva, prior to pellicle adsorption, and

subsequently deposit onto the sensor surface forming thicker more diffuse films (See Figure 5.7.). This explicates the increase in mass, thickness and decrease in density observed by the DPI measurements upon increasing the natural calcium concentration of saliva by 10 mM CaCl₂. In addition, the increase in elasticity could be due to the increase in calcium crosslinks within the film increasing the rigidity of the film.

Figure 5.7. Proposed model for the changes in the structure of the pellicle derived from saliva containing different concentrations of calcium: **(a)** Pellicle formed from saliva containing 0mM CaCl₂ or 1mM CaCl₂. **(b)** Pellicle formed from saliva containing 10mM CaCl₂. Proteins in saliva aggregate at 10mM CaCl₂ prior to pellicle adsorption. The aggregates subsequently deposit onto the sensor surface forming thicker more diffuse films.



It was also interesting to note that upon washing with de-ionised water the density of the pellicles return to that observed for saliva with no added calcium, suggesting that the nebulous protein adsorbed was easily removed, leaving a more dense and robust basal layer. The rapid loss of protein from the pellicle on rinsing with de-ionised water highlights the importance of maintaining the pH and ionic balance of saliva in order to preserve the stability of the pellicle. It is likely that upon introduction of de-

ionised water to the pellicle, ions and proteins, leached out into the water, primarily due to the hypotonicity of the de-ionised water. This rapid decrease in the ionic concentration of the pellicle would have increased the electrostatic repulsion between anionic moieties within proteins and reduced intermolecular interactions [91, 144, 226]. This destabilised the structure of the pellicle facilitating loss of loosely bound proteins, which explains the observed dramatic decrease in pellicle thickness and mass with concomitant increase in density (see Figure 5.2.).

To conclude, this study lays the foundations on how regulating the calcium concentration of saliva provides a mechanism that can control the physical properties of the salivary pellicle. In addition, the overall structure of the pellicle, in terms of mass and thickness is relatively insensitive to calcium at low concentrations, allowing a flexibility to adapt to changing physiological and environmental conditions was also observed. It is important to recognise that these *in vitro* results do not necessarily represent the true nature of how the salivary pellicle forms in the oral cavity. Furthermore, there was also a dilution of the saliva samples which could have confounded the results, and this needs to be taken into account when interpreting the data. Despite these limitations the results do provide some evidence as to how the pellicle may behave on oral surfaces when calcium concentrations change; although further research was required to develop a more realistic representation of pellicle formation in the oral cavity. This was subsequently observed, by studying the adsorption of saliva on hydroxyapatite and hydrophobic sensors, which were more representative of conditions in the mouth.

Chapter 6

Structural Changes of the Salivary Pellicle under Acidic Conditions

Introduction

Knowledge on the protective function of the salivary pellicle against acid erosion is mainly based on experiments that compare enamel test pieces exposed to differing acidic environments. A number of these studies show that enamel covered with a salivary pellicle reduces enamel mineral loss, decreases erosive lesion depth and enhances enamel re-hardening compared to pellicle free enamel [227-230]. These techniques are valuable in confirming the protective role that the pellicle plays in the mouth, but they provide limited information on the actual structural changes that the pellicle undergoes when exposed to acidic environments. For data regarding structural changes in the pellicle, one has to look at studies observing the organoleptic properties of food; in particular mouthfeel/texture studies.

Mouthfeel perception is of particular interest to the food industry as it is a physical property of food that can influence consumer choice. For example, food texture studies have shown that consumer preferences for dairy products was driven by the perception of smooth and creamy textures [231]. The pellicle is recognised as an important factor in texture perception. Subsequently the interaction between salivary proteins and astringent compounds have been studied using a number of techniques; such as turbidity [232], chromatography [233], tribology [234], nuclear magnetic resonance [235] and light scattering [236]. Current literature seems to agree that astringency is a physical stimulus arising from precipitation of salivary proteins (proline-rich proteins, histatins and bovine mucins have all been observed to precipitate through interaction with polyphenols) and consequent breakdown of the lubricating salivary pellicle[237].

The saliva contains a mixture of amphiphilic proteins that selectively adsorb to all soft (i.e. mucosa), and hard (i.e. enamel) tissues within the oral cavity [45] which determines all interfacial events taking place between the mouth and the environment, and therefore performs both a protective and a gustatory role [13, 68, 238]. Many studies [235, 236, 239-243] therefore have investigated the molecular basis of astringency by focusing on the interaction between proteins present in salivary pellicle and polyphenols. However, it has also been revealed that an increasing acidic environment can elicit a perception of dryness in the mouth, by reducing the interfacial shear elasticity of the salivary pellicle. Rosetti *et al.* [244] showed that increasing the concentration of citric acid in saliva reduced the interfacial shear elasticity of the salivary pellicle at the air liquid interface. This would support work carried out by Sowalsky & Noble [245] who observed that citric acid elicit a perception of oral dryness as a secondary attribute (sourness being the primary).

Citric acid is often added to beverages such as fruit juices and soft drinks helping to create a tart flavour, giving the impression of freshness, but also acts as a preservative by lowering the pH of the product. In the UK alone there has been an 8-fold increase in the consumption of soft drinks since the 1950s [246]. This increase in soft drink consumption has paralleled an increase in enamel erosion.

Consequently, the structural changes that the pellicle undergoes when exposed to citric acid is of interest in terms of its protective role in the mouth, but also with respect to the astringent sensations that occur when citric acid is consumed. The importance that the pellicle plays in these roles becomes apparent in individuals who suffer from dry mouth syndrome (i.e. Xerostomia) [57, 58, 213] common to

hyposalivators and patients with Sjogren's syndrome. Without adequate saliva in the mouth to produce an effective salivary pellicle, these individuals suffer from difficulties in swallowing, speech, mastication, an increase in dental caries and mucous membrane damage, as well as an altered sensory perception of food (i.e. Dysgeusia) [247].

In this chapter, the *in vitro* formation of the salivary pellicle and the structural modifications that the salivary pellicle undergoes when exposed to increasing concentrations of citric acid was examined. This was carried out by adsorbing stimulated whole mouth saliva (WMS) onto silicon oxide surfaces, using a quartz crystal microbalance with dissipation monitoring (QCMD) and a dual polarisation interferometer (DPI) to yield information on changes in the pellicle structure in terms of adsorbed mass, thickness and pellicle density when challenged with increasing concentrations of citric acid. The novel information, helps to reveal the changes in the complex interfacial film forming properties of human saliva [216], which plays a key role in maintaining the physiological processes of the oral cavity.

Materials & Methods

Solutions

Saliva: Stimulated WMS samples were obtained from 6 apparently healthy, non-smoking, male and female volunteers, ranging in age from 20 to 50 years. Saliva collection was undertaken according to the protocol previously described in chapter 2.

Buffers: Citric acid (sigma), sodium hydroxide (sigma) and Miliq water were used to make a series of 10mM citrate buffers at pH3, 4, 5, 6 and 7. pH was altered by neutralization with NaOH from pH 3 to pH 7. Solutions were prepared in deionised and filtered ultra-pure water (Nanopure Diamond, Barnstead Int., USA).

Sensor properties

The substrates used for the formation of the salivary pellicle were QCMD and DPI silica coated sensors. The root mean square surface roughness of the DPI sensors was 4.7nm, and 1.2 nm for the QCMD silica sensors; measured by MFP-3D atomic force microscope (Asylum Research, CA, USA)) as described in Chapter 3. The isoelectric point of silica is \approx pH 2 (Vansant *et al.*, 1995) so under the conditions used in this study (pH3-pH7), the silica would have carried a negative charge.

Sensor cleaning

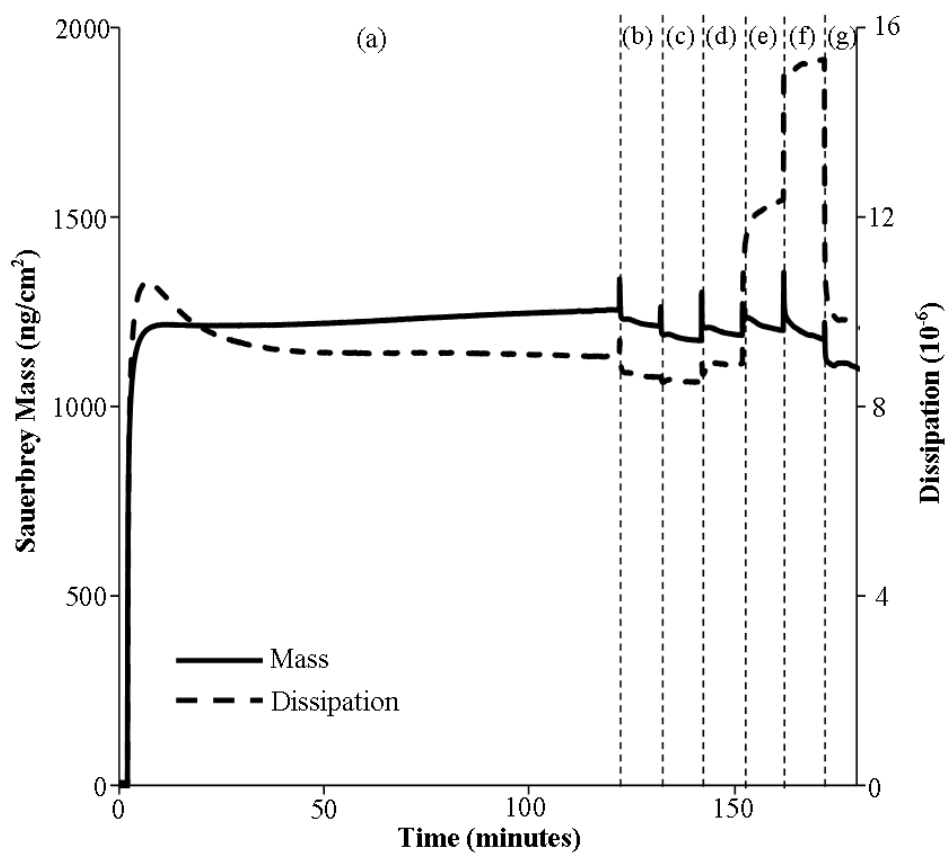
After the completion of the experiment, QCMD and DPI surfaces were cleaned with 2% w/v SDS (Sigma-Aldrich, UK), followed by 2% v/v Hellmanex (Müllheim, Germany), then copiously rinsed with ultra-pure water and subsequently dried with

oxygen free nitrogen gas. Finally, QCMD sensors were exposed to UV-ozone (Bio-Force Nanosciences Inc., Iowa, USA) for 20 min.

Quartz crystal microbalance with dissipation monitoring (QCMD)

The measurements were performed using a D300 QCMD (Q-Sense AB, Vastra Frolunda, Sweden) with a QAFC 302 axial flow measurement chamber maintained at 36.8°C as previously described. Saliva was allowed to adsorb to the sensor for 2 hours as formation of the pellicle reaches equilibrium between adsorption and desorption of salivary proteins within 90–120 min [126, 248, 249]. Furthermore, in previous studies 120-min pellicle differed neither from 24-h biofilms nor from 3-min short time pellicles regarding its protective potential [250-252]. Therefore 2 hours was deemed a satisfactory adsorption time. Subsequently the *in vitro* pellicle was rinsed with increasingly acidic solutions at 10 minute time intervals; until the last rinse when a pH7 citrate buffer solution was used (See Figure 6.1.).

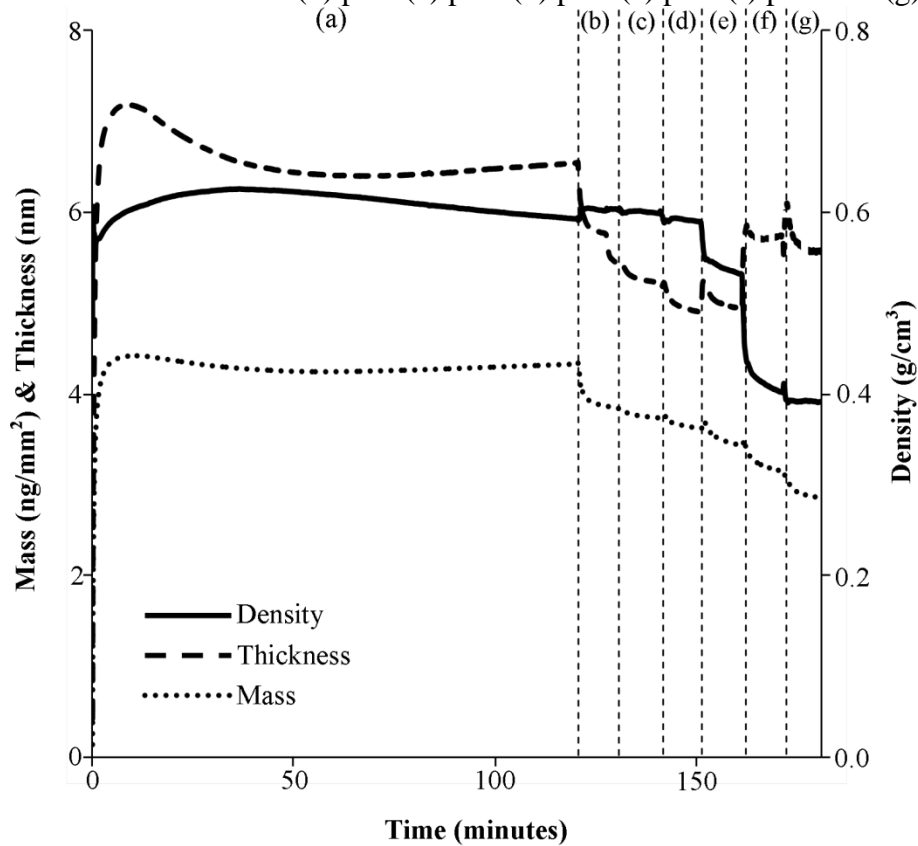
Figure 6.1. Salivary pellicle adsorption profile on a QCMD silica sensor after (a) 2 hour adsorption of the salivary pellicle and then subsequent rinsing of the adsorbed pellicle with citrate buffer at: (b) pH7 (c) pH6 (d) pH5 (e) pH4 (f) pH3 and (g) pH7.



Dual polarisation interferometer (DPI)

Measurements of surface layer thickness and refractive indices were performed in real time using an AnaLight Bio200 DPI, previously described in chapter 2. As with the QCMD experiment the saliva was allowed 2 hours to adsorb to the sensor and subsequently the *in vitro* pellicle was also rinsed with increasingly acid solutions as 10 minute time intervals; until the last rinse when a pH7 citrate buffer solution was used (See Figure 6.2.).

Figure 6.2. Salivary pellicle adsorption profile on a DPI silica sensor after (a) 2 hour adsorption of the salivary pellicle and then subsequent rinsing of the adsorbed pellicle with citrate buffer at: (b) pH7 (c) pH6 (d) pH5 (e) pH4 (f) pH3 and (g) pH7.



Statistics

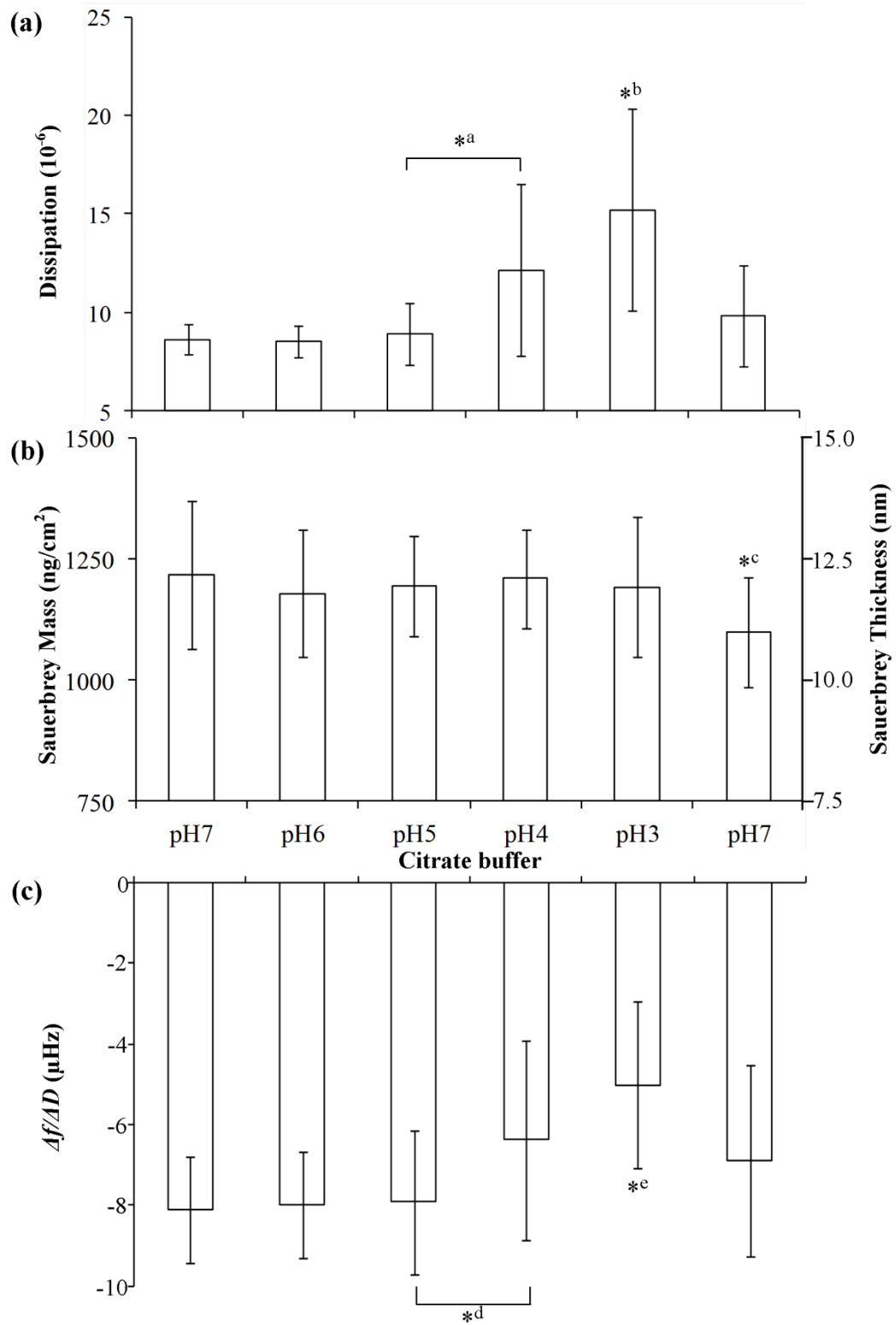
Significant differences in pellicle mass, thickness, density and dissipation was determined by two sample t tests at each of the pH rinse steps of the experiment (i.e. measurement of pellicle mass at pH7 against pellicle mass at pH 6, pH 5, pH4, pH 3 and finally at pH7) using GenStat (14th Edition, VSN International Ltd, Hemel Hempstead, UK). A p value < 0.05 was considered significant in all statistical analysis.

Results

QCMD

Upon the addition of saliva to the silica substrate a rapid adsorption of salivary proteins takes place (see Figure 6.1.). The formation of the pellicle began to reach equilibrium after 20 minutes adsorption, however the pellicle was given 2 hours to fully adsorb. Upon the first rinse step (i.e. citrate buffer at pH7) a small amount of loosely adsorbed material was removed from the pellicle. Subsequent rinsing with citrate buffer at pH 6 and pH 5 did not produce any significant structural changes to the pellicle. However, upon rinsing with pH4 citrate buffer; a significant increase in the dissipation of the pellicle took place from $9 \pm 2 \times 10^{-6}$ to $12 \pm 4 \times 10^{-6}$ (See Figure 6.2.). Another significant increase in dissipation took place when the pellicle was rinsed with a pH 3 citrate buffer solution; increasing the dissipation to $15 \pm 5 \times 10^{-6}$. However, when a citrate buffer of pH7 was reintroduced over the pellicle the dissipation returned to similar levels observed at the initial pH7 rinse. This suggests that the pellicle was able to adapt its structure to the acidity of the environment with which it is exposed.

Figure 6.3. Bar charts representing the mean (n=5) (a) Dissipation, (b) Sauerbrey mass, thickness and (c) ratio of $\Delta f/\Delta D$ for salivary pellicles under different pH conditions (i.e. pH 3- pH7). The pellicle undergoes predominant structural changes at pH 4 and pH 3.



Of interest was that these changes in the dissipation of the pellicle did not reciprocate a change in the pellicle mass. Only until the final rinse of the pellicle was a significant change in hydrated mass observed; where the pellicle dropped to $1100 \pm 114 \text{ ng/cm}^2$ (see Table 6.1.). This suggests that under the acidic conditions used in this experiment the pellicle was able to maintain a significant portion of hydrated mass despite significant changes in dissipation after several acidic rinse steps.

Table 6.1. QCMD data of the salivary pellicle under neutral and acidic conditions (pH7 – pH3)

pH rinse	Frequency (Hz)	Dissipation (10^{-6})	$\Delta f/\Delta D$ (μHz)	Sauerbrey Mass (ng/cm^2)	Sauerbrey Thickness (nm)
pH7 (1st rinse)	-69(± 9)	9 (± 1)	-8 (± 1)	1218 (± 152)	12.2 (± 1)
pH6	-67(± 8)	9 (± 1)	-8 (± 1)	1179 (± 132)	11.8 (± 1)
pH5	-68 (± 7)	9 (± 2)	-8 (± 2)	1195 (± 103)	11.9 (± 1)
pH4	-69 (± 7)	12 (± 4)* ¹	-6 (± 2)* ³	1209 (± 103)	12.1 (± 1)
pH3	-68 (± 8)	15 (± 5)* ²	-5 (± 2)* ⁴	1192 (± 143)	11.9 (± 1)
pH7 (Final rinse)	-63 (± 6)	10 (± 3)	-7 (± 2)	1100 (± 114)* ⁵	11.0(± 1)* ⁶

*¹ - Pellicle significantly more dissipative at pH 4 compared to pellicle at pH5

*² - Pellicle significantly more dissipative at pH 3 compared to all other rinses

*³ - Pellicle at pH 4 significantly more viscous relative to the pellicle at pH5

*⁴ - Pellicle at pH 3 significantly more viscous relative to the pellicle at all other rinses

*⁵ - Pellicle mass significantly less than all other pellicles after pH7 (final rinse)

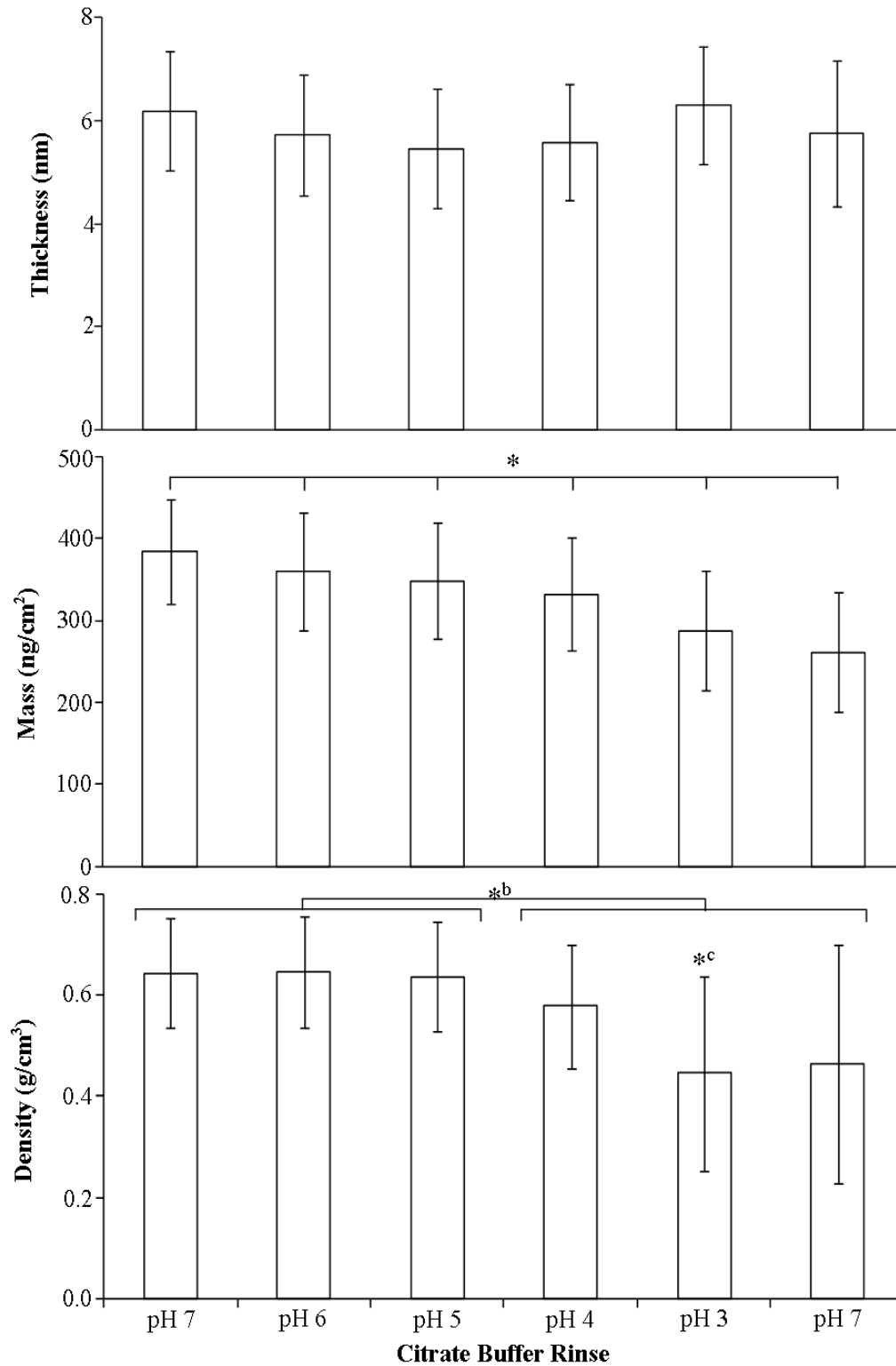
*⁶ - Pellicle thickness significantly less than all other pellicles after pH7 (final rinse)

DPI

As was observed with the QCMD results; upon the addition of saliva to the DPI silica substrate a very rapid adsorption of salivary proteins took place (see Figure 6.2.). The mean pellicle polymer mass was 385 ng/cm^2 after 2 hours adsorption. The formation of the pellicle began to plateau after 20 minutes adsorption; however, the pellicle was given a total 2 hours to fully adsorb, for reasons previously stated. Upon the first rinse step (i.e. citrate buffer at pH7) any loosely adsorbed material was removed. In fact, at each rinse a significant quantity of pellicle mass was removed,

despite the thickness of the pellicle remaining relatively consistent throughout the experiment (See Figure 6.4.).

Figure 6.4. Bar charts representing the mean (n=5) (a) Thickness, (b) Mass and (c) Density changes of the salivary pellicle under different pH conditions (i.e. pH 3- pH7). Significant changes in Mass and density but not hickness were observed.



This continual decrease in mass and stable thickness eventually gave rise to significant changes in pellicle density; dropping from $0.65 \pm 0.1 \text{ g/cm}^3$ to $0.46 \pm 0.2 \text{ g/cm}^3$. The change in density was most notable after the introduction of citrate buffer at pH4 and pH3 (See Table 6.2.). This change in pellicle density was shown to be irreversible when the final rinse of citrate buffer at pH7 had no effect on pellicle density. This suggests that after several acidic rinse steps the pellicle was able to maintain thickness despite significant changes in mass, resulting in a subsequent decrease in pellicle density.

Table 6.2. DPI data of the salivary pellicle under neutral and acidic conditions (pH7 – pH3)

pH rinse	Thickness (nm)	Density (g/cm ³)	Mass (ng/cm ²)
pH7 (1st rinse)	6.2 (± 1.2)	0.64 (± 0.1)	385 (± 63)* ⁴
pH6	5.7 (± 1.2)	0.65 (± 0.1)	360 (± 71)
pH5	5.5 (± 1.2)	0.64(± 0.1)	349 (± 71)
pH4	5.6 (± 1.1)	0.58 (± 0.1)* ¹	332 (± 69)
pH3	6.3 (± 1.1)	0.45 (± 0.2)* ²	288 (± 73)
pH7 (Final rinse)	5.8 (± 1.4)	0.46 (± 0.2)* ³	262 (± 74)

*¹ - Pellicle significantly less dense at pH4 rinse compared to all other rinses.
*² - Pellicle significantly less dense at pH3 rinse, excluding the final pH7 rinse
*³ - Pellicle significantly less dense at pH7 (final rinse), excluding the pH3 rinse
*⁴ - Significant difference in mass loss at each of the pH rinse steps

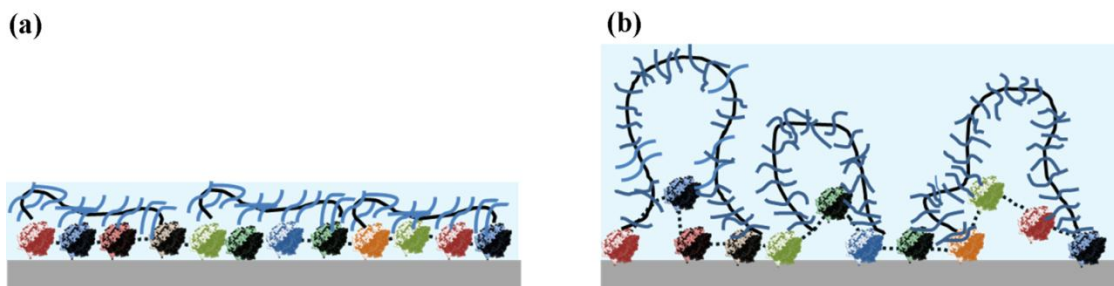
Discussion

Knowledge on the protective function of the salivary pellicle is mainly based on experiments performed *in vitro* with salivary pellicle coatings formed on enamel test pieces. These studies show that the enamel micro-hardness, mineral loss and surface roughness changes are less pronounced if the surfaces are coated with *in situ* formed pellicles. The evidence supporting the protective role of the pellicle is overwhelming [14, 15, 72, 151, 227, 229, 230, 251, 253-257]; however, these studies did not evaluate the structural modifications of the pellicle during an acidic challenge; and therefore what is not completely clear is: what structural modifications does the pellicle undergo when exposed to an acidic environment? And how do these structural modifications influence the protective role of the pellicle?

The present study therefore was designed to investigate the structure of the salivary pellicle at the solid/liquid interface by observing the formation of the salivary pellicle on silica QCMD and silica DPI sensors; and then exposing the pellicle to increasing acidic environments using citric acid. It was observed that the most significant changes in pellicle structure occurred when the pellicle was bathed in more acidic (i.e. pH4 and a pH3) citrate buffer solutions; with respect to the pellicle bathed in less acidic citrate buffers (i.e. pH7, pH6 and pH5). However, it is with the addition of the pH 4 citrate buffer that drastic structural changes begin to take place. At this concentration of hydrogen ions in solution the salivary pellicle became more diffuse, where the density of the pellicle decreased significantly ($p < 0.05$) from 0.64 ± 0.1 g/cm³ at pH 7 to 0.58 ± 0.1 g/cm³ at pH4. Whilst the data also showed that the pellicle became more viscous or 'softer' where the dissipation of the pellicle

increased significantly ($p < 0.05$) from $9 \pm 1 \times 10^{-6}$ at pH7 to $12 \pm 1 \times 10^{-6}$ at pH4 (see Figure 6.5.). It is evident from the data that an interaction between the pellicle proteins was triggered at \sim pH4; this is likely to be a consequence of a change in repulsion and attraction between proteins at this concentration of hydrogen ions.

Figure 6.5. (a) salivary pellicle showing glycosylated mucins over a layer of low-molecular weight proteins bathed in pH7 citrate buffer solution, representing a densely packed rigid film relative to (b) where a more diffuse and viscous salivary pellicle was observed when bathed in a more acidic (i.e. pH3 and pH4) citrate buffer solution.



In 2009 Siqueira & Oppenheim [49] identified that majority of peptides in the salivary pellicle were acidic in nature with 50% of all pellicle peptides having an isoelectric point (pI) of < 5.9 . Proctor *et al.* [39] also observed that a pellicle formed from parotid saliva was predominantly composed of statherin and concluded that this protein's pI was pH \sim 4.2. Other common pellicle proteins such as Cystatin-S and acidic proline rich proteins have similarly low pIs and therefore remain negatively charged at pH conditions found in the oral cavity [258]. On the one hand, this facilitates the adsorption to cationic calcium ions on the enamel surface, but on the other hand, when the pH of the environment is reduced to pH 4 pellicle proteins begin to change charge. Since the net electrostatic repulsive energy of these pellicle proteins is small at neutral pH, (relative to favourable non covalent interactions) most of the proteins in the pellicle remain stable. This was reflected in the negligible

change in the physical structure of the pellicle when rinsed with citrate buffers at pH7, and even with the slightly acidic pH6 and pH5 citrate buffers. However, when the citrate buffer was lowered to pH 4, significantly lower than the pI of most pellicle proteins, a noticeable change in physical structure was observed.

This structural change is likely a consequence of the interaction between hydrogen ions present in the acidic citrate buffer and the pellicle proteins; whereby hydrogen ions bind to the carboxyl groups and the amino groups of amino acids; neutralising their negative charges. The net charge of the pellicle proteins become positive and consequently an increase in electrostatic repulsion between amino acids took place. This then permits favourable non covalent interactions to be overcome; resulting in rearrangement of the protein molecules within the pellicle. This would explain the decrease in pellicle density and elasticity observed upon exposure to citrate buffers at pH 3 and pH4.

In 2007 Rossetti *et al.* [244] also observed a decrease in pellicle elasticity (at the air saliva interface) when citric acid was added to saliva. This was described as a consequence of aggregation and precipitation of salivary proteins adsorbed at the air interface. They hypothesised that astringency upon consumption of citric acid arises from the same disruption (e.g. aggregation and precipitation) of proteins in the salivary pellicle lubricating the oral tissue. Vardhanabhuti *et al.* [259] also observed that interactions between positively charged proteins and salivary proteins play a role in the astringency of whey protein drinks at low pH. Other acidic beverages such as fruit juices and soft drinks however, are the most common cause for enamel erosions in western societies; and the pH at which demineralisation occurs is approximately

5.5 (referred to as the critical pH [258] depending on the concentration of calcium and phosphate in saliva [260]). Yet the structural change of the salivary pellicle was only observed to take place at pH4 and below. It can be assumed therefore that the pellicle's resistance to change at pH 5 is partly responsible for the anti-erosive potential of the pellicle that forms on the tooth surface. It appears, that the complex structure and range of interactions within the pellicle prevent it from completely falling apart at low pH. Although the structure is clearly affected, it still has enough integrity and strength to keep the vast majority of the structure in place, and continue to protect the enamel, and rapidly restore itself when the pH increases again.

However, pH alone is not predictive of a food's potential to cause enamel erosion as other factors modify the progression of erosion. For example, yoghurt (pH ~4) shows no erosive capacity which is thought to be due to its high content of calcium and phosphate ions making it supersaturated with respect to the hydroxyapatite of enamel[138]. Furthermore, adding calcium to orange juice or sports drinks (e.g. Lucozade) has been shown to reduce the erosive potential of acidic beverages [73]. For example, Mahoney *et al.* also showed that an orange drink with a pH of 3.84 (and 32 mM calcium) caused no statistically significant changes in enamel, dentine hardness or elastic modulus [261]. It is also important to appreciate that the oral cavity prevents the dissolution of enamel via a number of other salivary based mechanisms, and does not just rely on the salivary pellicle for protection. For example: saliva directly acts on the erosive agent itself by diluting, clearing and buffering acids[9, 57]. In addition, the concentration of calcium and phosphate ions in saliva serves as a natural reservoir for the remineralisation of hydroxyapatite, which slows the dissolution rate of enamel [4, 11, 81, 262]. Therefore individual's salivary flow rates and eating habits also need to be considered when interpreting the

in vitro data presented. Nevertheless, this study gives an insight to the potential mechanisms involved upon structural changes of the pellicle when it is exposed to an acidic environment in the mouth; changes that are of interest to dental research; with regard to the anti-erosive potential of the pellicle; and the food industry, in terms of pellicle lubricity and mouth-feel.

Chapter 7

Structural and Compositional Changes in the Salivary Pellicle Induced Upon Exposure to SDS and STP

Introduction

The salivary pellicle is a protein rich film that forms on all surfaces within the mouth, and provides a barrier to dissolution of enamel by dietary acids, and concomitantly lubricates the mouth, facilitating the consumption and processing of food [13]. However, the pellicle is ambivalent in nature as it also provides the primary sites for the attachment of bacteria, which in certain cases can be responsible for the development of plaque; a risk factor for carie formation [18]. The pellicle therefore is juxtaposed between protecting the oral cavity from acidic and abrasive damage, whilst aiding the adsorption of plaque forming bacteria close to the tooth surface [55]. Widespread dentifrice products used in conjunction with tooth brushing act to reduce these plaque deposits, as well as tooth stain removal [147]. Certain ingredients such as, detergents (e.g. sodium dodecyl sulphate (SDS)) and abrasives (e.g. sodium carbonate) are common to most dentifrices. These ingredients are used to remove stained pellicle from dentition and loosen deposits on tooth surfaces that may become cariogenic over time [263]. In addition, chelants; known as condensed phosphates (e.g. sodium tripolyphosphate (STP)), display a strong affinity to enamel surfaces [264]. These anionic condensed phosphates have not only been shown to remove pellicle proteins that have become stained, but have also been shown to reduce plaque development [37]. The safety of pyrophosphate salts and detergents found in dentifrice products (such as STP and SDS) is now well established and today, condensed phosphates and detergents are found in most dentifrices worldwide [153, 158]. And whilst SDS is known to remove pellicle proteins [30], and STP has been shown to be effective in the *in vitro* removal of stain [161]; the impact of SDS and STP on salivary pellicle structure has not been investigated or characterised in

great detail. As the pellicle is the primary interface between the oral environment and the hard and soft tissue of the mouth, it plays an important role in oral physiological and pathological processes [68]. Consequently, a deeper understanding of the structural changes that SDS and STP induce in the salivary pellicle is important to understand. Therefore, this study investigates how STP and SDS impact the preformed salivary pellicle adsorbed onto DPI and QCMD silica and hydroxyapatite sensors and to identify the proteins SDS and STP displace using a hydroxyapatite FPLC column. Changes in the physical structure of the salivary pellicle (surface mass, density, thickness and viscoelasticity) and the identification of the proteins that SDS and STP displace are reported to help understand the way SDS and STP, not only remove the pellicle from the surface, but also what effect exposure to these chemicals has on the structure of the remaining salivary pellicle.

Materials & Methods

Saliva collection

Saliva was collected from apparently healthy volunteers according to a protocol previously assessed by an independent ethics panel as described in Chapter 2. 10 saliva samples (5 WMS & 5 PS) were exposed to hydroxyapatite and silica QCM-D and DPI sensors respectively. Subsequently each experiment was rinsed with either 10 mM SDS or 10 mM STP.

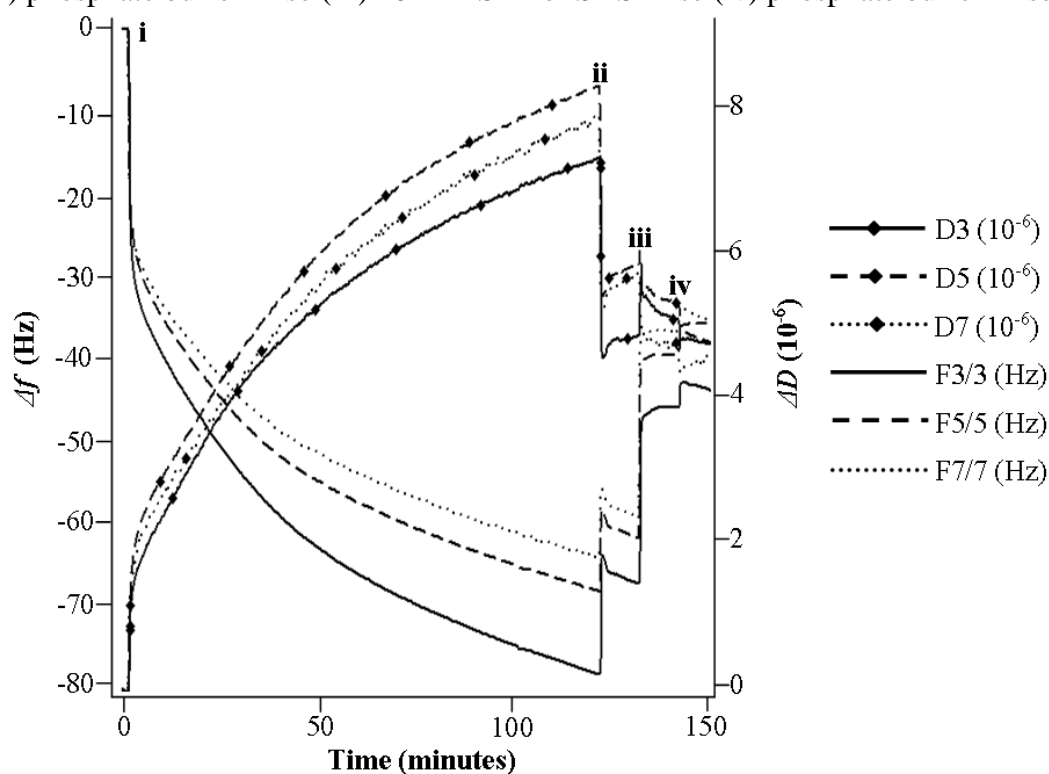
Solutions

The concentration of SDS and STP in oral hygiene products is around 1.5% w/w and 10% w/w respectively. In order to account for the dilution of STP and SDS by the saliva during use in the mouth, a concentration of 10mM of SDS (0.29% w/w) and 10mM STP (0.36% w/w) was used. 0.1M Phosphate buffer (Sigma-Aldrich) was used, with ultra-pure water as the solvent (Nanopure Diamond, Barnstead Int., USA).

Quartz crystal microbalance with dissipation monitoring (QCMD)

Changes in frequency and dissipation of the oscillating sensor were measured using a D300 QCMD (Q-Sense AB, Vastra Frolunda, Sweden) as previously described in Chapter 2. Saliva was allowed to adsorb for 2 hours onto either a silica or hydroxyapatite coated substrate before any rinsing took place. The adsorbed pellicle was then rinsed with a phosphate buffer to remove any loosely adsorbed material and allowed 10 minutes to equilibrate. Then the pellicle was rinsed with 10mM STP or 10mM SDS (depending on the experiment being carried out) and allowed to equilibrate for 10 minutes. Finally, phosphate buffer was used to rinse away any displaced pellicle proteins (See Figure 7.1. for experimental procedure).

Figure 7.1. QCMD Experimental procedure: Salivary pellicle adsorption profile for a parotid saliva sample on a QCMD hydroxyapatite sensor. (i) Addition of saliva (ii) phosphate buffer rinse (iii) 10 mM STP or SDS rinse (iv) phosphate buffer rinse.

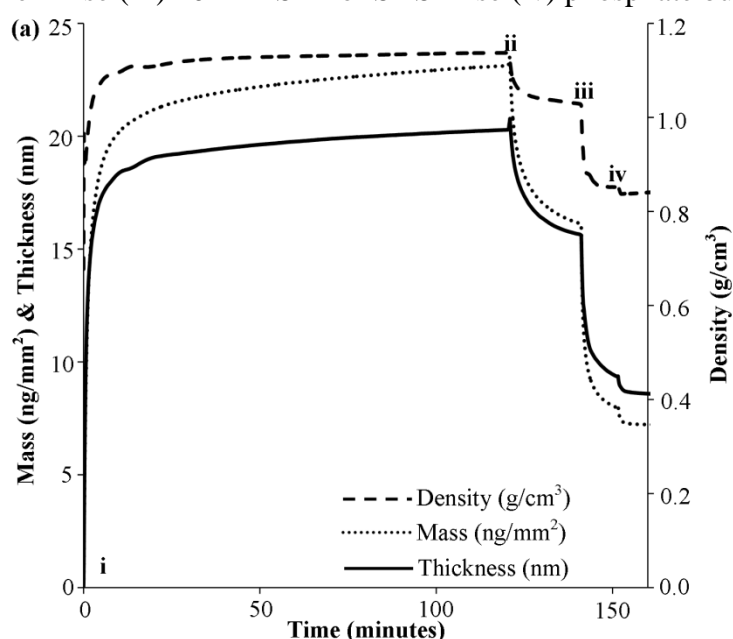


Dual polarisation interferometer (DPI)

Measurements of surface layer thickness and refractive indices (RI) were performed in real time using an AnaLight Bio200 DPI (Farfield Sensors Ltd., Manchester, UK). The sensor (silica or hydroxyapatite coated) was clamped in a temperature-controlled enclosure allowing the temperature to be maintained at 36.8°C for all experiments as previously described in Chapter 2. As with QCMD experiments, the adsorption of salivary proteins and subsequent rinsing steps were identical. i.e. Saliva was allowed to adsorb for 2 hours before any rinsing took place. The adsorbed pellicle was then rinsed with a phosphate buffer to remove any loosely adsorbed material and allowed 10 minutes to equilibrate. Then the pellicle was rinsed with 10mM STP or 10mM

SDS (depending on the experiment being carried out) and allowed 10 minutes to equilibrate. Finally, phosphate buffer was used to rinse away any displaced pellicle proteins (See Figure 7.2.); which shows the typical adsorption profile of a parotid saliva sample using the DPI.

Figure 7.2. DPI Experimental procedure: Salivary pellicle adsorption profile for parotid saliva sample on a DPI hydroxyapatite sensor. (i) Addition of saliva (ii) phosphate buffer rinse (iii) 10 mM STP or SDS rinse (iv) phosphate buffer rinse.



Sensor properties

The substrates used for the formation of the salivary pellicle were QCMD and DPI sensors coated with either hydroxyapatite (which constitutes the main mineral of the dental enamel) or silica. These surfaces differ in both their physical and chemical composition and were used in order to observe how the pellicle and the displacers (STP and SDS) behave on the two different surfaces. Under the neutral conditions (\approx pH7) used for the adsorption of the salivary pellicle in this study, the hydroxyapatite surface would have carried a slight positive charge and the silica a strong negative charge. These properties affect the interaction of SDS and STP as pellicle displacers and will be discussed later.

Fast protein liquid chromatography (FPLC)

Salivary protein fractionation was performed via a BioCAD SPRINT Perfusion Chromatography workstation (PerSeptive Biosystems, Massachusetts, USA); using ceramic hydroxyapatite particles (Bio-Rad Laboratories, Hertfordshire, UK) as the column packing media, which was replaced after each experiment. Saliva was injected into the column and allowed to adsorb for 2 hours. Un-adsorbed salivary proteins were then flushed out of the column (10 column volumes) by phosphate buffer. The remaining adsorbed proteins were then eluted using either 10mM SDS or 10mM STP (10 column volumes). Detection of proteins displaced by 10 mM SDS and 10 mM STP was performed at 220nm; eluted proteins were collected (2ml per fraction) using an Advantec SF-2120 super fraction collector (Advantec MFS Inc., CA, USA). Subsequently each 2 ml protein fraction collected was dialysed against milli-q water using Spectra/Por 3 dialysis tubing with a MWCO of 3.5 kDa (Spectrum Laboratories Inc., CA, USA) and then concentrated down to 0.5ml using a Speed-vac SPD131DDA (Thermo Scientific, Hampshire, UK).

SDS-PAGE

The pellicle protein fractions were further separated by molecular weight using SDS-PAGE. 10 µl protein samples were run on 8 cm x 9 cm, 4–12% NuPage MES BIS-TRIS pre-cast gels (Invitrogen) according to the manufacturer's instructions. The voltage was set at 200 V, 100 watts and a current of 350 mA per gel for 35 min. The gel was then fixed in a solution containing 50% methanol, 10% acetic acid and 40% ultra-pure water, and then stained with Coomassie Brilliant Blue R-250 (Thermo).

Mark 12™ unstained standard protein standards (Invitrogen) were used as molecular weight markers.

Tandem Mass Spectrometry (LC-MS/MS) & In situ trypsin hydrolysis of protein bands

Details previously explained on page 86-88 and page 99.

AFM

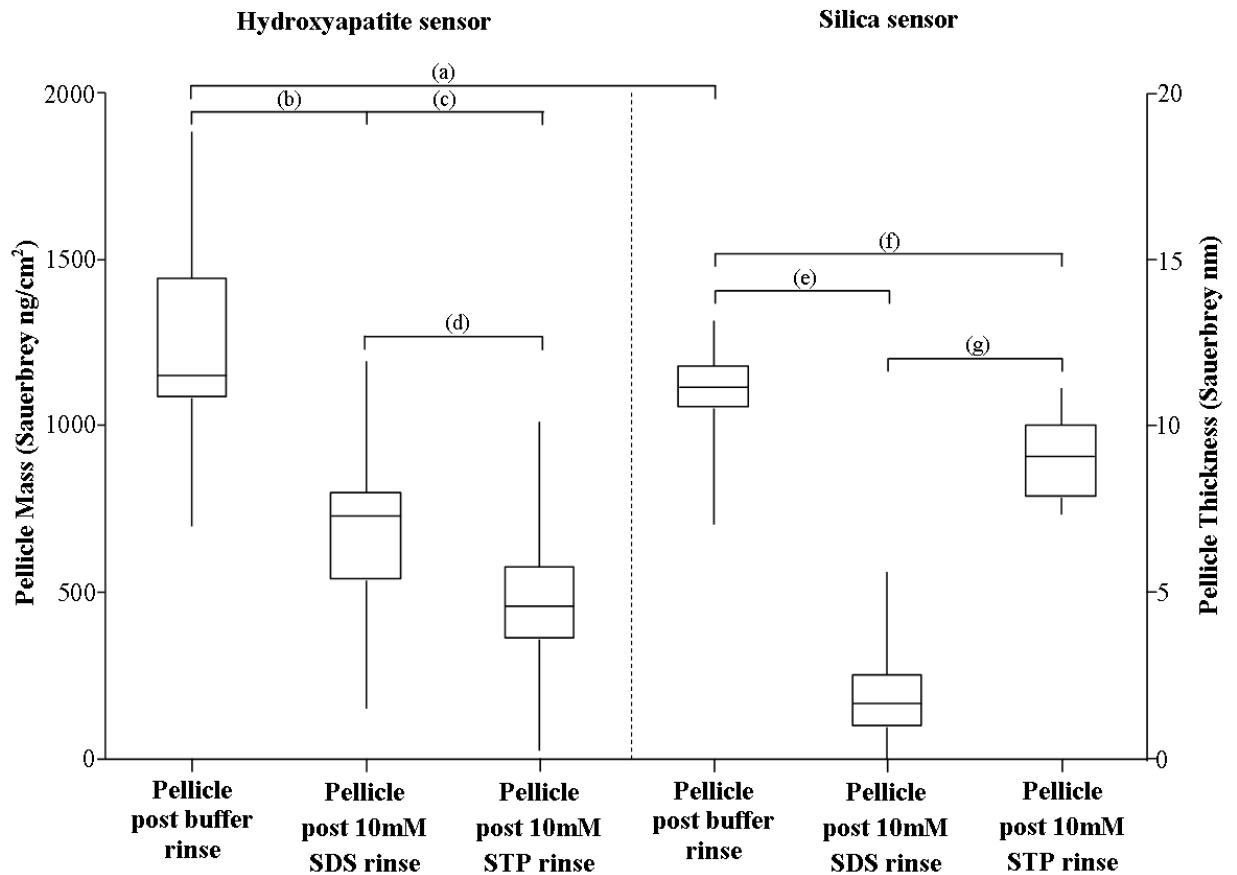
A hydroxyapatite coated QCMD sensor was placed in WMS for 2 hours and maintained at 36.8 °C to allow a pellicle to adsorb to the surface of the sensor. After exposure to saliva the sensor was rinsed with phosphate buffer and then mounted in an AFM holder. The pellicle adsorbed to the sensor surface was then imaged in liquid (phosphate buffer). The same sensor was then soaked in 10 mM STP for 10 minutes and then rinsed with phosphate buffer. The pellicle was then re-imaged in liquid (phosphate buffer).

Results

QCMD

In Figure 7.3. a box plot displays the change in pellicle mass and thickness on silica and hydroxyapatite sensors before and after exposure to 10mM SDS and 10mM STP. The mean mass for the combined PS and WMS salivary pellicles (1215 ± 289 ng/cm^2) was slightly higher on the hydroxyapatite sensor than on the silica sensor ($1103 \pm 139\text{ng}/\text{cm}^2$) but the difference was not statistically significant ($p=0.11$). After exposure to 10mM SDS the pellicle adsorbed onto hydroxyapatite sensor was reduced to $663 \pm 297\text{ng}/\text{cm}^2$ ($7 \pm 3\text{nm}$ thick). Whilst after exposure to 10mM STP it was reduced to $491 \pm 293\text{ng}/\text{cm}^2$ ($5 \pm 3\text{nm}$ thick). This showed that the remaining pellicle adsorbed onto the hydroxyapatite substrate was larger in mean thickness and mass when exposed to 10mM SDS as opposed to 10mM STP. However, a significant reversal of this result took place when SDS or STP was exposed to the pellicle adsorbed on the silica surface. This showed a large reduction in the remaining pellicle mass and thickness after exposure to 10mM SDS (mass: $194 \pm 171\text{ng}/\text{cm}^2$; thickness: $2 \pm 2\text{nm}$ thick); but only a small change when the pellicle was exposed to 10mM STP ($911 \pm 142\text{ng}/\text{cm}^2$; $9 \pm 1\text{nm}$ thick). This shows that STP was more effective at displacing pellicle from the hydroxyapatite surface, whilst conversely; SDS was more effective at displacing pellicle from the silica surface.

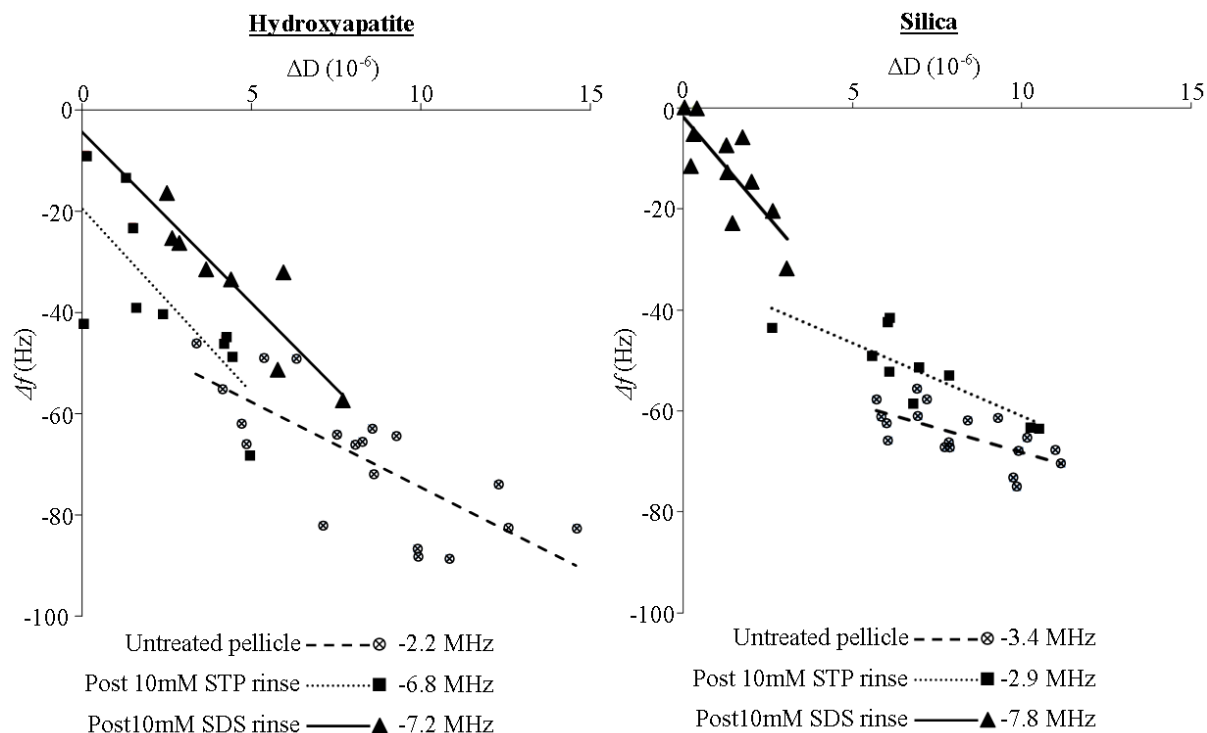
Figure 7.3. Box plot displaying the Sauerbrey mass (primary axis) and thickness (secondary axis) of the combined WMS and PS salivary pellicles on hydroxyapatite and silica sensors before and after rinsing with 10mM STP and 10mM SDS; and the statistical differences between them.



- (a) No significant difference ($p=0.113$) between pellicle adsorbed to hydroxyapatite and silica sensors
- (b),(c) Significant difference ($p < 0.001$) between pellicle before and after rinsing with 10mM SDS and 10mM STP
- (d) No significant difference ($p=0.18$) between pellicles after exposure to 10mM SDS or 10mM STP
- (e) Significant difference ($p < 0.001$) between pellicle before and after rinsing with 10mM SDS
- (f) Significant difference ($p = 0.001$) between pellicle before and after rinsing with 10mM STP
- (g) Significant difference ($p < 0.001$) between pellicles after exposure to 10mM SDS and 10mM STP

When the pellicle was exposed to 10mM SDS, it became predominantly more elastic relative to the untreated pellicle on both hydroxyapatite (-7.2 MHz) and silica (-7.8 MHz) sensors. However, when the pellicle was exposed to 10mM STP, it only became predominantly more elastic relative to the untreated pellicle on the hydroxyapatite (-6.8 MHz) sensor; and not on the silica (-2.9 MHz) sensor.

Figure 7.4. $\Delta f / \Delta D$ plot displaying the different elastic properties of the combined WMS and PS salivary pellicles before and after rinsing with SDS and STP on both hydroxyapatite and silica surfaces. (A test for outliers was performed using the “outlier test” function in the R statistical package and removed from the plots [Details p.294-296 in 265].

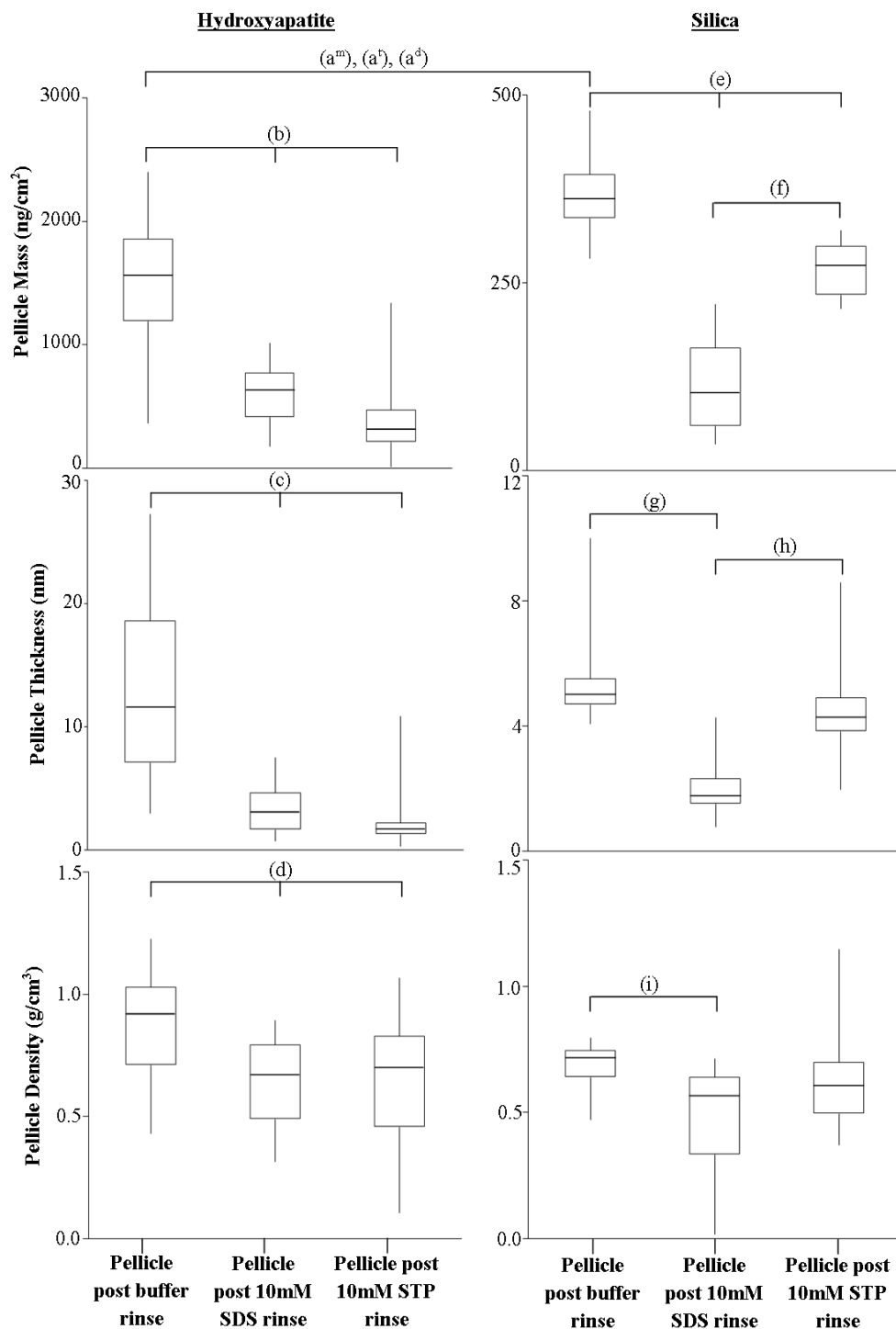


DPI

The structural properties (e.g. mass, thickness and density) of the pellicle adsorbed onto hydroxyapatite and silica sensors before and after exposure to 10mM SDS and 10mM STP is shown as a box plot in Figure 7.5. Unlike the QCMD results, there was a significant difference in the pellicle’s structure on the DPI hydroxyapatite sensor (mean mass: $1390 \pm 731 \text{ ng/cm}^2$) compared to the DPI silica sensor (mean mass: $366 \pm 52 \text{ ng/cm}^2$). After displacing the pellicle adsorbed on the hydroxyapatite sensors with 10mM SDS for 10 minutes, the remaining pellicle had a mean mass of $354 \pm 228 \text{ ng/cm}^2$ (displaced $\sim 70\%$ mass); a mean thickness of $\leq 6 \pm 3 \text{ nm}$; and a mean density of $\leq 0.6 \pm 0.2 \text{ g/cm}^3$. Similarly, after exposing the pellicle to 10 mM STP the

remaining pellicle had a mean mass of $246 \pm 289 \text{ ng/cm}^2$ (displaced $\sim 80\%$ mass); a mean thickness of $\leq 4 \pm 4 \text{ nm}$; and a mean density of $\leq 0.6 \pm 0.3 \text{ g/cm}^3$. However, when observing the remaining pellicle on the silica sensor after the application of 10mM SDS and 10mM STP, a drastic difference ($p < 0.05$) between the two was observed. After the application of 10mM SDS the remaining pellicle structure had a mean mass of $113 \pm 63 \text{ ng/cm}^2$ (displaced $\sim 70\%$ mass); a mean thickness of $2 \pm 1 \text{ nm}$; and a mean density of $0.5 \pm 0.2 \text{ g/cm}^3$. Whilst after the application of 10mM STP the remaining pellicle structure had a much higher mean mass ($268 \pm 38 \text{ ng/cm}^2$) only displacing $\sim 20\%$ of the pellicle mass; and higher mean thickness ($5 \pm 2 \text{ nm}$); and mean density ($0.6 \pm 0.2 \text{ g/cm}^3$). Demonstrating that STP was less effective at displacing from the silica surface compared to hydroxyapatite.

Figure 7.5. Box plot displaying the changes in thickness, mass and density of combined WMS and PS salivary pellicles adsorbed to a DPI hydroxyapatite and silica sensor before and after rinsing with 10mM STP and 10mM SDS.

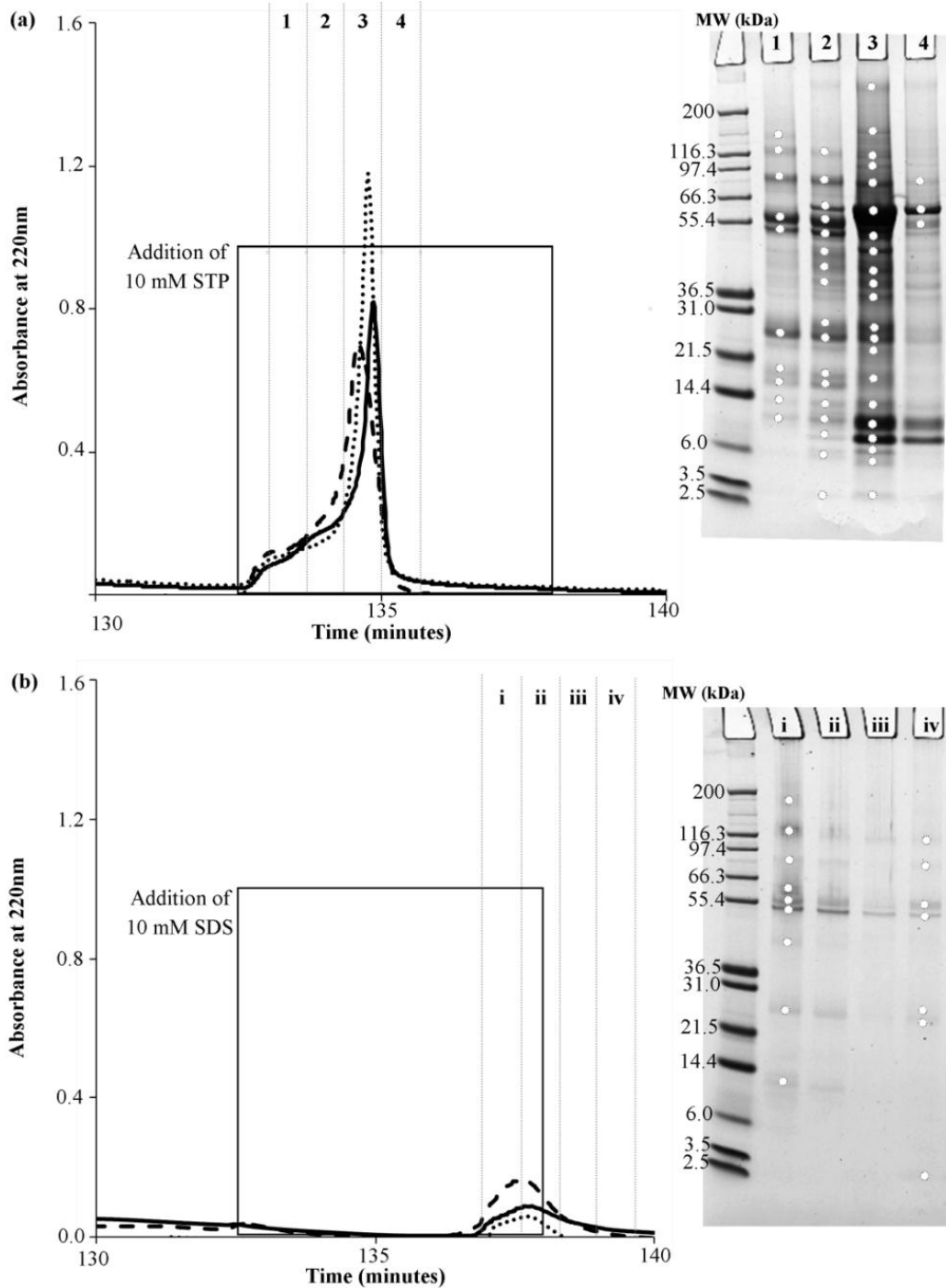


Sig. diff. ($p < 0.05$) between pellicle (Mass(a^m), Thickness(a^t), Density(a^d)) adsorbed to Hydroxyapatite and Silica
 Sig. diff. ($p < 0.05$) in pellicle Mass (b), Thickness (c), Density (d) after rinsing with 10mM SDS or 10mM STP
 Sig. diff. ($p < 0.05$) in pellicle mass (e), after rinsing with 10mM SDS or 10mM STP;
 (f) Sig. diff. ($p < 0.05$) between remaining pellicle mass rinsed with 10mM SDS and pellicles rinsed with 10mM STP
 (g) Sig. diff. ($p < 0.05$) in pellicle thickness, after rinsing with SDS and STP;
 (h) Sig. diff. ($p < 0.05$) between SDS and STP
 (i): Sig. diff. ($p < 0.05$) in pellicle mass, after rinsing with SDS

FPLC Protein identification

Whole mouth saliva was loaded into the hydroxyapatite-packed column and non adsorbed proteins flushed through. Adsorbed proteins subsequently displaced from the hydroxyapatite column using SDS or STP were collected to establish which proteins 10mM SDS and 10mM STP were displacing. The STP appeared to be much more effective at displacing proteins from the hydroxyapatite column than the SDS. The STP solution removed proteins as soon as contact was made with the column; whereas the SDS did not displace proteins until after ~5 minutes exposure (See figure 7.6.).

Figure 7.6. (a) Chromatogram showing the displacement of saliva proteins from hydroxyapatite by 10mM STP (three repeats) and the fractions collected (labelled 1-4); and the accompanying typical electrophoretic profile observed of those fractions separated by SDSPAGE (lanes 1-4). (b) Chromatogram showing the displacement of saliva proteins from hydroxyapatite by 10mM SDS (three repeats) and the fractions collected (labelled i - iv); and the accompanying typical electrophoretic profile observed of those fractions separated by SDSPAGE (labelled i - iv).



LC-MS/MS

Analysis of *in vitro* pellicle formed on the hydroxyapatite chromatography column was performed by a combination of chromatography, electrophoretic separation and tandem mass spectrometry. The displacement of salivary proteins from hydroxyapatite using 10 mM STP (see Table 7.1. **(a)**) showed the presence of 74 proteins from the major bands selected and 35 proteins using 10 mM SDS (see Table 7.1. **(b)**). Salivary proteins that are commonly found in the *in vivo* pellicle, such as; α -amylase, and cystatins, appear to be displaced by both STP and SDS. In addition, the identification of keratin (type II cytoskeletal 2 epidermal) in the *in vitro* pellicle suggests that the oral epithelium is also a source of pellicle proteins. The presence of a number of enzymes (e.g. α -amylase, carbonic anhydrase and lactoperoxidase) some of which have been shown to be immobilized in an active conformation in the pellicle layer [24] highlight the dynamic nature of the salivary pellicle that goes beyond a physical barrier.

Table 7.1. (a) Identified proteins displaced from hydroxyapatite using 10mM STP.

Accession number	protein name	Score	Mass (kDa)	Sig. sequences	PI
O60603	Toll-like receptor 2	845	90920	3	6.17
P00450	Ceruloplasmin	577	122983	18	5.44
P00558	Phosphoglycerate kinase 1	963	44985	24	8.3
P00738	Haptoglobin	845	45861	17	6.13
P01009	Alpha-1-antitrypsin	853	46878	15	5.37
P01023	Alpha-2-macroglobulin	1290	164613	36	6.03
P01024	Complement C3	476	188569	17	6.02
P01036	Cystatin-S	250	16489	2	4.95
P01040	Cystatin-A	240	11000	6	5.38
P01833	Polymeric immunoglobulin receptor	1705	84429	23	5.58
P01834	Ig kappa chain C region	401	11773	4	5.58
P01859	Ig gamma-2 chain C region	759	36505	11	7.66
P01860	Ig gamma-3 chain C region	133	42287	5	8.23
P01876	Ig alpha-1 chain C region	319	38486	4	6.08
P01877	Ig alpha-2 chain C region	469	37301	8	5.71
P02768	Serum albumin	1831	71317	33	5.92
P02774	Vitamin D-binding protein	477	54526	9	5.4
P02787	Serotransferrin	419	79294	12	6.81
P04040	Catalase	959	59947	24	6.9
P04080	Cystatin-B	193	11190	2	6.96
P04083	Annexin A1	1856	38918	27	6.57
P04745	Alpha-amylase 1	1098	58415	12	6.47
P05109	Calgranulin-A	220	10885	4	6.51
P06396	Gelsolin	541	86043	14	5.9
P06702	Calgranulin-B	319	13291	3	5.71
P06703	Calcyclin	186	10230	7	5.33
P06733	Alpha-enolase	848	47481	17	7.01
P07237	Protein disulfide-isomerase	525	57480	16	4.76
P07737	Profilin-1	384	15216	7	8.44
P09960	Leukotriene A-4 hydrolase	803	69868	15	5.8
P10599	Thioredoxin	256	12015	7	4.82
P12273	Prolactin-inducible protein	2847	16847	11	8.26
P12429	Annexin A3	760	36524	14	5.63
P12814	Alpha-actinin-1	1747	103563	37	5.25
P13796	Plastin-2	229	70814	8	5.29
P13928	Annexin A8	321	37086	7	5.56
P18206	Vinculin	927	124292	27	5.5
P18669	Phosphoglycerate mutase 1	394	28900	10	6.67
P22079	Lactoperoxidase	673	81149	18	8.89
P23141	Liver carboxylesterase	298	62766	9	6.15
P25311	Zinc-alpha-2-glycoprotein	977	34465	17	5.71
P29401	Transketolase	682	68519	10	7.58
P30044	Peroxiredoxin-5	260	22301	6	8.93
P30740	Leukocyte elastase inhibitor	1384	42829	14	5.9
P30838	Aldehyde dehydrogenase	617	50762	18	6.11
P31025	Lipocalin-1	1470	19409	15	5.39

Table 7.1. (a) Continued.

P37837	Transaldolase	986	37688	21	6.36
P40926	Malate dehydrogenase	393	35937	5	8.92
P50395	Rab GDP dissociation inhibitor beta	375	51087	14	6.11
P52209	6-phosphogluconate dehydrogenase	1292	53619	13	6.8
P54108	Cysteine-rich secretory protein 3	226	28524	11	8.09
P59665	Neutrophil defensin 1;	2229	10536	6	6.54
P59666	Neutrophil defensin 3	273	10580	3	5.71
P60174	Triosephosphate isomerase	363	31057	9	5.65
P60709	Actin, cytoplasmic 1	236	42052	8	5.29
P61626	Lysozyme C	841	16982	7	9.38
P62805	Histone H4	257	11360	4	11.36
P62937	Peptidyl-prolyl cis-trans isomerase A	238	18229	8	7.68
P63104	Protein kinase C inhibitor protein 1	436	27899	10	4.73
P68871	Hemoglobin subunit beta	981	16102	9	6.75
P69905	Hemoglobin subunit alpha	1049	15305	5	8.72
P80188	Neutrophil gelatinase-associated lipocalin	296	22745	8	9.02
Q01469	Fatty acid-binding protein	353	15497	6	6.6
Q0KKI6	Immunoglobulin light chain	775	24300	9	8.29
Q2TUW9	Lactoferrin	713	79812	22	8.51
Q6NS95	IGL@ protein	287	25475	6	6.19
Q6P5S2	UPF0762 protein C6orf58	793	38244	15	5.78
Q6PIL8	IGK@ protein	2920	26103	14	6.15
Q96DA0	Zymogen granule protein 16 homolog B	510	22725	8	6.74
Q9HC84	Mucin-5B	535	611584	14	6.2
Q9HD89	Resistin	348	12096	2	6.51
Q9NPP6	Immunoglobulin heavy chain variant	5177	45613	15	5.75
Q9Y6R7	IgGFc-binding protein	990	596443	25	5.14

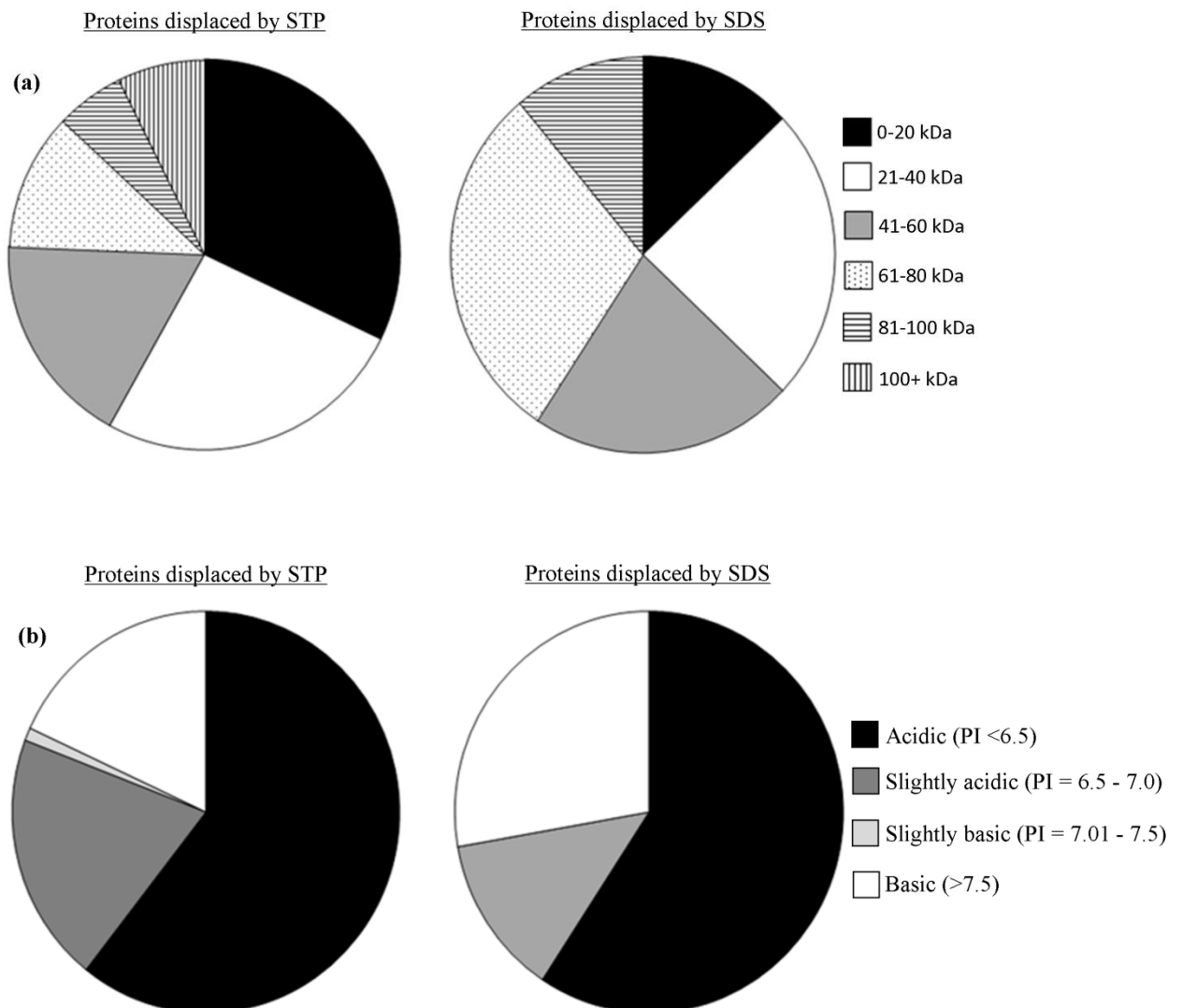
Table 7.1. (b). Identified proteins displaced from hydroxyapatite using 10mM SDS.

Accession number	protein name	Score	mass (kDa)	Sig. sequences	PI
P35908	Keratin, type II cytoskeletal 2 epidermal	1339	65678	27	8.07
C3PTT6	Pancreatic adenocarcinoma upregulated factor	975	21553	8	6.74
P00558	Phosphoglycerate kinase 1	457	44985	11	8.3
P01009	Alpha-1-antitrypsin	573	46878	14	5.37
P01011	Alpha-1-antichymotrypsin	288	47792	11	5.33
P01036	Cystatin-S	117	16489	3	4.95
P01591	Immunoglobulin J chain	172	18543	4	5.12
P01833	Polymeric immunoglobulin receptor	648	84429	17	5.58
P01859	Ig gamma-2 chain C region	330	36505	5	7.66
P01877	Ig alpha-2 chain C region	127	37301	3	5.71
P02768	Serum albumin	146	71317	5	5.92
P02787	Serotransferrin	337	79294	10	6.81
P04264	Keratin, type II cytoskeletal 1	1223	59020	24	8.15
P04406	Glyceraldehyde-3-phosphate dehydrogenase	256	36201	7	8.57
P04745	Alpha-amylase 1	1230	58415	25	6.47
P05109	Calgranulin-A	81	10885	2	6.51
P06744	Glucose-6-phosphate isomerase	145	63335	6	8.43
P07737	Profilin-1	261	15216	7	8.44
P09960	Leukotriene A-4 hydrolase	547	69868	14	5.8
P13645	Keratin, type I cytoskeletal 10	764	59020	12	5.13
P20061	Transcobalamin-1	206	48689	4	4.96
P22079	Lactoperoxidase	105	81149	6	8.89
P23280	Carbonic anhydrase 6	346	35459	8	6.51
P25311	Zinc-alpha-2-glycoprotein	822	34465	19	5.71
P30838	Aldehyde dehydrogenase	326	50762	7	6.11
P35527	Keratin, type I cytoskeletal 9	300	62255	7	5.14
P35908	Keratin, type II cytoskeletal 2 epidermal	943	65678	20	8.07
P59665	Neutrophil defensin 1	355	10536	6	6.54
P60174	Triosephosphate isomerase	286	31057	6	5.65
P61626	Lysozyme C	102	16982	2	9.38
P81605	Preproteolysin	70	11391	2	6.08
Q5EFE6	Anti-RhD monoclonal T125 kappa light chain	313	26024	4	8.7
Q6PIL8	IGK@ protein	745	26103	8	6.15
Q96DA0	Zymogen granule protein 16 homolog B	467	22725	6	6.74
Q96DR5	Parotid secretory protein	262	27166	6	5.35

The pellicle proteins identified were grouped according to their molecular weight (MW) to distinguish which types of proteins were being displaced when the pellicle was exposed to SDS or STP (See Figure 7.7. (a)). The STP displaced significantly more protein compared to SDS; and across a wider range of MWs, including a lot of high MW proteins. Whereas the SDS displaced fewer proteins; of which most were above 55 kD. In addition, the proteins were also grouped according to their isoelectric points (Figure 7.7. (b)). Considering that the pH value of stimulated saliva can increase up to pH 8 [9]; and that over 70% of all these proteins had isoelectric

points below pH 7; the majority of proteins displaced by STP or SDS were acidic in nature.

Figure 7.7. Qualitative classification of the *in vitro* pellicle proteins displaced by 10mM STP and 10 mM SDS according to (a) molecular weight and (b) isoelectric point. **N.B** STP displaced significantly more proteins than SDS. The following pie charts only show relative contributions of proteins displaced out of 100% and do not represent the total amount of protein displaced.



Discussion

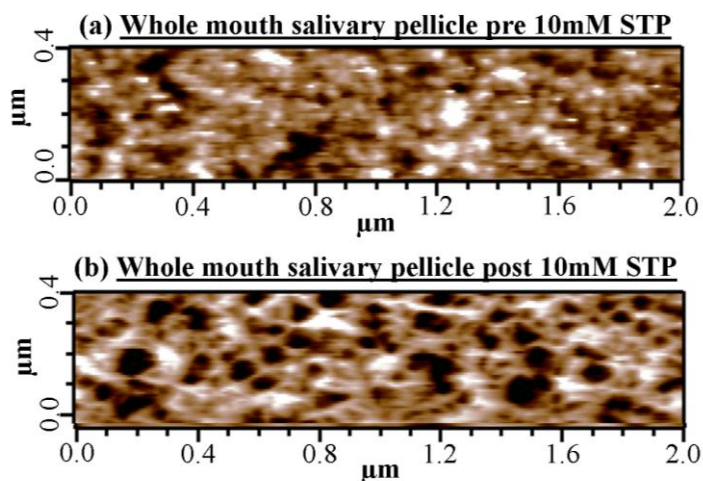
The first part of the present study used QCM-D and DPI to investigate the physical structure of the salivary pellicle at solid surfaces. These techniques made it possible to quantify the adsorption/desorption processes in real time, and observe the response of the pellicle structure upon exposure to SDS and STP [266, 267]. In both instruments 10mM STP had a more dramatic impact on the salivary pellicles adsorbed on the hydroxyapatite coated sensors as opposed to salivary pellicles adsorbed onto silica sensors. This difference in response was likely to be due to the electrostatic differences between the two surfaces (one negative (i.e. silica) and one positive (i.e. hydroxyapatite)). It was likely that STP was chelating cationic calcium ions of the hydroxyapatite coated sensors, and in by doing so, was strongly adsorbing to the hydroxyapatite [145]. In this way, STP appears to displace the salivary pellicle indirectly via competitive adsorption for the hydroxyapatite surface. However, relying solely on competitive adsorption to explain the displacement of pellicle from the hydroxyapatite surface using STP was not entirely satisfactory. This was because a small amount of pellicle displacement from the anionic silica surface when using STP was observed.

As the STP molecule is polyanionic and the surface of the silica sensor (under the conditions of this experiment) was also anionic, if competitive displacement was the only mode of action, one would see no displacement of pellicle adsorbed to the silica surface, as STP would be repulsed from the negative silica surface. However, this was not the case as STP displaced a small quantity of pellicle adsorbed onto the silica surface as well. One explanation for this phenomenon would be that STP was

interacting with the pellicle directly by chelating, and thus removing calcium ions that cross-link proteins within the pellicle itself. Because calcium ions have been shown to increase the strength of salivary films [39], their absence from the pellicle via STP chelation may result in a pellicle that is more loosely bound and therefore easier to displace.

SDS on the other hand was shown to displace significant quantities of pellicle from both silica and hydroxyapatite surfaces but, as has been observed in other studies [124, 268] the displacement was more pronounced on the silica sensor. Certain, surfactants are able to displace proteins by competitive adsorption with hydrophobic surfaces. Despite the surfaces in this study being only moderately hydrophobic, they will still be attractive to surfactants such as SDS. Although, the exact mechanism of protein displacement via surfactants is still unclear, work carried out by Mackie *et al.* [269] suggest that the protein films can be displaced by surfactants entering defects within the protein network and expanding these areas until the protein network breaks and is displaced; a process known as ‘orogenic displacement’ (See Figure 7.8.).

Figure 7.8. AFM image of (a) 2 hour adsorbed salivary pellicle. (b) The same pellicle after exposure to 10mM STP. The holes in the pellicle in image (b) represent areas where the pellicle network has been displaced by STP entering defects within the pellicle.



However, it has been shown that protein displacement potential of SDS is different depending on the surfaces that the proteins have adsorbed to [140] and that the mechanism behind the displacement of proteins from a silica surface using SDS has been suggested to be repulsion between negatively charged protein-SDS complexes and the negatively charged silica surface [270]. This would suggest that the SDS displaces the pellicle adsorbed onto the sensors by interacting directly with the proteins of the adsorbed pellicle. Nonetheless, a significant amount of pellicle remained attached to both hydroxyapatite and silica sensors after exposure of the pellicle to 10mM SDS and 10mM STP.

The remaining pellicle adsorbed onto the hydroxyapatite substrate was larger in mean thickness and mass after exposure to 10mM SDS than when exposed to 10mM STP. The increase in elasticity (observed in the $\Delta F/\Delta D$ plots); and the concomitant reduction in pellicle density (see figure 7.5.) after exposure to SDS and STP, would

suggest that the proteins that contributed to the viscous component of the pellicle were being removed, whilst the elastic component of the pellicle remained present. This would imply a curious structural transformation from a dense, viscoelastic structured pellicle, to an elastic but more diffuse pellicle after exposure to SDS and STP.

When SDS and STP were exposed to the pellicle adsorbed on the silica surface; a large reduction in the remaining pellicle mass and thickness only took place after exposure to 10mM SDS, (only a small change occurred when the pellicle was exposed to 10mM STP). It appears that SDS was able to reduce the viscous nature of the pellicle on both silica and hydroxyapatite surfaces, whereas the STP appeared to leave a more robust pellicle on the silica surface. Unlike SDS, STP does not contain any regions of hydrophobicity. Therefore STP does not displace pellicle proteins via hydrophobic interactions, and is also unlikely to interfere with any of the basic proteins attached to the negatively charged phosphate ions of the hydroxyapatite surface, such as Lysozyme and Histatins, due to its polyanionic nature. SDS on the other hand, is an amphiphilic anionic detergent that although negatively charged has a much lower charge density than the STP molecule, and can therefore directly solubilise proteins within the pellicle regardless of the charge of the sensor the pellicle had been adsorbed to. This was reflected in the fact that significant displacement of pellicle from all sensors occurred when exposed to SDS. However, contrary to this was the lack of protein displacement observed in the second part of this study, where pellicle proteins were exposed to 10mM SDS or 10mM STP via hydroxyapatite chromatography. Rykke *et al.* [271] observed the lack of protein (albumin) displacement from hydroxyapatite when exposed to SDS; suggesting that

the hydrocarbon tail of SDS lowered the desorbing potential of the molecule. If this was indeed the case, it would suggest that the interaction between pellicle proteins adsorbed onto the hydroxyapatite coating of the QCMD and DPI sensors are more susceptible to protein displacement than the hydroxyapatite of the FPLC column. Perhaps the underlying silica beneath the hydroxyapatite coatings of the DPI and QCMD sensors facilitates the displacement of pellicle proteins from the sensors. However, it may simply be that the difference in surface area to volume ratio of the hydroxyapatite column compared to the sensors is the primary reason for the differences observed. Other studies [124, 268] have also shown that SDS was less effective at protein displacement on hydroxyapatite surfaces when compared to silica. This compliments our observation of the minute quantities of pellicle displacement when the SDS was exposed to the pellicle adsorbed onto hydroxyapatite via FPLC. STP, on the other hand was very effective in displacing proteins from all hydroxyapatite surfaces and this was reflected particularly well in the ion exchange chromatogram Figure 7.6. (a).

The observation that the majority (~70%) of proteins displaced by SDS and STP were acidic in nature implies that the negatively charged sulphate group of SDS, and the negatively charged phosphate groups of STP, was where the key interactions between the cationic calcium ions of the hydroxyapatite surface and the adsorbed proteins was taking place. This interaction was much stronger for STP than it was for SDS. However, the high concentration of acidic proteins identified could be a consequence of the high concentration of acidic proteins throughout the pellicle [49] as opposed to any specific anionic (SDS) or cationic (Ca^{++}) interaction.

Complications in the analysis of data occurred as a consequence of the high variability in the adsorbed mass of pellicle observed between individuals; as has also been recorded in other studies [33]. This was highlighted by the high standard deviation observed for the mean WMS pellicle that adsorbed onto both QCMD and DPI hydroxyapatite sensors ($1215 \pm 289 \text{ ng/cm}^2$ and $1390 \pm 731 \text{ ng/cm}^2$ respectively). These differences are likely to be a consequence of the variable composition of the volunteer's saliva, a common difficulty encountered in salivary research [272]. The variability in measurements of biological samples such as saliva can conceal real trends in data sets when sample sizes or numbers of data points are relatively few. To increase the overall power of the system under study, the data from PS formed pellicles with that of WMS formed pellicles was combined. Increasing the number of data sets in this way confirmed if trends in the data were statistically significant [273]. This was considered a valid as the main aim of the study was to understand the impact of STP and SDS on the adsorbed pellicle as opposed to difference in PS and WMS pellicle.

Other differences in pellicle structure arose due to the physical and chemical properties of the sensors used in this study. For example, it has been shown that the protein profiles of the salivary pellicle adsorbed onto hydroxyapatite *in vitro* can differ from the salivary pellicle adsorbed onto enamel *in vivo*; even when formed from the same saliva [115]. However, [20, and 36] identified proteins *in vivo* to also be present *in vitro* thus validating the system used in the current study.

It is known that protein adsorption to a solid surface is affected by a number of parameters, such as the surface roughness of the sensor (see chapter 3), or the

hydrophobicity of the sensor [195]. As the DPI hydroxyapatite and silica sensors used in this study varied in a number of physical parameters, it was not possible to determine with certainty whether the saliva sample, or the sensor's substrate, had the greater effect on the amount of pellicle proteins adsorbing to the sensor surface. However, and importantly for the interpretation of the results in this study, the chemical properties of the sensors remained consistent. That is to say that both DPI and QCMD hydroxyapatite sensors would have remained positively charged and the silica sensors would have remained negatively charged at the pH used in these experiments. And it was this phenomenon that was exploited to distinguish the modes of action with which the polyanionic STP and amphiphilic SDS displaced pellicle from the surface of hydroxyapatite and silica sensors.

In conclusion the interaction of the polyanionic molecule STP with the salivary pellicle is strongly influenced by electrical charge of the surface that the pellicle has adsorbed to. For example, STP removes pellicle from hydroxyapatite via competitive adsorption for the cationic calcium ions on the hydroxyapatite surface, and by sequestering calcium ions that cross link proteins within the pellicle. However, STP is less effective when removing pellicle from silica surfaces mainly due to electrical repulsion from the silica. Conversely, SDS was affected less by the surface that the pellicle had adsorbed onto and was able to displace significant quantities of pellicle adsorbed on both hydroxyapatite and silica surfaces via a direct interaction with the pellicle. However, the pellicle displacing potential of SDS was shown to be less effective on pure hydroxyapatite compared to hydroxyapatite coated QCM-D and DPI sensors; and it maybe that the underlying sensor, beneath the hydroxyapatite

coatings, increases the adsorption potential of SDS, and should be considered when interpreting SDS protein displacement from sensors with a hydroxyapatite coating.

Chapter 8

Conclusion

The salivary pellicle plays an important role in maintaining oral health, however, a complete understanding of its genesis remains unresolved. In an attempt to provide more detail in the subject area this thesis has highlighted the physical properties of the salivary pellicle during its formation *in vitro* and when exposed to different components of food (e.g. calcium [33]& changes in pH) and dental hygiene products (e.g. STP & SDS). This information has been important in helping to further understand the formation of the salivary pellicle and its structure and composition on different surfaces (e.g. silica & hydroxyapatite). For example, it was shown how the physical properties of the pellicle (e.g. mass & viscoelasticity) are influenced by the physical properties of the sensor (e.g. hydrophobicity & surface roughness) to which the salivary proteins adsorb. This early work resulted in the selection of two types of surfaces (i.e. hydroxyapatite & silica) being used for the remainder of the project. The use of stimulated parotid saliva (mucin free) and stimulated whole mouth saliva on these surfaces made it possible to deduce an appreciation for the role that mucins play in the formation of the pellicle [274]. In particular, the mucins within saliva were shown to play two key roles during pellicle formation. Firstly they may favour the diffusion of low MW proteins to the enamel surface, by hindering the diffusion of high molecular weight proteins and secondly, the mucins help to form a less elastic, outer layer, thus lubricating the tooth surface and providing protection against potential abrasive stresses. Other components inherent to saliva, such as calcium, were also explored. It was found that increasing the natural calcium concentration of saliva by 10 mM CaCl₂ increased the aggregation of proteins in saliva; forming large protein aggregates prior to pellicle adsorption, which subsequently deposit onto the sensor surface forming thicker but less dense films [33]. However, the overall structure of the pellicle was shown to be insensitive to calcium at low concentrations,

allowing a flexibility to adapt to changing physiological and environmental conditions. Other environmental changes such as, changes in acidity were also observed. This gave an insight to the potential mechanisms involved upon structural changes of the pellicle when it was exposed to an acidic environment in the mouth when, for example, consuming acidic foods. A structural change of the salivary pellicle was only observed to take place at pH4 and below. This correlated with the pI of some of the proteins identified in the pellicle, reducing the binding with calcium and thus weakening the pellicle structure. However the pellicle remained largely intact, and this resistance to structural change was considered to be partly responsible for the anti-erosive potential of the pellicle that forms on the tooth surface. Finally, the investigation of STP and SDS was explored in order to try and understand the way these different dentifrice components displace the pellicle; and further, to what degree they affect the remaining pellicle structure. STP was shown to remove pellicle from hydroxyapatite via competitive adsorption for the cationic calcium ions on the hydroxyapatite surface, and by sequestering calcium ions that cross link proteins within the pellicle. SDS on the other hand, was shown to directly solubilise proteins within the pellicle regardless of the surface charge of the sensor. Identification of pellicle proteins that were displaced by SDS and STP were also investigated to understand how SDS and STP affect the structure and composition of the pellicle and the mechanisms of pellicle displacement. This new knowledge builds upon the current understanding of the salivary pellicle and may provide details towards the development of more realistic and effective salivary mimetics, which has currently not been possible due to the complex interfacial properties of saliva.

The multifunctional roles of saliva, in particular the formation, structure and composition of the salivary pellicle, represents a very focused area of scientific research. From a dental perspective, the interaction between the pellicle formed in the mouth and its interaction with dental components is starting to generate a lot of attention [34, 254, 255, 263, 275-278]. In particular, combining ingredients that not only remove biofilm build up; but also potentially interact with the pellicle to prevent subsequent bacterial adsorption, is a topic that may become widespread. Altering molecules present in the pellicle, which may bind to bacterial surface receptors, is one way that could prevent bacterial adsorption close to the tooth surface. Gibbons *et al.* [279] used enzymes added to toothpaste formulations to alter the carbohydrate moieties of the pellicle *in vitro*, which subsequently caused a reduction of bacterial adherence (N.B. Carbohydrates can be ligands used for bacterial adherence). Although, confirmation of those findings *in vivo* failed, it does perhaps open up the field to test other combinations of enzymes in oral hygiene formulations to see if pellicle modification takes place; and if any potential changes can result in the development of an effective prophylaxis against tooth decay. Recently, Hannig *et al.* [275] were able to show that certain mouthwash preparations containing hydroxyapatite microclusters displayed antiadherent and antibacterial effects.

There is also increasing interest from food scientists to understand the influence of the pellicle on the sensory perception of foods and how certain food ingredients interact with the pellicle [244, 280, 281]. For example, performing studies to unravel the chemical and physical mechanisms by which salivary components mediate the processing and perception of food could potentially help reveal the importance of the pellicle on taste and texture perception. Combining laboratory techniques that

measure the viscoelastic nature of the pellicle, alongside trained human sensory panels to evaluate changes in food texture or taste, may take us a step closer to elucidating the pellicle's role in the sensory perception of foods. Studies have looked at how polyphenols found in fruits and vegetables can induce a dry, puckering feeling in the mouth [217, 244, 259, 282]. A consequence of the pellicle losing its viscoelastic properties as pellicle proteins aggregate with polyphenols [238]. However, it may be more revealing to observe the effect of food components that can create a creamy sensation in the mouth. For example, it may be useful to look at the effect of different fatty acids found in foods on the viscoelastic effect they have on a preformed pellicle. Identifying any potential change in pellicle structure could provide important information on the changes that the pellicle undergoes when exposed to fat rich foods; foods that humans find desirable. This could potentially result in acquiring the knowledge required to modify foods in order to increase palatability or reduce fat content without the loss of texture.

Another area of research involves the possible regenerative properties and functions of the salivary pellicle. For example, evidence suggests that growth factors play a role in wound healing and the maintenance of oral and systemic health [283]. This raises several questions, each of which would be potential avenues of further pellicle research. For example, could the salivary pellicle be selectively enhanced to promote these growth factors? Or enhanced to selectively control bacterial adherence and aggregation? Would it be possible to promote the adsorption of buffering systems close to the tooth surface to prevent acid erosion? Or would it be possible to extract salivary components to develop more effective artificial salivas? A relatively straightforward future study would be to use the information gathered in this research

on the physical behaviour of the pellicle to design and develop improved artificial salivas. Research should focus on these topics by using *in vivo* pellicle models where possible or *in vitro* models as a substitute. Systematic investigation of the formation of the pellicle in this way is necessary to promote long-term changes of the *in vivo* formed pellicle layer. Whilst this research may represent a significant challenge, the results of such studies would provide important insights into the functional properties of the salivary pellicle, insights that are essential for the development of future pellicle based research.

References

- [1] A. Yin, H.C. Margolis, Y. Yao, J. Grogan and F.G. Oppenheim, Multi-component adsorption model for pellicle formation: The influence of salivary proteins and non-salivary phospho proteins on the binding of histatin 5 onto hydroxyapatite, *Arch. Oral Biol.*, 51 (2006) 102-110.
- [2] A. Thylstrup and O. Fejerskov, *Textbook of Clinical Cariology*, Munksgaard, 1994.
- [3] R.J. Turner and H. Sugiya, Understanding salivary fluid and protein secretion, *Oral Diseases*, 8 (2002) 3-11.
- [4] L.M. Sreebny, Saliva in health and disease: an appraisal and update, *Int. Dent. J.*, 50 (2000) 140-161.
- [5] L. Zheng, Y.J. Seon, J. McHugh, S. Papagerakis and P. Papagerakis, Clock Genes Show Circadian Rhythms in Salivary Glands, *J. Dent. Res.*, 91 (2012) 783-788.
- [6] R.G. Smith and A.P. Burtner, Oral side-effects of the most frequently prescribed drugs, *Special care in dentistry : official publication of the American Association of Hospital Dentists, the Academy of Dentistry for the Handicapped, and the American Society for Geriatric Dentistry*, 14 (1994) 96-102.

- [7] P.C. Denny, P.A. Denny, D.K. Klauser, S.H. Hong, M. Navazesh and L.A. Tabak, Age Related-Changes in Mucins from Human Whole Saliva, *J. Dent. Res.*, 70 (1991) 1320-1327.
- [8] H. Inoue, K. Ono, W. Masuda, Y. Morimoto, T. Tanaka, M. Yokota and K. Inenaga, Gender difference in unstimulated whole saliva flow rate and salivary gland sizes, *Arch. Oral Biol.*, 51 (2006) 1055-1060.
- [9] T.K. Fábíán, P. Fejérdy, P. Csermely and T.P. Begley, Saliva in Health and Disease, *Chemical Biology of*, in: *Wiley Encyclopedia of Chemical Biology*, John Wiley & Sons, Inc., 2007.
- [10] W.M. Edgar, Saliva and Dental Health - Clinical Implications of Saliva - Report of a Consensus Meeting, *Br. Dent. J.*, 169 (1990) 96-98.
- [11] S.P. Humphrey and R.T. Williamson, A review of saliva: Normal composition, flow, and function, *Journal of Prosthetic Dentistry*, 85 (2001) 162-169.
- [12] A.V. Amerongen, J.G.M. Bolscher and E.C.I. Veerman, Salivary proteins: Protective and diagnostic value in cariology?, *Caries Res.*, 38 (2004) 247-253.
- [13] G. Carpenter, Role of Saliva in the Oral Processing of Food, in: *Food Oral Processing*, Wiley-Blackwell, 2012, pp. 45-60.

- [14] M. Hannig, M. Fiebiger, M. Guntzer, A. Dobert, R. Zimehl and Y. Nekrashevych, Protective effect of the in situ formed short-term salivary pellicle, *Arch. Oral Biol.*, 49 (2004) 903-910.
- [15] C. Hannig, K. Becker, N. Hausler, W. Hoth-Hannig, T. Attin and M. Hannig, Protective effect of the in situ pellicle on dentin erosion-an ex vivo pilot study, *Arch. Oral Biol.*, 52 (2007) 444-449.
- [16] J. Kosoric, M.P. Hector and P. Anderson, The influence of proteins on demineralization kinetics of hydroxyapatite aggregates, *Journal of Biomedical Materials Research Part A*, 94A (2010) 972-977.
- [17] J. Kosoric, R. Williams, M. Hector and P. Anderson, A Synthetic Peptide Based on a Natural Salivary Protein Reduces Demineralisation in Model Systems for Dental Caries and Erosion, *Int J Pept Res Ther*, 13 (2007) 497-503.
- [18] C. Hannig and M. Hannig, The oral cavity-a key system to understand substratum-dependent bioadhesion on solid surfaces in man, *Clinical Oral Investigations*, 13 (2009) 123-139.
- [19] M.S. Kelly, J. Nuttall, N. Bradnock, G. Morris, J. Nunn, J. Pine, C. Pitts, N. Treasure, E. White, D., Adult Dental Health Survey — Oral Health in the United Kingdom 1998, in: O.f.N. Statistics (Ed.), The Stationery Office, London, 1998, pp. 1 - 577.

- [20] Y. Yao, J. Grogan, M. Zehnder, U. Lendenmann, B. Nam, Z. Wu, C.E. Costello and F.G. Oppenheim, Compositional analysis of human acquired enamel pellicle by mass spectrometry, *Arch. Oral Biol.*, 46 (2001) 293-303.
- [21] R. Gocke, F. Gerath and H. von Schwanewede, Quantitative determination of salivary components in the pellicle on PMMA denture base material, *Clin Oral Investig*, 6 (2002) 227-235.
- [22] Y. Yao, E.A. Berg, C.E. Costello, R.F. Troxler and F.G. Oppenheim, Identification of protein components in human acquired enamel pellicle and whole saliva using novel proteomics approaches, *J. Biol. Chem.*, 278 (2003) 5300-5308.
- [23] J. Li, E.J. Helmerhorst, R.F. Troxler and F.G. Oppenheim, Identification of in vivo pellicle constituents by analysis of serum immune responses, *J. Dent. Res.*, 83 (2004) 60-64.
- [24] C. Hannig, M. Hannig and T. Attin, Enzymes in the acquired enamel pellicle, *Eur. J. Oral Sci.*, 113 (2005) 2-13.
- [25] R. Vitorino, M.J. Calheiros-Lobo, J. Williams, A.J. Ferrer-Correia, K.B. Tomer, J.A. Duarte, P.M. Domingues and F.M. Amado, Peptidomic analysis of human acquired enamel pellicle, *Biomed. Chromatogr.*, 21 (2007) 1107-1117.
- [26] R. Vitorino, M.J. Calheiros-Lobo, J.A. Duarte, P.M. Domingues and F.M.L. Amado, Peptide profile of human acquired enamel pellicle using MALDI tandem MS, *Journal of Separation Science*, 31 (2008) 523-537.

- [27] C. Hannig, B. Spitzmueller and M. Hannig, Transaminases in the acquired pellicle, *Arch. Oral Biol.*, 54 (2009) 445-448.
- [28] D. Deimling, L. Breschi, W. Hoth-Hannig, A. Ruggeri, C. Hannig, Y. Nekrashevych, C. Prati and M. Hannig, Electron microscopic detection of salivary alpha-amylase in the pellicle formed in situ, *Eur. J. Oral Sci.*, 112 (2004) 503-509.
- [29] M. Hannig, A. Dobbert, R. Stigler, U. Muller and S.A. Prokhorova, Initial salivary pellicle formation on solid substrates studied by AFM, *Journal of Nanoscience and Nanotechnology*, 4 (2004) 532-538.
- [30] M. Hannig, A.K. Khanafer, W. Hoth-Hannig, F. Al-Marrawi and Y. Acil, Transmission electron microscopy comparison of methods for collecting in situ formed enamel pellicle, *Clinical Oral Investigations*, 9 (2005) 30-37.
- [31] N. Schwender, K. Huber, F. Al Marrawi, M. Hannig and C. Ziegler, Initial bioadhesion on surfaces in the oral cavity investigated by scanning force microscopy, *Applied Surface Science*, 252 (2005) 117-122.
- [32] J.H. Baek, T. Krasieva, S. Tang, Y. Ahn, C.S. Kim, D. Vu, Z. Chen and P. Wilder-Smith, Optical approach to the salivary pellicle, *Journal of Biomedical Optics*, 14 (2009).
- [33] A. Ash, M.J. Ridout, R. Parker, A.R. Mackie, G.R. Burnett and P.J. Wilde, Effect of calcium ions on in vitro pellicle formation from parotid and whole saliva, *Colloids and Surfaces B: Biointerfaces*, 102 (2013) 546-553.

- [34] D.H. Veeregowda, H.J. Busscher, A. Vissink, D.-J. Jager, P.K. Sharma and H.C. van der Mei, Role of Structure and Glycosylation of Adsorbed Protein Films in Biolubrication, *PLoS One*, 7 (2012).
- [35] M. Hannig, Ultrastructural investigation of pellicle morphogenesis at two different intraoral sites during a 24-h period, *Clin Oral Investig*, 3 (1999) 88-95.
- [36] U. Lendenmann, J. Grogan and F.G. Oppenheim, Saliva and dental pellicle--a review, *Adv Dent Res*, 14 (2000) 22-28.
- [37] R.P. Shellis, M. Addy and G.D. Rees, In vitro studies on the effect of sodium tripolyphosphate on the interactions of stain and salivary protein with hydroxyapatite, *J. Dent.*, 33 (2005) 313-324.
- [38] C. Hannig, D. Berndt, W. Hoth-Hannig and M. Hannig, The effect of acidic beverages on the ultrastructure of the acquired pellicle-An in situ study, *Arch. Oral Biol.*, 54 (2009) 518-526.
- [39] G.B. Proctor, S. Hamdan, G.H. Carpenter and P. Wilde, A statherin and calcium enriched layer at the air interface of human parotid saliva, *Biochem. J.*, 389 (2005) 111-116.
- [40] A. Nasmyth, On the structure, physiology, and pathology of the persistent capsular investments and pulp of the tooth., *Royal Medical and Chirurgical Society of London* 22 (1839) 310-328.

[41] S.W. Chase, The origin, structure, and duration of Nasmyth's membrane, *The Anatomical Record*, 33 (1926) 357-376.

[42] W.L. Siqueira, E.J. Helmerhorst, W. Zhang, E. Salih and F.G. Oppenheim, Acquired enamel pellicle and its potential role in oral diagnostics, in: D. Malamud, R.S. Niedbala (Eds.) *Ann Ny Acad Sci*, Vol 1098, Blackwell Publishing, Oxford, 2007, pp. 504-509.

[43] R.R. Andrews, The Development of the Teeth, and Some of the Contested Points in Regard To Their Development and Structure, *J. Dent. Res.*, 1 (1919) 353-385.

[44] H.E. Jordan, Further evidence concerning the function of osteoclasts, *The Anatomical Record*, 20 (1921) 280-295.

[45] C.J. Dawes, G.N. Tonge, C.H., The nomenclature of the integuments of the enamel surface of the teeth, *Br. Dent. J.*, 115 (1963) 65 - 68.

[46] D.I. Hay, The adsorption of salivary proteins by hydroxyapatite and enamel, *Arch. Oral Biol.*, 12 (1967) 937-946, IN931-IN933.

[47] E.E. Kousvelari, R.S. Baratz, B. Burke and F.G. Oppenheim, Basic Biological Sciences: Immunochemical Identification and Determination of Proline-rich Proteins in Salivary Secretions, Enamel Pellicle, and Glandular Tissue Specimens, *J. Dent. Res.*, 59 (1980) 1430-1438.

- [48] I. Al-Hashimi and M.J. Levine, Characterization of in vivo salivary-derived enamel pellicle, *Arch. Oral Biol.*, 34 (1989) 289-295.
- [49] W.L. Siqueira and F.G. Oppenheim, Small molecular weight proteins/peptides present in the in vivo formed human acquired enamel pellicle, *Arch. Oral Biol.*, 54 (2009) 437-444.
- [50] W.L. Siqueira, W.M. Zhang, E.J. Helmerhorst, S.P. Gygi and F.G. Oppenheim, Identification of protein components in in vivo human acquired enamel pellicle using LC-ESI-MS/MS, *Journal of Proteome Research*, 6 (2007) 2152-2160.
- [51] O. Santos, J. Kosoric, M.P. Hector, P. Anderson and L. Lindh, Adsorption behavior of statherin and a statherin peptide onto hydroxyapatite and silica surfaces by in situ ellipsometry, *J. Colloid Interface Sci.*, 318 (2008) 175-182.
- [52] D. Deimling, C. Hannig, W. Hoth-Hannig, P. Schmitz, J. Schulte-Monting and M. Hannig, Non-destructive visualisation of protective proteins in the in situ pellicle, *Clinical Oral Investigations*, 11 (2007) 211-216.
- [53] H. Fujikawa, K. Matsuyama, A. Uchiyama, S. Nakashima and T. Ujiie, Influence of salivary macromolecules and fluoride on enamel lesion remineralization in vitro, *Caries Res.*, 42 (2008) 37-45.
- [54] A. Joiner, U.M. Elofsson and T. Arnebrant, Adsorption of chlorhexidine and black tea onto in vitro salivary pellicles, as studied by ellipsometry, *Eur. J. Oral Sci.*, 114 (2006) 337-342.

- [55] M.S. Wolff and C. Larson, The cariogenic dental biofilm: good, bad or just something to control?, *Braz Oral Res*, 23 Suppl 1 (2009) 31-38.
- [56] R.G. Schipper, E. Silletti and M.H. Vinyerhoeds, Saliva as research material: Biochemical, physicochemical and practical aspects, *Arch. Oral Biol.*, 52 (2007) 1114-1135.
- [57] L.A. Tabak, In Defense of the oral cavity: The protective role of the salivary secretions, *Pediatric Dentistry*, 28 (2006) 110-117.
- [58] A. Vissink, J.B. Mitchell, B.J. Baum, K.H. Limesand, S.B. Jensen, P.C. Fox, L.S. Elting, J.A. Langendijk, R.P. Coppes and M.E. Reyland, Clinical Management of Salivary Gland Hypofunction and Xerostomia in Head-and-Neck Cancer Patients: Successes and Barriers, *International Journal of Radiation Oncology*Biology*Physics*, 78 (2010) 983-991.
- [59] C.I.H. Berg, L. Lindh and T. Arnebrant, Intraoral Lubrication of PRP-1, Statherin and Mucin as Studied by AFM, *Biofouling: The Journal of Bioadhesion and Biofilm Research*, 20 (2004) 65 - 70.
- [60] C. Hannig, K. Huber, I. Lambrichts, J. Graser, J. D'Haen and M. Hannig, Detection of salivary alpha-amylase and lysozyme exposed on the pellicle formed in situ on different materials, *Journal of Biomedical Materials Research Part A*, 83A (2007) 98-103.

- [61] A. Aguirre, B. Mendoza, M. Reddy, F. Scannapieco, M. Levine and M. Hatton, Lubrication of selected salivary molecules and artificial salivas, *Dysphagia*, 4 (1989) 95-100.
- [62] L. Lindh, On the adsorption behaviour of saliva and purified salivary proteins at solid/liquid interfaces, *Swedish dental journal. Supplement*, (2002) 1-57.
- [63] W.H. Schwarz, The Rheology of Saliva, *J. Dent. Res.*, 66 (1987) 660-666.
- [64] W.A. Vanderreijden, E.C.I. Veerman and A.V.N. Amerongen, Shear Rate-Dependent Viscoelastic Behavior of Human Glandular Salivas (Vol 30, pg 141, 1993), *Biorheology*, 30 (1993) 301-301.
- [65] W.H. Douglas, E.S. Reeh, N. Ramasubbu, P.A. Raj, K.K. Bhandary and M.J. Levine, Statherin: A major boundary lubricant of human saliva, *Biochem. Biophys. Res. Commun.*, 180 (1991) 91-97.
- [66] E.S. Reeh, W.H. Douglas and M.J. Levine, Lubrication of saliva substitutes at enamel-to-enamel contacts in an artificial mouth, *The Journal of Prosthetic Dentistry*, 75 (1996) 649-656.
- [67] I.C.H. Berg, M.W. Rutland and T. Arnebrant, Lubricating Properties of the Initial Salivary Pellicle — an AFM Study, *Biofouling: The Journal of Bioadhesion and Biofilm Research*, 19 (2003) 365 - 369.

[68] M. Hannig and A. Joiner, The structure, function and properties of the acquired pellicle, *Teeth and Their Environment: Physical, Chemical and Biochemical Influences*, 19 (2006) 29-64.

[69] M.J. Larsen and E.I.F. Pearce, Saturation of human saliva with respect to calcium salts, *Arch. Oral Biol.*, 48 (2003) 317-322.

[70] E.I.F. Pearce, On the Dissolution of Hydroxyapatite in Acid Solutions, *J. Dent. Res.*, 67 (1988) 1056-1058.

[71] F. Garcia-Godoy and M.J. Hicks, Maintaining the integrity of the enamel surface - The role of dental biofilm, saliva and preventive agents in enamel demineralization and remineralization, *J. Am. Dent. Assoc.*, 139 (2008) 25S-34S.

[72] A.T. Hara, M. Ando, C. Gonzalez-Canbezcas, J.A. Cury, M.C. Serra and D.T. Zero, Protective effect of the dental pellicle against erosive challenges in situ, *J. Dent. Res.*, 85 (2006) 612-616.

[73] A. Lussi, E. Hellwig, D. Zero and T. Jaeggi, Erosive tooth wear: Diagnosis, risk factors and prevention, *American Journal of Dentistry*, 19 (2006) 319-325.

[74] J.H. Meurman and R.M. Frank, Scanning electron-microscopic study of the effect of salivary pellicle on enamel erosion, *Caries Res.*, 25 (1991) 1-6.

- [75] B.T. Amaechi, S.M. Higham, W.M. Edgar and A. Milosevic, Thickness of acquired salivary pellicle as a determinant of the sites of dental erosion, *J. Dent. Res.*, 78 (1999) 1821-1828.
- [76] L. Bonifait, F. Chandad and D. Grenier, Probiotics for Oral Health: Myth or Reality?, *Journal of the Canadian Dental Association*, 75 (2009) 585-590.
- [77] F.J. Cassels, C.V. Hughes and J.L. Nauss, Adhesin receptors of human oral bacteria and modeling of putative adhesin-binding domains, *Journal of Industrial Microbiology and Biotechnology*, 15 (1995) 176-185.
- [78] J. Meurman and I. Stamatova, Probiotics: contributions to oral health, *Oral Diseases*, 13 (2007) 443-451.
- [79] J.M. ten Cate, Biofilms, a new approach to the microbiology of dental plaque, *Odontology*, 94 (2006) 1-9.
- [80] E.M. Comelli, B. Guggenheim, F. Stingle and J.-R. Neeser, Selection of dairy bacterial strains as probiotics for oral health, *Eur. J. Oral Sci.*, 110 (2002) 218-224.
- [81] A.N. Amerongen and E. Veerman, Saliva: the defender of the oral cavity, *Oral Diseases*, 8 (2002) 12-22.
- [82] A.M. Vacca Smith and W.H. Bowen, In situ studies of pellicle formation on hydroxyapatite discs, *Arch. Oral Biol.*, 45 (2000) 277-291.

- [83] C.M. Huang, Comparative proteomic analysis of human whole saliva, *Arch. Oral Biol.*, 49 (2004) 951-962.
- [84] W. Teughels, N. Van Assche, I. Sliepen and M. Quirynen, Effect of material characteristics and/or surface topography on biofilm development, *Clinical Oral Implants Research*, 17 (2006) 68-81.
- [85] M. Bruvo, D. Moe, S. Kirkeby, H. Vorum and A. Bardow, Individual Variations in Protective Effects of Experimentally Formed Salivary Pellicles, *Caries Res.*, 43 (2009) 163-170.
- [86] J. Li, E.J. Helmerhorst, R.B. Corley, L.E. Luus, R.F. Troxler and F.G. Oppenheim, Characterization of the immunologic responses to human in vivo acquired enamel pellicle as a novel means to investigate its composition, *Oral Microbiol. Immunol.*, 18 (2003) 183-191.
- [87] R. Vitorino, M.J.C. Lobo, J. Duarte, A.J. Ferrer-Correia, K.B. Tomer, J.R. Dubin, P.M. Domingues and F.M.L. Amado, In vitro hydroxyapatite adsorbed salivary proteins, *Biochem. Biophys. Res. Commun.*, 320 (2004) 342-346.
- [88] D.P. Bakker, B.R. Postmus, H.J. Busscher and H.C. van der Mei, Bacterial strains isolated from different niches can exhibit different patterns of adhesion to substrata, *Applied and Environmental Microbiology*, 70 (2004) 3758-3760.
- [89] S. Demodarshan, K.L. Parkin and O.R. Fennema, *Fennema's Food Chemistry*, CRC Press/Taylor & Francis, 2008.

- [90] J.J. Gray, The interaction of proteins with solid surfaces, *Current Opinion in Structural Biology*, 14 (2004) 110-115.
- [91] W. Norde, My voyage of discovery to proteins in flatland ... and beyond, *Colloids and Surfaces B-Biointerfaces*, 61 (2008) 1-9.
- [92] G. Goobes, R. Goobes, W.J. Shaw, J.M. Gibson, J.R. Long, V. Raghunathan, O. Schueler-Furman, J.M. Popham, D. Baker, C.T. Campbell, P.S. Stayton and G.P. Drobny, The structure, dynamics, and energetics of protein adsorption - lessons learned from adsorption of statherin to hydroxyapatite, *Magnetic Resonance in Chemistry*, 45 (2007) S32-S47.
- [93] I.E. Svendsen, L. Lindh, U. Elofsson and T. Arnebrant, Studies on the exchange of early pellicle proteins by mucin and whole saliva, *J. Colloid Interface Sci.*, 321 (2008) 52-59.
- [94] W. Norde, Adsorption of proteins at solid-liquid interfaces, *Cells and Materials*, 5 (1995) 97-112.
- [95] D. Myers, Adsorption, in: *Surfaces, Interfaces, and Colloids (Second Edition)*, 2002, pp. 179-213.
- [96] A. Young, M. Rykke and G. Rölla, Quantitative and qualitative analyses of human salivary micelle-like globules, *Acta Odontologica Scandinavica*, 57 (1999) 105-110.

- [97] L. Vitkov, M. Hannig, Y. Nekrashevych and W.D. Krautgartner, Supramolecular pellicle precursors, *Eur. J. Oral Sci.*, 112 (2004) 320-325.
- [98] C. Hannig, M. Wasser, K. Becker, M. Hannig, K. Huber and T. Attin, Influence of different restorative materials on lysozyme and amylase activity of the salivary pellicle in situ, *Journal of Biomedical Materials Research Part A*, 78A (2006) 755-761.
- [99] I. Iontcheva, F.G. Oppenheim and R.F. Troxler, Human salivary mucin MG1 selectively forms heterotypic complexes with amylase, proline-rich proteins, statherin, and histatins, *J. Dent. Res.*, 76 (1997) 734-743.
- [100] Y. Yao, M.S. Lamkin and F.G. Oppenheim, Pellicle precursor protein crosslinking: Characterization of an adduct between acidic proline-rich protein (PRP-1) and statherin generated by transglutaminase, *J. Dent. Res.*, 79 (2000) 930-938.
- [101] M.S. Lamkin, D. Migliari, Y. Yao, R.F. Troxler and F.G. Oppenheim, New in vitro model for the acquired enamel pellicle: Pellicles formed from whole saliva show inter-subject consistency in protein composition and proteolytic fragmentation patterns, *J. Dent. Res.*, 80 (2001) 385-388.
- [102] B. Rosan and R.J. Lamont, Dental plaque formation, *Microbes Infect.*, 2 (2000) 1599-1607.

[103] M. Rykke and T. Sonju, Amino acid composition of acquired enamel pellicle collected in vivo after 2 hours and after 24 hours, *Eur. J. Oral Sci.*, 99 (1991) 463-469.

[104] C.W.I. Douglas, Bacterial-Protein Interactions in the Oral Cavity, *Advances in Dental Research*, 8 (1994) 254-262.

[105] R.V. Soares, T. Lin, C.C. Siqueira, L.S. Bruno, X.J. Li, F.G. Oppenheim, G. Offner and R.F. Troxler, Salivary micelles: identification of complexes containing MG2, slgA, lactoferrin, amylase, glycosylated proline-rich protein and lysozyme, *Arch. Oral Biol.*, 49 (2004) 337-343.

[106] L. Kajisa, A. Prakobphol, M. Schiodt and S.J. Fisher, Effect of plasma on composition of human enamel and cementum pellicle, *Eur. J. Oral Sci.*, 98 (1990) 461-471.

[107] R.J. Boackle, S.L. Dutton, W.L. Robinson, J. Vesely, J.K. Lever, H.R. Su and N.S. Chang, Effects of removing the negatively charged N-terminal region of the salivary acidic proline-rich proteins by human leucocyte elastase, *Arch. Oral Biol.*, 44 (1999) 575-585.

[108] J.N. Zimmerman, W. Custodio, S. Hatibovic-Kofman, Y.H. Lee, Y. Xiao and W.L. Siqueira, Proteome and Peptidome of Human Acquired Enamel Pellicle on Deciduous Teeth, *International Journal of Molecular Sciences*, 14 (2013) 920-934.

- [109] L. McHugh and J.W. Arthur, Computational Methods for Protein Identification from Mass Spectrometry Data, PLoS Comput Biol, 4 (2008) e12.
- [110] M.W. Duncan, R. Aebersold and R.M. Caprioli, The pros and cons of peptide-centric proteomics, Nature biotechnology, 28 (2010) 659-664.
- [111] E.C. Dobbs, Surface Resistance of Human Enamel to Acid Decalcification, J. Dent. Res., 12 (1932) 581-584.
- [112] A.H. Meckel, The formation and properties of organic films on teeth, Arch. Oral Biol., 10 (1965) 585-597, IN585-IN516.
- [113] P. Schüpbach, F.G. Oppenheim, U. Lendenmann, M.S. Lamkin, Y. Yao and B. Guggenheim, Electron-microscopic demonstration of proline-rich proteins, statherin, and histatins in acquired enamel pellicles *in vitro*, Eur. J. Oral Sci., 109 (2001) 60-68.
- [114] A.B. Sonju Clasen, M. Hannig, K. Skjorland and T. Sonju, Analytical and ultrastructural studies of pellicle on primary teeth, Acta Odontol Scand, 55 (1997) 339-343.
- [115] A. Carlén, A. Börjesson, K. Nikdel and J. Olsson, Composition of Pellicles Formed in vivo on Tooth Surfaces in Different Parts of the Dentition, and in vitro on Hydroxyapatite, Caries Res., 32 (1998) 447-455.

- [116] A. Carlen, S.G. Rudiger, I. Loggner and J. Olsson, Bacteria-binding plasma proteins in pellicles formed on hydroxyapatite in vitro and on teeth in vivo, *Oral Microbiol. Immunol.*, 18 (2003) 203-207.
- [117] J. Li, E.J. Helmerhorst, Y. Yao, M.E. Nunn, R.F. Troxler and F.G. Oppenheim, Statherin is an in vivo pellicle constituent: identification and immun-quantification, *Arch. Oral Biol.*, 49 (2004) 379-385.
- [118] B.L. Slomiany, V.L.N. Murty, E. Zdebska, A. Slomiany, K. Gwozdziński and I.D. Mandel, Tooth Surface-Pellicle Lipids and their role in the Protection of Dental Enamel Against Lactic-Acid Diffusion in Man, *Arch. Oral Biol.*, 31 (1986) 187-191.
- [119] M.B. Kautsky and J.D.B. Featherstone, Effect of Salivary Components on Dissolution Rates of Carbonated Apatites, *Caries Res.*, 27 (1993) 373-377.
- [120] B.L. Slomiany, V.L.N. Murty, I.D. Mandel, S. Sengupta and A. Slomiany, Effect of Lipids on the Lactic-Acid Retardation Capacity of Tooth Enamel and Cementum Pellicles Formed invitro from Saliva of Caries-Resistant and Caries-Susceptible Human Adults, *Arch. Oral Biol.*, 35 (1990) 175-180.
- [121] M. Reich, C. Hannig, A. Al-Ahmad, R. Bolek and K. Kummerer, A comprehensive method for determination of fatty acids in the initial oral biofilm (pellicle), *J. Lipid Res.*, 53 (2012) 2226-2230.
- [122] T. Sonju, Investigations of some salivary glycoproteins and their possible role in pellicle formation., *Den Norske tannlaegeforenings tidende*, 85 (1975) 393-403.

- [123] C.W. Mayhall and W.T. Butler, The carbohydrate composition of experimental salivary pellicles, *Journal of Oral Pathology & Medicine*, 5 (1976) 358-370.
- [124] O. Santos, L. Lindh, T. Halhur and T. Arnebrant, Adsorption from saliva to silica and hydroxyapatite surfaces and elution of salivary films by SDS and delmopinol, *Biofouling*, 26 (2010) 697-710.
- [125] F. Rupp, M. Haupt, M. Eichler, C. Doering, H. Klostermann, L. Scheideler, S. Lachmann, C. Oehr, H.P. Wendel, E. Decker, J. Geis-Gerstorfer and C. von Ohle, Formation and Photocatalytic Decomposition of a Pellicle on Anatase Surfaces, *J. Dent. Res.*, 91 (2012) 104-109.
- [126] K.K. Skjorland, M. Rykke and T. Sonju, Rate of pellicle formation in vivo, *Acta Odontologica Scandinavica*, 53 (1995) 358-362.
- [127] B. Nyvad and O. Fejerskov, Scanning Electron Microscopy of Early Microbial Colonization of Human Enamel and Root Surfaces InVivo, *Scandinavian Journal of Dental Research*, 95 (1987) 287-296.
- [128] H.J. Busscher, H.M.W. Uyen, I. Stokroos and W.L. Jongebloed, A Transmission Electron-Microscopy Study of the Adsorption Patterns of Early Developing Artificial Pellicles on Human-Enamel, *Arch. Oral Biol.*, 34 (1989) 803-810.

[129] A.B. Sonju Clasen, M. Hannig and T. Sonju, Variations in pellicle thickness: a factor in tooth wear?, in: M. Addy (Ed.) Tooth wear and sensitivity : clinical advances in restorative dentistry, Martin Dunitz, London, 2000, pp. 189-194.

[130] A. Walz, K. Stuhler, A. Wattenberg, E. Hawranke, H.E. Meyer, G. Schmalz, M. Bluggel and S. Ruhl, Proteome analysis of glandular parotid and submandibular-sublingual saliva in comparison to whole human saliva by two-dimensional gel electrophoresis, *Proteomics*, 6 (2006) 1631-1639.

[131] M. Castagnola, D. Congiu, G. Denotti, A. Di Nunzio, M.B. Fadda, S. Melis, I. Messina, F. Misiti, R. Murtas, A. Olianas, V. Piras, A. Pittau and G. Puddu, Determination of the human salivary peptides histatins 1, 3, 5 and statherin by high-performance liquid chromatography and by diode-array detection, *J. Chromatogr. B*, 751 (2001) 153-160.

[132] M.D. McConnell, Y. Liu, A.P. Nowak, S. Pilch, J.G. Masters and R.J. Composto, Bacterial plaque retention on oral hard materials: effect of surface roughness, surface composition, and physisorbed polycarboxylate, *Journal of Biomedical Materials Research Part A*, 92A (2010) 1518-1527.

[133] J.H.H. Bongaerts, D. Rossetti and J.R. Stokes, The lubricating properties of human whole saliva, *Tribol. Lett.*, 27 (2007) 277-287.

[134] H.J. Busscher, D.J. White, H.J. Kamminga-Rasker, A.T. Poortinga and H.C. van der Mei, Influence of oral detergents and chlorhexidine on soft-layer

electrokinetic parameters of the acquired enamel pellicle, *Caries Res.*, 37 (2003) 431-436.

[135] H.C. van der Mei, D.J. White, H.J. Kamminga-Rasker, J. Knight, A.A. Baig, J. Smit and H.J. Busscher, Influence of dentifrices and dietary components in saliva on wettability of pellicle-coated enamel in vitro and in vivo, *Eur. J. Oral Sci.*, 110 (2002) 434-438.

[136] A.M. Vacca Smith and W.H. Bowen, The effects of milk and kappa-casein on salivary pellicle formed on hydroxyapatite discs in situ, *Caries Res*, 34 (2000) 88-93.

[137] P. Schupbach, J.R. Neeser, M. Golliard, M. Rouvet and B. Guggenheim, Incorporation of Caseinoglycomacropeptide and Caseinophosphopeptide into the Salivary Pellicle Inhibits Adherence of Mutans Streptococci, *J. Dent. Res.*, 75 (1996) 1779-1788.

[138] A. Lussi, T. Jaeggi and D. Zero, The role of diet in the aetiology of dental erosion, *Caries Res.*, 38 (2004) 34-44.

[139] P. Moynihan and P.E. Petersen, Diet, nutrition and the prevention of dental diseases, *Public Health Nutrition*, 7 (2004) 201-226.

[140] M. Cárdenas, U. Elofsson and L. Lindh, Salivary Mucin MUC5B Could Be an Important Component of in Vitro Pellicles of Human Saliva: An in Situ Ellipsometry and Atomic Force Microscopy Study, *Biomacromolecules*, 8 (2007) 1149-1156.

- [141] T. Jensdottir, P. Holbrook, B. Nauntofte, C. Buchwald and A. Bardow, Immediate Erosive Potential of Cola Drinks and Orange Juices, *J. Dent. Res.*, 85 (2006) 226-230.
- [142] N. Vassilakos, T. Arnebrant and P.O. Glantz, Adsorption of Whole Saliva onto Hydrophilic and Hydrophobic Solid-Surfaces - Influence of Concentration, Ionic-Strength and pH, *Scandinavian Journal of Dental Research*, 100 (1992) 346-353.
- [143] Y. Tanizawa, N. Johna, Y. Yamamoto and N. Nishikawa, Salivary films on hydroxyapatite studied by an in vitro system for investigating the effect of metal ions and by a quartz-crystal microbalance system for monitoring layer-by-layer film formation, *Journal of Cosmetic Science*, 55 (2004) 163-176.
- [144] L. Macakova, G.E. Yakubov, M.A. Plunkett and J.R. Stokes, Influence of ionic strength changes on the structure of pre-adsorbed salivary films. A response of a natural multi-component layer, *Colloids Surf B Biointerfaces*, 77 (2010) 31-39.
- [145] K. Kandori, S. Oda and S. Tsuyama, Effects of pyrophosphate ions on protein adsorption onto calcium hydroxyapatite, *Journal of Physical Chemistry B*, 112 (2008) 2542-2547.
- [146] I.S. Harding, N. Rashid and K.A. Hing, Surface charge and the effect of excess calcium ions on the hydroxyapatite surface, *Biomaterials*, 26 (2005) 6818-6826.

- [147] I.A. Meyers, M.J. McQueen, D. Harbrow and G.J. Seymour, The surface effect of dentifrices, *Australian Dental Journal*, 45 (2000) 118-124.
- [148] H.J. Busscher, D.J. White, H.C. van der Mei, A.A. Baig and K.M. Kozak, Hexametaphosphate effects on tooth surface conditioning film chemistry--in vitro and in vivo studies., *The Journal of clinical dentistry*, 13 (2002) 38-43.
- [149] M. Kuroiwa, T. Kodaka, M. Kuroiwa and M. Abe, Brushing-induced effects with and without a non-fluoride abrasive dentifrice on remineralization of enamel surfaces etched with phosphoric acid, *Caries Res*, 28 (1994) 309-314.
- [150] A. Joiner, A. Schwarz, C.J. Philpotts, T.F. Cox, K. Huber and M. Hannig, The protective nature of pellicle towards toothpaste abrasion on enamel and dentine, *J. Dent.*, 36 (2008) 360-368.
- [151] M. Hannig, The protective nature of the salivary pellicle, *Int. Dent. J.*, 52 (2002) 417-423.
- [152] D.J. White, A new and improved "dual action" whitening dentifrice technology--sodium hexametaphosphate., *The Journal of clinical dentistry*, 13 (2002) 1-5.
- [153] K.J. Fairbrother and P.A. Heasman, Anticalculus agents, *J. Clin. Periodontol.*, 27 (2000) 285-301.

- [154] D.J. White and E.R. Cox, In vitro studies of the anticalculus efficacy of an improved whitening dentifrice., *The Journal of clinical dentistry*, 12 (2001) 38-41.
- [155] T.S. Tilliss, Use of a whitening dentifrice for control of chlorhexidine stain, *J Contemp Dent Pract*, 1 (1999) 9-15.
- [156] A. Gaffar, T. Polefka, J. Afflitto, A. Esposito and S. Smith, In vitro evaluations of pyrophosphate/copolymer/NaF as an anticalculus agent, *Compendium (Newtown, Pa.) Supplement*, (1987) S242-250.
- [157] C. McGaughey, Binding of polyphosphates and phosphonates to hydroxyapatite, subsequent hydrolysis, phosphate exchange and effects on demineralization, mineralization and microcrystal aggregation, *Caries Res*, 17 (1983) 229-241.
- [158] R.W. Gerlach, Comparative intraoral tolerance of sodium hexametaphosphate and pyrophosphate antitartar dentifrices., *The Journal of clinical dentistry*, 13 (2002) 29-32.
- [159] N. Sharif, E. MacDonald, J. Hughes, R.G. Newcombe and M. Addy, The chemical stain removal properties of 'whitening' toothpaste products: studies in vitro, *Br Dent J*, 188 (2000) 620-624.
- [160] A.A. Baig, K.M. Kozak, E.R. Cox, J.R. Zoladz, L. Mahony and D.J. White, Laboratory studies on the chemical whitening effects of a sodium hexametaphosphate dentifrice., *The Journal of clinical dentistry*, 13 (2002) 19-24.

- [161] F. Ayad, B. Demarchi, A. Khalaf, R. Davies, R. Ellwood, B. Bradshaw, M.E. Petrone, P. Chaknis, W. DeVizio, A.R. Volpe and H.M. Proskin, A six-week clinical tooth whitening study of a new calculus-inhibiting dentifrice formulation, *Journal of Clinical Dentistry*, 11 (2000) 84-87.
- [162] K.A. Marx, Quartz crystal microbalance: A useful tool for studying thin polymer films and complex biomolecular systems at the solution-surface interface, *Biomacromolecules*, 4 (2003) 1099-1120.
- [163] B. Jaffe, *Piezoelectric Ceramics*, Elsevier Science, 1971.
- [164] G. Sauerbrey, Verwendung Von Schwingquarten Zur Wagung Dunner Schichten Und Zur Mikrowagung, *Zeitschrift Fur Physik*, 155 (1959) 206-222.
- [165] M.V. Voinova, M. Rodahl, M. Jonson and B. Kasemo, Viscoelastic acoustic response of layered polymer films at fluid-solid interfaces: Continuum mechanics approach, *Physica Scripta*, 59 (1999) 391-396.
- [166] G.H. Cross, N.J. Freeman and M.J. Swann, Dual Polarization Interferometry: A Real-Time Optical Technique for Measuring (Bio)molecular Orientation, Structure and Function at the Solid/Liquid Interface, in: *Handbook of Biosensors and Biochips*, John Wiley & Sons, Ltd, 2008.
- [167] H. Zhao, P.H. Brown and P. Schuck, On the Distribution of Protein Refractive Index Increments, *Biophysical Journal*, 100 (2011) 2309-2317.

[168] J.A.d. Feijter, J. Benjamins and F.A. Veer, Ellipsometry as a tool to study the adsorption behavior of synthetic and biopolymers at the air-water interface, *Biopolymers*, 17 (1978) 1759-1772.

[169] M. Westwood, T.R. Noel and R. Parker, The characterisation of polygalacturonic acid-based layer-by-layer deposited films using a quartz crystal microbalance with dissipation monitoring, a dual polarization interferometer and a Fourier-transform infrared spectrometer in attenuated total reflectance mode, *Soft Matter*, 6 (2010) 5502-5513.

[170] V.J. Morris, A.R. Kirby and A.P. Gunning, *Atomic force microscopy for biologists*, Imperial College Press, 2009.

[171] T. Kawasaki, Hydroxyapatite as a liquid chromatographic packing, *Journal of Chromatography A*, 544 (1991) 147-184.

[172] K.G. Kenrick and J. Margolis, Isoelectric focusing and gradient gel electrophoresis: a two-dimensional technique, *Analytical biochemistry*, 33 (1970) 204-207.

[173] R.H. Perry, R.G. Cooks and R.J. Noll, Orbitrap Mass Spectrometry: Instrumentation, Ion Motion and Applications, *Mass Spectrometry Reviews*, 27 (2008) 661-699.

[174] D.N. Perkins, D.J.C. Pappin, D.M. Creasy and J.S. Cottrell, Probability-based protein identification by searching sequence databases using mass spectrometry data, *Electrophoresis*, 20 (1999) 3551-3567.

[175] E.J. Helmerhorst and F.G. Oppenheim, Saliva: a dynamic proteome, *J. Dent. Res.*, 86 (2007) 680-693.

[176] R.P. Kusy and D.L. Schafer, Rheology of Stimulated Whole Saliva in a Typical Pre-Orthodontic Sample-Population, *Journal of Materials Science-Materials in Medicine*, 6 (1995) 385-389.

[177] K.S. Lashley, Reflex secretion of the human parotid gland, *Journal of Experimental Psychology*, 1 (1916) 461-493.

[178] P.K. Smith, R.I. Krohn, G.T. Hermanson, A.K. Mallia, F.H. Gartner, M.D. Provenzano, E.K. Fujimoto, N.M. Goeke, B.J. Olson and D.C. Klenk, Measurement Of Protein Using Bicinchoninic Acid, *Analytical Biochemistry*, 150 (1985) 76-85.

[179] K. Nakanishi, T. Sakiyama and K. Imamura, On the adsorption of proteins on solid surfaces, a common but very complicated phenomenon, *Journal of Bioscience and Bioengineering*, 91 (2001) 233-244.

[180] L. Vroman and A.L. Adams, Adsorption of Proteins out of Plasma and Solutions in Narrow Spaces, *J. Colloid Interface Sci.*, 111 (1986) 391-402.

- [181] S.M. Daly, T.M. Przybycien and R.D. Tilton, Adsorption of poly(ethylene glycol)-modified ribonuclease A to a poly(lactide-co-glycolide) surface, *Biotechnology and Bioengineering*, 90 (2005) 856-868.
- [182] C.F. Wertz and M.M. Santore, Adsorption and Reorientation Kinetics of Lysozyme on Hydrophobic Surfaces, *Langmuir*, 18 (2002) 1190-1199.
- [183] M. Castagnola, T. Cabras, G. Denotti, M.B. Fadda, G. Gambarini, A. Lupi, I. Manca, G. Onnis, V. Piras, V. Soro, S. Tambaro and I. Messina, Circadian Rhythms of Histatin 1, Histatin 3, Histatin 5, Statherin and Uric Acid in Whole Human Saliva Secretion, *Biological Rhythm Research*, 33 (2002) 213-222.
- [184] H. Gusman, C. Leone, E.J. Helmerhorst, M. Nunn, B. Flora, R.F. Troxler and F.G. Oppenheim, Human salivary gland-specific daily variations in histatin concentrations determined by a novel quantitation technique, *Arch Oral Biol*, 49 (2004) 11-22.
- [185] L. Lindh, P.O. Glantz, I. Carlstedt, C. Wickstrom and T. Arnebrant, Adsorption of MUC5B and the role of mucins in early salivary film formation, *Colloids and Surfaces B-Biointerfaces*, 25 (2002) 139-146.
- [186] G.R. Germaine and L.M. Tellefson, Potential role of lysozyme in bactericidal activity of in vitro-acquired salivary pellicle against *Streptococcus faecium* 9790, *Infection and immunity*, 54 (1986) 846-854.

- [187] A. Bengtsson and S. Sjoberg, Surface complexation and proton-promoted dissolution in aqueous apatite systems, *Pure and Applied Chemistry*, 81 (2009) 1569-1584.
- [188] E.F. Vansant, P. Van Der Voort and K.C. Vrancken, Modification with silicon compounds: Mechanistic studies, *Characterization and Chemical Modification of the Silica Surface*, 93 (1995) 193-297.
- [189] B. Ghafouri, C. Tagesson and M. Lindahl, Mapping of proteins in human saliva using two-dimensional gel electrophoresis and peptide mass fingerprinting, *Proteomics*, 3 (2003) 1003-1015.
- [190] J.P. Ouhayoun, F. Gosselin, N. Forest, S. Winter and W.W. Franke, Cytokeratin patterns of human oral epithelia: differences in cytoke-
ratin synthesis in gingival epithelium and the adjacent alveolar mucosa, *Differentiation; research in biological diversity*, 30 (1985) 123-129.
- [191] K. Rechendorff, M.B. Hovgaard, M. Foss, V.P. Zhdanov and F. Besenbacher, Enhancement of Protein Adsorption Induced by Surface Roughness, *Langmuir*, 22 (2006) 10885-10888.
- [192] M. Cardenas, J.J. Valle-Delgado, J. Hamit, M.W. Rutland and T. Arnebrant, Interactions of hydroxyapatite surfaces: Conditioning films of human whole saliva, *Langmuir*, 24 (2008) 7262-7268.

- [193] M. Johnsson, M.J. Levine and G.H. Nancollas, Hydroxyapatite Binding Domains in Salivary Proteins, *Crit. Rev. Oral Biol. Med.*, 4 (1993) 371-378.
- [194] E.A. Vogler, Protein adsorption in three dimensions, *Biomaterials*, 33 (2012) 1201-1237.
- [195] M. Rabe, D. Verdes and S. Seeger, Understanding protein adsorption phenomena at solid surfaces, *Advances in Colloid and Interface Science*, 162 (2011) 87-106.
- [196] C.J. van Oss, Long-range and short-range mechanisms of hydrophobic attraction and hydrophilic repulsion in specific and aspecific interactions, *Journal of Molecular Recognition*, 16 (2003) 177-190.
- [197] P.D.V. de Almeida, A.M.T. Gregio, M.A.N. Machado, A.A.S. de Lima and L.R. Azevedo, Saliva composition and functions: a comprehensive review, *J Contemp Dent Pract*, 9 (2008) 72-80.
- [198] C. Hannig, T. Attin, M. Hannig, E. Henze, K. Brinkmann and R. Zech, Immobilisation and activity of human alpha-amylase in the acquired enamel pellicle, *Arch. Oral Biol.*, 49 (2004) 469-475.
- [199] L. Lindh, P.O. Glantz, P.E. Isberg and T. Arnebrant, An in vitro study of initial adsorption from human parotid and submandibular/sublingual resting saliva at solid/liquid interfaces, *Biofouling*, 17 (2001) 227-239.

- [200] S.A. Rayment, B. Liu, G.D. Offner, F.G. Oppenheim and R.F. Troxler, Immunoquantification of human salivary mucins MG1 and MG2 in stimulated whole saliva: Factors influencing mucin levels, *J. Dent. Res.*, 79 (2000) 1765-1772.
- [201] A.B. Mann and M.E. Dickinson, Nanomechanics, chemistry and structure at the enamel surface, in: *Teeth and Their Environment: Physical, Chemical and Biochemical Influences*, Vol 19, Karger, Basel, 2006, pp. 105-131.
- [202] E. Neyraud, J.H.F. Bult and E. Dransfield, Continuous analysis of parotid saliva during resting and short-duration simulated chewing, *Arch. Oral Biol.*, 54 (2009) 449-456.
- [203] J.A. BanderasTarabay, M. GonzalezBegne, M. SanchezGarduno, E. MillanCortez, A. LopezRodriguez and A. VilchisVelazquez, Salivary flow rate and protein concentration in human whole saliva, *Salud Publica De Mexico*, 39 (1997) 433-441.
- [204] L.A. Tabak, M.J. Levine, N.K. Jain, A.R. Bryan, R.E. Cohen, L.D. Monte, S. Zawacki, G.H. Nancollas, A. Slomiany and B.L. Slomiany, Adsorption of human salivary mucins to hydroxyapatite, *Arch. Oral Biol.*, 30 (1985) 423-427.
- [205] S.E. Harding, S.S. Davis, M.P. Deacon and I. Fiebrig, Biopolymer mucoadhesives, in: S.E. Harding (Ed.) *Biotechnology and Genetic Engineering Reviews*, Vol 16, Vol 16, 1999, pp. 41-86.

- [206] D.H. Veeregowda, H.C. van der Mei, H.J. Busscher and P.K. Sharma, Influence of fluoride-detergent combinations on the visco-elasticity of adsorbed salivary protein films, *Eur. J. Oral Sci.*, 119 (2011) 21-26.
- [207] H.P. Erickson, Size and Shape of Protein Molecules at the Nanometer Level Determined by Sedimentation, Gel Filtration, and Electron Microscopy, *Biological Procedures Online*, 11 (2009) 32-51.
- [208] E.C. Moreno, M. Kresak, J.J. Kane and D.I. Hay, Adsorption of Proteins, Peptides, and Organic-Acids from Binary Mixtures onto Hydroxylapatite, *Langmuir*, 3 (1987) 511-519.
- [209] S.S. Olmsted, J.L. Padgett, A.I. Yudin, K.J. Whaley, T.R. Moench and R.A. Cone, Diffusion of macromolecules and virus-like particles in human cervical mucus, *Biophysical Journal*, 81 (2001) 1930-1937.
- [210] W.M. Saltzman, M.L. Radomsky, K.J. Whaley and R.A. Cone, Antibody Diffusion in Human Cervical-Mucus, *Biophysical Journal*, 66 (1994) 508-515.
- [211] P. Denny, F.K. Hagen, M. Hardt, L.J. Liao, W.H. Yan, M. Arellanno, S. Bassilian, G.S. Bedi, P. Boontheung, D. Cociorva, C.M. Delahunty, T. Denny, J. Dunsmore, K.F. Faull, J. Gilligan, M. Gonzalez-Begne, F. Halgand, S.C. Hall, X.M. Han, B. Henson, J. Hewel, S. Hu, S. Jeffrey, J. Jiang, J.A. Loo, R.R.O. Loo, D. Malamud, J.E. Melvin, O. Miroshnychenko, M. Navazesh, R. Niles, S.K. Park, A. Prakobphol, P. Ramachandran, M. Richert, S. Robinson, M. Sondej, P. Souda, M.A. Sullivan, J. Takashima, S. Than, J.H. Wang, J.P. Whitelegge, H.E. Witkowska, L.

Wolinsky, Y.M. Xie, T. Xu, W.X. Yu, J. Ytterberg, D.T. Wong, J.R. Yates and S.J. Fisher, The proteomes of human parotid and submandibular/sublingual gland salivas collected as the ductal secretions, *Journal of Proteome Research*, 7 (2008) 1994-2006.

[212] R.J. Lamont and H.F. Jenkinson, *Oral microbiology at a glance*, 2010.

[213] M.D. Turner and J.A. Ship, Dry mouth and its effects on the oral health of elderly people, *J. Am. Dent. Assoc.*, 138 (2007) 15S-20S.

[214] K. Nagy, E. Urban, O. Fazekas, L. Thurzo and E. Nagy, Controlled study of lactoperoxidase gel on oral flora and saliva in irradiated patients with oral cancer, *Journal of Craniofacial Surgery*, 18 (2007) 1157-1164.

[215] P. Dirix, S. Nuyts, V. Vander Poorten, P. Delaere and W. Van den Bogaert, Efficacy of the BioXtra dry mouth care system in the treatment of radiotherapy-induced xerostomia, *Supportive Care in Cancer*, 15 (2007) 1429-1436.

[216] S. Hahnel, M. Behr, G. Handel and R. Burgers, Saliva substitutes for the treatment of radiation-induced xerostomia--a review, *Support Care Cancer*, 17 (2009) 1331-1343.

[217] J.-W. Yao, C.-J. Lin, G.-Y. Chen, F. Lin and T. Tao, The interactions of epigallocatechin-3-gallate with human whole saliva and parotid saliva, *Arch. Oral Biol.*, 55 (2010) 470-478.

- [218] L.A. Sewon, S.M. Karjalainen, E. Soderling, H. Lapinleimu and O. Simell, Associations between salivary calcium and oral health, *J. Clin. Periodontol.*, 25 (1998) 915-919.
- [219] X. Arias-Moreno, O. Abian, S. Vega, J. Sancho and A. Velazquez-Campoy, Protein-Cation Interactions: Structural and Thermodynamic Aspects, *Current Protein & Peptide Science*, 12 (2011) 325-338.
- [220] M. Rykke, A. Young, G. Smistad, G. Rolla and J. Karlsen, Zeta potentials of human salivary micelle-like particles, *Colloids and Surfaces B-Biointerfaces*, 6 (1996) 51-56.
- [221] K. Kawasaki and K.M. Weiss, Mineralized tissue and vertebrate evolution: The secretory calcium-binding phosphoprotein gene cluster, *Proceedings of the National Academy of Sciences of the United States of America*, 100 (2003) 4060-4065.
- [222] M. Rykke, G. Smistad, G. Rølla and J. Karlsen, Micelle-like structures in human saliva, *Colloids and Surfaces B: Biointerfaces*, 4 (1995) 33-44.
- [223] R. Goobes, G. Goobes, C.T. Campbell and P.S. Stayton, Thermodynamics of statherin adsorption onto hydroxyapatite (vol 45, pg 5576, 2006), *Biochemistry*, 45 (2006) 10161-10161.

- [224] L. Lindh, P.O. Glantz, N. Stromberg and T. Arnebrant, On the adsorption of human acidic proline-rich proteins (PRP-1 and PRP-3) and statherin at solid/liquid interfaces, *Biofouling*, 18 (2002) 87-94.
- [225] G.N.M. Ferreira, A.C. Da-Silva and B. Tome, Acoustic wave biosensors: physical models and biological applications of quartz crystal microbalance, *Trends in Biotechnology*, 27 (2009) 689-697.
- [226] K.L. Jones and C.R. O'Melia, Protein and humic acid adsorption onto hydrophilic membrane surfaces: effects of pH and ionic strength, *Journal of Membrane Science*, 165 (2000) 31-46.
- [227] B.T. Amaechi and S.M. Higham, In vitro remineralisation of eroded enamel lesions by saliva, *J Dent*, 29 (2001) 371-376.
- [228] B.T. Amaechi and S.M. Higham, Eroded enamel lesion remineralization by saliva as a possible factor in the site-specificity of human dental erosion, *Arch Oral Biol*, 46 (2001) 697-703.
- [229] Y. Nekrashevych, M. Hannig and L. Stosser, Assessment of enamel erosion and protective effect of salivary pellicle by surface roughness analysis and scanning electron microscopy, *Oral health & preventive dentistry*, 2 (2004) 5-11.
- [230] Y. Nekrashevych and L. Stosser, Protective influence of experimentally formed salivary pellicle on enamel erosion - An in vitro study, *Caries Res.*, 37 (2003) 225-231.

- [231] J.P. Montmayeur and J. Coutre, *Fat Detection: Taste, Texture, and Post Ingestive Effects*, Taylor & Francis, 2010.
- [232] J. Horne, J. Hayes and H.T. Lawless, Turbidity as a Measure of Salivary Protein Reactions with Astringent Substances, *Chemical Senses*, 27 (2002) 653-659.
- [233] S. Kallithraka, J. Bakker and M.N. Clifford, Evidence that Salivary Proteins are Involved in Astringency, *Journal of Sensory Studies*, 13 (1998) 29-43.
- [234] J.F. Prinz and P.W. Lucas, Saliva tannin interactions, *Journal of Oral Rehabilitation*, 27 (2000) 991-994.
- [235] A.J. Charlton, N.J. Baxter, M.L. Khan, A.J.G. Moir, E. Haslam, A.P. Davies and M.P. Williamson, Polyphenol/Peptide Binding and Precipitation, *Journal of Agricultural and Food Chemistry*, 50 (2002) 1593-1601.
- [236] C. Poncet-Legrand, A. Edelmann, J.L. Putaux, D. Cartalade, P. Sarni-Manchado and A. Vernhet, Poly(l-proline) interactions with flavan-3-ols units: Influence of the molecular structure and the polyphenol/protein ratio, *Food Hydrocolloids*, 20 (2006) 687-697.
- [237] P.A.S. Breslin, M.M. Gilmore, G.K. Beauchamp and B.G. Green, Psychophysical evidence that oral astringency is a tactile sensation, *Chemical Senses*, 18 (1993) 405-417.

- [238] H.L. Gibbins and G.H. Carpenter, Alternative Mechanisms of Astringency – What is the Role of Saliva?, *Journal of Texture Studies*, (2013) n/a-n/a.
- [239] E. Monteleone, N. Condelli, C. Dinnella and M. Bertuccioli, Prediction of perceived astringency induced by phenolic compounds, *Food Quality and Preference*, 15 (2004) 761-769.
- [240] Q. Yan and A. Bennick, Identification of histatins as tannin-binding proteins in human saliva, *The Biochemical journal*, 311 (Pt 1) (1995) 341-347.
- [241] N. Naurato, P. Wong, Y. Lu, K. Wroblewski and A. Bennick, Interaction of Tannin with Human Salivary Histatins, *Journal of Agricultural and Food Chemistry*, 47 (1999) 2229-2234.
- [242] Y. Lu and A. Bennick, Interaction of tannin with human salivary proline-rich proteins, *Arch. Oral Biol.*, 43 (1998) 717-728.
- [243] N.J. Baxter, T.H. Lilley, E. Haslam and M.P. Williamson, Multiple Interactions between Polyphenols and a Salivary Proline-Rich Protein Repeat Result in Complexation and Precipitation†, *Biochemistry*, 36 (1997) 5566-5577.
- [244] D. Rossetti, G.E. Yakubov, J.R. Stokes, A.M. Williamson and G.G. Fuller, Interaction of human whole saliva and astringent dietary compounds investigated by interfacial shear rheology, *Food Hydrocolloids*, 22 (2008) 1068-1078.

- [245] R.A. Sowalsky and A.C. Noble, Comparison of the effects of concentration, pH and anion species on astringency and sourness of organic acids, *Chem Senses*, 23 (1998) 343-349.
- [246] A.J. Rugg-Gunn and J.H. Nunn, *Nutrition, Diet, and Oral Health*, Oxford University Press, 1999.
- [247] M. Ramos-Casals, A.G. Tzioufas, J.H. Stone, A. Siso and X. Bosch, Treatment of primary Sjogren syndrome: a systematic review, *JAMA : the journal of the American Medical Association*, 304 (2010) 452-460.
- [248] T. Sonju and G. Rolla, Chemical-Analysis of Acquired Pellicle Formed in 2 Hours on Cleaned Human Teeth in-vivo-Rate of Formation and Amino Acid Analysis *Caries Res.*, 7 (1973) 30-38.
- [249] Y. Kuboki, K. Teraoka and S. Okada, X-Ray Photoelectron Spectroscopic Studies of the Adsorption of Salivary Constituents on Enamel, *J. Dent. Res.*, 66 (1987) 1016-1019.
- [250] M. Hannig and M. Balz, Influence of in vivo formed salivary pellicle on enamel erosion, *Caries Res.*, 33 (1999) 372-379.
- [251] M. Hannig and M. Balz, Protective properties of salivary pellicles from two different intraoral sites on enamel erosion, *Caries Res.*, 35 (2001) 142-148.

- [252] M. Hannig, N.J. Hess, W. Hoth-Hannig and M. De Vrese, Influence of salivary pellicle formation time on enamel demineralization--an in situ pilot study, *Clin Oral Investig*, 7 (2003) 158-161.
- [253] G.F. Castro, M.F. Siqueira, Y. Xiao, P.M. Yamaguti and W.L. Siqueira, Effect of Dialyzed Saliva on Human Enamel Demineralization, *Caries Res.*, 47 (2013) 56-62.
- [254] S.C. Brevik, A. Lussi and E. Rakhmatullina, A new optical detection method to assess the erosion inhibition by in vitro salivary pellicle layer, *J. Dent.*, 41 (2013) 428-435.
- [255] A. Lussi, A. Bossen, C. Hoeschele, B. Beyeler, B. Megert, C. Meier and E. Rakhmatullina, Effects of enamel abrasion, salivary pellicle, and measurement angle on the optical assessment of dental erosion, *Journal of Biomedical Optics*, 17 (2012).
- [256] A. Wiegand, S. Bliggenstorfer, A.C. Magalhaes, B. Sener and T. Attin, Impact of the in situ formed salivary pellicle on enamel and dentine erosion induced by different acids, *Acta Odontologica Scandinavica*, 66 (2008) 225-230.
- [257] M.E. Barbour, R.P. Shellis, D.M. Parker, G.C. Allen and M. Addy, Inhibition of hydroxyapatite dissolution by whole casein: the effects of pH, protein concentration, calcium, and ionic strength, *Eur. J. Oral Sci.*, 116 (2008) 473-478.
- [258] C. Dawes, What is the critical pH and why does a tooth dissolve in acid?, *Journal (Canadian Dental Association)*, 69 (2003) 722-724.

[259] B. Vardhanabhuti, P.W. Cox, I.T. Norton and E.A. Foegeding, Lubricating properties of human whole saliva as affected by beta-lactoglobulin, *Food Hydrocolloids*, 25 (2011) 1499-1506.

[260] P. Anderson, M.P. Hector and M.A. Rampersad, Critical pH in resting and stimulated whole saliva in groups of children and adults, *International Journal of Paediatric Dentistry*, 11 (2001) 266-273.

[261] E. Mahoney, J. Beattie, M. Swain and N. Kilpatrick, Preliminary in vitro assessment of erosive potential using the ultra-micro-indentation system, *Caries Res*, 37 (2003) 218-224.

[262] M.W.J. Dodds, D.A. Johnson and C.K. Yeh, Health benefits of saliva: a review, *J. Dent.*, 33 (2005) 223-233.

[263] A. Joiner, Whitening toothpastes: a review of the literature, *J Dent*, 38 Suppl 2 (2010) e17-24.

[264] D.J. White, E.R. Cox, E.M. Suszcynskymeister and A.A. Baig, In vitro studies of the anticalculus efficacy of a sodium hexametaphosphate whitening dentifrice., *The Journal of clinical dentistry* 13 (2002) 33-37.

[265] J. Fox and S. Weisberg, *An R Companion to Applied Regression*, SAGE Publications, 2010.

- [266] J.D. Moore, M.A. Perez-Pardo, J.F. Popplewell, S.J. Spencer, S. Ray, M.J. Swann, A.G. Shard, W. Jones, A. Hills and D.G. Bracewell, Chemical and biological characterisation of a sensor surface for bioprocess monitoring, *Biosensors & Bioelectronics*, 26 (2011).
- [267] M.C. Dixon, Quartz crystal microbalance with dissipation monitoring: enabling real-time characterization of biological materials and their interactions, *J Biomol Tech*, 19 (2008) 151-158.
- [268] I.C.H. Berg, U.M. Elofsson, A. Joiner, M. Malmsten and T. Arnebrant, Salivary protein adsorption onto hydroxyapatite and SDS-mediated elution studied by in situ ellipsometry, *Biofouling*, 17 (2001) 173-187.
- [269] A.R. Mackie, A.P. Gunning, P.J. Wilde and V.J. Morris, Orogenic Displacement of Protein from the Air/Water Interface by Competitive Adsorption, *J Colloid Interface Sci*, 210 (1999) 157-166.
- [270] M. Wahlgren and T. Arnebrant, Adsorption of β -Lactoglobulin onto silica, methylated silica, and polysulfone, *J. Colloid Interface Sci.*, 136 (1990) 259-265.
- [271] M. Rykke, G. Rolla and T. Sonju, Effect of Sodium Lauryl Sulfate on Protein Adsorption to Hydroxyapatite Invitro and on Pellicle Formation Invivo, *Scandinavian Journal of Dental Research*, 98 (1990) 135-143.
- [272] N. Jehmlich, K.H.D. Dinh, M. Gesell-Salazar, E. Hammer, L. Steil, V.M. Dhople, C. Schurmann, B. Holtfreter, T. Kocher and U. Völker, Quantitative

analysis of the intra- and inter-subject variability of the whole salivary proteome, *Journal of Periodontal Research*, 48 (2013) 392-403.

[273] R.B. Bausell and Y.-F. Li, *Power analysis for experimental research: A practical guide for the biological, medical and social sciences*, 2002.

[274] A. Ash, G.R. Burnett, R. Parker, M.J. Ridout, N.M. Rigby and P.J. Wilde, Structural characterisation of parotid and whole mouth salivary pellicles adsorbed onto DPI and QCMD hydroxyapatite sensors, *Colloids Surf B Biointerfaces*, (2013).

[275] C. Hannig, S. Basche, T. Burghardt, A. Al-Ahmad and M. Hannig, Influence of a mouthwash containing hydroxyapatite microclusters on bacterial adherence in situ, *Clinical Oral Investigations*, 17 (2013) 805-814.

[276] W.L. Siqueira, M. Bakkal, Y.Z. Xiao, J.N. Sutton and F.M. Mendes, Quantitative Proteomic Analysis of the Effect of Fluoride on the Acquired Enamel Pellicle, *PLoS One*, 7 (2012).

[277] H.-S. Lee, S. Tsai, C.-C. Kuo, A.W. Bassani, B. Pepe-Mooney, D. Miksa, J. Masters, R. Sullivan and R.J. Composto, Chitosan adsorption on hydroxyapatite and its role in preventing acid erosion, *J. Colloid Interface Sci.*, 385 (2012) 235-243.

[278] F. Javier Silvestre, M. Paz Minguez and J.M. Sune-Negre, Clinical evaluation of a new artificial saliva in spray form for patients with dry mouth, *Medicina Oral Patologia Oral Y Cirugia Bucal*, 14 (2009) E8-E11.

- [279] R. Gibbons and I. Etherden, Enzymatic modification of bacterial receptors on saliva-treated hydroxyapatite surfaces, *Infection and immunity*, 36 (1982) 52-58.
- [280] J. Chen, Food oral processing - a review, *Food Hydrocolloids*, 23 (2009) 1-25.
- [281] E. Silletti, M.H. Vingerhoeds, W. Norde and G.A. Van Aken, The role of electrostatics in saliva-induced emulsion flocculation, *Food Hydrocolloids*, 21 (2007) 596-606.
- [282] E. Jobstl, J. O'Connell, J.P.A. Fairclough and M.P. Williamson, Molecular model for astringency produced by polyphenol/protein interactions, *Biomacromolecules*, 5 (2004) 942-949.
- [283] T. Zelles, K.R. Purushotham, S.P. Macauley, G.E. Oxford and M.G. Humphreys-Beher, Concise Review: Saliva and Growth Factors: The Fountain of Youth Resides in Us All, *J. Dent. Res.*, 74 (1995) 1826-1832.